Estudi del metabolisme del glicogen en la funció neuronal i la seva implicació en la malaltia de Lafora i l'envelliment

Jordi Vallès Ortega

TESI DOCTORAL

Estudi del metabolisme del glicogen en la funció neuronal i la seva implicació en la malaltia de Lafora i l'envelliment.

Jordi Vallès Ortega

Barcelona, gener 2012

Estudi del metabolisme del glicogen en la funció neuronal i la seva implicació en la malaltia de Lafora i l'envelliment.

Memòria presentada per
Jordi Vallès Ortega

Per a optar al grau de
Doctor per la Universitat de Barcelona

Tesi realitzada en el Laboratori d'Enginyeria Metabòlica i Teràpia de la Diabetis, pertanyent al Programa de Medicina Molecular de l'Institut de Recerca Biomèdica (IRB Barcelona), i dirigida pel Dr. Joan J. Guinovart Cirera

Tesi adscrita a la Universitat de Barcelona
Facultat de Biologia
Departament de Bioquímica i Biologia Molecular

Programa de Doctorat en Biotecnologia
Màster Oficial 2008-2009

Barcelona, gener 2012

El doctorand — El director de la Tesi

Jordi Vallès Ortega — Dr. Joan J. Guinovart Cirera

Als meus pares.

If I brought a pig in here and said,'This pig can talk' and the pig talked, you wouldn't say, 'Well that's just an n of 1, show me another pig.' You would say, 'Oh my god that's a talking pig!'

Dr. V.S. Ramachandran

AGRAÏMENTS

Tinc la sensació que he llegit en totes les tesis dels meus companys i amics les mateixes frases que estic a punt d'escriure. Però és cert que no voldria deixar-me ningú i que escric això a les tantes (potser és necessari escriure aquest apartat a última hora i amb el cansament de tot el que s'ha escrit anteriorment). Així que abans de dir gràcies demano perdó per qui se senti decebut per les paraules que acompanyen el seu nom o, simplement, per la manca de referència a l'ajuda que m'hagin donat tots aquells que oblidi.

Començo, com no pot ser d'una altra manera, pel Dr. Guinovart, el Joan, el Guino, vaja. Han passat uns quants anys des d'aquell dia en que jo era estudiant de tercer de carrera i volia fer pràctiques al teu laboratori. Com et veus d'aquí 10 anys? em vas preguntar. Més vell. Em vaig atrevir a respondre. Doncs bé, encara no han passat 10 anys, però m'han sortit unes quantes canes. Seriosament, vull agrair-te la confiança i el suport que m'has donat i em dónes. Tinc la sensació d'haver-me fet gran però no només d'edat. Si haig de destacar una cosa d'haver fer la tesi sota la teva direcció, és que he tingut l'oportunitat d'equivocar-me molts cops. No conec una manera millor d'aprendre. Gràcies.

David, el meu mentor. Aquell home estrany, sempre engominat, perico i desordenat que es va atrevir a començar un projecte sobre metabolisme del glicogen en neurones, que va tenir la santa paciència de donar-me joc durant el primer any de la meva tesi i que ha acabat sent un gran amic. Tinc masses coses per agrair-te i la majoria no es poden escriure aquí. Així que quan vingui a San Diego t'ho explico.

Mar, a tu què t'haig de dir? I en quin idioma? Que no serveixi de precedent però: aunque yo hable en catalán, lento y bajito y tú todo lo contrario, quiero que sepas que valoro mucho tu trabajo y tu empeño por hacer que todo esté en su sitio y funcione bien. Nunca olvidaré mis primeros westerns (las burbujas cuadradas del tamaño de mi cabeza, las bandas grises y las negras...) o la tensión de bajar contigo a cultivos. Cuando se aprendre algo contigo, nunca se olvida. Y he aprendido mucho de ti.

El laboratori tampoc funcionaria com funciona si no fos per l'equip tècnic: Anna, Emma, Manu, gràcies pel vostre suport i per fer aquella feina que ningú veu. També agrair a l'Ester, la Lydie i la Mari Carmen la seva disponibilitat. Espero que us vagi mot bé en les noves feines.

Joaquim, fem una cosa, jo t'escric els agraïments i tu me'ls repasses. Per desgràcia, en aquest apartat el control de cambios no serveix, perquè segur que em quedaré curt. Ja sé que, com tu dius, només fas la teva feina. Però sense la teva ajuda aquesta tesi i els articles que la formen no estarien on estan. Gràcies per la teva infinita paciència i disponibilitat. Parlar amb tu de ciència (i del que no és ciència) és un plaer.

El club del tupper (si tothom ens coneix així, no seré jo qui ho canviï): Carlos R., gracias por tus consejos, las lentejas, las madrugadas de Rosa Clarà, los goles sin ángulo, por invitarme a tu isla y a tu muy noble y leal Villa, por todo lo compartido y aún por compartir. Carles M., gràcies per sa tonyina amb soja, sa teva ajuda cada cop que se m'acudia fer alguna cosa de biologia molecular, per ses teves cançons, per acollir homeless per Sant Joan i a ses Festes de Gràcia (ses bones, no ses de BCN, i dó!), per ser el meu visino. He vist com t'afaitaven i ja tinc les barbes en remull! Lanuza, Rojo... què puc dir-te aquí que encara no t'hagi dit? No cal que parli de l'EVO, oi? Pirata? Gràcies pel pollastre rostit (i la musaka que em va donar energia per acabar la discussió!), pels esmorzars a les 12, les barbacoes, els vespres de cervesa i futbol, per deixar-te guanyar a squash o a frontón, pels gintònics que sobraven,... Per ser allà sempre, sense haver-t'ho de demanar. Vés pensant com es dirà l'empresa!

Els companys que encara no han marxat (o que acaben d'arribar): Isa, aquella noia que semblava tímida i que va entrar després de mi. Això vol dir que hauries de ser la següent, no? Ja quasi ho tens, n'estic segur que triomfaràs! Gràcies per convidar-nos a tots els pastissos que inexplicablement et sobren a casa, per tenir sempre un somriure per oferir i una estona per parlar. Quan tu dipositis podem anar a cel·lebra-ho al Hotel el Churra, no? Felipe, el bombero

chileno que vino a mantener el desorden en la poyata de David, nuestro central de hierro. Tú también estás invitado a Murcia, obvio! Los tres nos morimos de ganas de volver a ver al guatón ese... Mucha suerte en tu proyecto y gracias por tu compañerismo. Jordi, no, jo no, el Duran, gràcies per la teva feina, sense ella la meva tesi no hagués estat possible tal i com és ara. Giorgia, dai! La última predoc en entrar, gracias por tus clases de italiano macarrónico, por confiar en mis ideas, verás como al final saldrá, ya lo verás... Chris, the flyman, please correct me! Thanks for your suggestions and ideas, hope we'll have time to collaborate a little bit making flies live longer. Good luck!

I els que han aixecat el vol de can Guino: Dani, el que era el noi alt amb ulleres de pasta abans que jo, encara que mai em vas voler dir quants ul d'oligos es posaven a la PCR, les teves idees ens il·luminaven a tots. Delia, la flamant techtransfer, des que no hi ets sempre sobra xocolata, però se't troba a faltar. Laura, no puc atribuir només a Delia la volatilitat de la xocolata. Voleu dir que no és culpa del tungstat això? Ara recordava que jo et vaig ensenyar a fer els primers westerns, ara tu ja ets doctora i jo fa molt de temps que no miro films plens de bandes inexplicables... Moltes gràcies pels bons moments. Susana, mira que confiar en l'assaig de ramificació de glicogen per al teu article! Ens va costar conèixer-nos, però ha valgut molt la pena. Gràcies fer-me costat quan més ho he necessitat i per confiar en mi. Sé que puc comptar amb tu, sobretot si es tracta de sushi i daiquiri, no? Óscar, el químic que es va atrevir a buscar-li més fosfats a la sintasa, gràcies per no deixar-nos sols a primera hora del matí. Y los americanos, Adelaida, la doctora silenciosa del fondo, gracias por tus bailes, tu respeto y comprensión, por esas charlas a les 10 de la noche... ¿cierras tú? Espero que tengas mucho éxito en tu México lindo. Flor, por iniciarnos en el mundo de las moscas. Spichigher, pichí, aunque me costó acostumbrame a tus silvidos, tus interminables historias hacían las tardes más llevaderas. Seguramente te inventabas la mitad de las cosas, pero igualmente eran harto interesantes. Fabián, nunca pensé que de algún modo podría alegrarme de un incendio en un instituto austral de una ciudad desconocida. Tampoco imaginé tener un amigo nacido en el cono sur (la verdad es que nunca pensé que alguien pudiera vivir allí donde se inserta la bombilla del globo terráqueo que me regalaron por mi primera comunión). Pero ahí estás tú. Pasaste poco tiempo en el lab, pero fue suficiente para descubrir una magnífica persona y ganar un buen amigo. Nos vemos pronto. A ver si es cierto que las chorrillanas son mejores en Valpo que en el Pessebre.

També haig d'agrair l'ajuda de molta gent que de fora del lab, però que han contribuït a fer possible aquesta tesi: el Dr. Soriano i la gent del seu laboratori, que mai es van cansar de resoldre els meus dubtes i de deixar-me els seus reactius. Especialment el Lluís, de qui vaig aprendre com fer immunos de cervell, i el Carles, que van trobar temps per col·laborar amb nosaltres. Gràcies a ells he pogut portar endavant una tesi centrada en el sistema nerviós. De la mateixa manera, l'Anna Serafín, la seva actitud incansable per provar les tincions que fessin falta i per explicar-ho tot tan bé han estat clau. El Dr. Pumarola i la gent del seu laboratori, especialment la Merce, que van acceptar la col·laboració i totes les meves suggerències des del primer moment. Ha estat un luxe treballar amb vosaltres. Estic segur que això no acaba aquí. Analía (i Marta) gracias por dedicar tu tiempo a mi loco proyecto y a enseñarme tu arte en estereotaxia. Lamento que se quedara a medias porque trabajar contigo fue un placer, se contagia tu optimismo. Espero que te guste lo que hice en lugar de nuestro proyecto fallido. Gracias por aceptar, de nuevo, mi propuesta. Y por hablar de proyectos que quedaron sin terminar, también quiero recordar aquí al laboratorio del Dr. Ramón y Cajal: Carlos, Ma. Ángeles. Espero que los dos estéis bien. Quizá algún día escribamos el artículo, eh María? Y si ese día no llega, por lo menos nuestra aventura con laforina fue divertida. Gracias por los cafés en las alturas. A la gent del servei de microsopia: el Julien, però sobretot la Lídia i l'Anna. Després de tantes hores, qui es creuria ara que vaig tardar 2 anys a poder ajuntar imatges dels dos oculars del microscopi, eh? Gràcies per la disposició i el tracte. Heu vist quina portada més xula? I com no, gràcies al laboratori de la Dra. Caelles, a la Carme i al Joan per deixar-nos utlitzar el microoones i la cafetera i als seus membres: Lanuza, Tessa, Sara, Johan, Laura, Cris, Neus. Pels dinars al passadís gelat i altres activitats extraescolars. Si no podem fer ciència, sempre podem trobar-nos per beure vi, no?

Durant la tesi també he fet altres activitats que han contribuït, jo crec que molt positivament, a la meva formació. Vull donar les gràcies a tots els membres del primer IRB Student Council i a la Clara Caminal. Un no sap què costa organitzar una cosa, fins que no ho ha fet. I nosaltres ho hem fet. Me'n sento molt orgullós. Josep Maria, gràcies per donar-me l'oportunitat de participar en els

programes I,tu? Jo Bioquímica i Recerca en Secundària. Tots sabem que costa molt dir-te que no, però va valdre la pena no fer-ho.

Per últim, les persones més importants a la meva vida. Georgina, gràcies per aguantar el meu mal humor i les meves manies, per fer-me somriure, per donar-me força quan em calia. Al teu costat tots els camins semblen fàcils i el futur no m'espanta. I a la meva família: iaia, perquè aquesta tesi et farà encara més il·lusió que a mi, abuelo, me hubiera gustado que vivieras este momento. Por el orgullo que demostraban tus palabras cuando hablabas de mi. Als meus germanets, la Marta i el Manel, la meva tieta, els meus cosins, pel suport. Envoltat de la gent que t'estima és molt més fàcil pensar en ciència. I als meus pares, perquè vosaltres sou qui més s'ha esforçat en aquest projecte. Perquè tot el que sóc i tot el que pugui aconseguir és fruit del vostre treball incansable i la vostra fe amb mi. Gràcies per tot!

ÍNDEX

ÍNDEX

ABREVIACIONS

AD	*Alzheimer's disease*, Malaltia d'Alzheimer
AGEP	*Advanced glycosylation end-products*, Productes finals de glicosilació avançada
ALS	*Amyothrophic lateral sclerosis*, Esclerosi lateral amiotròfica
AMPc	Adenosina monofosfat cíclica
APBD	*Adult polyglucosan body disease*, Malaltia de cossos de poliglucosà en adults
BE	*Branching Enzyme.* Enzim ramificant
BGP	*Brain Glycogen Phosphorylase*, Glicogen fosforilasa de cervell
CA1	*Cornum Amonnis 1*, Asta d'Ammon 1
CA2	*Cornum Amonnis 2*, Asta d'Ammon 2
CA3	*Cornum Amonnis 3*, Asta d'Ammon 3
DBE	*Debranching Enzyme*, Enzim desramificant
DG	*Dentate Gyrus.* Gir dentat
G1P	*Glucose-1-phosphate*, Glucosa-1-fosfat
G6P	*Glucose-6-phosphate*, Glucosa-6-fosfat
GFAP	*Glial Fibrillary Acidic Protein*, Proteïna acídica fibrilar de la glia
GK	*Glucokinase*, Glucoquinasa
GP	*Glycogen Phosphorylase*, Glicogen fosforilasa
GS	*Glycogen Synthase*, Glicogen sintasa
GSK3	*Glycogen Synthse Kinase 3*, Quinasa de la glicogen sintasa 3
GYG	*Glycogenin*, Glicogenina
HD	*Huntington's disease*, Malatia de Huntington
HSP	*Heat shock protein*, Proteïna de xoc tèrmic
KO	*Knock out*, nul, deficient (manipulat genèticament per impedir la transcripció d'un gen determinat)
LGS	*Liver Glycogen Synthase*, Glicogen sintasa hepàtica
MGP	*Muscle Glycogen Phosphorylase*, Glicogen fosforilasa muscular.
MGS	*Muscle Glycogen Synthase*, Glicogen sintasa muscular
NF200	*200 kDa neurofilaments*, Neurofilaments de 200 kDa
PAS	*Periodic acid Schiff*, Àcid Periòdic i base de Schiff
PD	*Parkinson's disease*, Malaltia de Parkinson
PGB	*Polyglucosan Body*, Cossos de poliglucosà
PhK	*Phosphorylase kinase*, Fosforilasa quinasa
Pi	*Inorganic Phosphate*, Fosfat inorgànic
PKA	*cAMP-dependent Protein Kinase*, Proteïna quinasa depenent de AMPc
PP1	*Protein Phosphatase 1*, Proteïna fosfatasa 1
PTG	*Protein Targeting to Glycogen*, Proteïna dirigida al glicogen
PV	*Parvalbumin*, Parvalbúmina
siRNA	*Short interfering RNA*, Oligonucleòtids de RNA d'interferència.
SNC	Sistema nerviós central
UDP	*Uridine diphosphate*, Uridina difosfat
UPS	*Ubiquitin-proteasome system*, Sistema ubiqüitina-proteasoma
UTP	*Uridine triphosphate*, Uridina trifosfat
WT	*Wild type*, salvatge (sense manipulació genètica)

INTRODUCCIÓ GENERAL

INTRODUCCIÓ GENERAL

1. El glicogen

El glicogen és la principal reserva de carbohidrats del cos humà. Es tracta d'un polisacàrid de D-glucosa, és a dir un poliglucosà, altament ramificat que actua com a magatzem de glucosa i des d'on pot ser alliberada ràpidament en cas de demanda. El glicogen és un sistema de reserva de glucosa que proporciona diversos avantatges: s'acumula intracel·lularment sense incrementar la pressió osmòtica de la cèl·lula, pot ser metabolitzat ràpidament sense necessitat de consumir ATP i, al contrari del que passa amb els àcids grassos, pot ser utilitzat com a font d'energia en condicions anaeròbiques. Les reserves més grans de glicogen es troben al fetge i al múscul esquelètic. Hi ha al voltant de 100 g de glicogen al fetge alimentat i al voltant de 400 g de glicogen al múscul esquelètic en repòs (Champe and Harvey, 1994), és a dir, el glicogen suposa el 1-2% del pes del múscul esquelètic i el 6-8% del pes de fetge (Shulman et al., 1995). El glicogen hepàtic és alliberat en forma de glucosa a la circulació sistèmica en resposta a una baixada dels nivells de glucosa en sang, mantenint d'aquesta manera la normoglicèmia. El glicogen muscular, en canvi, és utilitzat com a font d'energia únicament per a les cèl·lules del mateix múscul esquelètic durant la contracció muscular.

També es troba glicogen al cervell i s'estima que aquest en conté entre 0.5 i 1.5 g, és a dir, al voltant del 0.1% del seu pes total. Per tant, no resulta estrany que s'hagi passat per alt durant tant de temps el rol del glicogen cerebral. De fet, el dogma generalitzat que apareix als llibres de text sobre el metabolisme del cervell defensa que aquest és energèticament depenent de la glucosa com a substrat i que no disposa de reserves d'energia. Per tant, a llarg termini el cervell està a la mercè de l'aportament constant de glucosa a través de la circulació sistèmica (Brown, 2004; Stryer, 1995). La permeabilitat selectiva de la barrera hemato-encefàlica limita la possibilitat que d'altres metabòlits presents a la sang, com per exemple el lactat, actuïn com a fonts d'energia per al cervell. Encara que no hi ha cap dubte que la glucosa és el principal suport energètic del cervell, estudis *in vitro* han mostrat que el teixit cerebral pot sobreviure durant llargs períodes amb substrats diferents a la glucosa com el lactat i el piruvat, altres sucres com la manosa o la fructosa, i cossos cetònics com el beta-hidroxibutirat i l'acetoacetat. Aquests fets suggereixen que *in vivo* el cervell podria sobreviure a base de substrats derivats de la glucosa generats dins de la parènquima cerebral. Tenint en compte que el glicogen es troba als astròcits, està posicionat idòniament per proveir substrats energètics a les neurones i resulta probable que el glicogen tingui un paper de suport en la funció cerebral.

1.1. Síntesi i degradació del glicogen

Les rutes generals de glicogènesi i glicogenòlisi són idèntiques en tots els teixits, però els enzims que hi intervenen i la seva regulació són fets a mida per a als requeriments específics de cadascun. La síntesi de glicogen parteix de la glucosa-6-fosfat (G6P), la disponibilitat intracel·lular de la qual és clau en aquest procés perquè es troba en un punt de creuament de diverses vies metabòliques. Els nivells de G6P depenen, com a mínim, del transport i fosforilació de glucosa extracel·lular, del flux glicolític/gliconeogènic, la ruta de les pentoses fosfat i la ruta de biosíntesi d'hexosamines (formació de glicoproteïnes i peptidoglicans) (Figura 1). Així que, malgrat aquest text es centri en el metabolisme del glicogen, cal tenir sempre present que aquest és un mecanisme integrat al l'estat metabòlic general de la cèl·lula (Bouche et al., 2004).

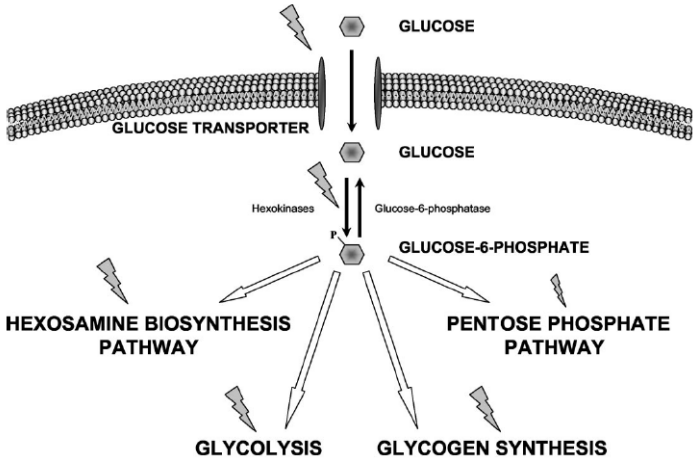

Figura 1. Rutes metabòliques de la glucosa-6-fosfat
(Bouche et al. 2004)

La síntesi de glicogen comença amb la conversió de glucosa-6-fosfat en glucosa-1-fosfat (G1P) per part de la fosfoglucomutasa (EC 5.4.2.2) La G1P reacciona amb uridina trifosfat (UTP), una reacció catalitzada per la UDP glucosa pirofosforilasa (EC 2.7.7.9), per produir UDP-glucosa alliberant dues molècules de fosfat inorgànic (Pi). La UDP-glucosa és el donador de tots els residus glucosil que s'afegeixen a la molècula de glicogen. La iniciació de la síntesi de glicogen té lloc gràcies a la glicogenina (GYG, EC 2.4.1.186) que transfereix la glucosa des de la UDP-glucosa a un residu tirosina específic de la seva cadena lateral. Així, catalitza la seva pròpia glicosilació fins a formar un oligòmer de 8 a 10 residus de glucosa que servirà com a encebador per a la posterior elongació del polímer de glucosa. L'elongació de la cadena té lloc mitjançant enllaços α-1,4-glucosídics entre el carboni 1 del grup glucosil de la UDP-glucosa que entra i el carboni 4 del residu glucosil acceptor de la cadena de glicogen creixent. La glicogen sintasa (GS, EC 2.4.1.11), que interacciona amb la GYG, catalitza aquesta reacció que requereix que la cadena acceptora tingui com a mínim una longitud de quatre unitats de glucosa. Com a resultat de la reacció de síntesi de glicogen s'allibera UDP, que és transformada de nou en UTP per la nucleòsid difosfat

quinasa (EC 2.7.4.6) i pot tornar a ser utilitzada per a la síntesi de UDP-glucosa. Si totes les glucoses s'afegissin a la molècula creixent de glicogen d'aquesta manera es formaria un polímer lineal. De fet, l'amilosa que es forma en les plantes és un polímer amb aquestes característiques. En canvi, de mitjana, aproximadament cada 8 residus de glucosa neix una ramificació deguda a un enllaç α-1,6-glucosídic format entre el carboni 1 de la molècula de glucosa entrant i el carboni 6 del residu glucosil acceptor. La ramificació té dos avantatges, incrementa la solubilitat del glicogen, i augmenta enormement el nombre d'extrems no reductors, fet que multiplica en gran mesura tan la capacitat d'incorporació com d'alliberació de residus de glucosa. Les ramificacions són introduïdes per acció de l'enzim ramificant amilo-(α-1,4-α-1,6)-transglicosilasa (BE, EC 3.2.1.3), el qual transfereix entre 4 i 7 unitats glucosil des de l'extrem no reductor de la cadena cap a un grup hidroxil situat en el carboni 6 d'un residu de glucosa de l'interior del polímer, formant un enllaç glicosídic α-1,6.

La degradació del glicogen (glicogenòlisi) no és simplement el procés invers a la seva síntesi, sinó que requereix enzims independents, fet que proporciona un major nivell de control sobre el contingut de glicogen. El producte de degradació de glicogen és principalment la G1P, que és transformada posteriorment en G6P per la fosfoglucomutasa, però també s'allibera glucosa. La proporció de G1P i glucosa depèn del nombre de residus glucosil que hi hagi entre punts de ramificació. El destí metabòlic d'aquests compostos és específic de teixit i depèn de la presència de glucosa-6-fosfatasa (EC 3.1.3.9). La glicogen fosforilasa (GP, EC 2.4.1.1) trenca l'enllaç glicosídic α-1-4 entre els residus glucosil als extrems no reductors del glicogen per formar G1P. L'activitat de la glicogen fosforilasa continua fins que queden quatre residus glucosil per arribar al punt de ramificació, llavors la reacció s'atura deixant com a resultat dextrans que no poden ser degradats. Les ramificacions poden ser eliminades gràcies a l'activitat amilo-1,6-α-glucosidase,4-α-glucanotransferasa de l'enzim desramificant (DBE). En primer lloc, l'activitat 4-α-glucotransferasa (glucosil 4:4 transferasa, EC 3.2.1.33) treu els tres residus glucosil més externs del punt de ramificació, deixant un únic residu en el punt de ramificació, i els afegeix a l'extrem no reductor de la molècula, on poden ser degradats per la glicogen fosforilasa. El residu glucosil restant (unit al glicogen per un enllaç α-1,6) és tallat mitjançant l'activitat amilo-1,6-α-glucosidasa (EC 3.2.1.33) alliberant glucosa. Així la cadena pot seguir sent degradada per la glicogen fosforilasa alliberant G1P fins a tornar a arribar als 4 residus glucosil de distància del següent punt de ramificació, llavors és repeteix el procés. El producte final de la degradació del glicogen és G6P (i glucosa), el metabolisme de la qual depèn de l'estat energètic de la cèl·lula. La síntesi i degradació del glicogen succeeixen simultàniament, per tant el contingut net de glicogen varia en funció de les necessitats immediates d'energia.

1.2. Glicogen sintasa (GS)

La GS és l'únic enzim capaç de sintetitzar llargs polímers de glucosa en mamífers. Existeixen dues isoformes d'aquest enzim corresponents a dos gens independents i que reben el nom dels principals teixits glicogenogènics on aquestes s'expressen. La isoforma muscular (MGS), codificada a partir del gen *GYS1*, s'expressa en la majoria de teixits -inclòs el cervell- però no en el fetge, l'únic teixit on s'expressa de la isoforma hepàtica (LGS), codificada pel gen *GYS2*.

Aquest apartat està enfocat a la MGS, ja que és la isoforma que s'expressa en el sistema nerviós central (SNC) i té un paper clau en el contingut d'aquest treball. La MGS és l'enzim que catalitza el pas limitant en la síntesi de glicogen i està altament regulat mitjançant diversos mecanismes que impliquen, al menys, modificacions covalents, al·lostèriques i de localització subcel·lular.

1.2.1. Regulació per fosforilació

Un mecanisme clau en la regulació de l'activitat glicogen sintasa és la inactivació per fosforilació, és a dir, la unió covalent de grups fosfat. Aquesta fosforilació pot ser catalitzada per diverses quinases en nou residus de serina localitzats als extrems N i C-terminal de la MGS. A N-terminal hi ha els llocs de fosforilació 2 i 2a, corresponents als aminoàcids 7 i 10. A l'extrem C-terminal trobem els llocs 3a, 3b, 3c, 4, 5, 1a i 1b, que corresponen als residus 640, 644, 648, 652, 656, 697 i 710 respectivament (Figura 2). La fosforilació dels diferents llocs causa la inactivació de l'enzim mitjançant la disminució de l'afinitat pel seu substrat UDP-glucosa (Roach et al., 1976) i el seu activador al·lostèric G6P (Roach and Larner, 1976; Salavert et al., 1979; Skurat et al., 2000) i un augment d'afinitat per ATP i Pi, que tendeixen a antagonitzar la G6P (Mathews and Van Holde, 1990). Així doncs, a grans trets, la forma desfosforilada és la forma activa de la MGS i la fosforilada la inactiva.

Les quinases que participen en aquesta inactivació són nombroses (Roach et al., 1991), entre elles es troben la proteïna quinasa C i la proteïna depenent de calmodulina/Ca2+ (CaM-PK), que fosforilen els llocs 1a i 1b respectivament. La quinasa depenent d'AMPc (PKA) fosforila els llocs 1a i 1b i el lloc 2 (Cohen and Hardie, 1991), que també és fosforilat per la quinasa depenent d'AMP (AMPK) (Carling and Hardie, 1989) o la fosforilasa quinasa (Roach et al., 1978). El lloc 2a és fosforilat per la caseïna quinasa 1 (Flotow and Roach, 1989), però només quan el lloc 2 està fosforilat (Skurat et al., 1994). Els centres de l'extrem C-terminal 3a, 3b, 3c i 4 són regulats principalment per la glicogen sintasa quinasa 3 (GSK3), fosforilació que es veu potenciada per la fosforilació prèvia del lloc 5 per part de la caseïna quinasa II (Roach, 1990). El lloc 3a també és fosforilat per la quinasa PASK (Wilson et al., 2005). La interacció d'aquestes quinases amb MGS i, per tant, la fosforilació s'inhibeixen en presència de glicogen.

Malgrat tot això, la fosforilació en les diferents serines no té el mateix impacte en l'activitat de l'enzim. Els llocs de fosforilació que han mostrat ser més importants en la seva regulació són el 2, 2a (Ser 7 i 10), 3a i 3b (Ser 640 i 644) (Skurat et al., 1994). Per aquest motiu el seu grau de fosforilació s'utilitza de forma generalitzada per avaluar l'estat d'activació de la MGS. Els altres llocs de fosforilació tenen un efecte menor o no tenen un efecte directe sobre l'activitat.

L'activació per desfosforilació de la MGS és catalitzada principalment per la proteïna fosfatasa 1 (PP1), que alhora està involucrada en la inactivació per desfosforilació de la GP. Així, l'acció d'aquesta fosfatasa activa la síntesi de glicogen alhora que inhibeix la seva degradació. La PP1 és un holoenzim que està implicat en la regulació d'altres processos cel·lulars a més d'aquest. Consta d'una subunitat catalítica (PP1c) molt promíscua que s'expressa de forma ubiqua (Bollen, 2001), i de múltiples subunitats reguladores que, mitjançant la seva expressió diferencial i la seva localització cel·lular, dirigeixen l'activitat de la subunitat catalítica cap a substrats específics. S'han descrit sis subunitats reguladores que dirigeixen la PP1 cap al glicogen i que, per tant, afavoreixen la seva acumulació: PPP1R3A (ó G_M, PP1G, R_{GL}), PPP1R3B (ó G_L), PPP1R3C (ó PTG, PPP1R5), PPP1R3D (ó PPP1R6), PPP1R3E i PPP1R3F. L'expressió de cada una d'aquestes subunitats és específica de diferents teixits, però aquesta especificitat varia entre els diferents mamífers (Montori-Grau et al., 2011). A grans trets, però, G_M s'expressa principalment en múscul esquelètic (Tang et al., 1991), G_L en fetge (Doherty et al., 1995) i R3E en múscul esquelètic, múscul cardíac i fetge (Munro et al., 2005). La PTG, que s'ha detectat en cervell (Berman et al., 1998; Printen et al., 1997), i la R6 (Armstrong et al., 1997) són ubiqües. La R3F s'ha identificat recentment en astrocitomes de ratolí i conté, com la subunitat G_M, un lloc d'unió a membrana (Kelsall et al., 2011). Les sis subunitats interaccionen amb el glicogen i la subunitat catalítica, facilitant l'activitat fosfatasa d'aquesta sobre els seus substrats GS, GP i la fosforilasa quinasa (PhK) que estan unides al polisacàrid. A més d'aquesta capacitat, la PTG també pot formar complexos entre PP1 i les proteïnes reguladores del metabolisme del glicogen perquè pot unir-se directament a elles. Per tant, la PTG actua com a bastida (*scaffold*) molecular, engalavernant la PP1 amb els seus substrats GS i GP sobre les partícules de glicogen, i incrementant així l'acumulació de glicogen (Berman et al., 1998; Fong et al., 2000; Greenberg et al., 2003; Lerin et al., 2000; O'Doherty et al., 2000; Printen et al., 1997)

1.2.2. Regulació al·lostèrica

Com s'ha comentat anteriorment, la modulació de l'activitat per fosforilació està lligada a canvis d'afinitat de la MGS no només pel seu substrat UDP-glucosa sinó també per moduladors al·lostèrics. Entre aquests moduladors trobem inhibidors com ara diversos nucleòtids (ATP, ADP, AMP i UPD) i el principal activador, la G6P, que s'uneix a una zona rica en arginines corresponent als residus 579, 580, 582, 586, 588 i 591 de la MGS humana (Pederson et al., 2000). Aquesta unió causa un canvi conformacional en l'enzim (Baskaran et al., 2010) que fa més accessible el centre catalític (situat al voltant del residu E510) i afavoreix així la catàlisi. (Figura 2). De fet, s'ha

demostrat recentment que el mecanisme principal pel qual la insulina promou l'acumulació de glicogen muscular *in vivo* és l'activació al·lostèrica i no la desfosforilació de la MGS (Bouskila et al., 2010). Quan la concentració de G6P és suficientment alta, la seva unió és capaç de revertir la inactivació de MGS induïda per fosforilació i conferir-li la seva activitat màxima (Villar-Palasi and Guinovart, 1997). Aquest efecte s'utilitza de forma habitual *in vitro* per determinar la quantitat de MGS i el seu estat d'activació en mostres biològiques. La mesura de l'activitat MGS en presència d'una concentració alta (6,6 mM en el cas del nostre laboratori) de G6P en la mescla de reacció permet determinar l'activitat MGS total (*activitat T*), que correspon a l'activitat MGS màxima i és directament proporcional a la quantitat d'enzim. La mesura de l'activitat sense afegir G6P a la mescla de reacció ens dóna l'activitat MGS intrínseca o independent de G6P (*activitat I*) que depèn del seu estat de fosforilació. El quocient entre les activitats I i T (*ratio I/T*) constitueix el grau d'activació de la MGS, on un valor igual a 1 correspondria a l'activació màxima i un valor igual a 0 significaria que l'enzim és totalment inactiu.

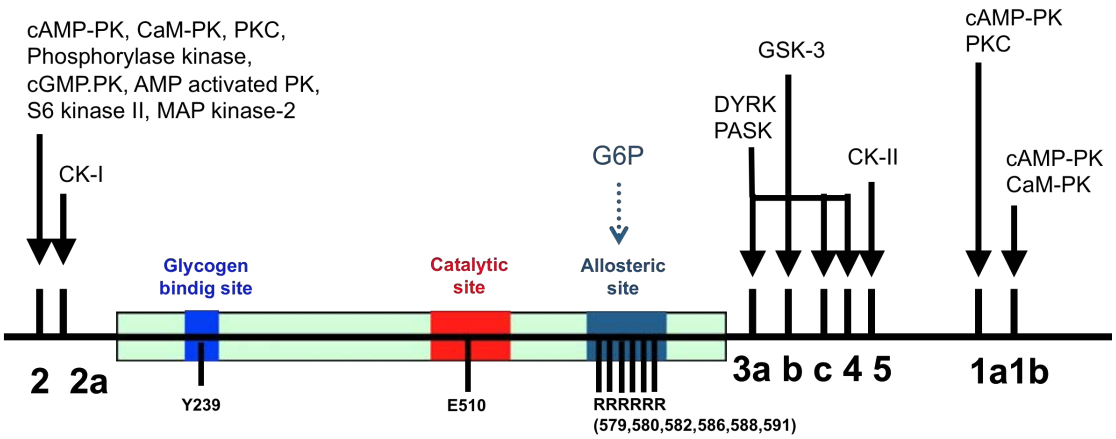

Figura 2. Regulació de la MGS

1.2.3. Regulació lligada a la localització cel·lular

La MGS, com la PTG, la GP i altres proteïnes de la maquinària del glicogen, té una afinitat alta pel glicogen i resulta molt difícil de trobar una situació fisiològica on aquesta no es trobi unida al polisacàrid. De fet, recentment s'ha identificat un lloc d'unió al glicogen (al voltant del residu Y239) diferent al centre catalític que té un paper clau en aquesta alta afinitat i, per tant, en la seva localització cel·lular (Diaz et al., 2011) (Figura 2). Malgrat això, canvis en la distribució cel·lular de la MGS promoguts per la seva interacció amb el glicogen i amb altres proteïnes (en presència o no de glicogen) podrien ser importants per a la seva regulació. Un exemple d'aquestes interaccions podria ser l'associació entre la MGS i la GYG. En múscul esquelètic de rata, la MGS transloca cap a una fracció enriquida en actina en resposta a la depleció de glicogen induïda per contracció muscular (Nielsen et al., 2001). Per poder tornar a sintetitzar glicogen de manera

eficient, la MGS necessita interaccionar amb la GYG. S'ha descrit que les dues proteïnes poden estar associades al citoesquelet d'actina (Baque et al., 1997; Nielsen et al., 2001). A més, s'ha descrit que la translocació pot ser depenent de fosforilació en els llocs 1b, 2 i 2a durant l'inici d'aquesta re-síntesi de glicogen en múscul (Prats et al., 2005). En diversos tipus de línies cel·lulars, la MGS transloca del citoplasma al nucli quan s'esgoten les reserves de glicogen en les cèl·lules cultivades en absència de glucosa i del nucli al citoplasma quan es torna a afegir glucosa al medi (Ferrer et al., 1997).

1.3. Glicogen Fosforilasa (GP)

En mamífers, es coneixen tres isoformes de GP que són codificades per gens independents. Reben el nom del teixit on s'expressen preferentment: la muscular (MGP), l'hepàtica (LGP) i la de cervell (BGP). Encara que la isoforma muscular també s'expressa en cervell (Browner et al., 1992). La GP també pot ser regulada per fosforilació (Thorens et al., 1990) i al·lostèricament (Wang et al., 2002). Al contrari que la GS, la fosforilació de la GP té lloc en un únic residu, la Ser14 en l'isoforma de múscul, i comporta l'activació de l'enzim. D'aquesta manera, el podem trobar en dues formes interconvertibles: la desfosforilada i inactiva (GP-b) i la fosforilada i activa (GP-a). Aquesta fosforilació és catalitzada per la fosforilasa quinasa (PhK). La PhK s'activa quan és fosforilada per la PKA en resposta a AMPc. A més, conté una subunitat calmodulina a través de la qual és activada, mitjançant un canvi conformacional, en resposta a nivells intracel·lulars elevats de Ca^{2+}. La desfosforilació de la GP i la PhK, com ja s'ha comentat anteriorment, té lloc per acció de PP1 i comporta la conversió de la forma activa GP-a a la inactiva GP-b.

La regulació al·lostèrica de la GP depèn de la isoforma i l'estat de fosforilació (Parodi et al., 1970). Pel que fa al SNC, les GP-b de múscul i de cervell presenten activació al·lostèrica per AMP i inhibició per ATP. De manera que en situacions de requeriment energètic, quan la relació AMP/ATP creix, es pot activar la GP-b i, per tant, la degració de glicogen. La unió d'AMP és cooperativa i es veu augmentada després de la fosforilació de GP (Roach, 2002). A més la GP també és regulada pels nivells de G6P, que actua com a inhibidor al·lostèric estabilitzant la seva forma inactiva. La unió d'aquest enzim pel seu substrat també pot ser entesa com part de la seva regulació al·lostèrica. Per exemple, la BGP presenta una menor afinitat pel glicogen que la MGP. Aquesta afinitat pot ser incrementada per AMP, de manera que la regulació per AMP/ATP adquireix major importància en la BGP per a estimular la degradació de glicogen, que faria que aquesta isoforma sigui més sensible a l'estat energètic de la cèl·lula. Al cervell, aquesta regulació pot adquirir major importància tenint en compte el seu baix contingut en glicogen (Crerar et al., 1995).

1.4. GràNul o orgànul de glicogen?

Més enllà de la concepció clàssica, que descriu el glicogen com una polímer de glucosa que es fa i es desfà en el citoplasma de la cèl·lula en funció dels requeriments energètics, cada cop més dades fan pensar en el glicogen com en un orgànul. El glicogen seria, doncs, una estructura dinàmica i finament regulada, amb el seu propi conjunt de proteïnes que interactuen entre elles i amb altres proteïnes i estructures de la cèl·lula.

En aquesta direcció, en un treball publicat recentment (Stapleton et al., 2010) s'identifiquen un gran nombre de proteïnes unides al glicogen hepàtic, entre les quals es troben la major part de les proteïnes del metabolisme del glicogen així com altres que no havien estat prèviament descrites, com la genetonina 1 o la ferritina. En aquest experiment també s'identifiquen altres proteïnes que normalment es localitzen en altres compartiments cel·lulars, com el lisosoma o el reticle endoplasmàtic i que es copurifiquen amb el glicogen, reflectint la relació que hi ha entre el glicogen i aquests compartiments cel·lulars.

En situació fisiològica el glicogen es localitza al citoplasma de les cèl·lules, normalment pròxim a estructures membranoses, com el reticle endoplasmàtic en fetge (Cardell et al., 1985) o el reticle sarcoplasmàtic en múscul (Shearer and Graham, 2004). En el cas del glicogen muscular, s'ha postulat que la seva unió al reticle sarcoplasmàtic pugui tenir lloc a través del domini d'unió a membranes de la subunitat reguladora de la proteïna fosfatasa 1 G_M (Tang et al., 1991) o de la proteïna genetonina 1 (Jiang et al., 2010). La genetonina 1, també coneguda com STBD1 (*Starch binding domain-containing protein 1*), permetria la interacció i ancoratge del gra de glicogen a membranes intracel·lulars. Té un domini d'interacció amb la proteïna GABARAPL1 (Jiang et al., 2011), que és membre de la família Atg8 de proteïnes associades a l'autofàgia. Aquesta interacció suggereix que la genetonina 1 podria tenir un paper en la degradació del glicogen per autofàgia, intervenint en el tràfic del glicogen cap als lisosomes. Els pacients amb la malaltia de Pompe, que tenen mutacions en el gen que codifica per la α–glucosidasa lisosomal, presenten acumulació de glicogen dins del lisosoma (Fukuda et al., 2006), fet que reforça la idea que, en condicions normals, el gràNul de glicogen pot ser transportat al lisosoma (Geddes and Stratton, 1977) i ser hidrolitzat per l'α–glucosidasa. L'acumulació de glicogen al lisosoma és perjudicial per a les cèl·lules dels pacients i acaba causant-los la mort.

1.5. Metabolisme del glicogen al cervell

El glicogen està present al sistema nerviós central (SNC) encara que a concentracions molt menors que al fetge o al múscul esquelètic. S'accepta que, a grans trets, el contingut de glicogen en aquests teixits segueix la proporció de 100:10:1 per a fetge/múscul esquelètic/cervell (Nelson et al., 1968). Per aquest motiu, no és sorprenent que s'hagi desestimat un possible paper del glicogen cerebral com a reserva energètica per a l'activitat continuada de l'òrgan i estigui

àmpliament acceptat que el cervell és depenent de la glucosa subministrada per la circulació sistèmica (Brown, 2004). Tot i així, s'ha proposat que el contingut de glicogen del cervell és un recurs energètic de curt termini que juga un paper en el recolzament d'activitats neurals locals i/o específiques com la formació de memòria (Suzuki et al., 2011), l'estimulació sensorial (Brown et al., 2003; Cruz and Dienel, 2002; Swanson et al., 1992) o els cicles del son (Franken et al., 2003; Gip et al., 2002; Kong et al., 2002; Petit et al., 2002; Scharf et al., 2008). A més, el glicogen cerebral es postula com un agent protector en situacions patològiques o d'estrès com la hipoglucèmia (Brown et al., 2003; Herzog et al., 2008; Wender et al., 2000), l'exercici exhaustiu (Matsui et al., 2011), la isquèmia (Brown et al., 2004) i les convulsions (Bernard-Helary et al., 2000; Cloix et al., 2010).

Les molècules de glicogen del SNC es poden reconèixer com a partícules electrodenses d'entre 10 i 30 nm de diàmetre; el pes molecular del glicogen pot arribar fins als 10^8 Daltons (Champe and Harvey, 1994). Tot i que existeix alguna evidència que en l'etapa embrionària el glicogen es pot trobar en teixit neural i glial (Bloom and Fawcett, 1968), en adults, el glicogen del SNC es troba essencialment als astròcits i la majoria de neurones no n'acumulen (Cataldo and Broadwell, 1986; Magistretti et al., 1993b; Wender et al., 2000). Això no implica que el glicogen tingui una preferència regional; ja que els astròcits, on s'acumula, són presents en totes les zones del cervell i són 10 vegades més abundants que les neurones. La major acumulació de glicogen astrocític s'ha descrit en àrees d'alta densitat sinàptica (Koizumi and Shiraishi, 1970a; Koizumi and Shiraishi, 1970b; Koizumi and Shiraishi, 1970c; Phelps, 1972). De fet, el contingut de glicogen dels astròcits està controlat per neurotransmisors, hormones i el nivell energètic local, de manera que està estretament lligat a l'activitat neuronal per una banda i amb la disponibilitat energètica del teixit per l'altra.

Com s'ha comentat anteriorment, els astròcits expressen les isoformes muscular (MGP) i cerebral (BGP) de la glicogen fosforilasa, però no la de fetge (Pfeiffer-Guglielmi et al., 2003). Això suggereix que la GP dels astròcits es troba sota control al·lostèric i respon a l'estat energètic de la cèl·lula, podent alliberar ràpidament metabòlits derivats del glicogen en situacions de demanda energètica (Brown et al., 2003). En particular, sembla ser que la isoforma cerebral requereix AMP per a activar-se completament i que la seva afinitat pel glicogen és menor que la de la isoforma muscular, de manera que és altament sensible a l'estat energètic de la cèl·lula (Pfeiffer-Guglielmi et al., 2003).

Els astròcits tenen el transportador de glucosa GLUT1 (Vannucci et al., 1997) però també expressen receptors d'insulina i el transportador sensible a la insulina GLUT4 (Brown, 2004). Tant la hiperglucèmia (Magistretti et al., 1993) com la insulina (Dringen and Hamprecht, 1992) augmenten el contingut de glicogen en cultius d'astròcits. D'aquest fet se'n pot concloure que els astròcits poden captar glucosa tan de manera depenent com independent d'insulina. En aquesta direcció, s'ha descrit que el contingut de glicogen als astròcits incrementa per acció de glucosa,

IGF I, IGF II, insulina i glutamat (Brown, 2004). El glutamat, un neurotransmisor excitador, augmenta els nivells de glicogen (Hamai et al., 1999), però la seva acció sembla tenir lloc mitjançant l'increment del transport transmembrana de glucosa (Magistretti et al., 1999).

El metabolisme del glicogen cerebral és un clar exemple d'acoblament metabòlic entre les neurones i la glia. La mobilització de les reserves de glicogen dels astròcits pot activar-se mitjançant neurotransmisors i neuromoduladors com la noradrenalina i el pèptid vasoactiu intestinal (VIP) que són alliberats per les neurones actives (Pellegri et al., 1996; Sorg and Magistretti, 1992). Aquestes molècules tenen dos efectes. En primer lloc provoquen una ràpida glicogenòlisi, en la qual els astròcits alliberen lactat que és aprofitat per les neurones com a substrat energètic (Dringen et al., 1993; Magistretti et al., 1993a; Poitry-Yamate et al., 1995). En segon lloc, tenen un efecte més lent però perllongat que causa la resíntesi de glicogen als astròcits. Aquesta resíntesi retardada té lloc mitjançant un mecanisme depenent d'AMPc que causa l'augment de l'expressió de MGS i PTG (Allaman et al., 2000; Pellegri et al., 1996; Sorg and Magistretti, 1992). L'adenosina també causa un increment en el glicogen astrocític mitjançant el mateix mecanisme (Allaman et al., 2003). Els astròcits no expressen glucosa-6-fosfatasa, per tant, no poden generar glucosa lliure a partir del glicogen (Dringen and Hamprecht, 1993; Magistretti et al., 1993a). Per contra, expressen l'enzim lactat deshidrogenasa V, que transforma preferentment el piruvat en lactat i el transportador MCT1 que permet exportar el lactat a l'espai extracel·lular (Koehler-Stec et al., 1998; Morgello et al., 1995; Pierre et al., 2000). Les neurones expressen el transportador MCT2, que permet incorporar el lactat extracel·lular inclús a concentracions molt baixes (Bergersen et al., 2001; Debernardi et al., 2003; Halestrap and Price, 1999; Pierre et al., 2002; Pierre et al., 2000), i l'enzim lactat deshidrogenasa I, que oxida el lactat a piruvat (Bittar et al., 1996) per a ser utilitzat en la oxidació aeròbica (Brown, 2004; Brown et al., 2003). Així doncs, la maquinària metabòlica dels astròcits i les neurones sembla que està adaptada a aquest acoblament energètic en el qual els astròcits transfereixen les seves reserves de glicogen a les neurones en forma de lactat quan la demanda energètica ho requereix. Però cada cop existeixen més evidències que el paper dels astròcits no es limita a aportar energia a les neurones sinó que la seva activitat pot modular o controlar l'activitat cerebral. De fet, s'ha descrit recentment que en resposta a un estat de deshidratació, el lactat alliberat pels astròcits pot controlar l'activitat de les neurones encarregades d'articular la conducta de consum de sal (Shimizu et al., 2007). Aquesta i altres observacions estan canviant la idea d'una funció cerebral estrictament dirigida per les neurones cap a un sistema més integrat, basat en la cooperació entre les neurones i les cèl·lules glials (Belanger et al., 2011).

Encara que les isoformes de GP que s'expressen al cervell es troben predominantment en astròcits i només s'ha descrit la presència de BGP en algunes neurones concretes del cervell (Ignacio et al., 1990; Pfeiffer-Guglielmi et al., 2003), sorprenentment, existeixen evidències que indiquen que la MGS no només s'expressa en astròcits sinó també en neurones (Inoue et al., 1988; Pellegri et al., 1996). Aquest fet suggereix un paper alternatiu de la MGS en aquestes

cèl·lules que no acumulen glicogen en condicions normals. El treball d'aquesta tesi ha estat centrat en intentar aclarir el possible paper de la MGS i del metabolisme del glicogen en neurones i les seves implicacions en situacions neurodegeneratives on s'observen alteracions relacionades amb el seu funcionament.

2. El glicogen en situacions patològiques.

2.1. Malalties d'emmagatzemament de glicogen (*glycogen storage diseases*, GSD).

Les malalties que s'ha identificat que són causades per un defecte en el metabolisme del glicogen s'agrupen en les anomenades malalties d'emmagatzemament del glicogen (*glycogen storage diseases,* GSD) (Ozen, 2007). Són un grup de malalties que es classifiquen segons la deficiència enzimàtica que les provoca i el teixit principalment afectat (Taula 1). La malaltia de Danon (OMIM300257), que és causada per mutacions en el gen *LAMP2* i que causa acumulació de glicogen als lisosomes en els músculs, també és referida, en alguns casos com GSD (GSDIIb en aquest cas) o pseudo-GSD.

Table 1 Various Types of Glycogen Storage Disease Types I-IV

Type	Deficient enzyme	Gene symbol
I (von Gierke)		
Ia	Glucose 6-phophatase	G6PC
Ib	G6P tranlocase (T1)	SLC37A4
Ic	Phophotranslocase (T2)	NPT4(?)
Id	Glucose translocase (T3)	?
II		
Infantile (Pompe disease)	Lysosomal α-glucosidase	*GAA*
Childhood	〃	〃
Juvenile	〃	〃
Adult	〃	〃
III (Cori disease)		
IIIa (Liver & muscle form)	Amylo-1,6-glucosidase	*AGL*
IIIb (liver form)	〃	〃
IIIc (muscle form)	〃	〃
IV (Andersen disease)		
Infantile form	Branching enzyme	GBE1
(Liver)	Branching enzyme	〃
(Neuomuscular)	〃	〃
Juvenile or adult form (Liver, muscle)	〃	〃
Polyglucosan body disease (APBD)	〃	〃

Table 2 Various Types of Glycogen Storage Disease Types V-X and 0

Type	Deficient enzyme	Gene symbol
V (McArdle disease)		
Adult form	Muscle phosphorylase	PYGM
Infantile form	〃	〃
VI (Hers disease)	Liver phosphorylase	PYGL
VII (Tarui disease)		
Severe form	Phosphofructokinase	PFKM
Mild form	〃	〃
Phosphorylase activation system defects		
VIII (VIa/IXA)	Phosphorylase kinase (liver PBK)	
(XLG I/II)	α-subunit of PBK	PHKA2
Autosomal recessive	β subunit of PBK	PHKB
IXB	γ or δ subunit of PBK (?)	PHKG2
IXC	Cardiac muscle PBK	?
IXD (adult form)	Muscle PBK	PHKA1
(Severe muscle form)		PHKA1(?), PHKG1(?)
X (multisystem)	Protein kinase(?)	?
GSD 0	Glycogen synthase (liver)	GYS2
	〃 (muscle)	GYS1

Taula 1. Malalties d'emmagatzemament del glicogen (GSD). (Shin, 2006)

En la majoria dels casos, l'efecte d'aquestes malalties en el sistema nerviós central no s'ha descrit en profunditat degut a que, si existeixen, generalment queden emmascarats per la gravetat dels símptomes dels principals teixits afectats. Tot i així, malgrat que hi ha poques dades al respecte, s'ha descrit acumulació anòmala de glicogen i dany cerebral en la malaltia de Pompe (GSDII) (Burrow et al., 2010; Sidman et al., 2008) que és causada, com es comenta anteriorment, pel dèficit de α–glucosidasa lisosomal. Els casos més clars d'acumulació aberrant de glicogen al cervell són la malaltia d'Andersen (GSDIV, OMIM232500) (Lamperti et al., 2009; Shin, 2006), causada per carències en l'enzim ramificador i la malaltia de cossos de poliglucosà en adults (*adult polyglucosan body disease,* APBD, OMIM263570). Aquesta última es classifica com una forma adulta de GSDIV o com una malaltia independent en funció de si es detecta o no una anomalia en el gen de l'enzim ramificador. Malgrat l'aparent manca de metabolisme del glicogen en neurones, en pacients de GSDIV i APBD, aquestes cèl·lules presenten acumulacions de glicogen insoluble i poc ramificat. Aquests dipòsits, positius per la tinció amb àcid periòdic-base de Schiff (*periodic acid Schiff,* PAS), reben el nom de cossos de poliglucosà (*polyglucosan bodies,* PGBs). Les malalties que causen aquesta acumulació de PGBs sovint reben el nom de PGDs (*polyglucosan body diseases*).

Un altre cas on s'acumulen PGBs en neurones, i per tant de PGD, és la malaltia de Lafora (*Lafora disease,* LD, EPM2, OMIM254780). Malgrat acumular aquesta forma aberrant de glicogen, no ha estat classificada com a GSD perquè inicialment se'n desconeixien les causes genètiques, i un cop descobertes, els gens identificats no pertanyien a cap de les proteïnes conegudes en la ruta clàssica de regulació del glicogen. L'estudi de les PGDs i, en especial, de la LD ha aportat nous coneixements sobre la regulació del glicogen neuronal i conforma el principal objectiu d'aquesta tesi doctoral.

2.2. La malaltia de Lafora (*Lafora disease*, LD).

La malaltia de Lafora (*Lafora disease,* LD, EPM2, OMIM254780) és una patologia neurodegenerativa fatal i la causa més freqüent d'epilèpsia mioclònica progressiva (EPM) al sud d'Europa. Tot i que existeixen casos de LD arreu del món, la seva prevalença varia en funció de la regió, essent més freqüent en àrees geogràficament aïllades o amb un alt grau d'endogàmia. En els països occidentals, s'estima que la prevalença de la LD està per sota de 1/1.000.000, fet que li dóna el caràcter de malaltia rara (ORPHA501). Les característiques de la malaltia, que la defineixen com a EPM, són mioclònia (sacsejades musculars sobtades), crisis tònico-clòniques (possiblement el símptoma epilèptic més conegut per la societat, anomenat durant molts anys "Gran Mal") i disfunció neurològica progressiva.

La LD va ser descrita el 1911 pel científic espanyol Gonzalo Rodríguez Lafora, deixeble de Aloysius Alzheimer i de Santiago Ramón y Cajal. El Dr. Rodríguez Lafora va descriure per primer cop la presència d'estructures esfèriques en el cervell de pacients amb epilèpsia mioclònica i

demència que havien debutat en la malaltia abans dels 19 anys (Lafora and Glueck, 1911). Aquestes estructures, que s'han anomenat cossos de Lafora (*Lafora bodies,* LBs), són el tret distintiu de la LD i des de llavors es fan servir per diferenciar aquesta malaltia d'altres tipus de EPM. Els LBs són dipòsits positius per la tinció PAS, formats principalment per glicogen poc ramificat (Sakai et al., 1970; Yokoi, 1967; Yokoi et al., 1967; Yokoi et al., 1968; Yokoi et al., 1975), és a dir, PGBs, que es troben en el soma, axons i dendrites de les neurones (Cavanagh, 1999). Tot i que en primera instància, el Dr. Rodríguez Lafora suggeria la presència d'aquests cossos també en cèl·lules glials (Lafora, 1913; Lafora and Glueck, 1911), aquest fet va ser motiu de controvèrsia entre els científics de l'època i l'observació no ha estat confirmada.

La LD s'hereta de manera autosòmica recessiva i s'ha associat a mutacions en dos gens, *EPM2A* i *EPM2B*, que no es van identificar fins més de 80 anys després del treball inicial del Dr. Rodríguez Lafora. El gen *EPM2A* codifica per laforina, una fosfatasa d'especificitat dual amb un domini d'unió a carbohidrats. El gen *EPM2B* (*NHLRC1*) codifica per malina, una E3 ubiqüitina lligasa. Malgrat l'identificació del gens involucrats en la malaltia, el paper d'aquestes proteïnes en la formació dels LBs i la patogènesi de la LD continua sense estar clar.

2.2.1. Manifestacions clíniques de la malaltia de Lafora

La malaltia de Lafora s'inicia, en la majoria dels casos, entre els 10 i els 17 anys d'edat, típicament amb crisis generalitzades tònico-clòniques o crisis visuals que s'acostumen a descriure com visió de punts de llum o estrelles (Acharya et al., 1995; Minassian, 2001; Minassian et al., 2000). Posteriorment es presenten les mioclònies, un tret característic de la malaltia, que poden ser generalitzades o localitzades. Les mioclònies localitzades afecten típicament a les extremitats superiors i a la musculatura facial peribucal i periorbital. La mioclònia té lloc durant el repòs i s'exagera per l'excitació, l'acció o l'estimulació lumínica i, generalment, desapareix amb el son. Les mioclònies massives es succeeixen en forma de convulsions generalitzades durant les quals es conserva la consciència de manera parcial. La mioclònia és el primer motiu de dependència de cadira de rodes, abans que aparegui qualsevol dèficit motor. Una altra de les característiques fonamentals de la malaltia són les convulsions occipitals que, amb molta freqüència, es presenten amb ceguesa transitòria, al·lucinacions visuals, convulsions fotomioclòniques o fotoconvulsives (Roger et al., 1967; Roger et al., 1983).

Un cop iniciada, la malaltia té una taxa variable d'empitjorament clínic, el qual depèn de la severitat de l'epilèpsia. Les convulsions i la mioclònia responen temporalment al tractament, però gradualment arriben a ser refractaris. La freqüència de les convulsions generalitzades és també variable, però tots els pacients pateixen mioclònies quasi continues durant les hores en que no dormen.

Poc després del començament de les crisis i les mioclònies apareix una demència ràpidament progressiva. Altres manifestacions neurològiques que tenen lloc durant el curs de la malaltia són neuropatia i miopatia perifèriques i ataxia (Ganesh et al., 2002b). A mesura que la malaltia va avançant, la majoria de pacients acaben presentant mioclònies continues i evolucionen cap a un estat vegetatiu terminal en el que han de ser alimentats per sonda. Degut a les convulsions, els pacients que no són alimentats per sonda pateixen aspiracions freqüentment i és comú que morin degut a una pneumònia per bronco-aspiració (Minassian, 2002). La majoria dels malalts moren abans de 10 anys del començament de la malaltia (Minassian, 2001; Minassian et al., 2000).

Els símptomes clínics són precedits per anomalies en l'electroencefalograma i possibles problemes d'aprenentatge, com es desprèn de l'observació dels germans petits dels casos confirmats (Minassian, 2001; Minassian et al., 2000).

2.2.2. Patologia de la malaltia de Lafora

Els malalts de Lafora, com ja s'ha dit anteriorment, pateixen un procés sever de neurodegeneració progressiva. En l'autòpsia d'aquests pacients, s'observa una clara pèrdua de neurones sense desmielinització ni inflamació aparents. Totes les regions del sistema nerviós central pateixen aquest procés de neurodegeneració encara que en graus diferents. Algunes de les regions més afectades són els còrtex cerebral i cerebelar, l'hipocamp, els nuclis del cerebel, els ganglis basals, i el tàlam. A més, també s'ha observat neurodegeneració a la retina (Carpenter et al., 1974; Janeway et al., 1967; Neville et al., 1974; Schwarz and Yanoff, 1965). En biòpsies de cervell de pacients, només s'observa una pèrdua neuronal petita en les fases més primerenques de la malaltia malgrat que ja presenten una simptomatologia clínica important, principalment en forma d'atacs epilèptics (Busard et al., 1987; Carpenter et al., 1974). Aquestes observacions indiquen que hi ha factors addicionals previs a la pèrdua de neurones que estan probablement implicats en greu epilèpsia de la malaltia de Lafora.

2.2.3. Els Cossos de Lafora (LBs)

Els cossos de Lafora (*Lafora Bodies,* LBs) són PGBs, és a dir, són dipòsits insolubles formats principalment per poliglucosà. A més d'aquest contingut en polisacàrid (que reacciona amb la tinció PAS), contenen al voltant de l'1,5% de fosfat i aproximadament un 6% de proteïna (Cavanagh, 1999; Sakai et al., 1969; Sakai et al., 1970; Yokoi, 1967; Yokoi et al., 1967; Yokoi et al., 1968; Yokoi et al., 1975). Després del descobriment, per part del Dr. Rodríguez Lafora, d'aquests cossos d'inclusió en neurones de pacients amb epilèpsia mioclònica, els LBs també s'han trobat en altres teixits com fetge, múscul esquelètic, cor, retina i pell, essent més abundants en cervell, cor i múscul esquelètic (Acharya et al., 1995; Berkovic et al., 1993; Busard et al., 1986; Busard et

al., 1987; Cavanagh, 1999; Drury et al., 1993; Harriman et al., 1955; Kobayashi et al., 1990; Minassian et al., 2000; Roger et al., 1967; Roger et al., 1983).

En el cervell, la mida dels LBs oscil·la entre 3 i 40 μm i tenen el nucli més dens que la perifèria. Els dipòsits més grans es troben generalment al soma de neurones i poden ocupar tot el citoplasma. Els cossos més petits són majoritaris i s'atribueixen a les dendrites. La presència de LBs en axons és infreqüent i, com s'ha comentat, no s'ha confirmat que altres tipus cel·lulars del cervell puguin presentar-ne (Cavanagh, 1999).

La GS és l'únic enzim capaç de sintetitzar cadenes llargues de glucosa en mamífers. El fet que els LBs estiguin formats principalment per poliglucosà, que pot ser considerat un glicogen poc ramificat, suggeria que, així com la resta de PGBs, podien originar-se per un defecte en el metabolisme del glicogen (Berkovic et al., 1993; Busard et al., 1986; Busard et al., 1987; Cavanagh, 1999; Collins et al., 1968; Drury et al., 1993; Kobayashi et al., 1990; Minassian, 2001; Minassian et al., 2000; Nikaido et al., 1971; Nishimura et al., 1980; Robitaille et al., 1980; Roger et al., 1967; Roger et al., 1983; Sakai et al., 1970; Toga et al., 1968).

2.2.4. Origen genètic de la malaltia de Lafora

Com s'ha comentat a l'inici del capítol, la malaltia de Lafora (LD) s'hereta de manera autosòmica recessiva. Fins ara s'han identificat dos gens, *EPM2A* i *EPM2B*, la mutació dels quals causa la malaltia. Tot i així, s'ha suggerit que com a mínim un tercer gen, encara desconegut, pot ser responsable de la malaltia en aproximadament un 20% de pacients de Lafora per als quals no s'ha identificat cap mutació en el gens coneguts. S'ha identificat un àmplia varietat de mutacions tan en *EPM2A* com en *EPM2B* (Figura 4 i 5).

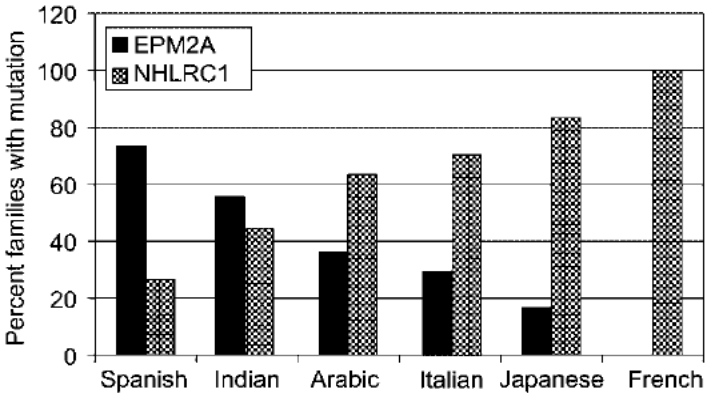

Figura3. Percentatge de famílies afectades per mutacions en *EPM2A* i *EPM2B* (*NHLRC1*). (Singh and Ganesh, 2009)

Cadascuna d'elles té una forta relació amb l'origen de la família afectada, fet que produeix una alta heterogeneïtat respecte el percentatge de pacients afectats d'un o altre gen en cada país. Pel que fa a l'estat espanyol, les mutacions a *EPM2A* causen aproximadament el 75% dels malalts

amb mutació coneguda, mentre que les mutacions en *EPM2B* causen el 25% restant (Figura 3) (Chan et al., 2004b; Singh and Ganesh, 2009).

Malgrat aquesta heterogeneïtat genètica, els pacients amb mutacions en qualsevol del dos gens presenten manifestacions clíniques indistingibles (Ganesh et al., 2006; Minassian et al., 1999).

2.2.4.1. *EPM2A* (laforina)

EPM2A (*epilepsy of progressive myoclonus type 2 gene A*) va ser el primer gen identificat i caracteritzat com a responsable de la malaltia de Lafora i es localitza en la regió cromosòmica 6q24 (Ganesh et al., 2000; Minassian et al., 1998; Sainz et al., 1997; Serratosa et al., 1995; Serratosa et al., 1999). El gen *EPM2A* està format per 4 exons i codifica per una proteïna de 331 aminoàcids, anomenada laforina, que conté un domini fosfatasa d'especificitat dual (DSPD) a l'extrem C-terminal (Ganesh et al., 2000; Wang et al., 2002) i un domini d'unió a carbohidrats (CBD) en l'N-terminal que promou la seva unió al glicogen (Figura 4) (Ganesh et al., 2001; Ganesh et al., 2002b; Minassian et al., 2000; Wang et al., 2002). Els dos dominis també es troben en els gens ortòlegs de rata i ratolí, fet que suggereix la seva conservació funcional en mamífers (Ganesh et al., 2001).

Al començament d'aquesta tesi, es coneixia poc sobre el paper de la laforina en el metabolisme del glicogen, de les seves proteïnes associades o substrats i de la seva implicació en el procés neuropatològic de la malaltia de Lafora. A més de la seva unió al glicogen, es va demostrar mitjançant assajos de doble híbrid que la laforina interaccionava amb ella mateixa i amb PTG (Fernandez-Sanchez et al., 2003). També es va observar que la laforina colocalitzava amb la GS (Chan et al., 2004a; Ganesh et al., 2004; Minassian, 2001). Aquestes dades situaven la laforina en el context d'un complex multiproteic associat a les partícules de glicogen juntament amb altres proteïnes clàssiques del metabolisme d'aquest polisacàrid.

La laforina s'uneix als PGBs amb major afinitat que al glicogen (Ganesh et al., 2004). Això feia pensar en un mecanisme de control en el qual la laforina podria unir-se al poliglucosà i, per mitjà del seu domini fosfatasa, aturar la seva formació o promoure la seva degradació. El paper de l'activitat fosfatasa de la laforina en l'etiopatologia de la LD ha estat àmpliament debatuda durant aquests anys. S'ha proposat que la laforina desfosforila, i per tant activa, la glycogen sintasa quinasa 3 (GSK3) (Lohi et al., 2005). L'activació de GSK3 inhibeix la síntesi de glicogen per fosforilació de la GS. També s'ha descrit que la laforina allibera el fosfat incorporat al glicogen durant la seva síntesi com a conseqüència d'errors catalítics de la GS (Tagliabracci et al., 2008; Tagliabracci et al., 2011; Tagliabracci et al., 2007; Worby et al., 2006). L'activitat fosfatasa de la laforina i la seva disfunció poden tenir un paper important en l'origen de la formació dels LBs. Per tant, mutacions en la laforina causarien la sobreactivació de la síntesi de glicogen i un increment del seu contingut en fosfat, fets que podrien alterar la seva estructura fent-la més

propícia per a la formació de LBs. Tot i així, aquestes hipòtesis no poden explicar com les mutacions en malina causen la malaltia.

Els ratolins deficients en laforina (laforina KO) presenten degeneració de les cèl·lules nervioses abans que els LBs siguin detectables. Això suggereix que la LD podria ser un trastorn neurodegeneratiu primari i que els LBs no juguen un paper central en l'epileptogènesi (Ganesh et al., 2002a). En aquests estadis primerencs, no es detecten LBs en algunes de les neurones que estan degenerant i no totes les que contenen inclusions degeneren, pel que la formació de LBs podria no ser necessària per a la neurodegeneració inicial. De totes maneres, no es pot descartar un paper causal d'aquests cossos en la disfunció neuronal ja que podrien induir estrès neuronal o ser neurotòxics. A mesura que la malaltia avança, la formació de LBs augmenta en les neurones d'aquests ratolins. És important destacar que els pacients amb APBD tenen inclusions molt similars als LBs però no presenten epilèpsia ni mioclònies (Robitaille et al., 1980). En canvi, desenvolupen de forma progressiva dèficits motors i sensorials i demència, símptomes que s'observen en pacients de la LD i que també estan associats al procés normal d'envelliment (Cavanagh, 1999). Totes aquestes observacions podrien relacionar l'acumulació de PGBs en cervell amb el desenvolupament d'aquests símptomes (Ganesh et al., 2004).

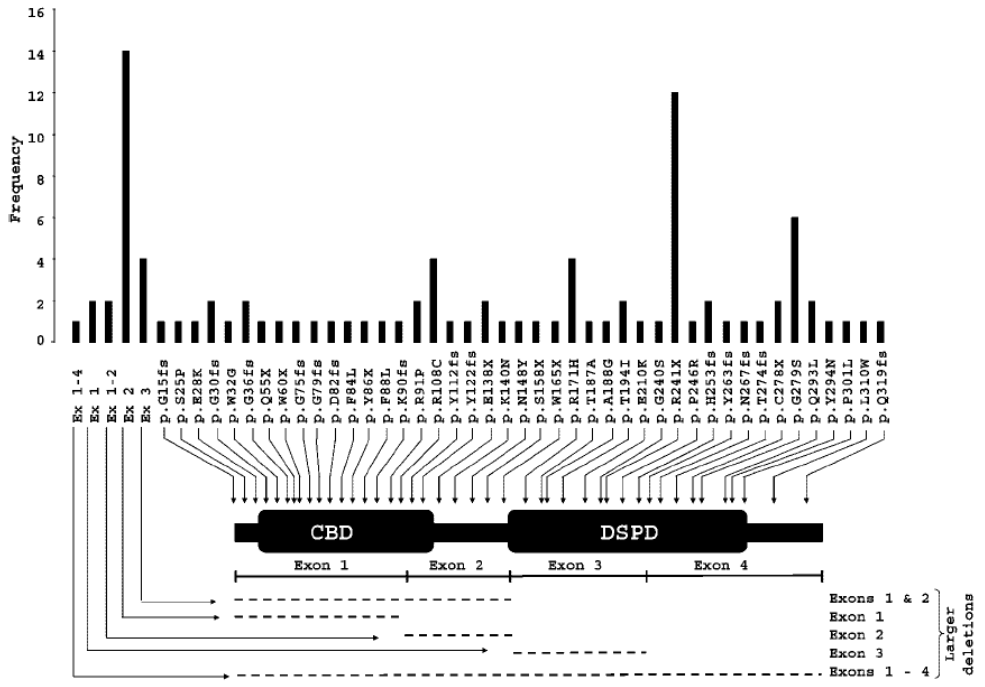

Figura 4. Representació de les mutacions descrites en el gen *EPM2A*
(Singh and Ganesh, 2009)

L'anàlisi de les mutacions del gen *EPM2A* en els malalts de Lafora ha identificat, fins l'any 2009, 48 mutacions diferents i diversos polimorfismes. Això inclou mutacions puntuals (de canvi d'aminoàcid o sense sentit, a codó stop), delecions i insercions (Figura 4) (Singh and Ganesh,

2009). S'assumeix que la major part de les mutacions originen una falta de laforina (mutacions sense sentit i insercions) o donen lloc a una laforina que ha perdut la seva capacitat d'unió al glicogen o la seva activitat fosfatasa (Fernandez-Sanchez et al., 2003; Ganesh et al., 2004; Ianzano et al., 2004; Wang et al., 2002). Una excepció és la mutació G240S, que manté l'activitat fosfatasa i s'uneix al glicogen però la seva interacció amb PTG està dràsticament reduïda (Fernandez-Sanchez et al., 2003).

2.2.4.2. *EPM2B* (malina)

El segon gen identificat associat a la LD va ser el *NHLRC1* (*NHL repeat containing 1*), més tard anomenat *EPM2B* (*epilepsy of progressive myoclonus type 2 gene B*), mapejat en la regió cromosòmica 6p22.3. El gen *EPM2B* té un sol exó i codifica per una proteïna de 395 aminoàcids denominada malina (Figura 5) (Chan et al., 2003a; Chan et al., 2003b). Aquesta proteïna té un domini de dits de zinc del tipus RING-HC i sis dominis NHL repetits d'interacció proteïna-proteïna (Freemont, 2000). La presència de dits de zinc RING és característica d'una classe de E3 ubiqüitina lligases (Freemont, 2000; Pickart, 2001). L'acció més coneguda que té lloc a través ubiqüitinilació de proteïnes és la degradació proteasomal, que requereix la unió d'una cadena de poliubiqüitines. Però en molt poc temps s'ha demostrat que la modificació post-traduccional per unió covalent de petites proteïnes com la ubiqüitina pot regular una àmplia varietat de processos com són canvis d'activitat, capacitat d'interacció o de localització cel·lular de les proteïnes modificades (Pickart, 2001; Sun and Chen, 2004; Weissman et al., 2011). Posteriorment a la seqüenciació del gen, l'activitat E3 ubiqüitina lligasa de malina va ser confirmada en diversos treballs (Gentry et al., 2005; Lohi et al., 2005).

Un dels descobriments clau per a entendre les causes de la malaltia de Lafora és el fet que els dominis NHL de la malina li permeten interaccionar i ubiqüitinilar la laforina, estimulant la seva degradació (Gentry et al., 2005). Aquests resultats no només mostraven, per primer cop, una relació directa entre les dues proteïnes alterades en la malaltia, sinó que a més situaven a la malina formant part d'un complex multiproteic amb laforina associat al gränul de glicogen. Aquest va ser el punt de partida del treball del Dr. Vílchez (Vilchez et al., 2007), en el qual vaig col·laborar i consisteix el primer article d'aquesta tesi (**Article 1**). Els resultats d'aquest treball, com es veurà més endavant, van revelar aspectes importants del mecanisme d'acció de laforina i malina i les conseqüències de la seva deficiència en el procés neurodegeneratiu de la LD. Els resultats que se'n desprenen representen la base de la resta del meu projecte doctoral.

En aquest punt, tal i com s'ha comentat anteriorment, ja existien nombroses dades sobre el model animal que recapitula el dèficit genètic de laforina (els ratolins laforina KO) (Ganesh et al., 2002a). Tot i això, moltes de les conclusions extretes de l'estudi d'aquest model no permetien explicar com les mutacions en malina causen la malaltia de Lafora. Per aquest motiu, i per tal d'analitzar *in vivo* les conclusions obtinguts en models cel·lulars en l'Article1, vam analitzar el

metabolisme del glicogen, la formació de LBs i el progrés neurològic de ratolins deficients en malina (malina KO) en un treball que va suposar gran part del meu projecte doctoral i que s'inclou com a segon article d'aquesta tesi (**Article 2**).

Al 2009 s'havien identificat 51 mutacions i diversos polimorfismes en el gen *EPM2B* (Figura 5). L'anàlisi de la relació genotip-fenotip de les mutacions en *EPM2B* mostra que pràcticament totes les mutacions resulten en la pèrdua de funció de malina (Chan et al., 2003b; Gomez-Abad et al., 2005; Singh and Ganesh, 2009). Les mutacions que afecten el domini RING bloquegen l'activitat ubiqüitina lligasa de la malina mentre que les mutacions en els dominis NHL interrompen la seva interacció amb la laforina. Per tant, les dues alteracions bloquegen la capacitat de malina d'ubiqüitinilar la laforina (Gentry et al., 2005).

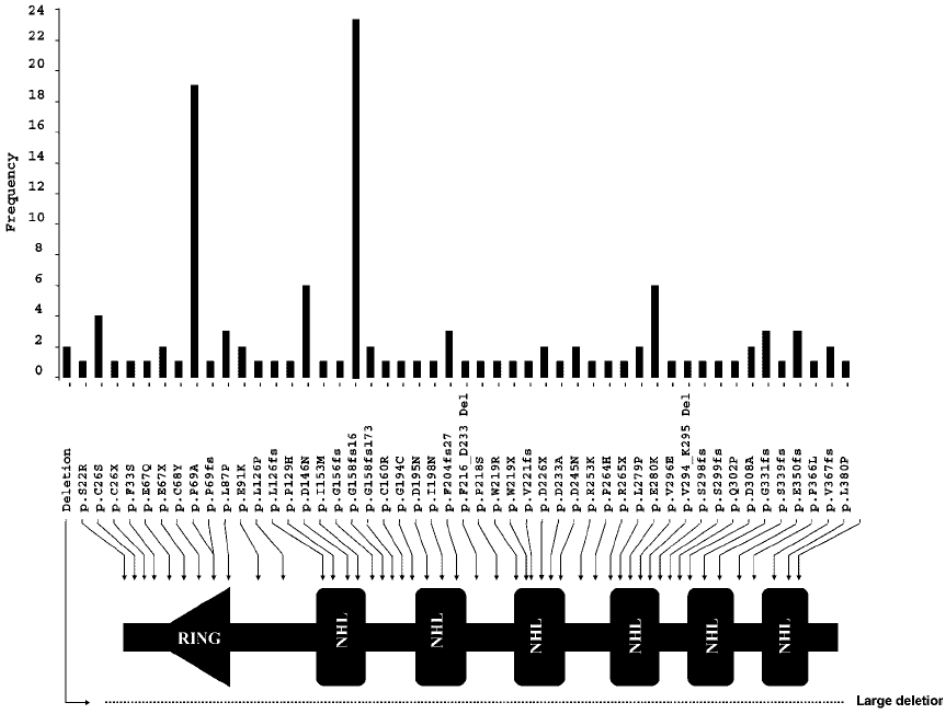

Figura 5. Representació de les mutacions descrites en el gen *EPM2B*
(Singh and Ganesh, 2009)

2.3. Corpora amylacea (CA)

Tal i com es comenta en els capítols anteriors, la formació de PGBs en el cervell s'ha associat a diferents tipus de malalties neurològiques amb símptomes clínics diversos. De fet, en moltes d'aquestes situacions patològiques, com la malaltia de Lafora, és encara motiu de discussió si l'acumulació d'aquests cossos d'inclusió és una de les causes o una conseqüència del dany de les cèl·lules del sistema nerviós central (SNC) (Cavanagh, 1999; Ganesh et al., 2004).

Un aspecte del SNC interessant per l'estudi d'aquesta relació entre la disfunció neuronal i la formació de PGBs són els cossos amilacis o Corpora Amylacea (CA). Els CA són PGBs que es troben al cervell d'humans i altres mamífers sans en edats avançades. Com a PGB, a més de poliglucosà, els CA contenen al voltant d'un 3% de fosfat i aproximadament un 4% de proteïnes (Sakai et al., 1969), algunes d'elles relacionades amb estrès cel·lular com l'ubiqüitina i les *heat shock proteins* (HSP) (Cisse et al., 1993; Martin et al., 1991). Aquestes inclusions associades a l'envelliment, que van ser descrites per primer cop per J.E. Purkinje el 1837, han estat àmpliament caracteritzades i ressenyades de manera exhaustiva (Cavanagh, 1999). Malgrat això, el tipus cel·lular on s'originen i, especialment, la causa o la funció de la formació dels CA encara no està clara. A més, encara que els CA són presents en tots el mamífers, les seves propietats i la localització a les diferents zones del cervell varia entre espècies.

Durant aquests darrers anys, s'ha realitzat un important esforç de recerca sobre els gens implicats en la malaltia de Lafora. Fruit d'aquest treball, diversos grups han suggerit que laforina i malina estan implicats en sistemes cel·lulars degradatius com les rutes endosoma-lisosomal o l'autofàgia (Aguado et al., 2010; Criado et al., 2011; Knecht et al., 2010; Puri and Ganesh, 2010; Puri et al., 2011) i en l'eliminació de proteïnes mal plegades a través del sistema ubiqüitina-proteasoma (Delgado-Escueta, 2007; Garyali et al., 2009; Rao et al., 2010a; Rao et al., 2010b). A més, s'ha proposat que aquestes activitats de laforina i malina protegeixen contra l'estrès de reticle endoplasmàtic (Liu et al., 2009; Vernia et al., 2009) i contra l'estrès tèrmic (Sengupta et al., 2011). Totes aquestes evidències fan que sigui interessant investigar si el metabolisme del glicogen, a més del seu paper com a reserva energètica, pot estar relacionat amb aquestes rutes cel·lulars degradatives.

En aquesta direcció, resulta interessant que l'acumulació de CA es vegi incrementada per diferents causes d'estrès com l'anòxia (Abe and Yagishita, 1995) i la isquèmia (Botez and Rami, 2001) o per situacions neuropatològiques com epilèpsies (Das et al., 2011; Erdamar et al., 2000; Loiseau et al., 1992; Loiseau et al., 1993; Radhakrishnan et al., 2007), esquizofrènia, síndrome de Down, malaltia d'Alzheimer (Cavanagh, 1999; Cisse et al., 1993; Fleming et al., 1986; Nishi et al., 2003; Nishimura et al., 2000; Singhrao et al., 1993) i altres condicions neurodegeneratives (Kosaka et al., 1981; Nishi et al., 2003; Robitaille et al., 1980). Aquestes observacions suggereixen més una relació entre la formació de CA i l'estrès o la mort cel·lular que no pas amb una alteració en la maquinària del metabolisme del glicogen.

Malgrat que la formació de CA en individuus sans és depenent de l'edat, la seva aparició és altament heterogènia fins i tot entre individuus de la mateixa espècie (Cavanagh, 1999). Per aquest motiu, l'estudi dels CA i la seva comparació amb els altres PGBs resulta complexa. Amb l'objectiu de minimitzar aquesta heterogeneïtat, vam establir aquesta comparació entre ratolins del mateix fons genètic, i envellits junts sota les mateixes condicions, en el treball que suposa el tercer article d'aquesta tesi (**Article 3**). En aquest treball, encara pendent de publicació, es

comparen les característiques dels CA que s'acumulen durant el procés normal d'envelliment amb els LBs presents en el nostre model de LD, els ratolins malina KO, els quals van mostrar acumulació de MGS en aquests cossos de poliglucosà (DePaoli-Roach et al., 2010); **Article 2**). A més a més, per tal d'avaluar el paper de la MGS en la formació dels CA, es van generar ratolins deficients en MGS (MGS KO). En aquest darrer treball es mostra que la matriu de poliglucosà sintetitzada per la MGS és necessària per a la formació de CA durant l'envelliment, i s'assenyala la semblança remarcable entre CA i LB, i les possibles implicacions d'aquestes observacions.

OBJECTIUS

OBJECTIUS

El glicogen del cervell sembla estar confinat en els astròcits. Tot i això, s'ha observat l'acumulació a les neurones de formes anòmales de glicogen, els poliglucosans, en diverses patologies neurodegeneratives i també en el procés d'envelliment natural. La nostra hipòtesi de treball és que les neurones tenen la maquinària per sintetitzar glicogen i que la pèrdua de control sobre aquesta maquinària genera una acumulació de glicogen que és nociva per a aquestes cèl·lules. Basant-nos en aquesta hipòtesi, volem investigar quin paper juguen els gens alterats en la malaltia de Lafora sobre el metabolisme del glicogen, i també quina és la funció fisiològica que justifica la presència de la maquinària metabòlica del glicogen en les neurones. Els objectius concrets per aquest treball són:

1) Caracterització de l'expressió de les proteïnes relacionades amb el metabolisme del glicogen en els diferents tipus cel·lulars del cervell.

2) Anàlisi de la funció dels gens mutats en la malaltia de Lafora sobre la regulació del metabolisme del glicogen i el seu paper en la formació de cossos de Lafora (LBs) en neurones.

3) Estudi de les conseqüències de l'acumulació de cossos de poliglucosà sobre la funció cerebral mitjançant la generació i anàlisi de models cel·lulars o animals de la malaltia de Lafora.

4) Caracterització dels mecanismes cel·lulars implicats en la formació de cossos de poliglucosà a la malaltia de Lafora (LBs) i durant de l'envelliment normal del cervell (Corpora Amylacea, CA).

5) Estudi del paper del metabolisme del glicogen en la formació de CA. Anàlisi de l'envelliment cerebral en models animals amb depleció o sobreexpressió de la glicogen sintasa.

RESUM DELS ARTICLES

Article 1.

Mecanisme supressor de la síntesi de glicogen en neurones i la seva desaparició en l'epilèpsia mioclònica progressiva.

Vilchez D, Ros S, Cifuentes D, Pujadas L, Vallès J, García-Fojeda B, Criado-García O, Fernández-Sánchez E, Medraño-Fernández I, Domínguez J, García-Rocha M, Soriano E, Rodríguez de Córdoba S, Guinovart JJ.

1. Les neurones tenen la maquinària necessària per a la síntesi de glicogen, però la mantenen inactiva.

L'anàlisi de cervell sencer de ratolí, cultiu primari de les seves neurones i de cèl·lules Neuro2a (N2a, procedents de neuroblastoma de ratolí) va mostrar que les neurones, igual que els astròcits, expressaven l'isoforma muscular de la GS (MGS) i no la isoforma hepàtica (LGS) (**Figura 1a,b**). A més, en contraposició amb els astròcits, les neurones no expressaven nivells detectables de GP, l'enzim responsable de la degradació del glicogen (**Figura 1b**). De totes maneres, malgrat expressar la MGS, ni les neurones ni les cèl·lules N2a acumulaven quantitats detectables d'aquest polisacàrid encara que fossin cultivades en un medi ric en glucosa (30mM) (**Figura 1c**). En canvi, els astròcits crescuts sota les mateixes condicions sí que presentaven una acumulació clara de glicogen (**Figura 1c**).

La incapacitat de les neurones per a sintetitzar glicogen podria ser deguda a una concentració de glucosa-6-fosfat (G6P) insuficient per a l'activació de la MGS, o a una quantitat insuficient de la pròpia MGS en aquest tipus cel·lular. Per avaluar aquestes possibilitats es va incrementar 5 cops la concentració de G6P intracel·lular mitjançant la sobreexpressió de glucoquinasa (GK) o d'hexoquinasa I (HK I) (**Figura 2a**). De la mateixa manera, mitjançant adenovirus recombinants, es va sobreexpressar la MGS en cultius primaris de neurones (**Figura 2b,c**). Cap de les dues estratègies va suposar una activació de la glicogen sintasa o una acumulació de glicogen, indicant que la manca de glicogen en aquest tipus cel·lular no és deguda a nivells de baixos de MGS o G6P. Es van obtenir resultats similars amb cèl·lules N2a (**Figura suplementària 1**). La MGS expressada en neurones es localitzava principalment en el nucli, fet característic de cèl·lules deplecionades de glicogen (**Figura 2c superior**). En canvi, la MGS en els astròcits s'agrupava al citoplasma, que és la localització típica per aquesta proteïna sota condicions de síntesi activa de glicogen (**Figura 2c inferior**). A més del control al·lostèric a través de G6P, el control de la síntesi de glicogen té lloc mitjançant la inactivació de la MGS per la fosforilació de múltiples serines dels extrems C i N terminals que efectuen diverses quinases. Els residus Ser640 i Ser7/10, que són els llocs de fosforilació que més redueixen l'activitat de l'enzim, es van trobar fosforilats en neurones i N2a (**Figura 2d i Figura suplementària 1**). Malgrat això, la Ser640 podia ser desfosforilada tractant les neurones amb 20 mM LiCl (**Figura 2e**), un inhibidor de la glicogen sintasa quinasa 3 (GSK3). Paral·lelament, la MGS desfosforilada canviava la seva localització subcel·lular i s'agrupava al citoplasma, coincidint amb el creixement de partícules de glicogen (**Figura 2c mig i**

Figura suplementària 1). La incubació de cultius primaris de neurones amb concentracions terapèutiques de LiCl (1-2 mM) durant 48 h no va produir cap canvi substancial en la MGS.

Es va induir una major desfosforilació de les serines 7, 10 i 640 en cultius primaris de neurones i en cèl·lules N2a mitjançant l'expressió de PTG (**Figura 3a i Figura suplementària 1**), una subunitat reguladora de PP1 que promou l'activació de MGS i interacciona amb la laforina. Aquesta desfosforilació va anar acompanyada per un marcat increment de l'acumulació de glicogen al llarg del soma, les dendrites i els axons (**Figura 3b,c i Figura suplementària 1**). Igual que el LiCl, la PTG induïa la relocalització de la MGS, que s'agrupava al citoplasma, colocalitzant amb les partícules de glicogen. L'activació de la MGS incrementava en les neurones que sobreexpressaven PTG, assolint valors propers als corresponents a l'estat màxim d'activació (**Figura 3b i Figura suplementària 1**) i l'enzim mostrava una mobilitat electroforètica augmentada, que és característica de l'enzim activat (desfosforilat) (**Figura 3a i Figura suplementària 1**). En conjunt, aquests resultats mostraven que les neurones tenen la maquinària apropiada per sintetitzar glicogen, però que aquest sistema està bloquejat, essencialment, mantenint la MGS en un estat fosforilat i, per tant, inactiu. En aquest context, és interessant indicar que la PTG gairebé no s'expressa en neurones. La relació transcripcional PTG/MGS era aproximadament 20 vegades menor en neurones que en altres cèl·lules que normalment acumulen glicogen. (**Figura 3d**). Com que els cossos de Lafora contenen polímers de glucosa poc ramificats, vam analitzar el grau de ramificació del glicogen dels experiments anteriors mitjançant el seu espectre d'absorció en presència de iode, en el qual un desplaçament cap a longituds d'ona majors indica una menor ramificació. El glicogen normal produïa un pic a 483 nm, mentre que l'aïllat de N2a o de neurones en cultiu s'enregistrava a 511 nm, indicant que aquest també era poc ramificat.

2. L'acumulació de glicogen és pro-apoptòtica en cèl·lules neuronals.

Per a determinar si l'acumulació d'aquest glicogen poc ramificat causa alteracions en cèl·lules neuronals, vàrem examinar si hi havia marcadors d'apoptosi en els cultius neuronals que havien estat forçats a acumular glicogen per sobreexpressió de PTG. Els cultius de neurones que acumulaven glicogen van mostrar un increment en l'apoptosi, comparats amb els controls, mitjançant els assajos de TUNEL (**Figura 4a**) i de caspasa-3 activa (**Figura 4b,c**). En canvi, astròcits que expressaven la mateixa quantitat de PTG, i per tant que sintetitzaven alts nivells de glicogen, no van mostrar activació de caspasa-3 (**Figura 4c**). Per tant, es podia concloure que l'acumulació de glicogen causa apoptosi específicament en les neurones.

3. El complex laforina-malina disminueix l'acumulació de glicogen.

Amb l'objectiu de determinar el paper de la laforina i la malina en la generació dels cossos de Lafora, vam analitzar si aquestes proteïnes tenien la capacitat de modular l'acumulació de

glicogen induïda per PTG en cèl·lules neuronals. Quan laforina o malina, per separat, es van coexpressar amb PTG en aquestes cèl·lules, no es va observar cap efecte sobre l'acumulació de glicogen induïda per aquesta última. Però quan laforina i malina, conjuntament, es van coexpressar amb PTG, l'activació de la síntesi de glicogen es bloquejava completament (**Figura 5a i Figura suplementària 2**). A més, es va detectar una clara reducció en els nivells de MGS i PTG. Els nivells de laforina també es van veure disminuïts, encara que en menor mesura (**Figura 5b i Figura suplementària 2**). En contraposició, la quantitat de malina incrementava quan es coexpressava amb laforina, suggerint que la malina era estabilitzada per la laforina. Per tant, els nivells de malina correlacionaven inversament amb els de PTG, MGS i laforina (**Figura 5b**). La reducció dels nivells de MGS correlacionava amb un decrement de sis vegades en l'activitat glicogen sintasa en les neurones que coexpressaven laforina i malina conjuntament, en comparació amb aquelles que expressaven només laforina.

Els inhibidors de proteasoma MG-132 i lactacistina bloquejaven el decrement en els nivells de MGS, PTG i laforina induïts pel complex laforina-malina (**Figura 5d i Figura suplementària 2**) i l'anàlisi per RT-PCR va confirmar que els nivells de trànscrits de MGS, PTG i laforina no estaven modificats, indicant que els canvis en els nivells de proteïna de MGS i PTG eren deguts a la seva degradació a través del sistema ubiqüitina-proteasoma i no pas per alteracions a nivell transcripcional. Aquestes dades suggerien que el complex laforina-malina és important per a la modulació dels nivells de MGS i PTG. D'aquesta manera, quan els nivells de laforina o malina baixessin, no es formarien complexos laforina-malina, i per tant no hi hauria degradació de MGS i PTG. A més, la quantitat de malina en absència de laforina era major quan s'inhibia el proteasoma. Aquesta observació suggereix que la malina també és degradada via ubiqüitina-proteasoma. (**Figura 5d**). En una cerca entre els pacients de la malaltia de Lafora, es va identificar la mutació de malina D146N, que afectava a la interacció entre laforina i malina sense alterar la seva l'activitat E3 ubiqüitina lligasa. És destacable que la malina D146N coexpressada conjuntament amb laforina (**Figura 6a**) no impedia l'acumulació de glicogen induïda per PTG i, al contrari que la malina salvatge, no induïda la degradació de MGS i PTG (**Figura 6b**). Per tant, la interacció entre malina i laforina és clau per l'acció d'aquestes dues proteïnes en el metabolisme del glicogen.

Si la laforina i la malina són necessàries per reduir els nivells de MGS i PTG, l'absència d'aquestes proteïnes en individus amb la malaltia de Lafora hauria de suposar un increment en els nivells de MGS i PTG. Per tal de comprovar-ho, es va imitar la condició patològica silenciant l'expressió de laforina en neurones mitjançant oligonucleòtids de RNA d'interferència (short interfering RNA, siRNA) (**Figura 6c**). El *knockdown* de laforina induït per dos siRNA diferents va causar un clar increment en els nivells de MGS i PTG respecte les cèl·lules transfectades amb siRNA control (**Figura 6d,e**). A més, aquelles cèl·lules acumulaven més glicogen en condicions glicogèniques (**Figura 6f**). Aquests resultats establien la implicació del sistema laforina-malina en el control de l'estabilitat de la MGS i la PTG i de l'acumulació de glicogen.

Article 2

Neurodegeneració i alteracions funcionals associades a l'acumulació de glicogen sintasa en un model de malaltia de Lafora.

Jordi Valles-Ortega*, Jordi Duran*, Mar Garcia-Rocha, Carles Bosch, Isabel Saez, Lluís Pujadas, Anna Serafin, Xavier Cañas, Eduardo Soriano, José M. Delgado-García, Agnès Gruart and Joan J. Guinovart

* Aquests autors han contribuït per igual.

1. Els ratolins amb deficiència de malina (malina *knock-out,* malina KO) acumulen glicogen poc ramificat en els cossos de Lafora (Lafora bodies, LBs).

En el nostre grup es van generar ratolins malina KO i es van criar fins gairebé l'edat d'1 any. Aquests animals acumulaven LBs, el tret distintiu de la malaltia de Lafora (Lafora disease, LD). Els LBs es podien trobar a diverses àrees del cervell, essent més abundants a l'hipocamp i al cerebel (**Figura 1A**). L'acumulació de LBs no era exclusiva del cervell, també va ser detectada en algunes fibres del múscul esquelètic i el cor (**Figura suplementària 1**). Aquestes inclusions creixien en nombre i mida amb l'edat, fet que es podia observar comparant ratolins de 4 i 11 mesos d'edat (**Figura 1A, Figura 7A**). A més, en els animals més vells, es van trobar LBs en regions del cervell que no estaven afectades als 4 mesos (**Figura 1A**). Aquests resultats eren consistents amb el caràcter progressiu de la malaltia de Lafora.

Els LBs són inclusions insolubles formades principalment per polímers de glucosa (poliglucosans) similars al glicogen però poc ramificats. Nosaltres vam mesurar el contingut en glicogen en homogenats de cervell sencer d'animals malina KO d'11 mesos d'edat, on la presència de LBs era més notòria. Aquests cervells presentaven un increment de 2.5 vegades en contingut de glicogen respecte els controls (**Figura 2A**). A més, l'homogenat es va sotmetre a centrifugació de baixa velocitat per tal d'analitzar la distribució d'aquest polisacàrid entre les fraccions soluble i insoluble. L'increment de glicogen detectat corresponia a aquell present en la fracció insoluble mentre que no es van trobar diferències significatives en la fracció soluble.

Es va mesurar el grau de ramificació del glicogen en els cervells malina KO mitjançant l'enregistrament de l'espectre d'absorció visible de glicogen purificat en presència de iode. Amb aquest mètode, el màxim d'absorció es desplaça cap a longituds d'ona majors en disminuir el grau de ramificació del polímer del glucosa. El glicogen aïllat de cervells KO era clarament menys ramificat (pic a 537 nm) que el de cervells control (pic a 492 nm) (**Figura 2B**).

2. Els ratolins malina KO acumulen MGS en els LBs.

La malina està involucrada en la degradació proteasomal de laforina i MGS (**Article 1**). Per aquest motiu vam analitzar el contingut i la distribució de la MGS en talls de cervell de ratolins

salvatges (*wild type,* WT) i malina KO. Vam utilitzar animals de 4 i 11 mesos per poder avaluar la progressió amb l'edat. Les inclusions de poliglucosà van resultar positives per anticossos contra MGS (**Figura 1B**), indicant així que els LBs contenen la proteïna MGS i el seu producte catalític (**Figura 1**). L'anàlisi per *western blot* va mostrar un gran increment en MGS en l'homogenat total dels cervells de malina KO respecte els controls. Els nivells d'aquesta proteïna es trobaven incrementats en la fracció insoluble, reforçant els resultats obtinguts per immunohistoquímica. Donat que les inclusions de poliglucosà aparentment incrementaven en nombre i mida amb l'edat, també vam analitzar els nivells d'altres proteïnes que s'uneixen al glicogen com la laforina, la glicogenina –l'enzim encebador de la síntesi de glicogen- i la glicogen fosforilasa. Els nivells de laforina (**Figura 3A**), de les isoformes muscular (MGP) i cerebral (BGP) de la glicogen fosforilasa, i de glicogenina (**Figura suplementària 3**) també es trobaven incrementats en la fracció insoluble. Curiosament, però, els nivells de MGP també estaven augmentats en la fracció soluble, on la MGS, la laforina i la BGP es mantenien inalterades.

L'anàlisi de l'estat de fosforilació de la MGS, utilitzant anticossos específics contra els llocs de fosforilació a N-terminal i C-terminal, va mostrar que encara que l'enzim present a la fracció soluble no mostrava diferències entre els ratolins KO i WT, la MGS present a la fracció insoluble dels ratolins KO estava menys fosforilada en els residus de Serina 7/10 (**Figura 3A i 3B**) i Serina 640 (**Figura 3A i 3C**), fet que correspondria a una forma més activa de l'enzim.

També vam mesurar l'activitat enzimàtica glycogen sintasa (GS) en homogenats totals i en les fraccions soluble i insoluble. L'activitat GS en presència de glucosa-6-fosfat (G6P) (**Figura 3D**) es pren habitualment com a mesura de la GS total. Sorprenentment, malgrat l'enorme increment en proteïna MGS vist per *western blot*, no es van trobar diferències en GS total mitjançant la mesura de la seva activitat. Aquests resultats indicaven que la proteïna MGS acumulada en els LBs no mostrava activitat, ni en presència del seu activador al·lostèric (G6P), en les condicions de l'assaig. El ratio d'activitat -/+ G6P, un indicador de l'estat d'activació de l'enzim, tampoc va presentar canvis en cap de les fraccions (**Figura 3E**) malgrat les diferències detectades per *western blot* en l'estat de fosforilació.

3. Progressió específica de tipus cel·lular en l'aparició de LBs: els LBs no només s'acumulen en neurones, sinó també en cèl·lules glials. Tant les interneurones PV+ de l'hipocamp com els astròcits expressen MGS i malina. Els dos tipus cel·lulars presenten LBs en ratolins malina KO.

L'estudi histològic de cervells de ratolí amb anticossos contra MGS va mostrar que, a més dels astròcits, les interneurones parvalbúmina positives (PV+) de l'hipocamp també expressen MGS (**Figura 4A**). Aquestes cèl·lules es poden trobar a les regions DG, CA1-2 i CA3 (no es mostra).

En el ratolí KO, l'únic exó de *Epm2b* va ser substituït per un casset de selecció que conté el gen de la β-galactosidasa (β-gal, *lacZ*) (**Figura suplementària 2A**). Com a conseqüència, els ratolins heterozigots per malina expressen βgal sota el control del promotor endogen de *Epm2b*. Per tal de superar el problema que suposava la manca d'un anticòs que reconegués la malina endògena, vam fer servir βgal com a reporter de l'expressió de malina en aquests animals. La immunodetecció de βgal va mostrar que, entre d'altres cèl·lules, alguns astròcits i totes les interneurones PV+ expressen malina a l'hipocamp, una de les zones del cervell més afectades en els ratolins malina KO (**Figura 4B**).

Mentre que els cervells KO de 4 mesos d'edat mostraven acumulació de LBs principalment associada als astròcits (**Figura 5 i Figura 6A**), els cervells d'11 mesos mostraven LBs en astròcits (**Figura 5, Figura 6A**) i en els cossos cel·lulars de neurones (**Figura 5**). Els LBs neuronals eren molt evidents en el soma de les interneurones PV+ de l'hipocamp i es trobaven de forma ocasional en els seus processos dendrítics (**Figura 6B**).

Per tal de corroborar els resultats anteriors, vam realitzar un estudi per microscòpia electrònica (EM) de l'hipocamp de ratolins KO d'11 mesos d'edat. Els astròcits presentaven sovint LBs dins del seu citoplasma (**Figura 6C c1 i c2**), en concordança amb les observacions fetes per microscòpia de fluorescència (**Figura 6a**). Vam centrar la nostra atenció en la zona dendrítica de CA1 i DG. Les dendrites van ser identificades pel gran nombre de microtúbuls organitzats en feixos i per la presència de contactes sinàptics en la seva superfície (**Figura 6C a2**) o en les espines dendrítiques que sortien d'elles (**Figura 6C b2**). Vam trobar dendrites que contenien grans LBs que deformaven la seva mida i la seva estructura (**Figura 6C a1, a2, b1 i b2**). En alguns casos, es van identificar gränuls de glicogen a la perifèria d'aquests LBs. A més, s'observaven freqüentment cèl·lules electro-denses amb les característiques estructurals típiques de les cèl·lules microglials, les quals envoltaven diversos LBs (**Figura 6C d**). Així doncs, vam concloure que els LBs s'acumulen en cèl·lules glials i en neurones.

4. Degeneració de les interneurones PV+ de l'hipocamp i gliosi en els ratolins malina KO.

Amb l'objectiu d'estudiar l'efecte de l'acumulació de LBs en les interneurones PV+, vam comptar el nombre d'aquestes neurones en l'hipocamp a 4 i 11 mesos d'edat. Vam trobar una marcada reducció en el nombre de neurones PV+ en els hipocamps malina KO d'11 mesos, un decrement que no s'observava als 4 mesos (**Figura 7A**). La disminució en la immunodetecció també s'observava en dendrites, fet que suggereix una alteració en la ramificació dendrítica (**Figura 7B**). Tenint en compte que la inducció de l'acumulació de poliglucosans causava mort neuronal per apoptosi en cultius primaris (**Article 1**), vam analitzar si la pèrdua neta de neurones causada per la deficiència de malina succeïa acompanyada d'un increment en la taxa d'apoptosi. Encara que no es van trobar trets clars d'apoptosi neuronal per TUNEL, activació de caspasa-3 o tinció amb FluoroJadeB (no es mostra), els hipocamps KO d'11 mesos d'edat presentaven un increment

evident de cèl·lules GFAP+ (**Figura suplementària 4**). Aquesta gliosi és una característica associada a la pèrdua neuronal que també s'observava en l'altre model de LD, el laforina KO, i estava en concordança amb la pèrdua d'interneurones PV+ observada en l'hipocamp dels animals malina KO.

5. Alteracions en la conducta dels ratolins malina KO.

Els ratolins KO es van desenvolupar normalment i eren fèrtils. Mostraven una postura i moviment normal i no van presentar diferències significatives en el test del *Rotarod*, en el que es mesura la capacitat de mantenir-se en un cilindre giratori, o en el *Beam walking test,* en el que es mesura la capacitat de caminar per una barra estreta. Tampoc van mostrar cap signe d'atàxia (no es mostra). El comportament exploratori dels ratolins KO va ser evaluat en un test a camp obert (*Open Field test,* **Figura suplementària 5**). Als 11 mesos d'edat, aquests animals eren hiperactius i evidenciaven un increment en la seva conducta exploratòria: es van trobar diferències significatives en el temps d'estada en el centre del camp, la distància recorreguda i el nombre de vegades que s'alçaven sobre les potes de darrera (*rearing*). Aquests resultats podien indicar una reducció de l'ansietat en els ratolins KO.

El condicionament operant és un bon test per tal de determinar les capacitats d'aprenentatge associatiu en la conducta d'alerta dels ratolins, així com d'altres habilitats cognitives i motores. Les dades recollides pel grup expert en conducta animal de José M. Delgado García i Agnès Gruart, mostren que les capacitats d'aprenentatge dels ratolins KO eren similars a les dels ratolins control. Per altra banda, l'estudi electrofisiològic que van dur a terme en el mateix grup, va mostrar alteracions neurològiques importants en els ratolins malina KO que es resumeixen a continuació.

6. Propietats funcionals de les sinapsis de CA3-CA1 en l'hippocamp de ratolins WT i malina KO en conducta d'alerta: els ratolins malina KO presenten hiperexcitabilitat sinàptica.

Les tècniques disponibles de enregistrament *in vivo* permeten l'estudi de les sinapsis de l'hipocamp en ratolins desperts. Mitjançant aquestes tècniques, es va concloure que els ratolins KO presentaven una excitabilitat sinàptica augmentada (**Figura 8A**). En canvi, els resultats també suggerien que els processos plàstics de curt termini associats a les sinapsis de CA3-CA1 de l'hipocamp no estaven afectades en els animals KO (**Figura 8B**).

7. Comparació de la potenciació de llarg termini (*Long-term potentiation, LTP*) provocada en ratolins WT i malina KO en conducta d'alerta.

Els ratolins KO presentaven LTPs majors i de major durada que els controls (**Figura 8C**), un fet que pot ser atribuït a la seva excitabilitat sinàptica augmentada, però que no es tradueix en una habilitat incrementada per a tasques d'aprenentatge associatiu.

8. Efectes de la injecció d'àcid kaínic en ratolins malina KO: els ratolins malina KO són propensos a patir atacs epilèptics.

Les soques C57BL6, en comparació amb ratolins d'altres fons genètics, presenten una elevada resistència a desenvolupar atacs epilèptics i els ratolins malina KO tenen un fons genètic C57BL6. Es va testar la susceptibilitat dels ratolins WT i KO a una única injecció d'àcid kaínic. Tal i com es mostra en el **Figura 9**, els ratolins malina KO presentaven propensió a patir sacsejades d'origen hipocampal, alguns cops mioclòniques, després d'una única injecció d'àcid kaínic. Aquesta reacció no es va observar mai en els animals control.

Article 3

El paper central de la glicogen sintasa en la formació de la corpora amylacea: similituds entre la malaltia de Lafora i l'envelliment fisiològic.

Jordi Valles-Ortega, Jordi Duran, Mercedes Márquez, David Vílchez, Lluís Pujadas, Joaquim Calbó, Eduardo Soriano, Martí Pumarola i Joan J. Guinovart

1. Canvis d'expressió de glicogen sintasa muscular (MGS) i malina en el procés d'envelliment del cervell: la formació de dipòsits de MGS al cervell de ratolins vells correlaciona amb una baixada de l'expressió de malina. L'acumulació d'aquests dipòsits té lloc a les mateixes àrees del cervell que en ratolins malina KO.

Amb l'objectiu d'analitzar possibles canvis en el patró d'expressió de la MGS en diferents zones del cervell durant l'envelliment, es va realitzar la immunodetecció amb anticossos específics contra aquesta proteïna en cervells de ratolins WT de 15 dies, 21 dies, 3 mesos, 6 mesos i 16 mesos d'edat (**Figures 1, 2 i 3**). En els cervells de 15 dies postnatals, el marcatge de MGS era més fort en astròcits que en la majoria de les neurones. Però les cèl·lules de Purkinje al cerebel (**Figura 2**) i les interneurones GABAèrgiques, especialment a l'hipocamp (**Figura 1**), presentaven una senyal comparable a la dels astròcits. L'expressió de MGS en les neurones de Purkinje es va mantenir des del dia 15 fins als 16 mesos sense canvis apreciables (**Figura 2**). En canvi, l'expressió a les interneurones dequeia clarament amb l'edat. Mentre que es podien trobar nombroses interneurones intensament marcades a l'hipocamp als 15 dies, la senyal era menor en els ratolins de 21 dies i gairebé inapreciable a partir dels 3 mesos d'edat (**Figure 1**). Encara que els astròcits expressaven MGS durant tot el període, mostraven una senyal menys intensa i difosa des dels 21 dies fins als 3 mesos i més intensa i definida a partir dels 6 mesos. Cal destacar que els cervells de 16 mesos d'edat presentaven dipòsits positius per MGS. Aquestes acumulacions en els ratolins vells es van observar principalment a l'hipocamp (**Figura 1**), la capa granular interna del cerebel (**Figura 2**) i les capes externes del còrtex piriforme (**Figura 3**).

Per tal d'analitzar el patró d'expressió de malina al cervell durant l'envelliment, vam utilitzar el gen *lacZ* insertat sota el promotor de malina en els ratolins KO com a reporter de l'activitat transcripcional (**Article 2**). Això va ser especialment útil perquè no hi ha cap anticòs disponible que detecti els nivells endògens de proteïna malina. La tinció X-gal de cervells heterozigots per malina des de 15 dies fins a 16 mesos va revelar una extensa senyal del reporter de malina a les diferents àrees del cervell, incloent l'hipocamp (**Figura 1**), el cerebel (**Figura 2**) i el còrtex piriforme (**Figura 3**). A l'hipocamp i al còrtex piriforme, aquesta senyal semblava incrementar des del dia 15 al dia 21 després del naixement, essent aquest increment especialment notable al gir dentat (DG) (**Figura 1**). Al cerebel, la tinció X-gal aparentment no incrementava a partir del dia 15 postnatal. Però, és de destacar que la senyal del reporter de malina dequeia gradualment durant l'envelliment en les tres zones del cervell (**Figures 1, 2 i 3**). Aquesta reducció era molt evident a la capa granular interna del cerebel, una de les regions del cervell amb major presència

de dipòsits de MGS (**Figura 2**). Tenint en compte que la malina regula la MGS induint la seva degradació proteasomal (**Article 1**) i que la depleció de malina causa acumulació de MGS (**Article 2**), és probable que el decrement observat en l'activitat transcripcional de malina comporti una disminució en els seus nivells de proteïna i, en conseqüència, una regulació a l'alça dels nivells de proteïna MGS. Resulta remarcable que els ratolins WT vells mostraven acumulació de MGS a les mateixes zones del cervell que estaven afectades en ratolins malina KO més joves (**Figura 4**). Per aquest motiu, vàrem enfocar el nostre estudi en aquestes zones del cervell.

2. Diferents proteïnes relacionades amb el metabolisme del glicogen s'acumulen en els dipòsits de poliglucosà tant de ratolins WT vells com de models de LD. Cap d'aquestes acumulacions s'observa en els ratolins MGS KO.

Tal i com s'ha comentat anteriorment, els CA, que es troben als cervells de mamífers vells, són coneguts per contenir poliglucosans. Tenint en compte que la MGS catalitza la síntesi de glicogen i que es troba acumulada amb l'edat, vàrem analitzar si el glicogen i les seves proteïnes associades eren presents en els dipòsits dels ratolins WT vells i els vam comparar amb els dels ratolins malina KO, els quals presenten un marcat increment en MGS (**Article 2**) que s'acumula a les mateixes àrees del cervell que en els ratolins WT vells (**Figura 4**). A més, per tal d'avaluar la importància de la MGS en el procés de formació dels CA, vàrem generar i estudiar els ratolins MGS KO (**Figura suplementària 1, veure mètodes**).

En aquest estudi es van comparar cervells de ratolins WT, malina KO i MGS KO de la mateixa edat (16 mesos). Primer de tot, vam analitzar el seu contingut en poliglucosà. Encara que el nombre i la mida d'aquestes acumulacions eren òbviament majors en el model de LD (LBs), els dipòsits presents en els cervells WT i malina KO eren igualment positius per la tinció PAS (**Figures 5A, 6A i 7A**), produïen una coloració lilosa amb la tinció amb iode (**Figures 5B, 6B i 7B**) i immunoreaccionaven amb l'anticòs anti-poliglucosà (**Figura 8A**), confirmant que els dos tipus de dipòsit contenen polimers de glucosa poc ramificats i que, per tant, poden ser anomenats PGBs. Aquests PGBs es trobaven principalment a l'hipocamp (**Figura 5**), el cerebel (**Figura 6**) i el còrtex piriforme (**Figura 7**) en cervells WT i malin KO coincidint amb l'acumulació de MGS (**Figures 5A, 6A i 7A**). A més, la laforina (**Figures 5A, 6A i 7A**) i la BGP (**Figura 8B**) també s'acumulaven als PBGs tan de cervells WT com malina KO. No es va trobar cap acumulació de poliglucosà, laforina, BGP (no es mostra) ni, òbviament, MGS en cap regió dels cervells dels ratolins MGS KO. És interessant comentar que en absència de MGS la laforina es localitza principalment al nucli cel·lular (**Figures 5, 6 i 7**).

3. Les molècules característiques (marcadors) de CA només s'acumulen en presència de dipòsits de poliglucosà en ratolins vells i es troben sobreacumulats en els ratolins model de LD: la MGS i, per tant, la síntesi de glicogen és necessària per la formació de CA.

3.1 Marcadors específics de tipus cel·lular: els astròcits interactuen amb els PGBs que es formen en el soma d'interneurones PV+ tan en ratolins WT vells com malina KO.

La presència de marcadors glials –com GFAP- i neuronals –com neurofilaments de 200 kDa (NF200)- ha estat utilitzada per diferents autors amb l'objectiu d'elucidar el tipus cel·lular originari dels CA i els diferents resultats obtinguts no són unívocs. Això és degut segurament a l'heterogeneïtat de les mostres i de les tècniques utilitzades per la seva determinació, i probablement també a la pròpia heterogeneïtat dels CA.

Diversos autors han descrit que els CA reaccionen amb anticossos contra GFAP, però també molts altres han publicat que els CA són negatius per GFAP. Nosaltres vam descriure per primer cop la presència de LBs fortament associats i dintre d'astròcits en cervells malina KO (**Article 2**) fent servir el sistema d'imatge confocal. En aquest treball es van obtenir imatges per microscòpia confocal de ratolins de 16 mesos WT i malina KO per tal de comparar la distribució entre tipus cel·lulars dels PGBs presents en els seus cervells. Els astròcits van mostrar una forta associació amb aquests dipòsits tant en ratolins WT com malina KO. Els PGBs es podien trobar al soma d'astròcits o envoltats pels seus processos positius per GFAP (**Figura 8**).

Vàrem avaluar la implicació de les cèl·lules neuronals en la formació de PGBs mitjançant l'anàlisi de la presència de NF200 i parvalbúmina (PV) en aquests dipòsits. Les interneurones PV+ de l'hipocamp expressen MGS i malina, i acumulen LB en el ratolí malina KO (**Article 2**). Es van trobar PGBs que contenien PV (**Figura 9A**) i NF200 (**Figura 9B**) tan en cervells WT com malina KO. Encara que els PGBs de l'hipocamp i del cerebel es marcaven molt lleugerament per NF200, els del còrtex piriforme es tenyien clarament amb aquest marcador. No es va trobar acumulació de PV ni de NF200 als cervells dels ratolins MGS KO, on es conservava la tinció normal de les neurones amb aquests marcadors (**Figura 9**).

A més, com que es va trobar associació dels PGBs amb astròcits i interneurones en els cervells WT i malina KO, vàrem obtenir imatges confocal d'alta resolució per poliglucosà, GFAP i PV amb l'objectiu d'analitzar a fons la interacció dels dipòsits amb aquests tipus cel·lulars. Els PGBs positius per PV, situats en les neurites o adherits a fragments d'interneurones, es trobaven freqüentment associats a processos astroglials positius per GFAP tant en ratolins WT com en ratolins malina KO (**Figura 10**). Sorprenentment, en ratolins WT vells, es van trobar PGBs en el soma d'interneurones positives per PV en l'interfície entre l'espai intracel·lular i l'extracel·lular, on estaven en contacte amb processos astrocítics (**Figura 10**). Extraordinàriament, fins i tot alguns PGBs situats completament a l'interior d'interneurones dels cervells malina KO mostraven associació amb astròcits. Es van observar filaments positius per GFAP que entraven dintre del soma neuronal i contactaven amb els dipòsits de poliglucosà (**Figura 10**).

3.2 Marcadors relacionats amb estrès cel·lular.

Diversos estudis han analitzat la composició de la fracció proteica dels CA mitjançant immunodetecció i s'ha descrit la presència de diversos marcadors en aquests dipòsits. Els marcadors relacionats amb l'estrès oxidatiu i amb l'eliminació de proteïnes com AGEP, ubiqüitina i HSP70 estan especialment ben identificats com a components de la CA. Els PGBs presents tan en cervells WT com malina KO contenien AGEP (**Figura 11**), ubiqüitina (**Figura 12A**) i HSP70 (**Figura 12B**) mentre que no es va trobar acumulació de cap d'aquests marcadors en cap regió cerebral dels ratolins MGS KO de la mateixa edat.

4. Proteïnes que formen agregats en altres malalties neurodegeneratives: els CA i els LBs també contenen proteïnes que s'agreguen en patologies com la malaltia de Parkinson.

En aquest estudi també vam analitzar altres proteïnes que, encara que són conegudes per estar involucrades en altres malalties com la d'Alzheimer i la de Parkinson, també han estat relacionades amb els PGBs. Aquest és el cas de la proteïna tau, que forma agregats en un ratolí model de la LD (laforina KO); i de l'α-sinucleïna, que s'ha trobat acumulada en diferents casos de malalties associades a cossos de poliglucosà (PGDs). Tan en el cervells de ratolins WT com malina KO, es van trobar alguns PGBs que contenien α-sinucleïna. Tot i així, eren difícils d'identificar al cerebel i no es van trobar al còrtex piriforme de cervells WT mentre que aquests PGBs positius per α-sinucleïna es trobaven fàcilment a l'hipocamp dels cervells WT i en les tres regions dels cervells malina KO (**Figura 13A**). No es van trobar acumulacions d'α-sinucleïna en els ratolins MGS KO (**Figura 13A**). Per altra banda, encara que s'ha descrit la presència de tau en els CA i els LBs de cervells humans, no es van poder identificar PGBs positius per tau en cervells WT i l'anticòs només va reaccionar lleugerament contra els PGBs de l'hipocamp de ratolins malina KO (**Figura 13 B**). No es van trobar acumulacions de tau en els cervells MGS KO (**Figura 13 B**). A més, cap dels PGBs es va tenyir amb Congo Red o Metanamina (**no es mostra**), tincions utilitzades normalment per a la detecció de substàncies amiloides.

ARTICLES

ARTICLE 1

nature neuroscience

ARTICLES

Mechanism suppressing glycogen synthesis in neurons and its demise in progressive myoclonus epilepsy

David Vilchez[1], Susana Ros[1], Daniel Cifuentes[1], Lluís Pujadas[1], Jordi Vallès[1], Belén García-Fojeda[2], Olga Criado-García[2], Elena Fernández-Sánchez[2], Iria Medraño-Fernández[2], Jorge Domínguez[1], Mar García-Rocha[1], Eduardo Soriano[1], Santiago Rodríguez de Córdoba[2,3] & Joan J Guinovart[1,3]

Glycogen synthesis is normally absent in neurons. However, inclusion bodies resembling abnormal glycogen accumulate in several neurological diseases, particularly in progressive myoclonus epilepsy or Lafora disease. We show here that mouse neurons have the enzymatic machinery for synthesizing glycogen, but that it is suppressed by retention of muscle glycogen synthase (MGS) in the phosphorylated, inactive state. This suppression was further ensured by a complex of laforin and malin, which are the two proteins whose mutations cause Lafora disease. The laforin-malin complex caused proteasome-dependent degradation both of the adaptor protein targeting to glycogen, PTG, which brings protein phosphatase 1 to MGS for activation, and of MGS itself. Enforced expression of PTG led to glycogen deposition in neurons and caused apoptosis. Therefore, the malin-laforin complex ensures a blockade of neuronal glycogen synthesis even under intense glycogenic conditions. Here we explain the formation of polyglucosan inclusions in Lafora disease by demonstrating a crucial role for laforin and malin in glycogen synthesis.

Glucose is the main source of energy in the brain; however, glycogen is not stored in neurons and is present only in astroglial cells[1]. Nevertheless, in several pathologies, polymers of glucose, normally referred to as polyglucosan bodies, accumulate in neuronal tissue[2]. One such pathology is Lafora-type progressive myoclonus epilepsy[3–5] (EPM2, OMIM 254780). The hallmark of Lafora disease is the presence of large inclusions (Lafora bodies) in the axons and dendrites of neurons[6,7]. These inclusions are composed of poorly branched polymers of glucose, which can be considered to be abnormal glycogen molecules. However, the mechanism by which polyglucosan bodies accumulate in Lafora disease remains unknown. Lafora disease typically manifests during adolescence with generalized tonic-clonic seizures, myoclonus, absences, drop attacks or partial visual seizures. As the disease progresses, afflicted individuals suffer a rapidly progressive dementia with apraxia, aphasia and visual loss, leading to a vegetative state and death, usually in the first decade from the onset of the initial symptoms. Seizures are commonly the first manifestation of the disease and may be generalized (tonic-clonic, absences, myoclonic, tonic or atonic) or focal (usually with visual symptoms). Electroencephalograms show both generalized and focal epileptiform discharges[8–13].

Lafora disease is inherited as an autosomal recessive disorder and shows genetic heterogeneity. It has been associated with mutations in two genes. *Epilepsy, progressive myoclonus 2a* (*EPM2A*) is mutated in approximately 48% of individuals with Lafora disease and encodes laforin, a dual-specificity protein phosphatase with a functional carbohydrate-binding domain[14–18]. A second gene, *Epilepsy, progressive myoclonus 2b* (*EPM2B*), is mutated in 30–40% of those with Lafora disease and encodes malin, an E3 ubiquitin ligase[18–20]. Malin interacts with laforin and causes its ubiquitination[20]. Individuals with mutations in laforin or malin are neurologically and histologically indistinguishable, which strongly suggests that these two proteins operate through common physiological pathways[18].

To examine how defects in either laforin or malin contribute to the formation of Lafora bodies, we have examined their role in neurons. We show that the laforin-malin complex blocks glycogen synthesis in these cells by inducing the proteasome-dependent degradation of MGS and PTG.

RESULTS

Neurons keep the machinery for glycogen synthesis inactive

Analysis of whole mouse brain, differentiated mouse Neuro2a (N2a) cells and primary cultured mouse neurons showed that neurons express MGS (**Fig. 1a**,**b**). Expression of the liver glycogen synthase (LGS) isoform was absent in these specimens (**Fig. 1a** and data not shown). Furthermore, neurons did not express glycogen phosphorylase, the enzyme that is responsible for the degradation of this polysaccharide (**Fig. 1b**). Notably, despite the expression of MGS, neurons and N2a cells did not accumulate detectable amounts of glycogen when cultured in medium containing high concentrations of glucose (30 mM) (**Fig. 1c**). In contrast, astrocytes grown under the same conditions showed marked accumulation of this polysaccharide (**Fig. 1c**; see ref. 1).

[1]Institute for Research in Biomedicine and University of Barcelona, Barcelona Science Park, Josep Samitier 1-5, E-08028 Barcelona, Spain. [2]Centro de Investigaciones Biológicas, Consejo Superior de Investigaciones Científicas, Ramiro de Maeztu 9, E-28040 Madrid, Spain. [3]These authors contributed equally to this work. Correspondence should be addressed to J.J.G. (guinovart@pcb.ub.es) and S.R.d.C. (SRdeCordoba@cib.csic.es).

Received 9 August; accepted 21 September; published online 21 October 2007; doi:10.1038/nn1998

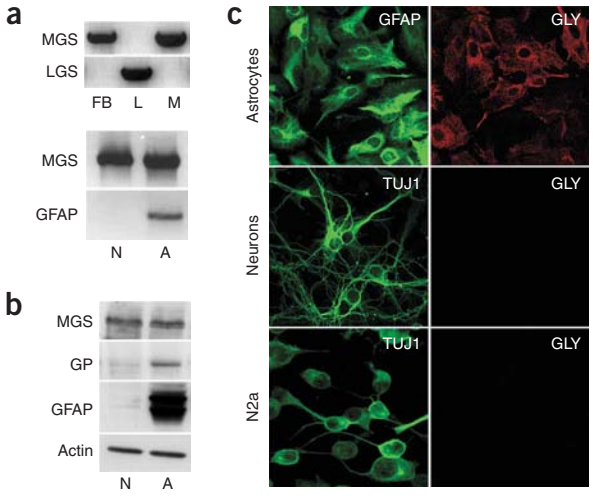

Figure 1 Neurons express MGS, but do not accumulate glycogen. (**a**) Upper, RT-PCR analysis of MGS and LGS in mouse forebrain (FB), liver (L) and muscle (M). Lower, RT-PCR analysis of MGS in primary cultures of neurons (N) and astrocytes (A). GFAP was used as an astroglial marker. Note the absence of signal in neurons. (**b**) Western blot analysis of homogenates of primary cultured neurons and astrocytes with antibodies to MGS, glycogen phosphorylase (GP) and GFAP. The astrocyte marker GFAP was almost undetectable in neuronal cultures. Actin was used as a control for gel loading. (**c**) Confocal microscopy images of primary cultured astrocytes, neurons and N2a cells growing in medium with 30 mM glucose. Cells were processed for immunofluorescence analysis with glycogen antibodies (GLY). GFAP and TUJ1 antibodies were used as markers of glial and neuronal cells, respectively. All images were acquired using a 63× objective with an additional 1.4 confocal magnification.

The inability of neurons to synthesize glycogen could be a consequence of a lack of sufficient intracellular concentrations of glucose-6-phosphate (G6P), the metabolite required for the activation of MGS[21–23], or of sufficient amounts of MGS in this cell type. However, a fivefold increase in the amount of intracellular G6P in primary cultured neurons by overexpression of glucokinase or hexokinase I did not result in glycogen synthase activation or glycogen accumulation (**Fig. 2a**). Similarly, overexpression of MGS in primary cultured neurons using recombinant adenoviruses did not increase glycogen deposition (**Fig. 2b,c**). These results indicate that the lack of glycogen accumulation in these cells was not a result of low levels of MGS or G6P. Similar results were obtained in N2a cells (**Supplementary Fig. 1** online). MGS expressed in neurons localized mostly in the nucleus (**Fig. 2c**, upper), which is a characteristic of cells that are depleted of glycogen[24,25]. In contrast, MGS in astrocytes clustered in the cytoplasm, which is a typical location for this protein under conditions of active glycogen synthesis (**Fig. 2c**, lower).

Control of glycogen synthesis is achieved mainly through the inactivation of MGS by phosphorylation of multiple serine residues at the C and N termini by a range of kinases[26]. Western blot analysis showed that MGS in primary cultured neurons and N2a cells was phosphorylated at the Ser640 and Ser7/10 residues, the phosphorylation sites that reduce the activity of the enzyme the most[26] (**Fig. 2d** and **Supplementary Fig. 1**). However, Ser640 can be effectively dephosphorylated by treating neurons with 20 mM LiCl (**Fig. 2e**), a glycogen synthase kinase 3 inhibitor[27]. Concomitantly, dephosphorylated MGS altered its subcellular localization and accumulated at specific sites in the cytoplasm, coinciding with growing glycogen particles (**Fig. 2c**, middle panel and **Supplementary Fig. 1**). Incubation of primary cultured neurons with LiCl at therapeutic concentrations (1–2 mM) for up to 48 h did not produce any substantial effect on MGS.

Extensive MGS dephosphorylation at Ser640 and Ser7/10 was induced in primary cultured neurons and N2a cells by PTG (**Fig. 3a** and **Supplementary Fig. 1**), a regulatory subunit of protein

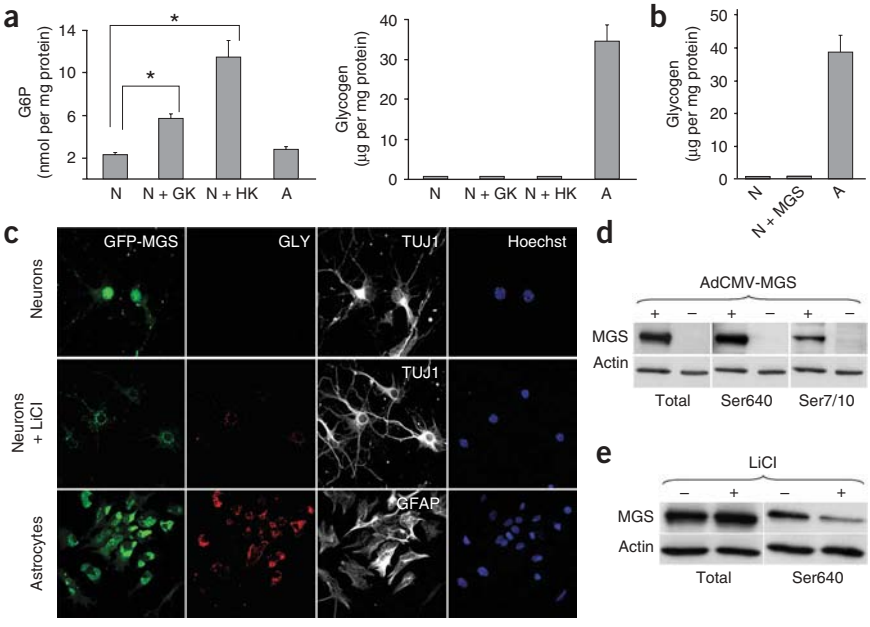

Figure 2 Effects of increased intracellular levels of G6P or overexpression of MGS. (**a**) Graphs show the intracellular levels of G6P (left) and the glycogen content (right) of neurons overexpressing glucokinase (N + GK) or hexokinase I (N + HK) (MOI 100) and uninfected neurons (N). A fivefold increase in the intracellular levels of G6P did not increase glycogen accumulation. G6P levels represent the mean ± s.e.m. ($n = 5–7$) of three independent experiments. *$P < 0.001$ noninfected versus AdCMV-GK, AdCMV-HK I–infected. Glycogen content represents the mean ± s.e.m. ($n = 6–10$) of three independent experiments. (**b**) Glycogen content (mean ± s.e.m., $n = 6$) of three independent experiments in primary cultures of neurons and astrocytes. Glycogen was undetectable in noninfected and AdCMV-MGS–infected (N + MGS, MOI 100) neuronal cells. (**c**) Immunofluorescence analysis with GLY and specific markers of neurons (TUJ1) and astrocytes (GFAP). Cell nuclei were stained with Hoechst 33342. Cells were treated with AdCMV-GFP-MGS (MOI 50 for neurons and 5 for astrocytes). MGS-overexpressing neurons accumulated glycogen when treated with 20 mM LiCl for 24 h (middle). All images were acquired using a 63× objective with an additional 1.4 confocal magnification. (**d**) Western blot analysis of AdCMV-MGS–infected (+, MOI 100) versus noninfected (–) neurons. We used antibodies recognizing total MGS and phosphorylated MGS on Ser640 and Ser7/10. (**e**) Western blot analysis of MGS-overexpressing neurons incubated in the presence (+) or absence (–) of 20 mM LiCl (24 h) with antibodies to MGS and Ser640.

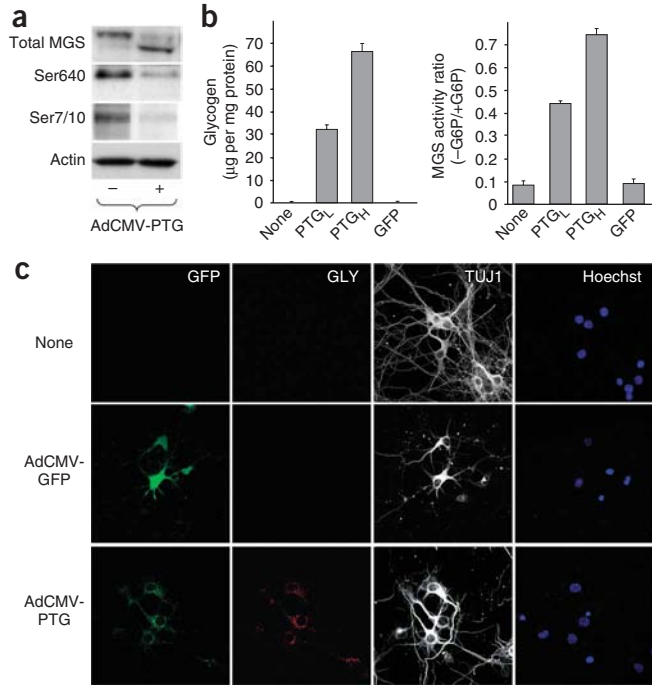

d

Tissue	MGS	PTG	PTG/MGS
Primary neurons	1	1	1
Skeletal muscle	72	1,386	19
Primary astrocytes	2.4	87	36

Figure 3 PTG expression activates neuronal MGS and results in glycogen accumulation. (**a**) Western blot analysis of neurons treated (+) or not (–) with AdCMV-PTG (MOI 100) and then incubated with antibodies that recognize total MGS and phosphorylated MGS on Ser640 and on Ser7/10. PTG overexpression stimulated the dephosphorylation of MGS at these sites. (**b**) Glycogen content and MGS activity ratio (–G6P/+G6P) of neurons treated with AdCMV-PTG at low (PTG_L, 50) and high (PTG_H, 100) MOI. None = noninfected neurons. PTG overexpression had a marked effect on the stimulation of neuronal glycogen deposition and MGS activity. Glycogen content represents the mean ± s.e.m. ($n = 6$–10) of three independent experiments. MGS activity ratio represents the mean ± s.e.m., $n = 6$–12, of three independent experiments. (**c**) Glycogen immunocytochemistry of primary cultures of neurons infected with AdCMV-PTG (MOI 50). TUJ1 and Hoechst 33342 staining were used as markers of neurons and nuclei, respectively. Glycogen accumulated in cell soma and in neurites. As a control for adenovirus infection, neurons were treated with AdCMV-GFP (MOI 50). All images were acquired using a 63× objective with an additional 1.4 confocal magnification. (**d**) RT-PCR. MGS and PTG transcript levels were compared with the values obtained in primary cultures of neurons, which were assigned a value of 1. The PTG/MGS transcript ratio in neurons was lower than the ratio in muscle or astrocytes.

phosphatase 1 that promotes the activation of MGS[28–30] and that interacts with laforin[31]. This dephosphorylation was accompanied by a marked increase in glycogen accumulation throughout the soma, neurites and axons (**Fig. 3b**,**c** and **Supplementary Fig. 1**). Like LiCl, PTG induced the intracellular relocation of MGS, which became clustered in the cytoplasm, colocalizing with glycogen particles (data not shown). The activation state of MGS increased in neurons overexpressing PTG, reaching values that were close to those of full activation (**Fig. 3b** and **Supplementary Fig. 1**), and the enzyme showed increased electrophoretic mobility, which is characteristic of the activated (dephosphorylated) enzyme (**Fig. 3a** and **Supplementary Fig. 1**). Taken together, these findings demonstrate that neurons have the appropriate machinery to synthesize glycogen, but this system is essentially blocked by keeping MGS in a phosphorylated, inactive state. In this context, it is of interest that PTG is scarcely expressed in neurons[32]. The PTG-MGS transcript ratio was approximately 20-fold lower in neurons than in cells that normally accumulate glycogen (**Fig. 3d**).

Because Lafora bodies are composed of poorly branched glucose polymers, we complexed samples isolated from neuronal cells with iodine and recorded the spectra, as described[33], to measure the degree of ramification of the glycogen produced in the experiments described above. Shifting of the absorption maximum to a higher wavelength is indicative of less branching. Normal glycogen gave a peak at 483 nm, whereas that isolated from N2a or primary cultured neurons peaked at 511 nm, indicating that it was poorly branched.

Glycogen accumulation is pro-apoptotic in neuronal cells

To ascertain whether accumulation of this poorly branched glycogen causes alterations in neuronal cells, we examined whether apoptotic markers were present in primary cultured neurons that were forced to accumulate glycogen by overexpression of PTG. Glycogen-accumulating primary cultured neurons showed increased apoptosis compared with controls when measured by TUNEL staining (**Fig. 4a**) and active caspase-3 assays (**Fig. 4b**,**c**).

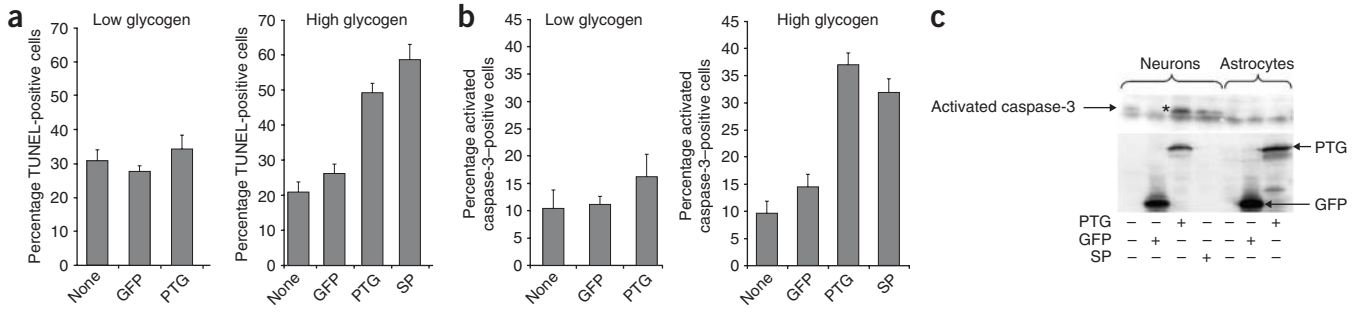

Figure 4 Accumulation of glycogen promotes apoptosis in primary cultured neurons. (**a**) Percentage of TUNEL-positive neurons accumulating low and high levels of glycogen. Glycogen accumulation was modulated by expression of PTG (AdCMV-PTG, MOI 50) for 24 h (low glycogen) or 96 h (high glycogen). GFP in the figure refers to AdCMV-GFP–treated cells (MOI 50). We used a 24-h treatment with 0.1 μM staurosporine as a positive control (SP). The percentage of TUNEL-positive cells was estimated in 8–14 fields (mean ± s.e.m.) in three coverslips for each treatment condition (500–600 total cells). (**b**) Percentage of activated caspase-3–positive neurons (mean ± s.e.m., 8–14 coverslip fields of three independent experiments, 550–600 total cells) in the same experimental conditions shown in **a**. (**c**) Western blot analysis of activated caspase-3 in primary cultured neurons and astrocytes in the same experimental conditions shown in **a** (96 h). Asterisk indicates the activated caspase-3. The lower panel shows a western blot with the GFP antibody.

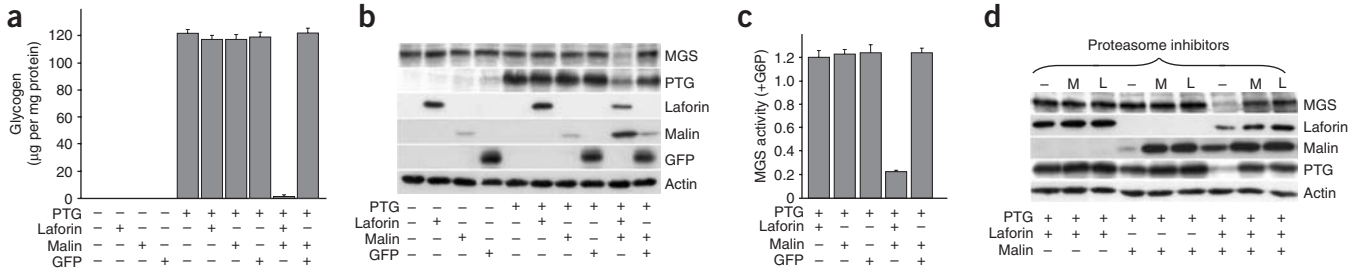

Figure 5 Blockade of glycogen synthesis by laforin and malin. (**a**) Glycogen content of N2a cells (mean ± s.e.m., $n = 14–23$, of 6 independent experiments) incubated with the recombinant adenoviruses indicated, used at a MOI of 20, with the exception of AdCMV-PTG, which was used at a MOI of 5. Malin and laforin coexpression blocked the glycogen accumulation induced by PTG. (**b**) Western blot analysis of N2a cells treated with recombinant adenoviruses in the same conditions as described in **a**. Note that MGS, PTG and laforin signals were markedly reduced when laforin and malin were coexpressed. Actin was used as a control for gel loading. (**c**) Total MGS activity (+G6P) of N2a cells (mean ± s.e.m., $n = 6–8$, of three independent experiments) after infection with AdCMV-PTG, AdCMV-laf, AdCMV-malin and AdCMV-GFP in the same conditions as described in **a**. Total MGS activity was reduced when laforin was coexpressed with malin. (**d**) Western blot analysis of N2a cells incubated with the recombinant adenoviruses indicated in the figure and treated with the proteasome inhibitors MG-132 1 μM (M) or lactacystin 5 μM (L) for 18 h. Proteasome inhibitors were added 4 h after the incubation with the adenoviruses. Cells were processed for western blot 22 h after infection. All of the viruses were used at a MOI of 10, except for AdCMV-PTG, which was used at a MOI of 2. Treatment with proteasome inhibitors blocked the degradation of MGS, laforin and PTG observed in cells expressing both malin and laforin and increased the total amount of malin.

In contrast, astrocytes expressing the same amount of PTG, and therefore synthesizing high levels of glycogen, did not show an activation of caspase-3 (**Fig. 4c**). Therefore, glycogen deposition triggered apoptosis specifically in cultured neurons.

The laforin-malin complex downregulates glycogen synthesis

To determine the role of laforin and malin in the generation of Lafora bodies, we analyzed whether these proteins have the capacity to modulate the PTG-induced accumulation of glycogen in neuronal cells. When laforin and malin were separately coexpressed with PTG in these cells, we did not observe an effect on PTG-induced glycogen accumulation (**Fig. 5a** and **Supplementary Fig. 2** online). However, when both laforin and malin were coexpressed simultaneously with PTG, they completely blocked the activation of glycogen synthesis (**Fig. 5a** and **Supplementary Fig. 2**). In addition, we detected a marked reduction of MGS and PTG levels (**Fig. 5b** and **Supplementary Fig. 2**). The levels of laforin were also diminished, although to a lesser extent (**Fig. 5b**). In contrast, the amount of malin was substantially increased when it was coexpressed with laforin, suggesting that malin is stabilized by laforin. Therefore, malin levels were inversely correlated with those of MGS, PTG and laforin (**Fig. 5b**). The reduction of MGS protein levels was correlated with a sixfold decrease in MGS activity in cells expressing both laforin and malin compared with cells expressing laforin alone (**Fig. 5c**). The effects of malin and laforin on MGS and PTG were specific, as other proteins involved in glycogen metabolism, such as hexokinase I or glycogen synthase kinase 3, were not degraded by the combined action of laforin and malin (data not shown). The proteasome inhibitors MG-132 and lactacystin[34] blocked the decrease of MGS, PTG and laforin levels that was induced by the malin-laforin complex (**Fig. 5d** and **Supplementary Fig. 2**). Quantitative real-time PCR (RT-PCR) analysis confirmed that MGS, laforin and PTG transcript levels were unaffected, indicating that the changes in MGS and PTG protein levels were a consequence of protein degradation through the ubiquitin-proteasome pathway and were not caused by alterations at the transcription level (data not shown). These data suggest that the laforin-malin complex is important in the modulation of MGS and PTG levels. Proteasome-dependent degradation of laforin, together with PTG and MGS, may act as a safety switch; that is, when laforin levels are reduced, no laforin-malin complexes are formed, and therefore MGS and PTG degradation will not occur. In addition, the amount of malin expressed in the absence of laforin was higher when these proteasome inhibitors were present. This observation suggests that malin is also degraded through the ubiquitin-proteasome pathway (**Fig. 5d**).

In a survey of individuals with Lafora disease, we identified a malin mutation (D146N) that specifically disrupts the interaction between laforin and malin without altering the E3 ubiquitin ligase activity of the latter (M.C. Solaz-Fuster, J.V. Gimeno-Alcañiz, S.R., M.E. Fernández-Sánchez, B.G.-F., O.C.-G., D.V., J.D., M.G.-R., M. Sánchez-Piris, C. Aguado, E. Knecht, J. Serratosa, J.J.G., P. Sanz and S.R.d.C., unpublished data). Notably, D146N did not impair PTG-induced glycogen accumulation in the presence of laforin (**Fig. 6a**) and, in contrast to wild-type malin, failed to induce the degradation of MGS and PTG (**Fig. 6b**). Therefore, the malin-laforin interaction is crucial for the action of these two proteins on neuronal glycogen metabolism.

If laforin and malin are required to decrease the levels of MGS and PTG, the absence of these proteins in individuals with Lafora disease should result in increased MGS and PTG levels. To test this, we mimicked the pathological condition by silencing laforin expression in neuronal cells using short interfering RNA (siRNA) oligonucleotides (**Fig. 6c**). The knockdown of laforin by two distinct siRNAs caused a marked increase in MGS and PTG levels compared with those in cells transfected with control siRNA (**Fig. 6d**,**e**). More glycogen accumulated in these cells under glycogenic conditions (**Fig. 6f**). These results establish the involvement of the laforin-malin system in the control of MGS and PTG stability and glycogen synthesis.

DISCUSSION

Our findings demonstrate the existence of a previously unknown regulatory mechanism for glycogen accumulation in neurons, which operates through the proteasome-mediated degradation of both MGS and PTG, with the latter being the key protein for MGS activation (see schematic in **Supplementary Fig. 3** online). MGS is a highly regulated enzyme. It is activated by G6P and inactivated by phosphorylation at multiple sites[35]. Furthermore, it is also regulated by changes in its subcellular localization in response to the metabolic status of the cell[24]. The mechanism demonstrated here, mediated by the laforin-malin complex, represents an additional control step that is superimposed on

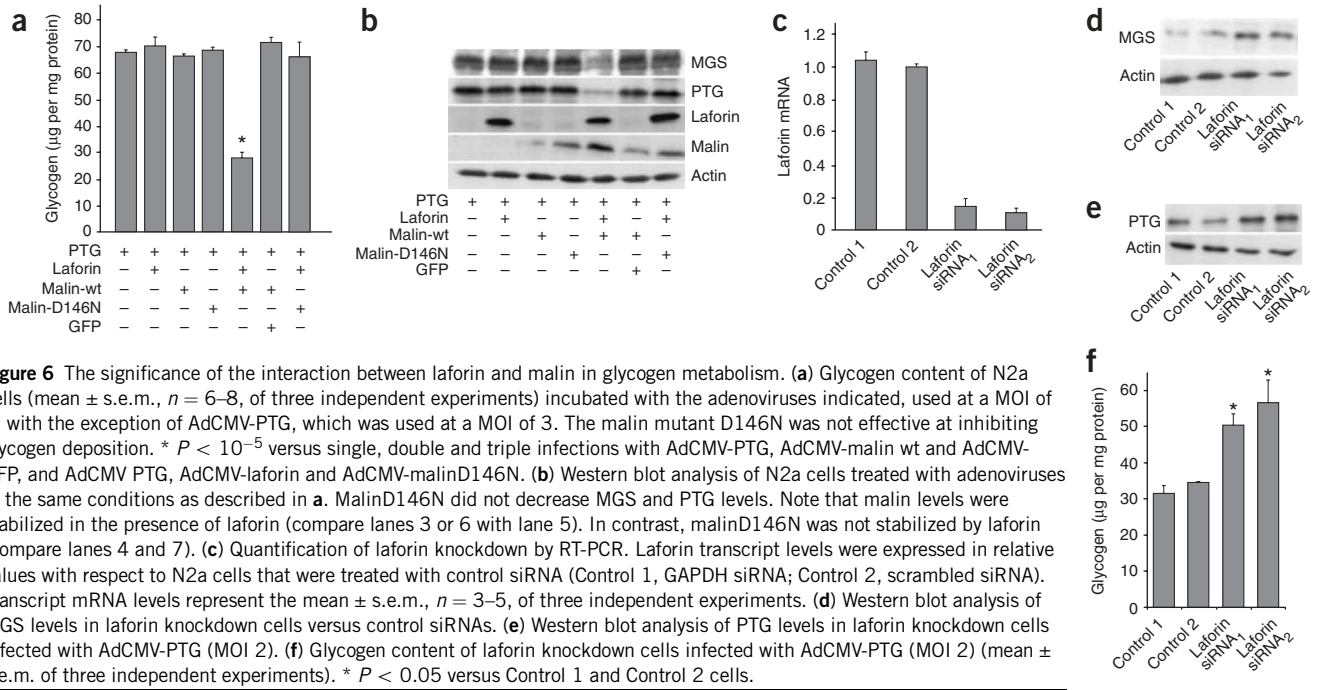

Figure 6 The significance of the interaction between laforin and malin in glycogen metabolism. (**a**) Glycogen content of N2a cells (mean ± s.e.m., $n = 6$–8, of three independent experiments) incubated with the adenoviruses indicated, used at a MOI of 5, with the exception of AdCMV-PTG, which was used at a MOI of 3. The malin mutant D146N was not effective at inhibiting glycogen deposition. * $P < 10^{-5}$ versus single, double and triple infections with AdCMV-PTG, AdCMV-malin wt and AdCMV-GFP, and AdCMV PTG, AdCMV-laforin and AdCMV-malinD146N. (**b**) Western blot analysis of N2a cells treated with adenoviruses in the same conditions as described in **a**. MalinD146N did not decrease MGS and PTG levels. Note that malin levels were stabilized in the presence of laforin (compare lanes 3 or 6 with lane 5). In contrast, malinD146N was not stabilized by laforin (compare lanes 4 and 7). (**c**) Quantification of laforin knockdown by RT-PCR. Laforin transcript levels were expressed in relative values with respect to N2a cells that were treated with control siRNA (Control 1, GAPDH siRNA; Control 2, scrambled siRNA). Transcript mRNA levels represent the mean ± s.e.m., $n = 3$–5, of three independent experiments. (**d**) Western blot analysis of MGS levels in laforin knockdown cells versus control siRNAs. (**e**) Western blot analysis of PTG levels in laforin knockdown cells infected with AdCMV-PTG (MOI 2). (**f**) Glycogen content of laforin knockdown cells infected with AdCMV-PTG (MOI 2) (mean ± s.e.m. of three independent experiments). * $P < 0.05$ versus Control 1 and Control 2 cells.

the previously known ones described above, and adds a further level of complexity to the control of glycogen synthesis. Although prevalent in neurons, this mechanism is probably involved in the regulation of glycogen synthesis more generally, as laforin and malin are not restricted to neurons. This mechanism probably serves to prevent excessive glycogen accumulation in certain tissues or under specific physiological conditions.

Furthermore, we demonstrate here that, against general belief, neurons have the machinery to synthesize glycogen, but this capacity is silenced by the inactivation of neuronal MGS through extensive phosphorylation and by the mechanism described here, which further ensures the blockage of glycogen synthesis by degrading both MGS and PTG. Altogether, these apparently redundant control mechanisms for glycogen synthesis may reflect the need to prevent glycogen accumulation in neurons. Neurons do not express detectable amounts of glycogen phosphorylase, the key enzyme for glycogen degradation. Therefore, the degradation of glycogen, should it accumulate, would not be feasible. Furthermore, when MGS becomes active, neurons accumulate poorly branched glycogen (polyglucosan). This observation illustrates the necessity of strictly controlling MGS activity in neurons.

As we have shown, deposition of this poorly branched glycogen is associated with deleterious effects in neuronal cells, as it activates the apoptotic program. Consequently, the previously unknown regulatory mechanism for glycogen synthesis that we report here is probably critical for preventing the accumulation of a dangerous molecule in the cytoplasm of neurons. Disturbance of this mechanism, as a consequence of loss-of-function mutations in laforin or malin, would explain the accumulation of intracellular inclusion bodies of glycogen-like composition in neurons (and in other cell types). We do not know the extent to which this phenomenon may be responsible for the cardinal clinical manifestations of Lafora disease. Although our results are consistent with the hypothesis that glycogen deposition triggers the alterations of neuronal function in Lafora disease, we cannot exclude the possibility that other potential targets of the laforin-malin complex are also involved in the pathogenesis of this disease. Whether this complex also triggers the degradation of other proteins is unknown.

In addition, our results raise the question of why neurons have maintained MGS expression throughout evolution if it must be kept strictly inactive under normal conditions. One possibility is that the genomic structure of the MGS gene (*Gys1*) does not allow for the silencing of MGS expression in neurons without interfering with the expression of other relevant neuronal genes or with the expression of MGS in other cell types. Alternatively, MGS may have a second, as yet undiscovered, fundamental function in neurons.

METHODS

Primary cultures of neurons and astrocytes. We obtained telencephalic neuron cultures from mouse embryos at embryonic day 16 (OF1 mice, Charles River Laboratories) as described[36] (**Supplementary Methods** online). These experiments were approved by the Barcelona Science Park's Animal Experimentation Committee and were carried out in accordance with the European Community Council Directive and the US National Institutes of Health guidelines for the care and use of laboratory animals. Enzymes and biochemical reagents were from Sigma, unless otherwise indicated. All other chemicals were of analytical grade. We cultured cells in serum-free Neurobasal medium (Invitrogen) supplemented with 2 mM L-glutamine (Invitrogen), 30 mM D-glucose, 5 mM $NaHCO_3$ (Invitrogen), penicillin (100 U ml^{-1}, Invitrogen), streptomycin (100 mg ml^{-1}, Invitrogen) and B27 supplement diluted 1:50 (Invitrogen). After 1 d of culture, we treated cells with uridine (50 μg ml^{-1}) and 5-fluoro-2′-deoxyuridine (20 μg ml^{-1}) to minimize the contamination by astrocytes. Primary cultures of neurons were infected at 5 d in culture for 12 h with adenoviruses at diverse multiplicities of infection (MOI) depending on the experiments. After removal of the virus-containing media, infected cells were maintained for 48 h in neuronal culture medium. For primary cultures of astrocytes, we cultured dissociated cells in Neurobasal medium supplemented with 2 mM L-glutamine, 30 mM D-glucose, 5 mM $NaHCO_3$, penicillin (100 U ml^{-1}), streptomycin (100 mg ml^{-1}), 5% horse serum and 5% fetal bovine serum (FBS). Primary cultures of astrocytes were incubated for 2 h with adenoviruses at diverse MOIs. After removal of the virus-containing media, astrocytes were incubated for 48 h with astrocyte culture medium.

N2a cells. We cultured N2a cells (American Type Culture Collection, CCL-131) in Dulbecco's modified eagle medium (DMEM, Invitrogen) supplemented with

2 mM L-glutamine, 25 mM D-glucose, penicillin (100 U ml^{-1}), streptomycin (100 mg ml^{-1}) and 10% FBS. Cells differentiated after being cultured for 72 h in FBS-free DMEM (with supplements). N2a cells were incubated for 2 h with adenoviruses at various MOIs. After removal of the virus-containing media, N2a cells were incubated for 48 h with N2a differentiation medium.

Preparation of recombinant adenovirus. Recombinant adenoviruses coding for rat liver glucokinase (AdCMV-GK)[37], rat liver hexokinase I (AdCMV-HKI)[37], green fluorescent protein (GFP) (AdCMV-GFP)[22], human MGS (AdCMV-MGS)[22] and human MGS fused to GFP (AdCMV-GFP-MGS)[25] have been described. We generated recombinant adenoviruses coding for the mouse PTG fused to GFP (AdCMV-PTG), human laforin (AdCMV-laf), wild-type (wt) human malin (AdCMV-malin) and mutant D146N human malin (AdCMV-malinD146N) fused to hemagglutinin epitope (HA). We obtained the coding sequence for PTG by amplification of mouse hepatocyte genomic DNA using the oligonucleotide primers 5′-CCG AAT TCG GNA CGA GAT GTG CTA GAT CC-3′ and 5′-CGC CAG TGT GCT GGA ATT CTC AAG TAG-3′. The coding sequence for PTG was then ligated into the pEGFP-C1 vector (Clontech), which was previously digested with *Bgl*II. The generation of the pCINeo-Laforin vector was described previously[31]. The coding sequence of human malin was amplified from human spleen genomic DNA by PCR using the oligonucleotide primers 5′-GGA TCC TAT GGC GGC CGA AGC-3′ and 5′-GAG ATC TCA CAA TTC ATT AAT GGC AGA C-3′, and was cloned into the mammalian expression vector pcDNA3, which contained an N-terminal HA tag. This pcDNA3–Malin wt–HA vector was used as the template for the introduction of mutation D146N by PCR, using the QuikChange Site-Directed Mutagenesis Kit (Stratagene). Then pEGFP-PTG, pCINeo-Laforin, pcDNA3–Malin wt–HA and pcDNA3–Malin D146N–HA vectors were used as templates for subcloning all of the selected cDNAs into the pAC.CMVpLpA plasmid[38] using the BD In Fusion PCR Cloning kit (Clontech) and appropriate oligonucleotides (5′-CGA GCT CGG TAC CCG GGA TAC CAC CAT GGC C-3′ and 5′-CTG CAG GTC GAC TCT AGA TCA GCG AGC TCT AG-3′ for laforin, 5′-CGA GCT CGG TAC CCG GGC GAC TCA CTA TAG GC-3′ and 5′-CTG CAG GTC GAC TCT AGT CGA CTC TAG ACC AG-3′ for wt malin-HA and malin D146N-HA, and 5′-CGA GCT CGG TAC CCG GGC GGG TAC CGG TCG CC-3′ and 5′-AAG CTA TAG CTA CTT GCT AGA GTC GAC CTG CAG-3′ for PTG-GFP).

To obtain the infective particles, human kidney 293 cells (cultured in DMEM supplemented with 10% FBS) were cotransfected with pAC.CMV plasmids containing the PTG-GFP, laforin, wt malin-HA or malin D146N-HA cDNAs and the pJM17 plasmid[39], and then amplified[38]. We confirmed the absence of errors by extracting and sequencing viral DNA[38] from all of the adenoviruses generated.

RNA interference. We used two independent siRNAs to target laforin: laforin $siRNA_1$ (Ambion, predesigned siRNA#16708: sense, 5′-GCA CAA CAA GAC UUU UCU Ctt-3′, and antisense, 5′-GAG AAA AGU CUU GUU GUG Ctt-3′) and laforin $siRNA_2$ (Custom SMARTpool siRNA designed to target laforin, Dharmacon). We used GAPDH human, mouse and rat siRNAs as positive controls and Negative Control #1 siRNA (Ambion, catalog #4624) as a negative control. We transfected a concentration of 100 nM of each siRNA into N2a cells using Lipofectamine 2000 (Invitrogen), following the manufacturer's instructions. We measured the efficiency of laforin knockdown by RT-PCR analysis.

Electrophoresis and immunoblotting. Cell-culture plates were processed for protein extract preparation (**Supplementary Methods**). Proteins were resolved by 10% SDS-PAGE, transferred onto a nitrocellulose membrane (Schleicher and Schuell) and probed with the following antibodies: rabbit antibody to human MGS (MGS3), which recognizes MGS independently of its phosphorylation state[25], sheep antibody to MGS phosphorylated on Ser7 and 10 (PGSser7/10, a gift from D.G. Hardie, University of Dundee, UK)[40], rabbit antibody to MGS phosphorylated on Ser640 (PGSser641, Cell Signaling), rabbit antibody to glial fibrillary acidic protein (GFAP, DakoCytomation), rabbit antibody to GFP (Immunokontact), mouse antibody to β-actin, mouse antibody to HA and mouse antibody to laforin. Antibody to brain glycogen phosphorylase was produced by Eurogentec: chickens were immunized against a peptide at the C terminus (GVEPSDLQIPPPNLPKD, amino acids 826–842) of mouse brain glycogen phosphorylase. For further details about the secondary antibodies used in this study see the **Supplementary Methods**.

Immunocytochemistry. Cells seeded on poly-L-lysine–coated coverslips were fixed for 30 min in PBS containing 4% (w/v) paraformaldehyde. After fixation, cells were incubated with $NaBH_4$ (1 mg ml^{-1}) for 10 min and permeabilized for 20 min with PBS containing 0.2% (v/v) Triton X-100. Blocking and incubation with the primary and secondary antibodies were carried out as previously described[25]. Coverslips were washed, air-dried and mounted onto glass slides using Mowiol as mounting medium. We used primary antibodies to MGS3 and GFAP, mouse antibody to β-III-tubulin (TUJ1) and a monoclonal antibody against glycogen (a gift from O. Baba, Tokyo Medical and Dental University)[41]. In some cases, nuclei were stained with Hoechst 33342 (Molecular Probes). For information about the secondary antibodies used, see the **Supplementary Methods**. Fluorescence images were obtained with a Leica SPII Spectral microscope (Leica Lasertechnik). The light source was an argon/krypton laser (75 mW), and optical sections (0.1 μm) were obtained.

Apoptosis assays. Neurons seeded onto poly-L-lysine–coated coverslips were fixed for 30 min in PBS containing 4% (w/v) paraformaldehyde and processed for TUNEL or active caspase-3 staining. TUNEL assays were carried out using the ApopTag Peroxidase *in situ* Apoptosis Detection Kit (Chemicon), following the manufacturer's instructions. Active caspase-3–positive cells were visualized by immunocytochemistry using the cleaved caspase-3 antibody (Cell Signaling) (**Supplementary Methods**). The TUNEL- and active caspase-3–positive cells were photographed with a Nikon Eclipse E-600 microscope using a 40× objective. The percentage of positive cells was estimated in 8–14 fields from each of three coverslips (three independent experiments) for each treatment condition (500–600 total cells). Total number of cells was evidenced after staining of nuclei with Hoechst 33342.

RNA purification and retro-transcription. Total RNA was isolated from mouse tissue and reverse transcribed as described in the **Supplementary Methods**. A series of specific primers were designed to specifically amplify a fragment of the coding sequence of mouse MGS, LGS and GFAP (**Supplementary Methods**).

Quantitative RT-PCR. We followed the standard RT-PCR protocol of the ABI Prism 7700 Detection System, together with the ready-made TaqMan primer and probe sets (Applied Biosystems). Each sample was analyzed in triplicate wells with 30 ng of first-strand cDNA in a total reaction volume of 20 μl. The temperature profile consisted of 40 cycles of 15 s at 95 °C and 1 min at 60 °C. Data was analyzed with the comparative 2ΔΔCt method using ribosomal 18S as endogenous control.

Metabolite determinations. To measure glycogen content, we scraped cell monolayers into 30% KOH and heated the extract for 15 min at 100 °C. We measured glycogen as described previously[42]. To assess glycogen branching, we used a previously described method based on the iodine absorption spectrum[33]. The intracellular concentration of G6P was measured by a spectrophotometric assay[43].

Determination of MGS activity. Cell-culture plates were processed as described in the **Supplementary Methods**. Protein concentration was measured by the Bradford method[44]. MGS activity was measured in homogenates in the absence or presence of 6.6 mM G6P, as described previously[45]. The activity measured in the absence of G6P represents the active form of MGS (I or a form), whereas the activity measured in the presence of 6.6 mM G6P represents total MGS activity. The –G6P/+G6P activity ratio is a nonlinear measurement of the activation state of the enzyme. Values below 0.1 indicate an essentially fully inactive enzyme, whereas those above 0.7 are equivalent to full activation[46].

Statistical analysis. Results were analyzed for significance by ANOVA and unpaired Student's *t* test. $P < 0.05$ was considered to be significant.

Note: Supplementary information is available on the Nature Neuroscience website.

ACKNOWLEDGMENTS

We thank J. Massagué for providing a critical review of the manuscript, P. Sanz and J.M. Serratosa for their advice, A. Adrover and E. Veza for their technical support, and T. Yates for correcting the manuscript. We also thank R.R. Gomis for the AdCMV-PTG virus, O. Baba for the monoclonal antibody to glycogen and D.G. Hardy for the gift of the PGSser7/10 antibody. This study was supported by grants from the *Fundació La Caixa*, *Fundació La Marató de TV3*, *Fundación Marcelino Botín*, the Spanish Ministry of Education and Science (SAF2005-00913; BFU2005-02253) and the *Instituto de Salud Carlos III* (CIBER-ER; RD06/0015/0030).

AUTHOR CONTRIBUTIONS

D.V. conducted most of the experiments, data analysis and interpretation. S.R. generated the AdCMV-laf, AdCMV-malin and AdCMV-malinD146N recombinant adenoviruses. D.C. carried out the RT-PCR experiments. L.P. contributed to the primary neuron cultures and the apoptosis assays. J.V. carried out the analysis of glycogen branching. S.R., D.C. and J.V. also contributed to other experiments. B.G.-F., O.C.-G., E.F.-S. and I.M.-F. generated the monoclonal laforin antibody, pCINeo-Laforin vector and pcDNA3-Malin-HA vector. J.D. supervised several experiments and the data analysis, and contributed to writing the manuscript. M.G.-R. supervised the western blot and immunofluorescence experiments. E.S. contributed with his knowledge of the nervous system. S.R.d.C. and J.J.G. planned and supervised the project, co-wrote the manuscript and contributed to every aspect of the project.

Published online at http://www.nature.com/natureneuroscience
Reprints and permissions information is available online at http://npg.nature.com/reprintsandpermissions

1. Brown, A.M. Brain glycogen re-awakened. *J. Neurochem.* **89**, 537–552 (2004).
2. Cavanagh, J.B. Corpora-amylacea and the family of polyglucosan diseases. *Brain Res. Brain Res. Rev.* **29**, 265–295 (1999).
3. Berkovic, S.F., Andermann, F., Carpenter, S. & Wolfe, L.S. Progressive myoclonus epilepsies: specific causes and diagnosis. *N. Engl. J. Med.* **315**, 296–305 (1986).
4. Lafora, G.R. Über das corkommen amyloider körperchen im innern der ganglienzellen; zugliech ein zum studium der amyloiden substanz im nervensystem. *Virchows Arch. Pathol. Anat.* **205**, 294–303 (1911).
5. Lafora, G.R. & Glueck, B. Beitrag zur histogpathologie der myoklonischen epilepsie. Z. *Gesamte Neurol. Psychiatr.* **6**, 1–14 (1911).
6. Collins, G.H., Cowden, R.R. & Nevis, A.H. Myoclonus epilepsy with Lafora bodies. An ultrastructural and cytochemical study. *Arch. Pathol.* **86**, 239–254 (1968).
7. Sakai, M., Austin, J., Witmer, F. & Trueb, L. Studies in myoclonus epilepsy (Lafora body form). II. Polyglucosans in the systemic deposits of myoclonus epilepsy and in corpora amylacea. *Neurology* **20**, 160–176 (1970).
8. Acharya, J.N., Satishchandra, P. & Shankar, S.K. Familial progressive myoclonus epilepsy: clinical and electrophysiologic observations. *Epilepsia* **36**, 429–434 (1995).
9. Berkovic, S.F., Cochius, J., Andermann, E. & Andermann, F. Progressive myoclonus epilepsies: clinical and genetic aspects. *Epilepsia* **34** (Suppl 3): S19–S30 (1993).
10. Kobayashi, K., Iyoda, K., Ohtsuka, Y., Ohtahara, S. & Yamada, M. Longitudinal clinicoelectrophysiologic study of a case of Lafora disease proven by skin biopsy. *Epilepsia* **31**, 194–201 (1990).
11. Minassian, B.A. Lafora's disease: towards a clinical, pathologic and molecular synthesis. *Pediatr. Neurol.* **25**, 21–29 (2001).
12. Shahwan, A., Farrell, M. & Delanty, N. Progressive myoclonic epilepsies: a review of genetic and therapeutic aspects. *Lancet Neurol.* **4**, 239–248 (2005).
13. Van Heycop Ten Ham, M.W. Lafora disease, a form of progressive myoclonues epilepsy. *Handb. Clin. Neurol.* **15**, 382–422 (1974).
14. Minassian, B.A. *et al.* Mutations in a gene encoding a novel protein tyrosine phosphatase cause progressive myoclonus epilepsy. *Nat. Genet.* **20**, 171–174 (1998).
15. Minassian, B.A. *et al.* Mutation spectrum and predicted function of laforin in Lafora's progressive myoclonus epilepsy. *Neurology* **55**, 341–346 (2000).
16. Serratosa, J.M. *et al.* A novel protein tyrosine phosphatase gene is mutated in progressive myoclonus epilepsy of the Lafora type (EPM2). *Hum. Mol. Genet.* **8**, 345–352 (1999).
17. Wang, J., Stuckey, J.A., Wishart, M.J. & Dixon, J.E. A unique carbohydrate binding domain targets the lafora disease phosphatase to glycogen. *J. Biol. Chem.* **277**, 2377–2380 (2002).
18. Ganesh, S., Puri, R., Singh, S., Mittal, S. & Dubey, D. Recent advances in the molecular basis of Lafora's progressive myoclonus epilepsy. *J. Hum. Genet.* **51**, 1–8 (2006).
19. Chan, E.M. *et al.* Mutations in NHLRC1 cause progressive myoclonus epilepsy. *Nat. Genet.* **35**, 125–127 (2003).
20. Gentry, M.S., Worby, C.A. & Dixon, J.E. Insights into Lafora disease: malin is an E3 ubiquitin ligase that ubiquitinates and promotes the degradation of laforin. *Proc. Natl. Acad. Sci. USA* **102**, 8501–8506 (2005).
21. Ferrer, J.C. *et al.* Control of glycogen deposition. *FEBS Lett.* **546**, 127–132 (2003).
22. Gomis, R.R., Cid, E., Garcia-Rocha, M., Ferrer, J.C. & Guinovart, J.J. Liver glycogen synthase but not the muscle isoform differentiates between glucose 6-phosphate produced by glucokinase or hexokinase. *J. Biol. Chem.* **277**, 23246–23252 (2002).
23. Skurat, A.V., Dietrich, A.D. & Roach, P.J. Glycogen synthase sensitivity to insulin and glucose-6-phosphate is mediated by both NH2- and COOH-terminal phosphorylation sites. *Diabetes* **49**, 1096–1100 (2000).
24. Ferrer, J.C., Baque, S. & Guinovart, J.J. Muscle glycogen synthase translocates from the cell nucleus to the cystosol in response to glucose. *FEBS Lett.* **415**, 249–252 (1997).
25. Cid, E., Cifuentes, D., Baque, S., Ferrer, J.C. & Guinovart, J.J. Determinants of the nucleocytoplasmic shuttling of muscle glycogen synthase. *FEBS J.* **272**, 3197–3213 (2005).
26. Skurat, A.V., Wang, Y. & Roach, P.J. Rabbit skeletal muscle glycogen synthase expressed in COS cells. Identification of regulatory phosphorylation sites. *J. Biol. Chem.* **269**, 25534–25542 (1994).
27. MacAulay, K. *et al.* Use of lithium and SB-415286 to explore the role of glycogen synthase kinase-3 in the regulation of glucose transport and glycogen synthase. *Eur. J. Biochem.* **270**, 3829–3838 (2003).
28. Printen, J.A., Brady, M.J. & Saltiel, A.R. PTG, a protein phosphatase 1–binding protein with a role in glycogen metabolism. *Science* **275**, 1475–1478 (1997).
29. Fong, N.M. *et al.* Identification of binding sites on protein targeting to glycogen for enzymes of glycogen metabolism. *J. Biol. Chem.* **275**, 35034–35039 (2000).
30. Berman, H.K., O'Doherty, R.M., Anderson, P. & Newgard, C.B. Overexpression of protein targeting to glycogen (PTG) in rat hepatocytes causes profound activation of glycogen synthesis independent of normal hormone- and substrate-mediated regulatory mechanisms. *J. Biol. Chem.* **273**, 26421–26425 (1998).
31. Fernandez-Sanchez, M.E. *et al.* Laforin, the dual-phosphatase responsible for Lafora disease, interacts with R5 (PTG), a regulatory subunit of protein phosphatase 1 that enhances glycogen accumulation. *Hum. Mol. Genet.* **12**, 3161–3171 (2003).
32. Allaman, I., Pellerin, L. & Magistretti, P.J. Protein targeting to glycogen mRNA expression is stimulated by noradrenaline in mouse cortical astrocytes. *Glia* **30**, 382–391 (2000).
33. Schlamowitz, M. On the nature of rabbit liver glycogen. II. Iodine absorption spectrum. *J. Biol. Chem.* **190**, 519–527 (1951).
34. Lee, D.H. & Goldberg, A.L. Proteasome inhibitors: valuable new tools for cell biologists. *Trends Cell Biol.* **8**, 397–403 (1998).
35. Villar-Palasi, C. & Guinovart, J.J. The role of glucose-6-phosphate in the control of glycogen synthase. *FASEB J.* **11**, 544–558 (1997).
36. Simo, S. *et al.* Reelin induces the detachment of postnatal subventricular zone cells and the expression of the Egr-1 through Erk1/2 activation. *Cereb. Cortex* **17**, 294–303 (2007).
37. Seoane, J. *et al.* Glucose-6-phosphate produced by glucokinase, but not hexokinase I, promotes the activation of hepatic glycogen synthase. *J. Biol. Chem.* **271**, 23756–23760 (1996).
38. Becker, T.C. *et al.* Use of recombinant adenovirus for metabolic engineering of mammalian cells. *Methods Cell Biol.* **43** (Pt A): 161–189 (1994).
39. McGrory, W.J., Bautista, D.S. & Graham, F.L. A simple technique for the rescue of early region I mutations into infectious human adenovirus type 5. *Virology* **163**, 614–617 (1988).
40. Hojlund, K. *et al.* Increased phosphorylation of skeletal muscle glycogen synthase at NH2-terminal sites during physiological hyperinsulinemia in type 2 diabetes. *Diabetes* **52**, 1393–1402 (2003).
41. Baba, O. [Production of monoclonal antibody that recognizes glycogen and its application for immunohistochemistry.]. *Kokubyo Gakkai Zasshi.* **60**, 264–287 (1993).
42. Chan, T.M. & Exton, J.H. A rapid method for the determination of glycogen content and radioactivity in small quantities of tissue or isolated hepatocytes. *Anal. Biochem.* **71**, 96–105 (1976).
43. Lang, G. & Michal, G. D-glucose-6-phosphate and D-Fructose-6-phosphate. in *Methods of Enzymatic Analysis* (ed. Bergmeyer, H. U.) 1238–1242 (Academic Press, New York, 1974).
44. Bradford, M.M. A rapid and sensitive method for the quantitation of microgram quantities of protein utilizing the principle of protein-dye binding. *Anal. Biochem.* **72**, 248–254 (1976).
45. Thomas, J.A., Schlender, K.K. & Larner, J. A rapid filter paper assay for UDPglucose-glycogen glucosyltransferase, including an improved biosynthesis of UDP-14C-glucose. *Anal. Biochem.* **25**, 486–499 (1968).
46. Guinovart, J.J. *et al.* Glycogen synthase: a new activity ratio assay expressing a high sensitivity to the phosphorylation state. *FEBS Lett.* **106**, 284–288 (1979).

Supplementary Figure 1 Vilchez et al.

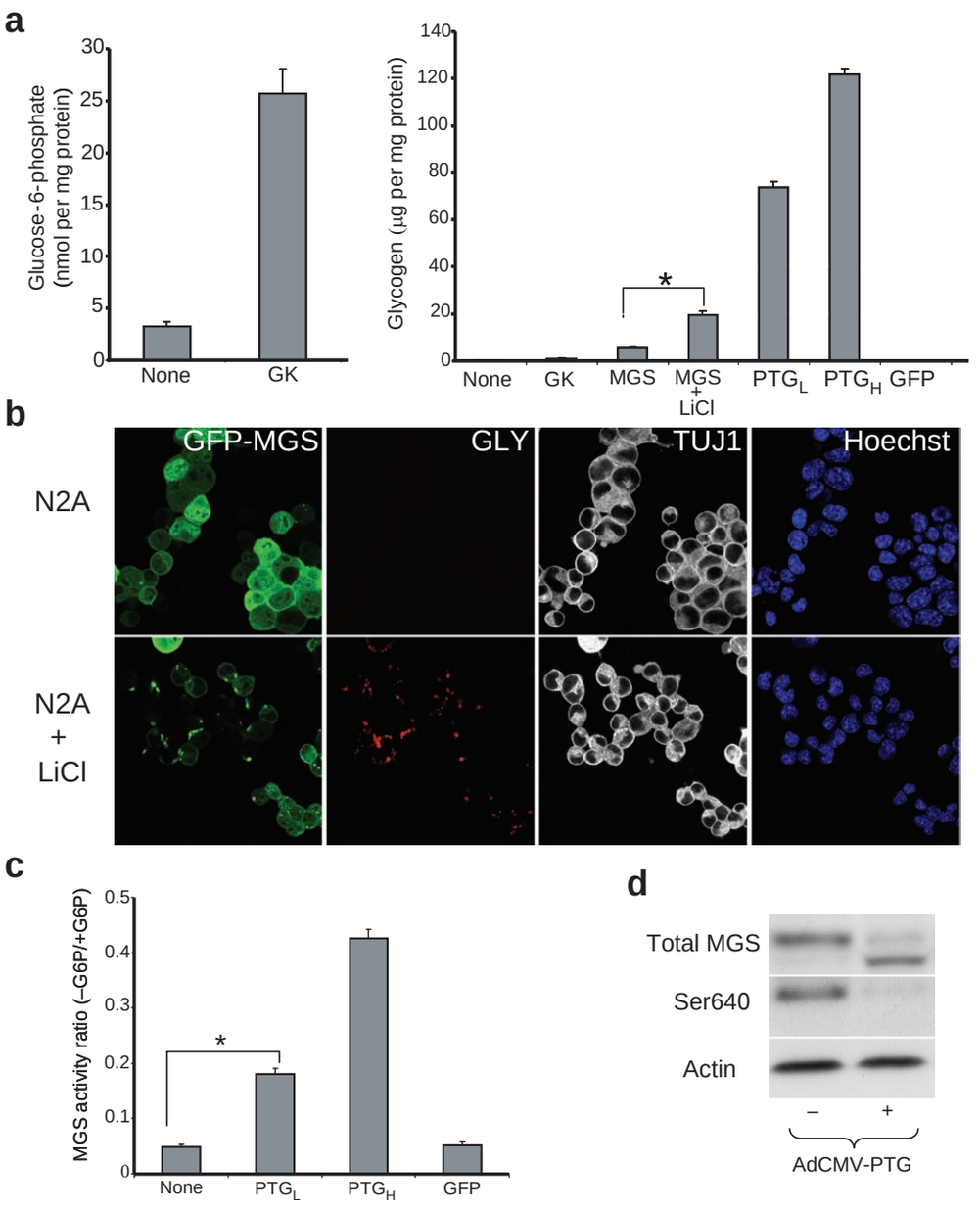

Supplementary Figure 1. Glycogen metabolism in N2a cells. **(a)** Graphs show the intracellular levels of G6P (left) and glycogen content (right) of N2a cells that were incubated with AdCMV-GK (MOI 10), AdCMV-MGS (MOI 10), AdCMV-GFP (MOI 10) and AdCMV-PTG at low (3) and high (5) MOI. None = non-infected neurons. A 7.9-fold increase in the levels of G6P did not have significant effects on glycogen accumulation. MGS-overexpressing cells accumulated glycogen after treatment with 20 mM LiCl for 24 h (*p<0.005 AdCMV-MGS vs. AdCMV-MGS + 20 mM LiCl). PTG had a dramatic effect on the stimulation of glycogen deposition. G6P levels represent the mean ± s.e.m. (n=5-9) of three independent experiments. Glycogen content represents the mean ± s.e.m. (n=6-24) of four independent experiments. **(b)** Immunofluorescence analysis with anti-glycogen (GLY) and a specific neuronal marker (TUJ1) of N2a cells treated with AdCMV-GFP-MGS (MOI 5). Cell nuclei were stained with Hoechst 33342. MGS-overexpressing cells accumulated glycogen when treated with 20 mM LiCl for 24 h. All images were acquired using a 63x objective with additional 1.4 confocal magnification. **(c)** MGS activity ratio (–G6P/+G6P) of N2a cells treated with AdCMV-GFP (MOI 5), AdCMV-PTG at low (3) and high (5) MOI. None = non-infected neurons. MGS activity ratio represents the mean ± s.e.m., n=7-9, of 3 independent experiments. *p<10-8 non-infected vs. AdCMV-PTGL. **(d)** Western blot analysis of N2a cells treated (+) or not (–) with AdCMV-PTG (MOI 10) incubated with antibodies that recognize total, and phosphorylated MGS in Ser640.

Supplementary Figure 2 Vilchez et al.

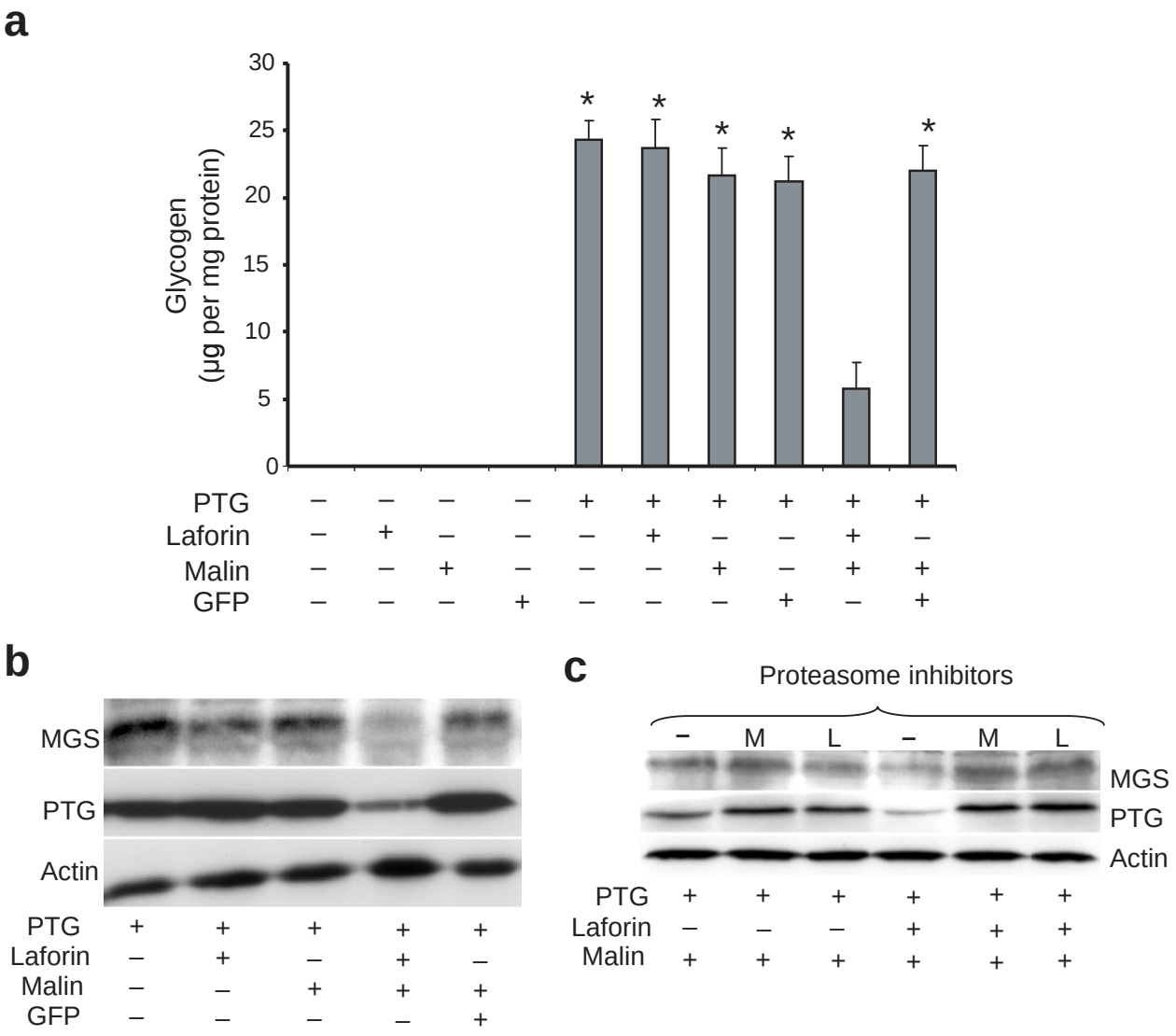

Supplementary Figure 2. The laforin-malin complex downregulates glycogen synthesis in primary cultured neurons. **(a)** Glycogen content (mean ± s.e.m. of 3 independent experiments) of primary cultured neurons incubated with the recombinant adenoviruses shown in the figure used at a MOI of 40, except AdCMV-PTG, which was used at a MOI of 30. Malin and laforin co-expression blocked the glycogen accumulation induced by PTG. *p<0.001 vs. non-infected, single infections with AdCMV-laf, AdCMV-malin or AdCMV-GFP and triple infection with AdCMV-PTG + AdCMV-laf + AdCMV-malin. **(b)** Western blot analysis of neurons treated with recombinant adenoviruses in the same conditions as described in **a**. Note that MGS and PTG signals were dramatically reduced when laforin and malin were co-expressed. **(c)** Proteasome inhibition blocks degradation of MGS and PTG by laforin and malin. Neurons were incubated with the recombinant adenoviruses indicated in the figure in the same conditions as described above and treated with the proteasome inhibitors, MG-132 5mM (M) or lactacystin 15 mM (L), for 24 h. Proteasome inhibitors were added 24 h after the incubation with the adenoviruses.

Supplementary Figure 3 Vilchez et al.

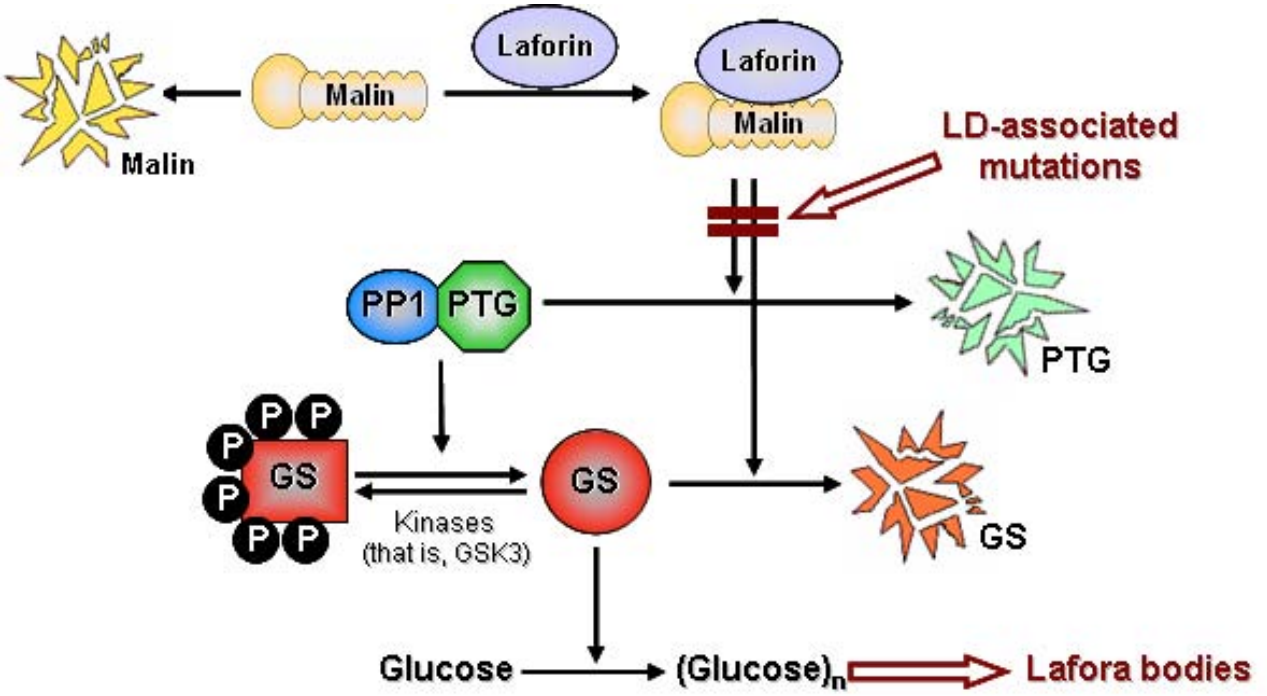

Supplementary Figure 3. Proposed role of laforin-malin complex in glycogen synthesis regulation.

Mechanism suppressing glycogen synthesis in neurons and its demise in progressive myoclonus epilepsy.

David Vilchez[1], Susana Ros[1], Daniel Cifuentes[1], Lluís Pujadas[1], Jordi Vallès[1], Belen Garcia-Fojeda[2], Olga Criado-Garcia[2], Elena Fernández-Sánchez[2], Mª Iria Medraño[2], Jorge Domínguez[1], Mar García-Rocha[1], Eduardo Soriano[1], Santiago Rodríguez de Córdoba[2],* and Joan J. Guinovart[1,*]

Supplementary Methods

Enzymes and biochemical reagents were from Sigma, unless otherwise indicated. All other chemicals were of analytical grade.

Primary cultures of neurons and astrocytes. Telencephalic neurons cultures were obtained from mouse embryos at embryonic day 16 (OF1 mice, Charles River Laboratories). The experiments were approved by the Barcelona Science Park's Animal Experimentation Committee and were carried out in accordance with the European Community Council Directive and the National Institute of Health guidelines for the care and use of laboratory animals. Briefly, mouse brains were dissected in PBS containing 0.6% glucose (w/v). After removal of the meninges, the telencephalon was mechanically and enzymatically dissociated with 0.25% trypsin (Invitrogen). Dissociated cells were then seeded on plates (Nunc) pre-treated with poly-L-lysine (10 μg ml^{-1}) and maintained in serum-free Neurobasal medium (Invitrogen) supplemented with 2 mM L-glutamine (Invitrogen), 30 mM D-(+)-glucose, 5 mM sodium bicarbonate (Invitrogen), penicillin/streptomycin (100 U ml^{-1}, 100 mg ml^{-1}, Invitrogen) and B27 supplement diluted 1/50 (Invitrogen). After one day in culture, we treated

the cells with Uridine/5-fluoro-2'-deoxyuridine (50 µg ml^{-1}, 20 µg ml^{-1}) to minimize contamination by astrocytes. The purity of the cultures was determined by immunocytochemistry with neuron- (anti β-III-tubulin (TUJ1, BAbCO), and astrocyte- (anti-glial fibrillar acidic protein, GFAP (DakoCytomation))-specific antibodies. In these conditions, we obtained primary cultures with 99% of neurons and we did not detect GFAP-positive cells. The cells were maintained 8 days in culture (8 DIV) unless otherwise indicated. For primary cultures of astrocytes, the procedure used to isolate and culture these cells was identical to that described for neurons except that after trypinisation, dissociated cells were cultured in Neurobasal medium supplemented with 2 mM L-glutamine, 30 mM D-(+)-glucose, 5 mM $NaHCO_3$, Penicillin/streptomycin (100 U ml^{-1}, 100 mg ml^{-1}), 5% horse serum and 5% fetal bovine serum. The cells were maintained in culture for 10 DIV.

Electrophoresis and immunoblotting. Cell-culture plates were flash-frozen in liquid nitrogen and processed for protein extract preparation. Frozen cell monolayers from 100-mm-diameter plates were scraped using 500 µl of cold homogenization buffer, which consisted of 25 mM Tris-HCl, pH 7.4, 25 mM NaCl, 0.2% (v/v) Triton X-100, 0.1% SDS, 10 mM sodium fluoride, 1 mM sodium pyrophosphate, 2 mM sodium orthovanadate, 0.5 mM EGTA, 25 nM okadaic acid, 10 µg ml^{-1} aprotinin, 10 µg ml^{-1} leupeptin, and 10 µg ml^{-1} pepstatin. After 15 min in ice, the extracts were passed 10 times through a 25G needle. Protein concentration of the homogenates was determined using the BCA protein assay (Pierce). Proteins were resolved by 10% SDS-PAGE, transferred onto a nitrocellulose membrane (Schleicher and Schuell) and probed with the following

antibodies: rabbit antibody against human MGS (MGS3), which recognizes MGS independently of its phosphorylation state[25]; sheep anti-phosphorylated MGS in Ser7 and 10 (PGSser7/10) (a gift from D.G. Hardie[40]); rabbit anti-phosphorylated GS in Ser640 (PGSser641, Cell Signaling); rabbit anti-GFAP (DakoCytomation); rabbit anti-green fluorescent protein (GFP) (Immunokontact); mouse anti-β-actin; mouse anti-HA; and mouse anti-laforin (Monoclonal laforin antibody A7 against human laforin is an IgG1κ mouse monoclonal antibody raised against recombinant GST::laforin expressed in *E. coli*). Antibody against brain glycogen phosphorylase was produced by Eurogentec: chickens were immunized against a peptide at the C-terminus of the protein. The peptide contained the C-terminal amino acids of mouse brain glycogen phosphorylase (^{826}GVEPSDLQIPPPNLPKD^{842}).

Secondary antibodies conjugated to horseradish peroxidase against rabbit (GE-Healthcare), mouse (DakoCytomation), sheep (DakoCytomation) and chicken immunoglobulins (Chemicon) were used. Immunoreactive bands were visualized using ECLplus kit (GE Healthcare) following the manufacturer's instructions.

Immunocytochemistry. Cells seeded on poly-L-lysine-coated coverslips were rinsed three times with PBS and fixed for 30 min in PBS containing 4% (w/v) paraformaldehyde. After fixation, cells were incubated with $NaBH_4$ (1mg ml^{-1}) for 10 min and permeabilized for 20 min with PBS containing 0.2% (v/v) Triton X-100. The following steps were performed as previously described[22]. Finally, coverslips were washed, air-dried, and mounted onto glass slides using Mowiol as mounting medium.

The primary antibodies used were: rabbit antibody against human MGS[25],

mouse antibody against laforin, mouse antibody anti β-III-tubulin TUJ1 (BAbCO), and a monoclonal antibody against glycogen (a generous gift from Dr. Otto Baba)[41]. In some cases nuclei were stained with Hoechst 33342 (Molecular Probes). The secondary antibodies used were: Alexa Fluor 546-conjugated goat anti-rabbit (Molecular Probes); Alexa Fluor 546-conjugated goat anti-mouse (Molecular Probes); Oregon Green-conjugated goat anti-mouse (Molecular Probes); and tetramethylrhodamine (TRITC)-conjugated goat anti-mouse IgM secondary antibody (Chemicon). Fluorescence images were obtained with a Leica SPII Spectral microscope (Leica Lasertechnik). The light source was an argon/krypton laser (75 mW), and optical sections (0.1 µm) were obtained.

Apoptosis assays. Neurons seeded on poly-L-lysine-coated coverslips were fixed for 30 min in PBS containing 4% (w/v) paraformaldehyde and processed for Terminal transferase dUTP nick end-labeling of DNA strand breaks (TUNEL) or active caspase-3 staining. TUNEL assay was carried out using the ApopTag Peroxidase *In Situ* Apoptosis Detection Kit (Chemicon) following the manufacturer's instructions. Active caspase-3-positive cells were visualized by immunocytochemistry using the Cleaved Caspase-3 antibody (Asp175) from Cell Signalling. This antibody recognizes endogenous levels of the large fragment (17/19 kDa) of activated caspase-3 and does not recognize full length capase-3 or other cleaved caspases. The TUNEL- and active caspase-3-positive cells were photographed with a Nikon Eclipse E-600 microscope using a 40x objective. The percentage of positive cells was estimated in 8-14 fields in each of three coverslips (three independent experiments) for each treatment condition (500-600 total cells). Total number of cells was evidenced after

staining of nuclei with Hoechst 33342.

In addition, the level of caspase-3 activation was determined by Western blot analysis using the Cleaved Caspase-3 antibody.

RNA purification and retrotranscription. Total RNA was isolated from mouse tissue after homogenization with 10 vol (p/v) of TRIzol reagent (Invitrogen), centrifugation at 12,000*g* for 5 min, extraction with chloroform and precipitation with isopropanol. The final pellet was washed with 75% ethanol, dessicated and resuspended in RNAse-free water. RNA was further purified with RNeasy minicolumns (RNeasy Total RNA Isolation Kit, QIAGEN) following the manufacturer's instructions. RNA isolation from cultured cells was perfomed with RNeasy minicolumns following the manufacturer's instructions. Quantification was done spectrophotometrically at 260 nm.

Up to 5 µg of total RNA from each sample was reverse transcribed for 50 min at 42ºC in a 15 µl reaction volume using 200 units of Superscript III reverse transcriptase (SuperScript First-strand Synthesis System for RT-PCR, Invitrogen) in the presence of 50 ng random hexamers. A series of specific primers were designed to specifically amplify a fragment of approximately 500 bp from the coding sequence of mouse muscle GS (5´ CCTTTTAGTGGGGAGCCTC and 5´GGACTCAGGGGCTCAGTGGG'), mouse liver GS (5´ GAGGATGCATAAGAGTAACGTC and 5´AAGTGGTTCAGAGAAAACGGTG) and mouse GFAP (5´ TCGAATGACTCCTCCACTCCCTGCC and 5´ CTTCCTGTTCGCGCATTTGCCG).

Determination of MGS activity. Frozen cell monolayers from 100-mm-diameter plates were scraped using 300 µl of homogenization buffer, which consisted of 10 mM Tris (pH 7.0), 150 mM KF, 15 mM EDTA, 0.6 M sucrose, 15 mM 2-mercaptoethanol, 10 µg ml^{-1} leupeptin, 10 µg ml^{-1} aprotinin, 10 µg ml^{-1} pepstatin, 1 mM benzamidine, 1 mM sodium orthovanadate, 25 nM okadaic acid and 1 mM phenylmethylsulfonyl fluoride. Homogenization was performed with a 25G needle. Protein concentration was measured following Bradford method[44] using the Bio-Rad Protein Assay reagent. MGS activity was measured in homogenates in the absence or presence of 6.6 mM G6P, as described previously[45]. The activity measured in the absence of G6P represents the active form of the enzyme (I or a form), whereas that measured in the presence of 6.6 mM G6P represents total GS activity. The –G6P / +G6P activity ratio is a non-linear measurement of the activation state of the enzyme. Values below 0.1 indicate an essentially fully inactive enzyme while those above 0.7 are equivalent to full activation[46].

ARTICLE 2

EMBO Molecular Medicine

Neurodegeneration and functional impairments associated with glycogen synthase accumulation in a mouse model of Lafora disease

Jordi Valles-Ortega[1,2†], Jordi Duran[1,3†], Mar Garcia-Rocha[1], Carles Bosch[1,4,5], Isabel Saez[1,2], Lluís Pujadas[1,4,5], Anna Serafin[6], Xavier Cañas[6], Eduardo Soriano[1,4,5], José M. Delgado-García[7], Agnès Gruart[7], Joan J. Guinovart[1,2,3]*

Keywords: glycogen synthase; glycogen; Lafora; malin; neurodegeneration

DOI 10.1002/emmm.201100174

Received June 20, 2011
Revised July 22, 2011
Accepted July 29, 2011

Lafora disease (LD) is caused by mutations in either the laforin or malin gene. The hallmark of the disease is the accumulation of polyglucosan inclusions called Lafora Bodies (LBs). Malin knockout (KO) mice present polyglucosan accumulations in several brain areas, as do patients of LD. These structures are abundant in the cerebellum and hippocampus. Here, we report a large increase in glycogen synthase (GS) in these mice, in which the enzyme accumulates in LBs. Our study focused on the hippocampus where, under physiological conditions, astrocytes and parvalbumin-positive (PV^+) interneurons expressed GS and malin. Although LBs have been described only in neurons, we found this polyglucosan accumulation in the astrocytes of the KO mice. They also had LBs in the soma and some processes of PV^+ interneurons. This phenomenon was accompanied by the progressive loss of these neuronal cells and, importantly, neurophysiological alterations potentially related to impairment of hippocampal function. Our results emphasize the relevance of the laforin–malin complex in the control of glycogen metabolism and highlight altered glycogen accumulation as a key contributor to neurodegeneration in LD.

INTRODUCTION

Glycogen is the principal storage form of glucose in animal and human cells. It is mainly produced in the liver and muscles, and glycogen levels in the brain are low compared to these two tissues. In the brain, this polysaccharide is stored in astrocytes, while most neurons do not accumulate it under normal conditions (Cataldo & Broadwell, 1986; Wender et al, 2000).

Glycogen is produced by glycogen synthase (GS), the only enzyme able to synthesize glucose polymers in mammals, and degraded by glycogen phosphorylase (GP). Mammals express two isoforms of GS encoded by *GYS1* and *GYS2*. The latter encodes the liver isoform (LGS) and its expression is restricted to the liver, while the former encodes the muscle isoform (MGS) and is widely expressed excluding the liver. MGS is regulated by phoshorylation at nine serine residues located in the amino- and carboxy-terminal domains of the enzyme. Phoshorylation by

(1) Institute for Research in Biomedicine (IRB Barcelona) Barcelona, Spain
(2) Department of Biochemistry and Molecular Biology, University of Barcelona, Barcelona, Spain
(3) Centro de Investigación Biomédica en Red de Diabetes y Enfermedades Metabólicas Asociadas (CIBERDEM), Madrid, Spain
(4) Department of Cell Biology, University of Barcelona, Barcelona, Spain
(5) Centro de Investigación Biomédica en Red para Enfermedades Neurodegenerativas (CIBERNED), Madrid, Spain
(6) Laboratory Animal Applied Research Platform, Barcelona Science Park, Barcelona, Spain
(7) Division of Neurosciences, Pablo de Olavide University, Seville, Spain
***Corresponding author:** Tel: +34 93 403 71 11; Fax: +34 93 403 71 14; E-mail: guinovart@irbbarcelona.org

†These authors contributed equally to this work.

several kinases, including GSK3, induces the inactivation of the enzyme, while dephosphorylation causes its activation (Skurat et al, 1994). GS is also allosterically activated by glucose-6-phosphate (G6P) in the brain (Goldberg & O'Toole, 1969) and in other tissues (Bouskila et al, 2010; Villar-Palasi & Guinovart, 1997). High levels of G6P fully activate GS even when the enzyme is phosphorylated.

In the brain, MGS is fully functional in astrocytes; neurons also express this isoform but it is kept in an inactive state under normal conditions. Both the muscle (MGP) and the brain (BGP) isoforms of GP are expressed in brain. Interestingly, astrocytes express both MGP and BGP while most neurons do not express GP (Pfeiffer-Guglielmi et al, 2003; Vilchez et al, 2007). Despite the apparent lack of glycogen metabolism in these cells, in some diseases poorly branched and insoluble glycogen, the so-called polyglucosan bodies (PGBs), accumulate in neurons [Adult Polyglucosan Body Disease (APBD, OMIM263570), Andersen Disease (GSD IV, OMIM232500) and Lafora Disease (LD; EPM2, OMIM254780)].

Lafora disease (LD) typically manifests during adolescence with generalized tonic-clonic seizures, myoclonus, absences, drop attacks or partial visual seizures. As the disease progresses, afflicted individuals suffer a rapidly progressing dementia with apraxia, aphasia, and visual loss, leading to a vegetative state and death usually in the first decade from the onset of the initial symptoms. The hallmark of LD is the presence of large inclusions of PGBs, the so-called Lafora bodies (LBs), in the somas and processes of neurons in the brain and in other tissues such as muscle and heart (Cavanagh, 1999). The mechanism by which this abnormal glycogen accumulates remains unclear. LD is inherited as an autosomal recessive disorder and has been associated with mutations in two genes: *EPM2A*, which encodes laforin, a dual-specificity protein phosphatase with a functional carbohydrate-binding domain; and *EPM2B*, which encodes malin, an E3 ubiquitin ligase. Malin ubiquitinates and promotes the degradation of laforin (Gentry et al, 2005). Individuals with mutations in *EPM2A* or *EPM2B* are neurologically and histologically indistinguishable. In spite of the long recognized aberrant accumulation of glycogen in LD, a direct link between glycogen metabolism and this neurodegenerative disease has remained elusive for decades and is still a matter of controversy.

The role of the laforin phosphatase activity in the etiopathology of LD has been widely debated. Laforin has been reported to dephosphorylate, and thus activate, glycogen synthase kinase 3 (GSK3) (Lohi et al, 2005). GSK3 activation inhibits glycogen synthesis by GS phosphorylation. Laforin has also been described to release the phosphate incorporated into glycogen by GS during its synthesis (Tagliabracci et al, 2008, 2011, 2007). So mutations in laforin would cause the overactivation of glycogen synthesis and increased phosphate content, which would alter glycogen structure, making it more prone to LB formation. Nevertheless, these hypotheses based only on the phosphatase activity of laforin fail to explain how malin deficiency causes LD.

We previously demonstrated that the laforin–malin complex blocks glycogen accumulation in cultured neurons by inducing the proteasome-dependent degradation of MGS and protein targeting to glycogen (PTG), a protein phosphatase-1 regulatory subunit responsible for the activation of MGS by dephosphorylation (Vilchez et al, 2007). In addition, PTG overexpression in cultured neurons induces the accumulation of poorly branched glycogen and cell death. Thus, we proposed that altered glycogen metabolism caused by either laforin or malin deficiency underlies LB formation and neurodegeneration in LD. Laforin disruption in mice is described to cause neurodegeneration, myoclonus epilepsy and impaired behavioural response together with LB formation (Ganesh et al, 2002) and increased levels of MGS protein are found in the brain of this model (Tagliabracci et al, 2008).

Reports on 3-month-old (DePaoli-Roach et al, 2010) and 6-month-old (Turnbull et al, 2010) mouse models of malin deficiency have recently been published. Neither describes neurological alterations. Here, we have extended the study of malin-deficient mice to 11 months. At this age, they presented neurodegeneration, increased synaptic excitability, and propensity to suffer myoclonic seizures together with increased levels of MGS in the brain. Our study analyses the hippocampal cell type-specific progression of LB appearance and it is the first to report the early presence of LBs in astroglial cells. We describe the expression of MGS and malin in a particular subset of interneurons (PV^+ cells), the later appearance of LB in these cells, and their degeneration and progressive loss. In addition, we report on the hippocampal functional impairment of the malin KO animals.

RESULTS

Malin KO mice accumulate poorly branched glycogen in LBs

We bred malin KO mice up to about 1 year of age. These animals accumulated LBs, the hallmark of LD. LBs were present in several areas of the brain, being most abundant in the hippocampus and cerebellum (Fig 1A). No comparable structures in corresponding regions of control littermate animals were found. LB accumulation was not exclusive to the brain, as they were also detected in some fibres of skeletal muscle and heart (Supporting Information Fig 1). The inclusions increased in number and size with age, as can be seen by comparing 4- and 11-month-old mice (Figs 1A and 7B). Moreover, in the older mice, LBs were detected in regions of the brain that were unaffected at 4 months (Fig 1A). This result is consistent with the accumulative nature of LD.

LBs are insoluble inclusions characterized by poorly branched glycogen-like polymers (Chan et al, 2005; Delgado-Escueta, 2007; Ganesh et al, 2006). We measured glycogen content in whole brain homogenates of 11-month-old malin KO animals, where the presence of LBs was most prominent. These brains showed a 2.5-fold increase in glycogen content (Fig 2A). In addition, low speed centrifugation was performed to analyse the distribution of this polysaccharide between the soluble and insoluble fractions. The increment in glycogen detected corresponded to that present in the insoluble fraction while no significant changes were found in the soluble fraction.

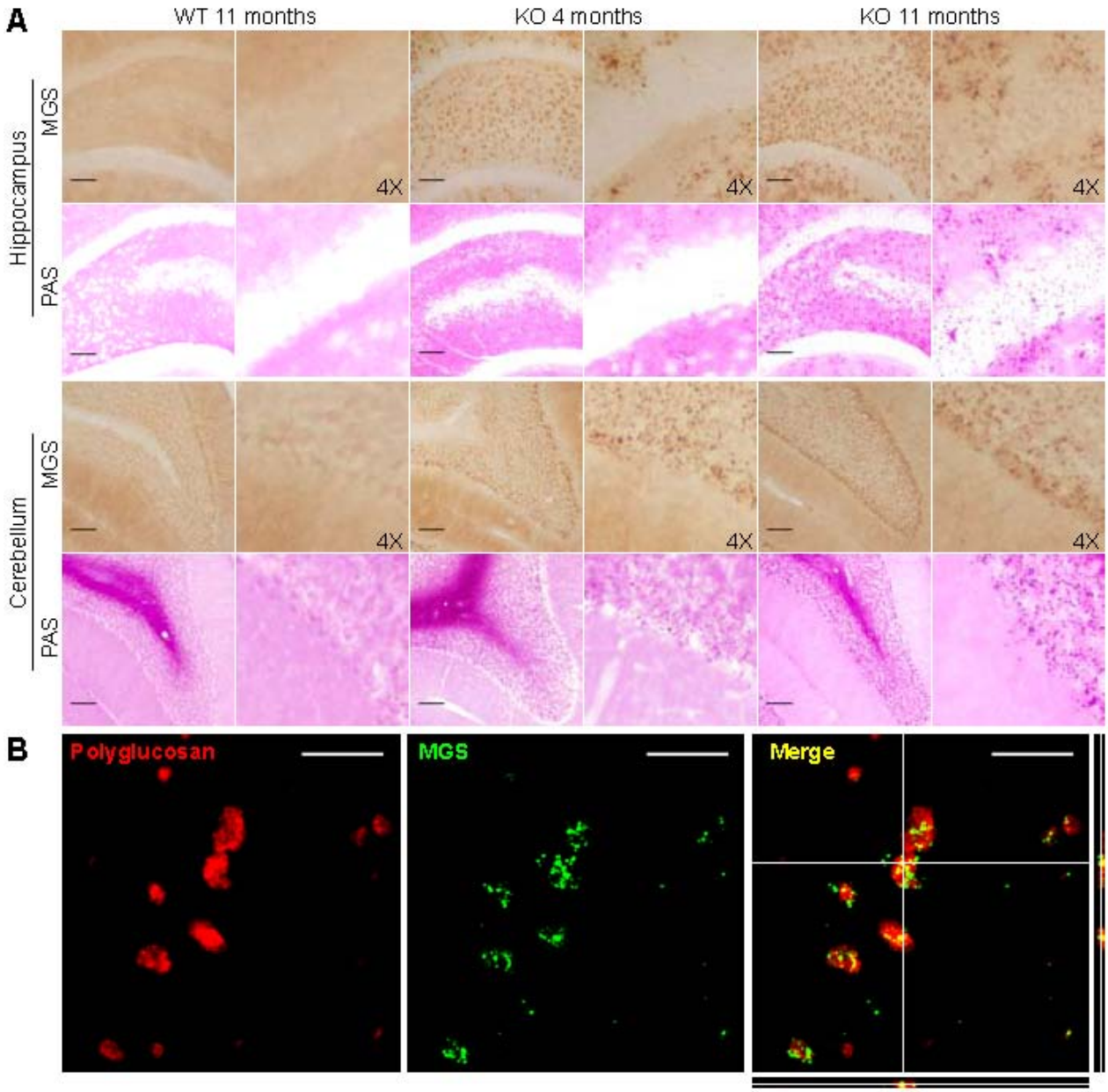

Figure 1. Histological localization of LBs in malin KO mouse brains. LBs are MGS-positive.

A. Periodic acid-Schiff staining (PAS) and immunostaining with an antibody against muscle glycogen synthase (MGS) are shown for the hippocampus and cerebellum of 4- and 11-month-old malin KO and 11-month-old WT littermate controls. Scale bar = 100 μm, 4X = 4-fold magnification.

B. Representative orthogonal confocal sections of LBs showing co-localization (yellow) of polyglucosan (red) and MGS (green) in malin KO brains. Scale bar = 10 μm.

The degree of glycogen branching in KO brains was measured by recording the visible absorption spectrum of purified glycogen in the presence of iodine. The lower the branching of the glucose polymer, the greater the displacement of its absorption maximum to longer wavelengths (Krisman, 1962). Glycogen isolated from a pool of KO brains was clearly less branched (peak at 537 nm) than that from control brains (peak at 492 nm) (Fig 2B).

Malin KO mice accumulate MGS in LBs

Malin has been reported to be involved in the proteasomal clearance of laforin (Gentry et al, 2005) and MGS (Vilchez et al, 2007). Therefore, we analysed the MGS content and distribution in brain sections from WT and malin KO mice. For this purpose, we used 4- and 11-month-old animals to evaluate the progression with age. The polyglucosan inclusions were immunostained for MGS (Fig 1B), thereby indicating that LBs

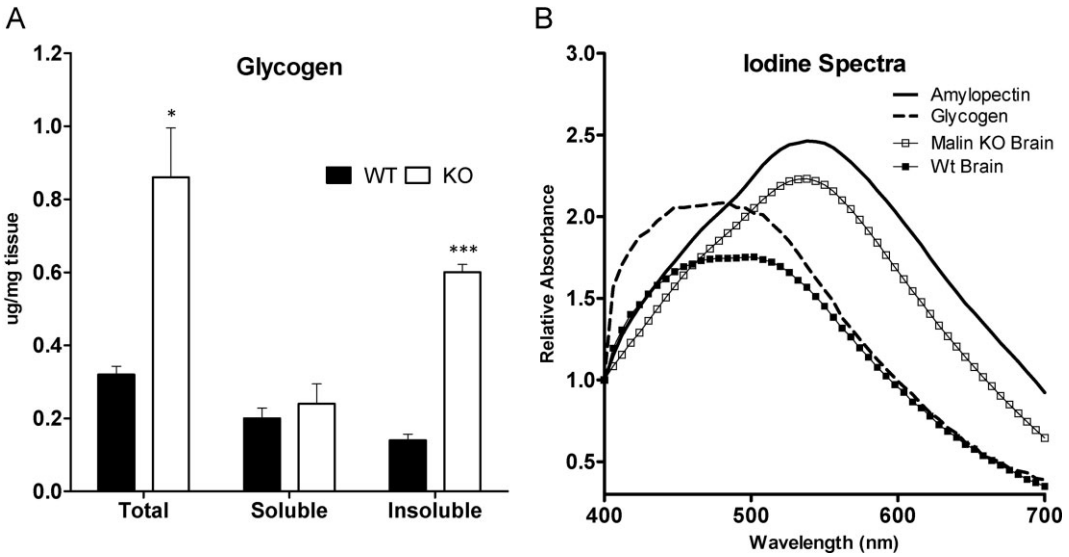

Figure 2. Analysis of glycogen in malin KO mouse brains. Glycogen is increased and accumulated in the pellet. Brain extracts from 11-month-old wild-type (WT) and malin knock-out (KO) mice were analysed. Total homogenates and the soluble and insoluble fractions resulting from low speed centrifugation were used for the biochemical analysis.

A. Glycogen content. Data are expressed as mean ± SEM. $^{*}p < 0.05$. $^{***}p < 0.001$. WT ($n = 6$), KO ($n = 6$).

B. Iodine spectra of glycogen purified from total brain homogenates. Amylopectin from corn and glycogen from mouse liver are shown for reference.

contain the GS protein and its catalytic product (Fig 1). Western blot analysis showed highly increased MGS in total homogenate from malin KO brains compared to controls. The levels of this protein were increased in the insoluble fraction, thus strengthening the results obtained from histochemistry. As polyglucosan inclusions apparently increased in number and size with age, we also analysed the levels of other glycogen-binding proteins as laforin, glycogenin—the priming enzyme for glycogen synthesis—and GP. The levels of laforin (Fig 3A), glycogen phosphorylase muscle (MGP) and brain (BGP) isoforms, and glycogenin (Supporting Information Fig 3) were also found to be increased and accumulated in the insoluble fraction. Interestingly, MGP levels were also increased in the soluble fraction where MGS, laforin, and BGP levels remained unchanged.

Analysis of the GS phoshorylation state using specific antibodies for the N-terminal and C-terminal phoshorylation sites showed that, while the enzyme in the soluble fraction did not show changes between KO and WT mice, the enzyme present in the insoluble fraction was less phosphorylated in KO mice compared to WT in Serine residues 7 and 10 (Fig 3A and B) and 640 (Fig 3A and C), corresponding to a more active form of GS.

We also measured GS enzymatic activity in total homogenates and in the soluble and insoluble fractions. GS activity in the presence of G6P (Fig 3D) is usually taken as a measure of total GS. Surprisingly, despite the large increase in GS protein levels seen by Western blot analysis, no significant differences in total GS activity were found by activity measurements. This result indicated that MGS protein accumulated in LBs does not show activity even in presence of its allosteric activator (G6P) in the conditions assayed. The ± G6P activity ratio, an indicator of the activation state of the enzyme, was also unchanged in all fractions (Fig 3E).

Cell-type specific progression of LB appearance

The histological study of mouse brains with antibodies against MGS showed that, in addition to astrocytes, PV^{+} interneurons of the hippocampus also express MGS (Fig 4A). These cells can be found in the DG, CA1-2 and CA3 (not shown).

In the KO mice, the only exon of *EPM2B* is substituted by a selection cassette containing the βgal gene (Supporting Information Fig 2). Consequently, malin heterozygous mice express βgal under the control of the endogenous promoter of *EPM2B*. To overcome the lack of an antibody recognizing the endogenous malin protein, we used βgal as a reporter of malin expression in these animals. βgal immunodetection showed that, among other cells, some astrocytes and all PV^{+} interneurons express malin in the hippocampus, one of the most affected regions of the malin KO brain (Fig 4B).

While 4-month-old KO brains showed mainly astrocyte-associated LB accumulation (Figs 5 and 6A), 11-month-old counterparts showed LBs in astrocytes (Figs 5 and 6A) and in the cell bodies of neurons (Fig 5). Neuronal LBs were very conspicuous in the neuronal somata of hippocampal PV^{+} interneurons and were occasionally found in their dendritic processes (Fig 6B).

To substantiate the above findings, we performed an electron microscopy study on hippocampal tissue from 11-month-old KO mice. Astrocytes often displayed LBs in their cytoplasm (Fig 6C c1 and c2), in agreement with the light microscopy observations (Fig 6A). We focused our attention on the dendritic

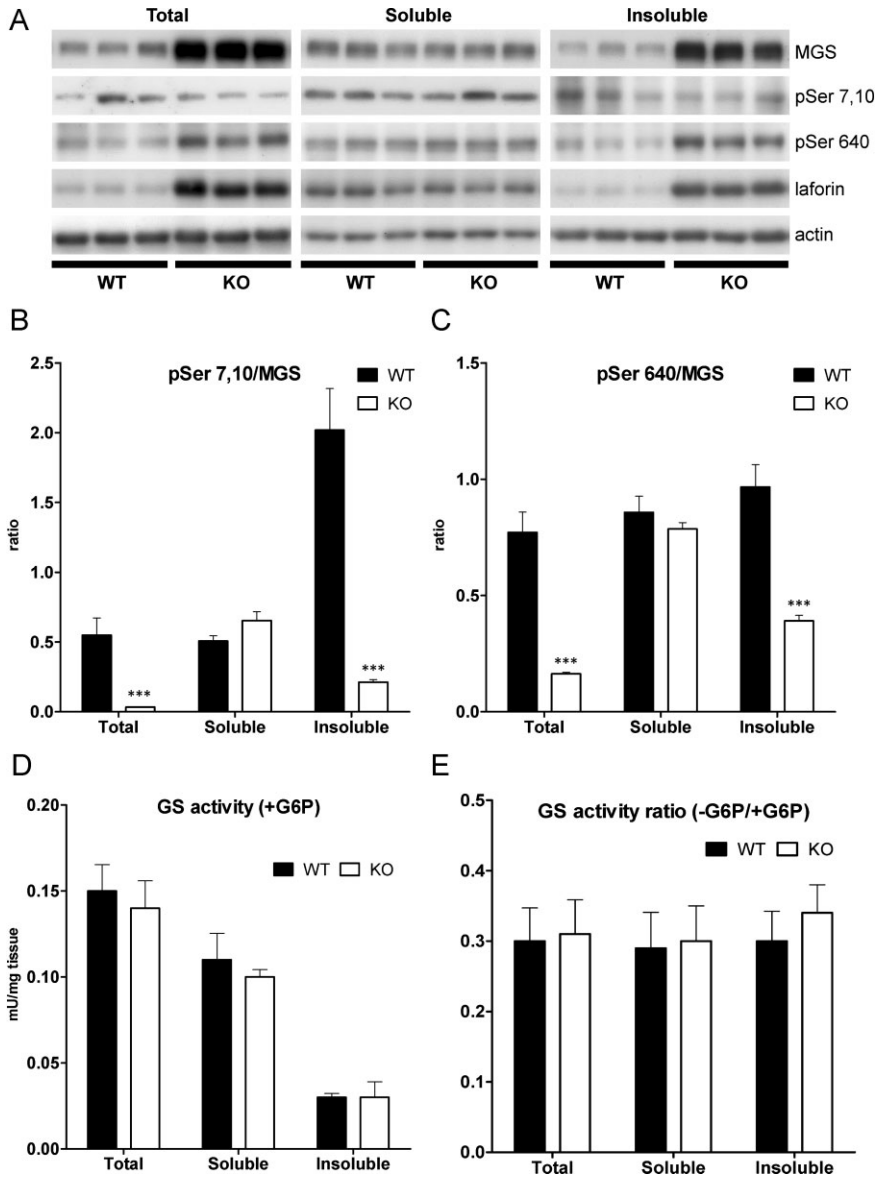

Figure 3. Analysis of MGS in malin KO mouse brains. MGS protein is increased and accumulated in the insoluble fraction. Brain extracts from 11-month-old wild-type (WT) and malin knock-out (KO) mice were analysed. Total homogenates and the soluble and insoluble fractions resulting from low speed centrifugation were used for the biochemical analysis.

A. Western blotting for MGS, GS phosphoserine 7 and 10 (pSer 7,10), GS phosphoserine 640 (pSer 640) and laforin. Actin was used as loading control.

B,C. GS phoshorylation state. Densitometries from Western blot analysis are expressed as ratio of the signals from the enzyme phosphorylated at specific sites to total protein.

D. Glycogen synthase (GS) activity measured in the presence of G6P.

E. GS activity ratio (−G6P/+G6P). Data are expressed as mean ± SEM. $^{*}p < 0.05$. $^{***}p < 0.001$. WT ($n = 6$), KO ($n = 6$).

profiles of the CA1 and DG. Dendrites were identified by the large number of microtubules organized in bundles and by the presence of synaptic contacts on their surface (Fig 6C a2) or on dendritic spines arising from them (Fig 6C b2). We found dendrites filled by large LBs, which distorted their size and fine structure (Fig 6C a1, a2, b1 and b2). In some cases, glycogen granules were identifiable at the periphery of these LBs. In addition, we frequently observed dark, electron-dense cells displaying the typical fine structural features of microglial cells, which engulfed large numbers of LBs (Fig 6C d). We thus concluded that LBs accumulate in glial cells and in neurons.

Degeneration of PV^+ interneurons in the malin KO hippocampus

To study the effect of LB accumulation on PV^+ interneurons, we counted the number of these neurons in the hippocampus at 4 and 11 months of age. We found a marked reduction in the number of PV^+ neurons in the hippocampus of 11-month-old KO mice; a decrease that was not detected at 4 months of age (Fig 7A). Decreased immunolabelling of PV^+ dendrites was also observed, which may suggest an impairment of dendritic arbors (Fig 7B). Since the induction of polyglucosan accumulation causes neuronal death by apoptosis in primary cultures (Vilchez et al, 2007), we analysed whether the net neuronal loss caused by malin deficiency correlated with increased rates of apoptosis. Although no clear neuronal apoptotic features were found by TUNEL, Caspase-3 activation or FluoroJadeB staining (not shown), 11-month-old KO hippocampi showed a clear increase in $GFAP^+$ cells (Supporting Information Fig 4). This gliosis has been reported to be associated to neuronal loss in other model of LD (Turnbull et al, 2011) and it is in concordance with the observed loss of PV^+ interneurons in malin KO hippocampi.

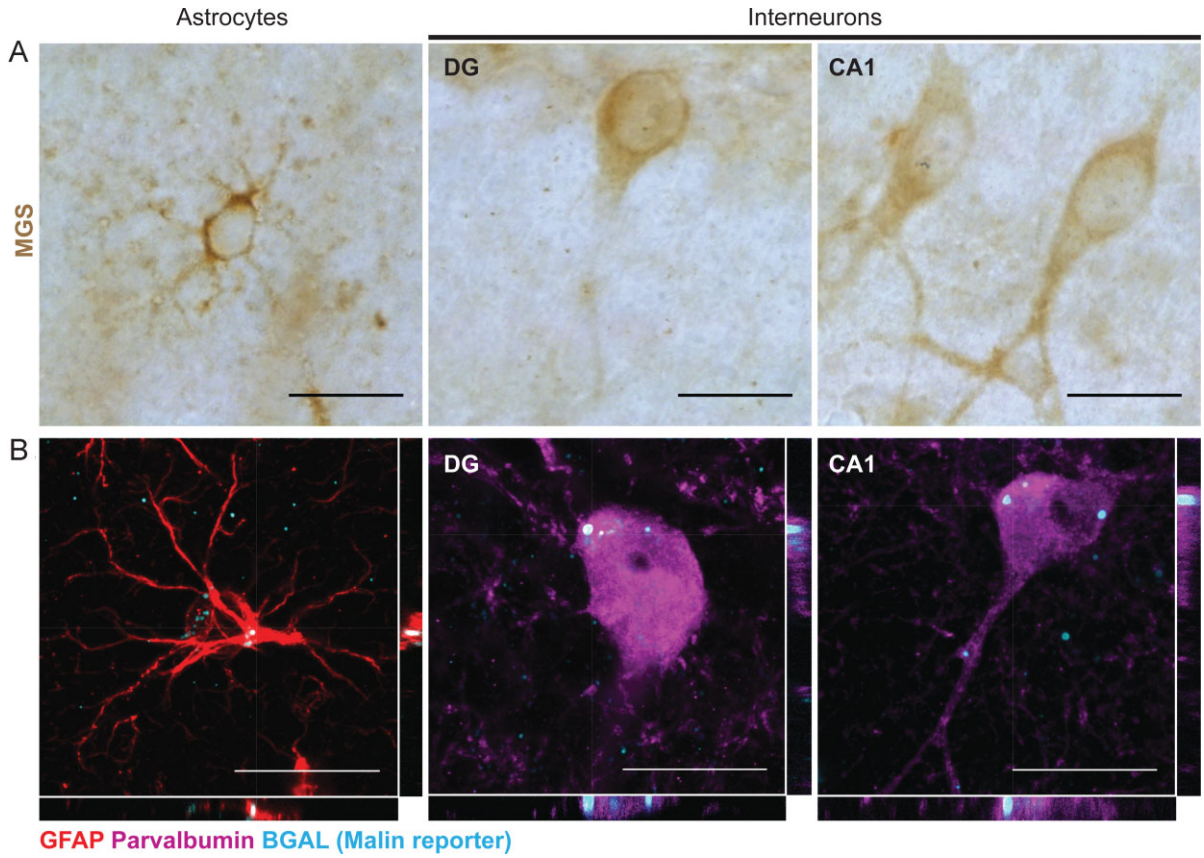

Figure 4. Hippocampal interneurons and astrocytes express MGS and malin. Hippocampal astrocytes and interneurons from dentate gyrus (DG) and CA1 regions of WT (**A**) and malin heterozygous (**B**) hippocampi of same-aged mice are shown.

A. Immunostaining with an antibody against MGS (brown).

B. Representative orthogonal confocal sections showing immunostaining with antibodies against glial fibrillary acidic protein (GFAP) (red), parvalbumin (PV) (magenta) and βgal (cyan). Scale bar = 20 μm.

Behavioural alterations in malin KO mice

Malin KO mice developed normally and were fertile. They displayed normal gait and showed no significant differences to WT mice in the Rotarod test or in the Beam walking test. They did not present any sign of cerebellar ataxia (data not shown). Exploratory behaviour of the KO mice was evaluated in an Open Field Test (Supporting Information Fig 5). At 11 months of age, these animals were hyperactive and showed an increase in exploratory behaviour. Significant differences were found in the time spent in the centre of the arena, the distance run and the number of rearings. These results indicate that KO mice have reduced anxiety.

Operant conditioning is an excellent learning test to determine associative learning capabilities of alert behaving mice, as well as other cognitive and motor abilities (Madronal et al, 2010). Collected results indicate that both WT and KO mice acquired a fixed-ratio (1:1) schedule (i.e. to press the lever one time to obtain a food pellet as reward) in the same number of sessions (WT, 5.2 ± 0.3 days; KO, 4.7 ± 0.2 days, $p = 0.282$, Student's *t*-test). From the 6th–10th sessions, both groups of animals obtained a similar number of pellets per session (WT, 23.2 ± 2.1; KO, 22.1 ± 2.6, $p = 0.152$, Student's *t*-test; not illustrated). In accordance, learning capabilities of KO mice were similar to that presented by their littermate controls.

Functional properties of hippocampal CA3-CA1 synapses in alert behaving WT and KO mice

Available *in vivo* recording techniques allow the study of hippocampal synapses in awake mice (Gruart et al, 2006; Madronal et al, 2009). Both WT and transgenic KO mice presented increases in the slope of fEPSP evoked at the CA1 area following the presentation of paired pulses (40 ms of inter-pulse interval) of increasing intensity at the ipsilateral Schaffer collaterals (Fig 8A). Nevertheless, KO mice presented significantly larger fEPSP amplitudes than WT animals at high stimulus intensities (>0.2 mA), suggesting an enhanced synaptic excitability.

We also looked for facilitation at the CA3-CA1 synapse. It is known that the synaptic facilitation evoked by the presentation of a pair of pulses is a typical presynaptic short-term plastic property of the hippocampal CA3-CA1 synapse, which has

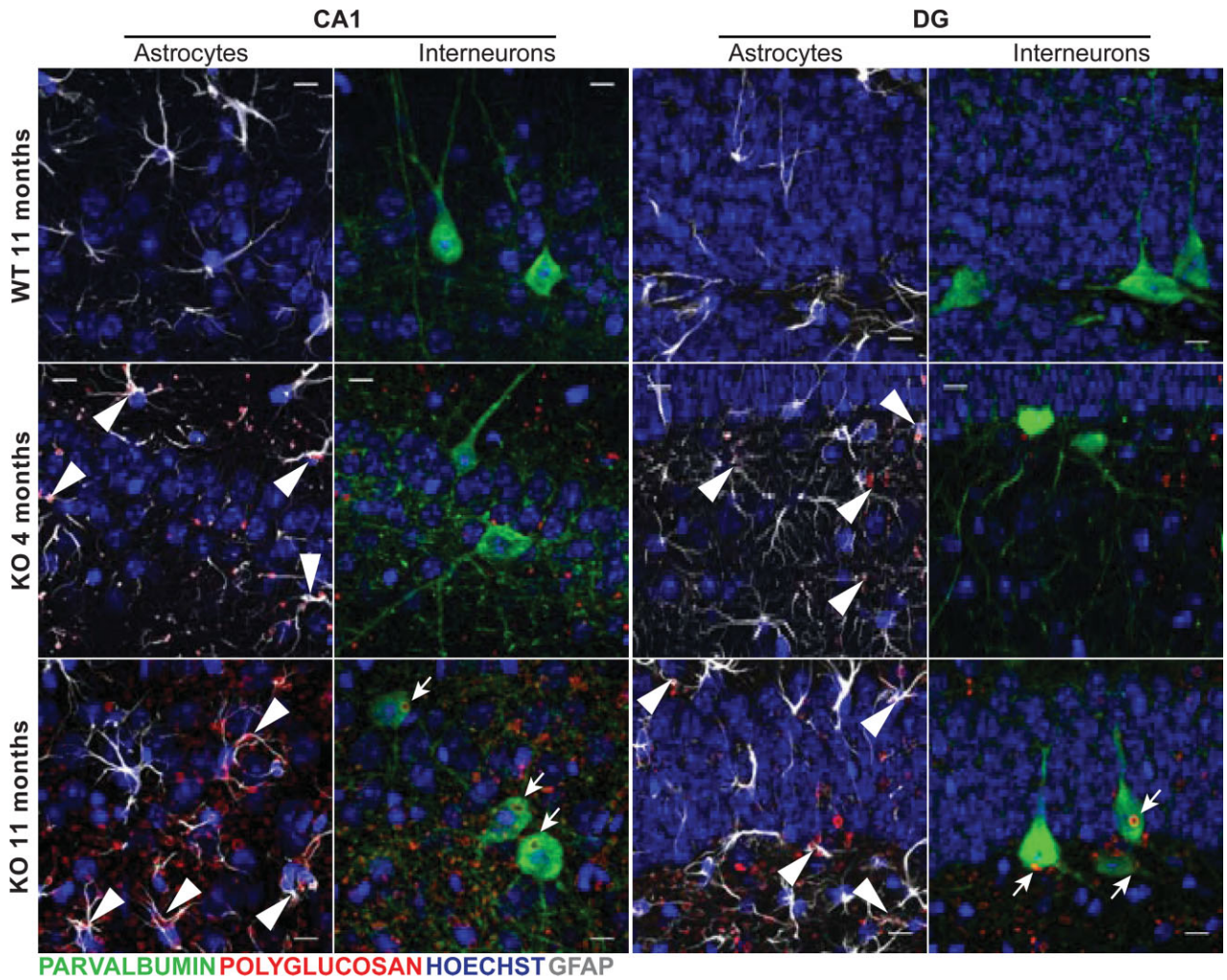

Figure 5. Age-associated progression of LB formation in the malin KO hippocampus. Confocal images are shown for DG and CA1 hippocampal regions of 4- and 11-month-old malin KO mice and 11-month-old WT littermate controls. Antibodies were used against parvalbumin (green), polyglucosan (red) and GFAP (white). Hoechst (blue) was used for nuclear staining. 4-month-old malin KO mice show mainly astrocyte-associated polyglucosan accumulation (arrowheads). 11-month-old malin KO animals show both astrocyte-associated (arrowheads) and interneuronal intracellular (arrows) accumulation. Control mice do not show comparable polyglucosan accumulation. Scale bar = 10 μm.

been related to the process of neurotransmitter release (Zucker & Regehr, 2002). But, as illustrated in Fig 8B, no significant differences between the two groups were observed at any of the selected intervals. In accordance, it can be suggested that short-term plastic processes are not affected in malin KO animals.

Comparison of long-term potentiation evoked in alert behaving WT and malin KO mice

For the long-term potentiation (LTP) study, and in order to obtain a baseline, WT and KO mice were stimulated every 20 s for ≥15 min at Schaffer collaterals (Fig 8C). When a stable baseline was obtained, mice were presented with the HFS protocol (see Materials and Methods section). After HFS, the same single stimulus used to generate the baseline records was presented at the initial rate (3/min) for another 60 min. Recording sessions were repeated up to 5 days later for 30 min each. Both groups presented a significant LTP, but with some differences between them. Indeed, the LTP response presented by KO mice was significantly larger than that presented by controls for more than 24 h. Thus, it can be proposed that KO mice present larger and longer-lasting LTPs than their respective littermate controls, a fact that could be ascribed to their enhanced synaptic excitability, but that is not translated into an increased ability for associative learning tasks.

Effects of kainic acid injection in malin KO mice

The C57BL6 strains are seizure-resistant in comparison to other mouse genetic backgrounds (McLin & Steward, 2006) and as

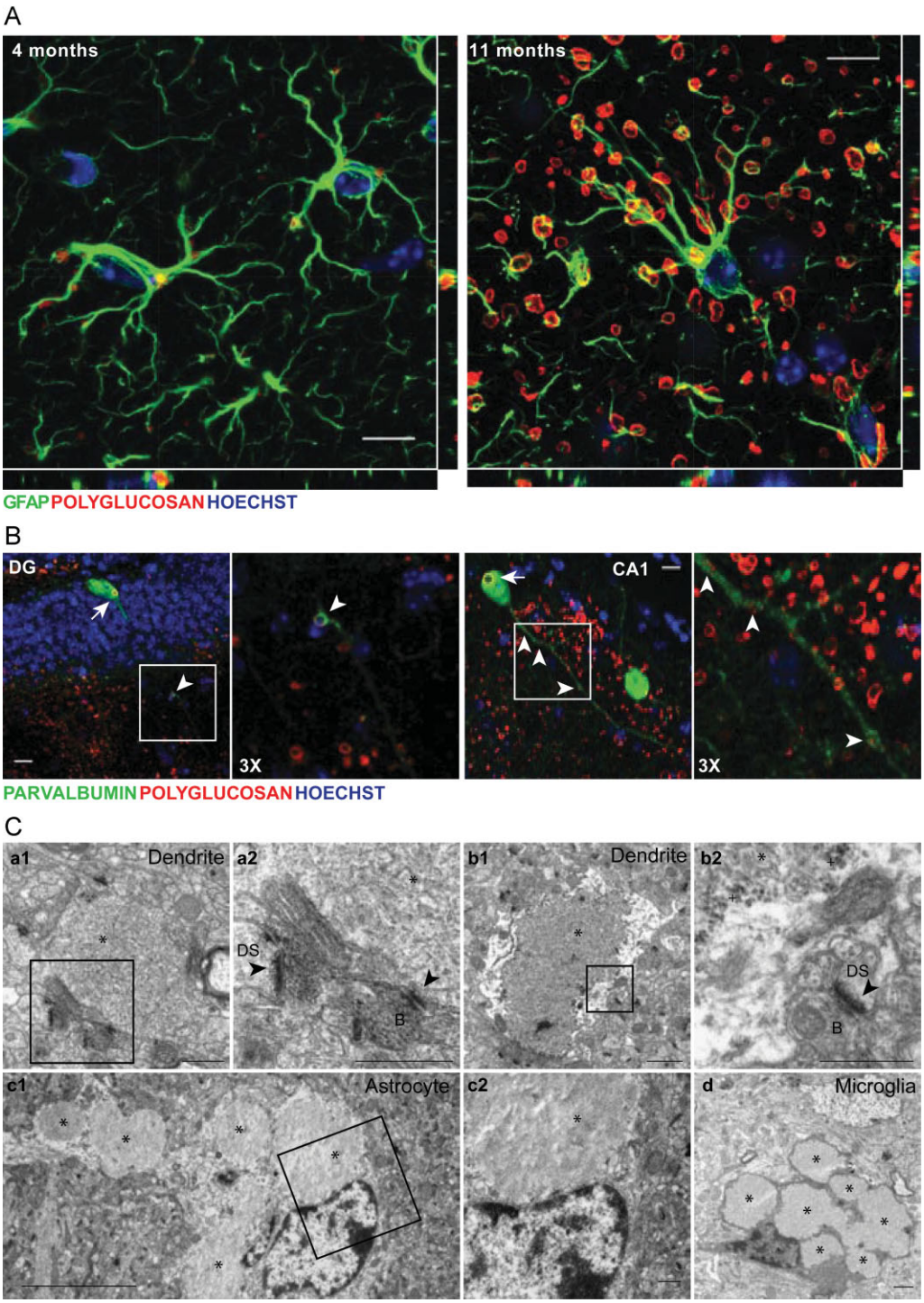

Figure 6. Localization of LBs in hippocampal astroglia, microglia and neurons. Representative images from 4-month-old (**A**) and 11-month-old (**A–C**) malin KO hippocampus.

A. Orthogonal confocal sections are shown for astrocytes containing polyglucosan accumulation in the hippocampus of 4- and 11-month-old KO mice. Antibodies were used against GFAP (green) and polyglucosan (red). Hoechst (blue) was used for nuclear staining. Scale bar = 10 μm.

B. Confocal images are shown for DG and CA1 hippocampal regions. Antibodies were used against parvalbumin (green) and polyglucosan (red). Hoechst (blue) was used for nuclear staining. Polyglucosan accumulation can be observed within the somas (white arrows) and some processes (white arrowheads) of PV^+ interneurons. Scale bar = 10 μm. 3X = 3-fold magnification.

C. Electron microscopy images are shown for CA1. Micrographs depict the presence of LBs and glycogen granules in dendrites (a1, a2, b1, b2). LBs were also found in astrocytes (c1, c2). Microglial cells with some engulfed LBs were observed (d). *, Lafora Body; +, glycogen granule; black arrowhead: postsynaptic density; B: synaptic bouton; DS: dendritic spine. a2, b2 and c2 are magnifications of the boxes in a1, b1 and c1. Scale bars are 5 μm in c1 and 0.5 μm in a1, a2, b1, b2, c2 and d.

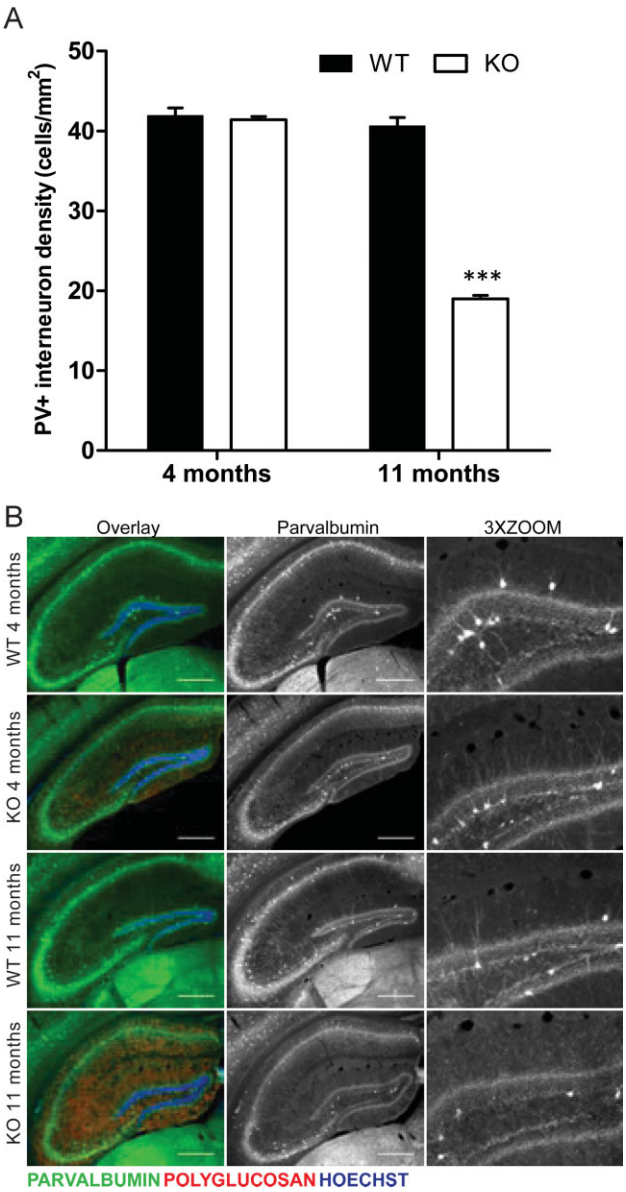

Figure 7. Malin KO mice show degeneration of PV$^+$ interneurons in the hippocampus. Immunofluorescence analyses are shown for hippocampus of 4- and 11-month-old malin KO mice and WT littermate controls. Antibodies were used against parvalbumin (green) and polyglucosan (red). Hoechst (blue) was used for nuclear staining.

A. Density of hippocampal PV$^+$ somas. 11-month-old malin KO mice show a 50% loss of PV$^+$ interneurons while no difference is observed in 4-month-old malin KO animals when compared with controls. Scale bar = 400 μm. 3X ZOOM = 3-fold magnification. Data are expressed as mean ± SEM. $^{***}p < 0.001$.

B. Representative images of hippocampus sections are shown as overlay of the three channels (Overlay) and the split of parvalbumin channel in greyscale (Parvalbumin). A clear decrease in the processes branching from PV$^+$ interneurons can be observed in the 11-month-old malin KO hippocampus.

indicated, malin KO were generated on a C57BL6 background. We investigated the susceptibility of both WT and KO mice to a single i.p. injection of kainic acid. As illustrated in Fig 9A, all injected KO mice presented spontaneous hippocampal seizures, accompanied on occasions (2 out of 6) by myoclonus. In contrast, no WT animal displayed clonic hippocampal seizures. Interestingly, the presence of seizures significantly reduced the amplitude and slope of fEPSPs evoked at the CA3-CA1 synapse (Fig 9B). Train stimulation of Schaffer collaterals evoked long-lasting after-discharges in KO, but not in WT, mice (Fig 9C). Finally, the presence of spontaneous clonic seizures and/or of experimentally evoked after-discharges reduced significantly the theta rhythm normally present in the hippocampus of awake mice (Fig 9D). In short, malin KO animals presented a propensity to generate hippocampal seizures not noticed in controls, following a single injection of kainic acid.

DISCUSSION

Here, we generated malin KO mice as an animal model of LD. We used this model to address fundamental questions regarding the role of malin in the control of glycogen metabolism and the impact of its demise at the histological, biochemical and behavioural level. In relation to recent publications on the same subject, we have extended the characterization of the model up to 11 months of age, a point at which the neurological consequences of the defect are already clearly visible. Our results point out the importance of the regulation of MGS by laforin and malin and highlight a key role of glycogen metabolism in the etiopathology of LD.

The KO animals showed LBs in several brain regions, these bodies being most conspicuous in the cerebellum and hippocampus. Glycogen content in the brains of these animals more than doubled that of the WT. This increase was accounted for solely by the polysaccharide present in the insoluble fraction. This observation thus supports the notion that the increase corresponds to the polyglucosan content of LBs. However, LBs contained not only polyglucosan but also MGS, the enzyme responsible for its synthesis. The accumulation of LBs occurs even with increased levels of soluble GP. These results can be understood as a response to polyglucosan accumulation and suggest that the aberrant glycogen synthesized in malin KO brains is resistant to GP degradation. In addition, in concordance with the apparent increase in the number of LBs, we also found increased levels of glycogenin in the insoluble fraction of KO brains, suggesting that this enzyme is also required for the initiation of polyglucosan synthesis.

It has been reported that phosphate is introduced into glycogen by catalytic error of GS and removed from it by the phosphatase activity of laforin. The hyperphosphorylation of glycogen would lead to a reduction of its solubility, this feature being the underlying determinant of LD according to recent publications (Tagliabracci et al, 2008, 2011; Turnbull et al, 2010). In the malin KO mice, although an increase of total laforin levels has been reported, a decrease in soluble laforin has been suggested to be responsible for the formation of LBs (DePaoli-Roach et al, 2010). Our data demonstrate that although laforin was augmented in the insoluble fraction, it remained unchanged

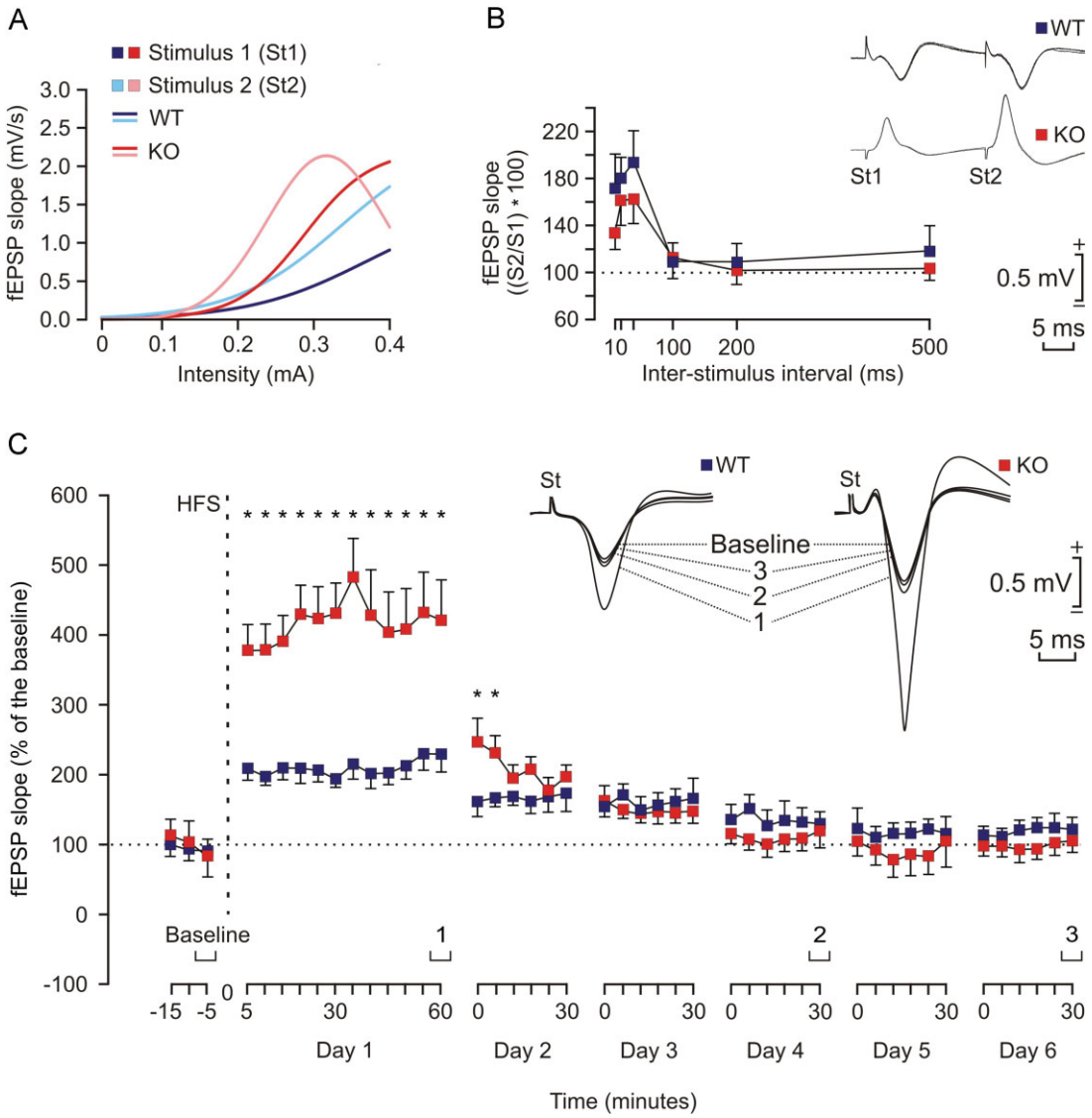

Figure 8. Electrophysiological properties of hippocampal synapses in WT and KO alert behaving mice.

A. Input/output curves of fEPSPs evoked at the CA1 area by paired (40 ms of interval) pulses presented to Schaffer collaterals at increasing intensities (in mA) in WT (1st pulse, dark blue; 2nd pulse, light blue) and KO (1st pulse, dark red; 2nd pulse, light red) mice ($n = 4$ animals/group). The best nonlinear adjustments ($r \geq 0.99$; $p \leq 0.001$) to the collected data are illustrated. KO mice presented significantly larger ($p < 0.01$) input/output curves than WT animals.

B. There were no significant differences in paired-pulse facilitation between WT (blue) and KO (red) mice. The data shown are mean ± SEM slopes of the 2nd fEPSP expressed as a percentage of the 1st for six (10, 20, 40, 100, 200, 500) inter-pulse intervals. Some fEPSP paired traces (20 ms of inter-pulse interval) collected from representative WT and KO mice are illustrated.

C. The two graphs illustrate the time course of LTP evoked in the CA1 area (fEPSP mean ± SEM) following high frequency stimulation HFS for WT (blue) and KO (red) mice. The HFS was presented after 15 min of baseline recordings, at the time marked by the dashed line. LTP evolution was followed for up to 6 days. The fEPSP is given as a percentage of the baseline (100%) slope. Although the two groups presented a significant increase (ANOVA, two-tailed) in fEPSP slope following HFS when compared with baseline records, values collected from the KO group were significantly ($^{*}p < 0.001$) larger than those collected from WT mice at the indicated times.

in the soluble fraction. Therefore, a decrease in the amount of soluble laforin cannot be invoked as the cause of LB accumulation in our model.

In agreement with the impressive accumulation of MGS observed by immunostaining, Western blot analysis of malin KO brain extracts showed that total MGS was dramatically increased and accumulated in the insoluble fraction. We found that the enzyme in the LBs was less phosphorylated and therefore expected to be more active. However, we did not detect increased GS activity even in the presence of G6P. This imbalance between total protein amounts and activity has previously been reported for the other model of LD, the laforin KO (Tagliabracci et al, 2008). These results could be explained by GS being unable to exert its activity under the assay

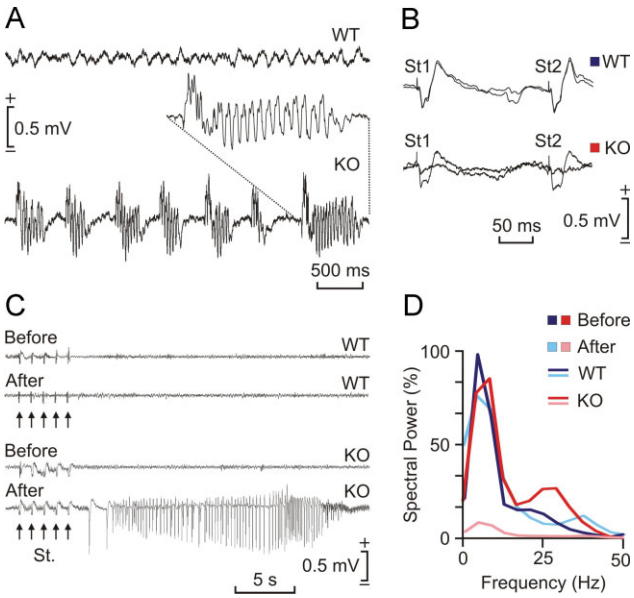

Figure 9. Effects of kainic acid injection in malin KO mice.

A. Representative hippocampal EEG recordings carried out in a WT (top) and in a KO mice 30 min after kainic acid injection (8 mg/kg, i.p.). Note the presence of repetitive clonic seizures in the KO animal. The inset shows an enlargement of a typical seizure.

B. Representative hippocamapal CA3-CA1 fEPSPs collected from a WT and a KO animal before and after kainic acid injection. Note that the presence of clonic seizures reduced significantly the amplitude of the evoked fEPSP in the KO mouse.

C. Differential effects of train stimulation (St.: five 200 Hz, 100 ms trains of pulses at a rate of 1/s) of WT and KO mice before and after kainic acid injection. Note the long-lasting seizure evoked in the KO animal when stimulated following kainic acid injection.

D. Spectral analysis of hippocampal EEG recordings collected from WT and KO mice before (WT, dark red; KO, dark blue) and after (WT, light red; KO, light blue) kainic injection. Note that the presence of repetitive seizures cancel out the normal theta (4–8 Hz) present in hippocampal EEG in behaving mice.

conditions because it is trapped in the LBs. Alternatively, GS accumulated in the LBs could be truly inactivated through structural changes, aggregation or unknown posttranslational modifications that prevented it from undergoing the allosteric activation induced by an excess of G6P. To the best of our knowledge, LD models are the only examples in which accumulations of this abnormal MGS have been described. So the mechanism by which the activity of this enzyme is impaired could be a unique characteristic of the disease and opens new questions on the regulation of glycogen metabolism.

The MGS accumulation observed in malin KO brains (11 months) is also comparable to that described for laforin KO brains at the same age (9–12 months) (Tagliabracci et al, 2008). Recent work (Turnbull et al, 2011) shows that PTG depletion prevents LB formation and the epileptic phenotype of laforin KO mice. Taken together, these observations reinforce the notion that the malin–laforin complex is involved in the degradation of PTG and MGS (Vilchez et al, 2007).

Although the presence of LBs in glial cells of patients was a matter of debate at the beginning of the 20th century (del Río-Hortega, 1925; Lafora, 1913), to the best of our knowledge, our study is the first to demonstrate astroglial LBs. This finding solves a long established paradox in LD. Research into this disease has been focused on neurons and the presence of LBs in these cells is considered the hallmark of LD. However, the presence of aberrant glycogen depositions in neurons but not in astrocytes is paradoxical as astrocytes, but not neurons, are considered to be the glycogenic cells in the brain. The immunohistological studies of the hippocampus, one of the most affected zones in the malin KO brains, showed that astrocytes and PV^+ interneurons express MGS and malin and that both types of cells accumulate LBs when malin is knocked out. This finding supports the idea that LBs are formed as a result of the deregulation of glycogen machinery. Interestingly, polyglucosan accumulation appeared first in astrocytes. The chronology of the appearance of LBs correlates with the degenerative character of LD as the increase in polyglucosan deposits in PV^+ somas coincided with loss of these interneurons. These observations are in agreement with previous results from our group suggesting that neurons are much more sensitive than astrocytes to cell death induced by glycogen overaccumulation (Vilchez et al, 2007).

Hippocampal PV^+ cells are inhibitory interneurons. They contribute in the generation of synchronous population discharge patterns and their impairment is thought to be involved in epileptogenesis and seizure activity (Magloczky & Freund, 2005). In fact, a decrease in their number occurs in some cases of epilepsy (Castro et al, 2011; Dinocourt et al, 2003), Alzheimer's disease (Brady & Mufson, 1997; Takahashi et al, 2010), Creutzfeldt-Jakob disease (Guentchev et al, 1997), schizophrenia (Nullmeier et al, 2011; Zhang & Reynolds, 2002), and other disorders such as Ammon's horn sclerosis (Zhu et al, 1997) and dementia with Lewis bodies (Bernstein et al, 2011). Our results suggest that malin KO mice undergo late-onset degeneration of PV^+ interneurons, which correlates with intracellular LB formation. Therefore, although the loss of PV immunoreactivity cannot be ruled out as it has been also described in some cases of epileptic hippocampus (Arellano et al, 2004; Sloviter, 1991; Wittner et al, 2005), the enhanced synaptic excitability and the propensity to myoclonic seizures that we observed in these animals could be attributed to the loss of hippocampal PV^+ interneurons. The induction of glycogen accumulation in neuron primary cultures causes death by apoptosis (Vilchez et al, 2007). Thus, the loss of interneurons could be attributed to the accumulation of this polysaccharide. Given that we did not detect this neurodegeneration when LBs were extra-neuronal (4 months), we propose that the neuronal accumulation of MGS protein and its synthetic product polyglucosan is crucial for the progression of LD.

In spite of the severe neurodegeneration found in the malin KO mice, apoptotic neurons were not found in our preparations. The same observation has been made in the brain of laforin KO mice, other model of LD (Ganesh et al, 2002). The study of neurodegenerative diseases like Alzheimer's, Huntington's and Amyotrophic Lateral Sclerosis has shown that it is very difficult to detect apoptosis *in vivo* (Mattson, 2000). This is because

apoptosis usually occurs quite rapidly (within hours), thus hindering the detection of cells showing classic features of this process in a neurodegenerative event that takes months.

Taken together, our results provide important insights into the molecular basis of LD. First, they confirm *in vivo* the role of malin in regulating MGS and glycogen accumulation. Second, they provide the first evidence of LB presence in astroglial cells. And finally, they link the expression of malin and MGS with a particular subset of neurons, the formation of LBs in these cells, their progressive loss, and the neurological decline associated with LD. We propose that the failure of MGS regulation is a key point for the progression of LD, thus making MGS a possible target for the treatment of this devastating disease.

MATERIALS AND METHODS

Chemicals and reagents

Amyloglucosidase, α-amylase (from human saliva) and 3,3′-diaminobenzidine tetrahydrochloride (DAB) were from Sigma–Aldrich. Antibodies against MGS (from Cell Signalling and Epitomics), pSer640-GS (from Cell Signaling), pSer7,10-GS (from Kinasource), glycogenin (from Abnova), actin (from Sigma), glial fibrillary acidic protein (GFAP, from Millipore and Dako), parvalbumin (from Swant), β-galactosidase (βgal, from Promega), polyglucosan (from Kamiya) and laforin (a gift from Dr. Santiago Rodríguez de Córdoba) were used in this study. Antibodies to GP isoforms were produced by Eurogentec. Guinea Pigs were immunized against a synthetic peptide corresponding to the C-terminus (amino acids 826-841) of muscle glycogen phosphorylase (MGP). Chickens were immunized against a synthetic peptide corresponding to the C-terminus (amino acids 826–842) of mouse brain glycogen phosphorylase (BGP) (Vilchez et al, 2007).

Generation of *EPM2B* KO mice

EPM2B-disrupted ES C57BL/6N (10571D-E2) cells were obtained from the Knockout Mouse Project Repository (KOMP), University of California, Davis, CA. In these cells, the complete EPM2B coding region plus 391 nucleotides of the 3′-untranslated region are replaced with a cassette containing the LacZ and Neo^R genes. LacZ is fused in-frame at the EPM2B ATG (Supporting Information Fig 2A). After confirmation of targeting by PCR analyses (Supporting Information Fig 2B), the cells were injected into C57BL/6J blastocysts, and these were then implanted in the uterus of pseudo-pregnant C57BL/6J females for the generation of chimeric mice. One chimeric male positive for the disruption was mated with C57BL/6J females to test for germline transmission. Heterozygous F1 mice were intercrossed to generate the animals used in this study. WT, heterozygous and homozygous null mice were identified by PCR genotyping using oligonucleotide primer pairs for both the 5′-end and the 3′-end of the EPM2B-disrupted region (Supporting Information Fig 2B). Further confirmation of the disruption was obtained by RT-PCR of EPM2B mRNA (Supporting Information Fig 2C).

Animal studies

All procedures were approved by the Barcelona Science Park's Animal Experimentation Committee and were carried out in accordance with the European Community Council Directive and National Institutes of Health guidelines for the care and use of laboratory animals. Mice were allowed free access to a standard chow diet and water and maintained on a 12-h/12-h light/dark cycle under specific pathogen-free conditions in the Animal Research Center at the Barcelona Science Park. After weaning at 3 weeks of age, tail clippings were taken for genotyping by PCR.

Behavioural and electrophysiological tests

Methodological information regarding the open field test, the operant conditioning procedures, the input/output curves, the electroencephalographic (EEG) recordings and the kainate injection and recording of seizure activities can be found in Supporting Information Methods.

Sample preparation, homogenation and fractionation for biochemical analysis

The animals used for biochemical analysis were anesthetized and sacrificed by decapitation. Heads were directly froze on liquid nitrogen and stored at −80°C until use. Tissue samples were added to 10 volumes of ice-cold homogenization buffer containing 10 mM Tris-HCl (pH 7), 150 mM KF, 15 mM EDTA, 15 mM 2-mercaptoethanol, 0.6 M sucrose, 25 nM okadaic acid, 1 mM sodium orthovanadate, 10 μg/ml leupeptin, 10 μg/ml aprotinin, 10 μg/ml pepstatin, 1 mM benzamidine and 1 mM phenylmethanesulfonyl fluoride. They were then homogenized (Polytron) at 4°C. For sample fractionation, homogenates were centrifuged at $13000 \times g$ for 15 min at 4°C. Sediments were resuspended with the same volume as supernatant of the corresponding buffer. Total homogenates, supernatants and sediments were recovered for GS activity, Western blotting and glycogen determination. Insoluble fractions were treated with amylase 110 U/ml for 3 h at 37°C to analyse glycogenin by Western blotting.

Glycogen synthase activity determination

Glycogen synthase activity was measured in total homogenates, supernatants and sediments in the presence of 4.4 mM UDP-glucose and absence or presence of 6.6 mM G6P, representing active or total activity, respectively, as previously described (Thomas et al, 1968).

Glycogen analysis

Total homogenates, supernatants and sediments were boiled in 30% KOH for 15 min and glycogen was determined by an amyloglucosidase-based assay as described in Chan and Exton (Chan & Exton, 1976). To assess glycogen branching, we used the method described by Krisman (Krisman, 1962).

Histology

Animals were anesthetized and perfused transcardiacally with phosphate buffered saline (PBS) containing 4% of paraformaldehyde. Brains were removed, postfixed with PBS-4% paraformaldehyde, cryoprotected with PBS-30% sucrose and frozen. To obtain tissue sections, brains were sectioned coronally at 30 μm, distributed in 10 series, and maintained at −20°C in PBS-30% glycerol-30% ethylene glycol for free-floating processing. In the case of animals used in electrophysiological experiments, selected sections

The paper explained

PROBLEM:

Lafora disease (LD) is a fatal progressive epilepsy caused by mutations in either *EPM2A*, which encodes laforin, or *EMP2B*, which encodes malin. At the beginning of the 20th century, more than 80 years before the discovery of the genes causing this disease, the presence of abnormal glycogen inclusions (later referred to as LBs) in neurons of the patients was described as the hallmark of the disease. However, the mechanism behind the formation of abnormal glycogen in LD is still a matter of debate, as is the link between LB formation and neurodegeneration. We approached these questions by studying malin-deficient mice.

RESULTS:

Our work is centred on the hippocampus, one of the most affected areas of the brain in LD. Here, we describe the expression of GS—the only enzyme able to produce glycogen in mammals—and malin in astrocytes and interneurons, and we analyse the progressive appearance of LBs in these cells in the malin-deficient mouse. We found a dramatic increase in GS in the brain of this animal model. The enzyme accumulated on LBs in an insoluble non-active form. Here, we have found a link between the late formation of LBs in a particular subset of interneurons, their degeneration and the characteristic neuropathology associated with LD. Furthermore, this is the first study to report the presence of LBs in astrocytes.

IMPACT:

Our findings provide new insights into the etiology of LD. Although glycogen is stored normally in astrocytes, evidence of LBs in these cells has never been reported. The detection of LBs in glial cells widens our vision by showing that the formation of aberrant glycogen is not limited to neurons. We highlight the high susceptibility of neurons, a cell type that does not normally store glycogen, to cell death induced by the accumulation of this polysaccharide and conclude that the malin/laforin complex is crucial for GS regulation and glycogen accumulation. We propose that GS is a potential target for the treatment of LD.

including the dorsal hippocampus were mounted on gelatinized glass slides and stained using the Nissl technique with 0.1% toluidine blue, to determine the location of stimulating and recording electrodes.

Electron microscopy

Animals were perfused with 2% glutaraldehyde-2% paraformaldehyde in 0.12 M phosphate buffer. After post-fixation in the same solution overnight, tissue slices were transferred to 2% osmium tetroxide, stained with 2% uranyl acetate, dehydrated and finally embedded in Araldite. Ultrathin sections from medial hippocampal samples were collected on formvar-coated slot grids and stained with lead citrate. Electron micrographs were taken using a Tecnai Spirit transmission electron microscope.

Immunocytochemistry

For immunodetection of antigens, sections were washed in PBS and PBS-0.1% Triton X-100, blocked for 2 h at RT with PBS containing 10% of normal goat serum (NGS), 0.2% of gelatin, and $F(ab')_2$ fragment anti-mouse IgG when required. Primary antibodies were incubated overnight at 4°C with PBS–5% NGS. For immunohistofluorescence, dye-labelled secondary antibodies and Hoechst 33342 were incubated for 2 h at RT in PBS-5% NGS, mounted in Mowiol and stored at −20°C. Confocal images were taken with a Leica SP5 microscope. For immunohistochemistry, sequential incubation with biotinylated secondary antibodies and streptavidin-HRP was performed in PBS-5% NGS. Bound antibodies were visualized by reaction using 0.03% diaminobenzidine and 0.002% H_2O_2, and sections were dehydrated and mounted (Eukitt). For PAS staining, selected brain sections were oxidized with 5% periodic acid for 10 min, stained with Schiff reagent for 30 min, dehydrated and mounted (Eukitt).

Cell counting

For quantification in the hippocampus, the number of parvalbumin-positive (PV^+) cells was counted every 10th section for each animal; data were normalized to the area counted in 30-μm-thick sections ($n = 8$–10 sections per animal, 3 animals per group). Areas measured for quantification were determined using ImageJ software.

Statistical analysis

Data are expressed as mean ± SEM. Statistical significance was determined by unpaired Student's *t*-test using GraphPad Prism software (version 5; GraphPad Software, Inc.). Statistical significance was assumed at $p \leq 0.05$.

Author contributions

JVO participated in the design and coordination of the study, carried out the histological analyses of brains, the quantification of PV^+ interneurons, and the glycogen branching assay and drafted the manuscript; JD conceived the study, participated in its design and coordination, generated, bred and genotyped the mice, carried out the histological analyses of muscle and heart, performed the behavioural studies and helped to draft the manuscript; MGR carried out the biochemical studies; CB performed the electron microscopy study; JMDG and AG performed the operant conditioning test and the electrophysiological studies; IS helped to analyse the mice; LP helped to study the brain MGS expression; AS helped to perform the histological analyses; XC and ES participated in the coordination of the study; JJG directed the study. All the authors read and approved the final manuscript.

Acknowledgements

The authors thank Anna Adrover, Emma Veza, Montserrat Climent and Natàlia Plana (IRB Barcelona), Marisa Larramona (Barcelona Science Park) and María Sánchez-Enciso (Pablo de Olavide University) for their technical assistance. Thanks also go to Stephen Forrow (IRB Barcelona Mouse Mutant Core Facility) and Julian Colombelli, Lídia Bardia and Anna Lladó (IRB Barcelona Advanced Digital Microscopy Core Facility) and Carmen López (University of Barcelona Electron Microscopy Unit) for advice, Joaquim Calbó and Florencia Tevy for critical review and to Tanya Yates for correcting the English version of the manuscript. This work was supported by the Ministerio de Ciencia y Innovación, Spain [grant numbers BFU2008-00769, BFU2008-03390/BMC, and BFU2008-00899], the Instituto de Salud Carlos III [PhD fellowship number FI06/00375] to [JV], the Torres Quevedo programme [PTQ-08-03-07880] to [AS] and a grant from the Fundación Marcelino Botín and the CIBER de Diabetes y Enfermedades Metabólicas Asociadas (ISCIII, Ministerio de Ciencia e Innovación).

Supporting information is available at EMBO Molecular Medicine online.

The authors declare that they have no conflict of interest.

For more information

OMIM Lafora Disease:
http://www.ncbi.nlm.nih.gov/omim/254780

Genes:

Malin:
http://www.ncbi.nlm.nih.gov/gene/378884

Laforin:
http://www.ncbi.nlm.nih.gov/gene/7957

MGS:
http://www.ncbi.nlm.nih.gov/gene/2997

References

Arellano JI, Munoz A, Ballesteros-Yanez I, Sola RG, DeFelipe J (2004) Histopathology and reorganization of chandelier cells in the human epileptic sclerotic hippocampus. Brain 127: 45-64

Bernstein HG, Johnson M, Perry RH, LeBeau FE, Dobrowolny H, Bogerts B, Perry EK (2011) Partial loss of parvalbumin-containing hippocampal interneurons in dementia with Lewy bodies. Neuropathology 31: 1-10

Bouskila M, Hunter RW, Ibrahim AF, Delattre L, Peggie M, van Diepen JA, Voshol PJ, Jensen J, Sakamoto K (2010) Allosteric regulation of glycogen synthase controls glycogen synthesis in muscle. Cell Metab 12: 456-466

Brady DR, Mufson EJ (1997) Parvalbumin-immunoreactive neurons in the hippocampal formation of Alzheimer's diseased brain. Neuroscience 80: 1113-1125

Castro OW, Furtado MA, Tilelli CQ, Fernandes A, Pajolla GP, Garcia-Cairasco N (2011) Comparative neuroanatomical and temporal characterization of FluoroJade-positive neurodegeneration after status epilepticus induced by systemic and intrahippocampal pilocarpine in Wistar rats. Brain Res 1374: 43-55

Cataldo AM, Broadwell RD (1986) Cytochemical identification of cerebral glycogen and glucose-6-phosphatase activity under normal and experimental conditions. II. Choroid plexus and ependymal epithelia, endothelia and pericytes. J Neurocytol 15: 511-524

Cavanagh JB (1999) Corpora-amylacea and the family of polyglucosan diseases. Brain Res Brain Res Rev 29: 265-295

Chan TM, Exton JH (1976) A rapid method for the determination of glycogen content and radioactivity in small quantities of tissue or isolated hepatocytes. Anal Biochem 71: 96-105

Chan EM, Andrade DM, Franceschetti S, Minassian B (2005) Progressive myoclonus epilepsies: EPM1, EPM2A, EPM2B. Adv Neurol 95: 47-57

del Río-Hortega P (1925) Papel de la microglía en la formación de los cuerpos amiláceos del tejido nervioso. Boletín Sociedad Española Historia Natural 25: 127-141

Delgado-Escueta AV (2007) Advances in lafora progressive myoclonus epilepsy. Curr Neurol Neurosci Rep 7: 428-433

DePaoli-Roach AA, Tagliabracci VS, Segvich DM, Meyer CM, Irimia JM, Roach PJ (2010) Genetic depletion of the malin E3 ubiquitin ligase in mice leads to lafora bodies and the accumulation of insoluble laforin. J Biol Chem 285: 25372-25381

Dinocourt C, Petanjek Z, Freund TF, Ben-Ari Y, Esclapez M (2003) Loss of interneurons innervating pyramidal cell dendrites and axon initial segments in the CA1 region of the hippocampus following pilocarpine-induced seizures. J Comp Neurol 459: 407-425

Ganesh S, Delgado-Escueta AV, Sakamoto T, Avila MR, Machado-Salas J, Hoshii Y, Akagi T, Gomi H, Suzuki T, Amano K *et al* (2002) Targeted disruption of the Epm2a gene causes formation of Lafora inclusion bodies, neurodegeneration, ataxia, myoclonus epilepsy and impaired behavioral response in mice. Hum Mol Genet 11: 1251-1262

Ganesh S, Puri R, Singh S, Mittal S, Dubey D (2006) Recent advances in the molecular basis of Lafora's progressive myoclonus epilepsy. J Hum Genet 51: 1-8

Gentry MS, Worby CA, Dixon JE (2005) Insights into Lafora disease: malin is an E3 ubiquitin ligase that ubiquitinates and promotes the degradation of laforin. Proc Natl Acad Sci USA 102: 8501-8506

Goldberg ND, O'Toole AG (1969) The properties of glycogen synthetase and regulation of glycogen biosynthesis in rat brain. J Biol Chem 244: 3053-3061

Gruart A, Munoz MD, Delgado-Garcia JM (2006) Involvement of the CA3-CA1 synapse in the acquisition of associative learning in behaving mice. J Neurosci 26: 1077-1087

Guentchev M, Hainfellner JA, Trabattoni GR, Budka H (1997) Distribution of parvalbumin-immunoreactive neurons in brain correlates with hippocampal and temporal cortical pathology in Creutzfeldt-Jakob disease. J Neuropathol Exp Neurol 56: 1119-1124

Krisman CR (1962) A method for the colorimetric estimation of glycogen with iodine. Anal Biochem 4: 17-23

Lafora GR (1913) Nuevas investigaciones sobre los cuerpos amiláceos del interior de las células nerviosas. Trab Lab Investi Biológ Univ Madrid 11: 29-42

Lohi H, Ianzano L, Zhao XC, Chan EM, Turnbull J, Scherer SW, Ackerley CA, Minassian BA (2005) Novel glycogen synthase kinase 3 and ubiquitination pathways in progressive myoclonus epilepsy. Hum Mol Genet 14: 2727-2736

Madronal N, Gruart A, Delgado-Garcia JM (2009) Differing presynaptic contributions to LTP and associative learning in behaving mice. Front Behav Neurosci 3: 7

Madronal N, Lopez-Aracil C, Rangel A, del Rio JA, Delgado-Garcia JM, Gruart A (2010) Effects of enriched physical and social environments on motor performance, associative learning, and hippocampal neurogenesis in mice. PLoS One 5: e11130

Magloczky Z, Freund TF (2005) Impaired and repaired inhibitory circuits in the epileptic human hippocampus. Trends Neurosci 28: 334-340

Mattson MP (2000) Apoptosis in neurodegenerative disorders. Nat Rev Mol Cell Biol 1: 120-129

McLin JP, Steward O (2006) Comparison of seizure phenotype and neurodegeneration induced by systemic kainic acid in inbred, outbred, and hybrid mouse strains. Eur J Neurosci 24: 2191-2202

Nullmeier S, Panther P, Dobrowolny H, Frotscher M, Zhao S, Schwegler H, Wolf R (2011) Region-specific alteration of GABAergic markers in the brain of heterozygous reeler mice. Eur J Neurosci 33: 689-698

Pfeiffer-Guglielmi B, Fleckenstein B, Jung G, Hamprecht B (2003) Immunocytochemical localization of glycogen phosphorylase isozymes in rat nervous tissues by using isozyme-specific antibodies. J Neurochem 85: 73-81

Skurat AV, Wang Y, Roach PJ (1994) Rabbit skeletal muscle glycogen synthase expressed in COS cells. Identification of regulatory phosphorylation sites. J Biol Chem 269: 25534-25542

Sloviter RS (1991) Permanently altered hippocampal structure, excitability, and inhibition after experimental status epilepticus in the rat: the "dormant basket cell" hypothesis and its possible relevance to temporal lobe epilepsy. Hippocampus 1: 41-66

Tagliabracci VS, Turnbull J, Wang W, Girard JM, Zhao X, Skurat AV, Delgado-Escueta AV, Minassian BA, Depaoli-Roach AA, Roach PJ (2007) Laforin is a glycogen phosphatase, deficiency of which leads to elevated phosphorylation of glycogen in vivo. Proc Natl Acad Sci USA 104: 19262-19266

Tagliabracci VS, Girard JM, Segvich D, Meyer C, Turnbull J, Zhao X, Minassian BA, Depaoli-Roach AA, Roach PJ (2008) Abnormal metabolism of glycogen phosphate as a cause for Lafora disease. J Biol Chem 283: 33816-33825

Tagliabracci VS, Heiss C, Karthik C, Contreras CJ, Glushka J, Ishihara M, Azadi P, Hurley TD, Depaoli-Roach AA, Roach PJ (2011) Phosphate incorporation during glycogen synthesis and Lafora disease. Cell Metab 13: 274-282

Takahashi H, Brasnjevic I, Rutten BP, Van Der Kolk N, Perl DP, Bouras C, Steinbusch HW, Schmitz C, Hof PR, Dickstein DL (2010) Hippocampal interneuron loss in an APP/PS1 double mutant mouse and in Alzheimer's disease. Brain Struct Funct 214: 145-160

Thomas JA, Schlender KK, Larner J (1968) A rapid filter paper assay for UDPglucose-glycogen glucosyltransferase, including an improved biosynthesis of UDP-14C-glucose. Anal Biochem 25: 486-499

Turnbull J, Wang P, Girard JM, Ruggieri A, Wang TJ, Draginov AG, Kameka AP, Pencea N, Zhao X, Ackerley CA *et al* (2010) Glycogen hyperphosphorylation underlies lafora body formation. Ann Neurol 68: 925-933

Turnbull J, Depaoli-Roach AA, Zhao X, Cortez MA, Pencea N, Tiberia E, Piliguian M, Roach PJ, Wang P, Ackerley CA *et al* (2011) PTG depletion removes Lafora bodies and rescues the fatal epilepsy of Lafora disease. PLoS Genet 7: e1002037

Vilchez D, Ros S, Cifuentes D, Pujadas L, Valles J, Garcia-Fojeda B, Criado-Garcia O, Fernandez-Sanchez E, Medrano-Fernandez I, Dominguez J *et al* (2007) Mechanism suppressing glycogen synthesis in neurons and its demise in progressive myoclonus epilepsy. Nat Neurosci 10: 1407-1413

Villar-Palasi C, Guinovart JJ (1997) The role of glucose 6-phosphate in the control of glycogen synthase. FASEB J 11: 544-558

Wender R, Brown AM, Fern R, Swanson RA, Farrell K, Ransom BR (2000) Astrocytic glycogen influences axon function and survival during glucose deprivation in central white matter. J Neurosci 20: 6804-6810

Wittner L, Eross L, Czirjak S, Halasz P, Freund TF, Magloczky Z (2005) Surviving CA1 pyramidal cells receive intact perisomatic inhibitory input in the human epileptic hippocampus. Brain 128: 138-152

Zhang ZJ, Reynolds GP (2002) A selective decrease in the relative density of parvalbumin-immunoreactive neurons in the hippocampus in schizophrenia. Schizophr Res 55: 1-10

Zhu ZQ, Armstrong DL, Hamilton WJ, Grossman RG (1997) Disproportionate loss of CA4 parvalbumin-immunoreactive interneurons in patients with Ammon's horn sclerosis. J Neuropathol Exp Neurol 56: 988-998

Zucker RS, Regehr WG (2002) Short-term synaptic plasticity. Annu Rev Physiol 64: 355-405

Supporting Information Figure Legends

Supporting Information Fig. 1. Malin KO bodies are MGS- and PAS-positive (Skeletal Muscle and Heart). Presence of MGS- and PAS-positive inclusions in skeletal muscle and heart of 11-month-old WT mice, and of 4- and 11-month-old malin KO mice. Scale bar 100µm. 4x = 4-fold magnification.

Supporting Information Figure 2. Generation and validation of the malin KO mouse. (**A**) Schematic representation of the targeted disruption. Arrows indicate the position of the primers used for genotyping. (**B**) 5'-end and 3'-end genotyping. Bands corresponding to the WT and the KO allele are indicated. (**C**) RT-PCR confirming the absence of malin mRNA in the KO.

Supporting Information Figure 3. Analysis of GP and glycogenin in the insoluble fraction. Brain extracts from 11-month-old wild-type (WT) and malin knock-out (KO) mice were analyzed. Soluble and insoluble fractions resulting from low speed centrifugation were used for the biochemical analysis. (**A**) Western blotting for muscle glycogen phosphorylase (MGP) and brain glycogen phosphorylase (BGP). (**B**) Western blotting for glycogenin in amylase-treated insoluble fraction. Actin was used as loading control.

Supporting Information Figure 4. Gliosis in malin KO hippocampus. Representative images of 11-months WT and KO hippocampus are shown. Antibodies were used against GFAP (green) and polyglucosan (red). Hoechst (blue) was used for nuclear staining. Scale bar 100µm.

Supporting Information Figure 5. Open field test. WT and KO mice were tested for open field activity for 30 min. Percentage of time spent in the center of the arena, distance run and number of rearings were scored. Data are expressed as mean ± SEM. *=$p<0.05$, **=$p<0.01$, ***=$p<0.001$. WT (n=9), KO (n=9).

Supporting Information Methods

Open Field Test. A square open field arena with an area of 40cm×40 cm and walls 30 cm high was used. A mouse was placed in the center and allowed to move freely for 30 min while being recorded by a video camera mounted above the open field. The recordings were scored later by a motion-recognition software that detects and analyzes mouse movements (Smart Junior, Panlab). At the end of each trial the surface of the arena was cleaned with 90% ethanol. A square central area accounting for 16% of the total area was defined as 'center'.

Operant conditioning procedures. Following early descriptions from some of us (Gottlieb et al., 2006; Madronal et al., 2010)**,** training took place in Skinner box modules measuring 12.5×13.5×18.5 cm (MED Associates, St. Albans, VT, USA). Each Skinner box was housed within a sound-attenuating chamber, which was constantly illuminated (19 W lamp) and exposed to a 45 dB white noise (Cibertec, S.A., Madrid, Spain). Each Skinner box was equipped with a food dispenser from which pellets (Noyes formula P; 45 mg; Sandown Scientific, Hampton, UK) could be delivered by pressing a lever. Before training, mice were handled daily for 7 days and food-deprived to 80% of their free-feeding weight. For operant conditioning, animals were trained to press the lever to receive pellets from the feeder using a fixed-ratio (1:1) schedule. Sessions lasted for 20 min. Animals were maintained on this 1:1 schedule until they reached the selected criterion, namely when they obtained ≥ 20 pellets/session for two successive sessions. Conditioning programs, lever presses, and delivered reinforcements were monitored and recorded by a computer, using a MED-PC program (MED Associates, St. Albans, VT, USA).

Input/output curves, paired pulse facilitation and long-term potentiation (LTP) in behaving mice. Animals were prepared following procedures described elsewhere (Gruart et al., 2006). Under deep anesthesia (ketamine, 35 mg/kg and xylazine, 2 mg/kg, i.p.) mice were implanted with bipolar electrodes aimed at the right Schaffer collateral-commissural pathway of the dorsal hippocampus (2 mm lateral and 1.5 mm posterior to Bregma; depth from brain surface, 1.0-1.5 mm; Paxinos and Franklin, 2001) and with two recording electrodes aimed at the ipsilateral CA1 area (1.2 mm lateral and 2.2 mm posterior to Bregma; depth from brain surface, 1.0-1.5 mm). Electrodes were made from 50 μm, Teflon-coated, tungsten wire (Advent Research, Eynsham, UK). The final location of the recording electrode in the CA1 area was determined according to the field potential depth profile evoked by single pulses presented to the Schaffer collateral pathway (Gruart et al., 2006). A bare silver wire was affixed to the bone as ground. Implanted wires were soldered to a six-pin socket (RS Amidata, Madrid, Spain), which was fixed to the skull with dental cement (see (Gruart et al., 2006) for details).

For input/output curves, mice were stimulated at the Schaffer collaterals with paired pulses (40 ms of inter-stimulus interval) at increasing intensities (0.02-0.4 mA). We also checked the effects of paired pulses at a range of (10, 20, 40, 100, 200, and 500 ms) inter-stimulus intervals when using intensities corresponding to 40% and 60% of the amount required to evoke a saturating response. In all the cases, the pair of pulses of a given intensity was repeated ≥ 5 times with time intervals ≥ 30 s, to avoid as much as possible interferences with slower short-term potentiation (augmentation) or depression processes (Zucker & Regehr, 2002). Moreover, to avoid any cumulative effect, intensities and intervals were presented at random.

To evoke LTP in behaving mice, we followed procedures described previously (Gruart et al., 2006). Field EPSP baseline values were collected 15 min prior to LTP induction using single 100 μs, square, biphasic pulses. Pulse intensity was set at 30–40% of the amount required to evoke a maximum fEPSP response (0.15–0.25 mA) ─ i.e., well below the threshold for evoking a

population spike. For LTP induction, animals were presented with a high-frequency stimulation (HFS) session consisting of five 200 Hz, 100 ms trains of pulses at a rate of 1/s repeated six times, at intervals of 1 min. Thus, a total of 600 pulses were presented during the HFS session. In order to avoid evoking large population spikes and/or the appearance of EEG seizures, the stimulus intensity during HFS was set at the same as that used for generating baseline recordings. After each HFS session, the same single stimuli were presented every 20 s for 60 additional min and for 30 min the followings five days.

Electroencephalographic (EEG) recordings. EEG recordings were carried out with the awake animal placed in a small (5 × 5 × 5 cm) box, to avoid over walking movements. Recordings were carried out for 5 min. The power spectrum of the hippocampal EEG activity was computed with Mat Lab 7.4.0 software (MathWorks, Natick, MA, USA), using the fast Fourier transform with a Hanning window, expressed as relative power and averaged across each recording session (Munera et al., 2000).

Kainate injection and recording of seizure activities. To study the propensity of WT and KO mice to generate convulsive seizures, animals were injected (i.p.) with the AMPA/kainate receptor agonist kainic acid (8 mg/kg; Sigma, Saint Louis, Missouri, USA) dissolved in 0,1 M phosphate buffered saline (PBS) pH = 7.4. The electrocorticographic activity of the hippocampal pyramidal CA1 area was recorded for 2 h after the injection. Injected animals were presented with a stimulus session (five 200 Hz, 100 ms trains of pulses at a rate of 1/s) 1 h after the injection (see Rangel et al., 2009 for details).

Supporting Information References

Gottlieb M, Leal-Campanario R, Campos-Esparza MR, Sanchez-Gomez MV, Alberdi E, Arranz A, Delgado-Garcia JM, Gruart A, Matute C (2006) Neuroprotection by two polyphenols following excitotoxicity and experimental ischemia. Neurobiol Dis 23**:** 374-386

Gruart A, Munoz MD, Delgado-Garcia JM (2006) Involvement of the CA3-CA1 synapse in the acquisition of associative learning in behaving mice. J Neurosci 26**:** 1077-1087

Madronal N, Lopez-Aracil C, Rangel A, del Rio JA, Delgado-Garcia JM, Gruart A (2010) Effects of enriched physical and social environments on motor performance, associative learning, and hippocampal neurogenesis in mice. PLoS One 5**:** e11130

Munera A, Gruart A, Munoz MD, Delgado-Garcia JM (2000) Scopolamine impairs information processing in the hippocampus and performance of a learned eyeblink response in alert cats. Neurosci Lett 292**:** 33-36

Rangel A, Madronal N, Gruart A, Gavin R, Llorens F, Sumoy L, Torres JM, Delgado-Garcia JM, Del Rio JA (2009) Regulation of GABA(A) and glutamate receptor expression, synaptic facilitation and long-term potentiation in the hippocampus of prion mutant mice. PLoS One 4**:** e7592

Zucker RS, Regehr WG (2002) Short-term synaptic plasticity. Annu Rev Physiol 64**:** 355-405

Supporting Information Figure 1

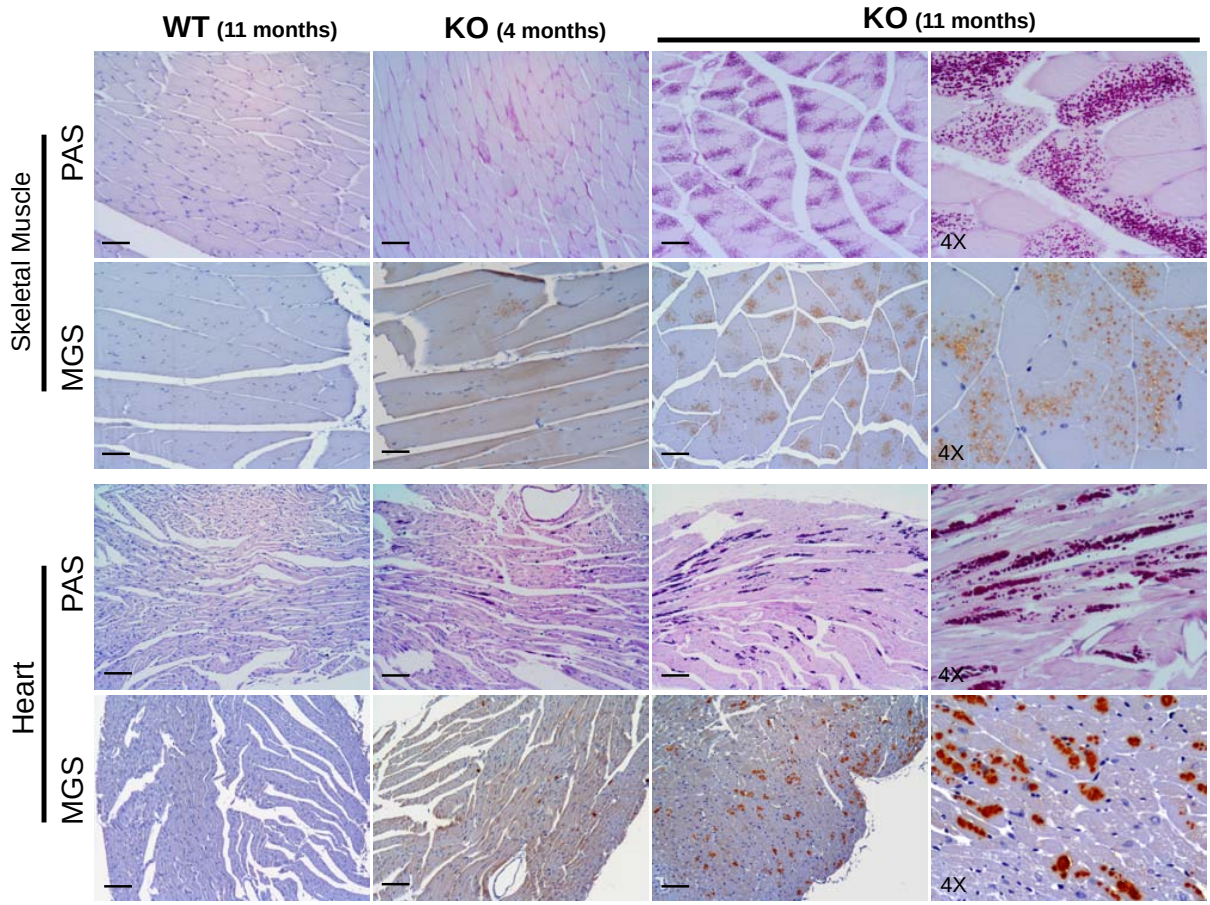

Supporting Information Figure 2

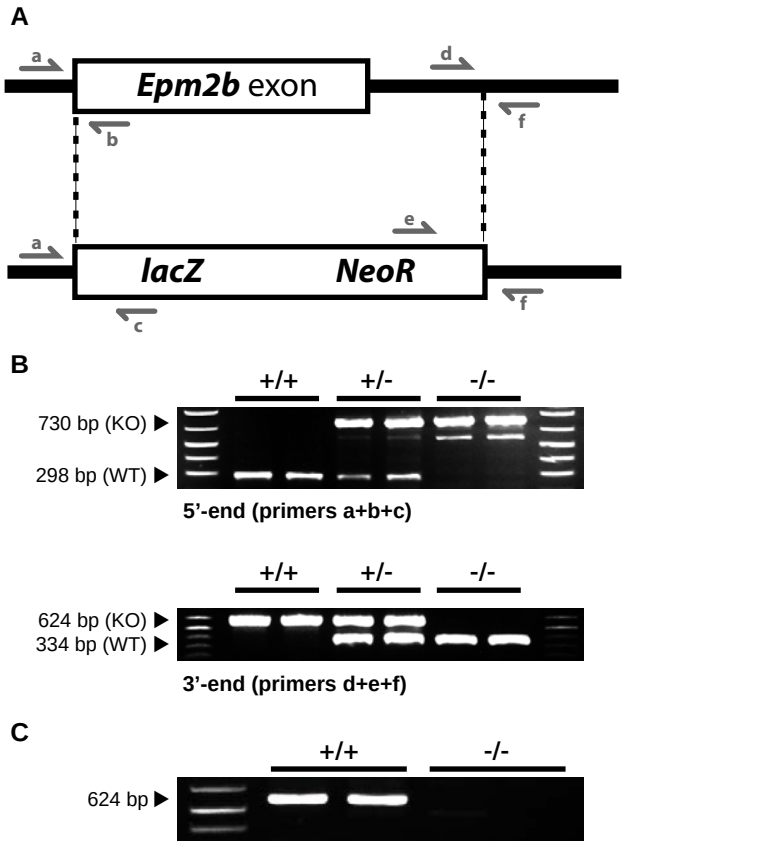

Supporting Information Figure 3

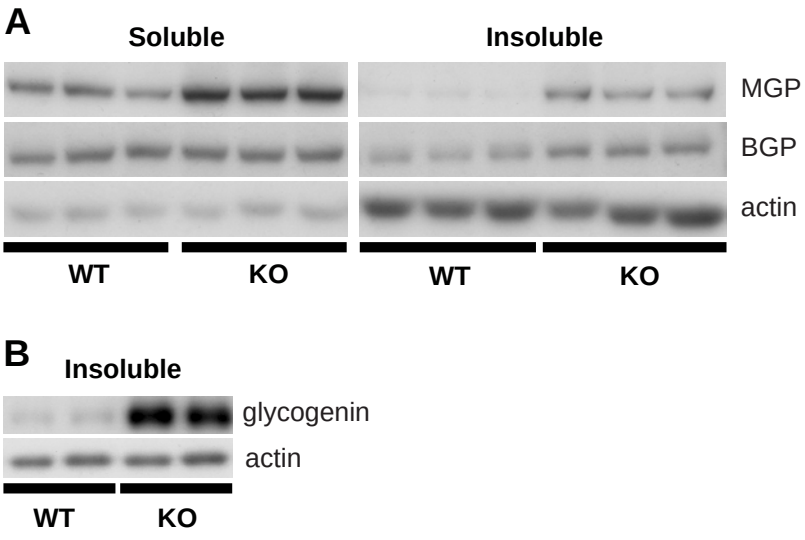

Supporting Information Figure 4

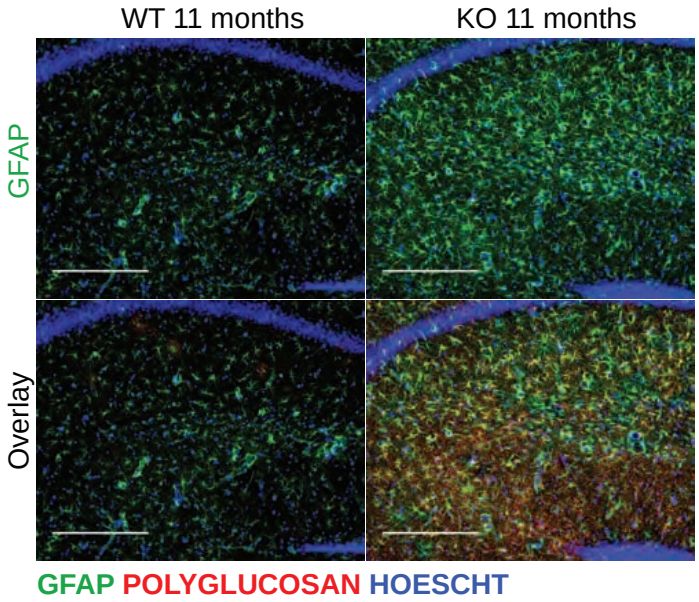

Supporting Information Figure 5

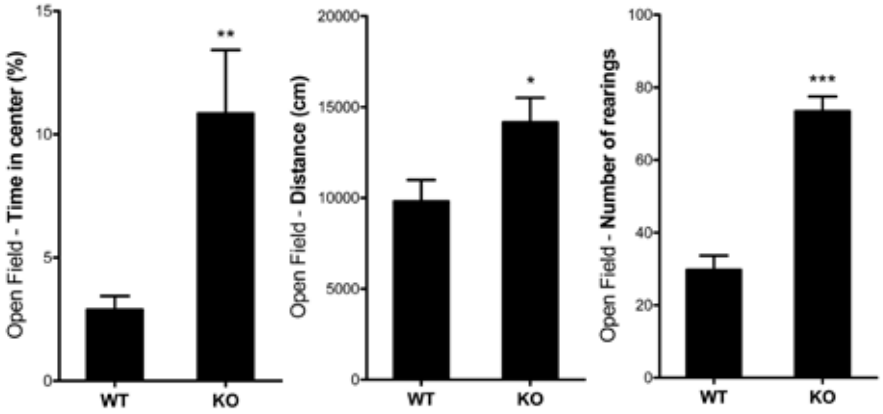

ARTICLE 3

A central role of glycogen synthase in corpora amylacea formation: similarities between Lafora disease and physiological aging.

Jordi Valles-Ortega, Jordi Duran, Mercedes Márquez, Lluís Pujadas, David Vílchez, Eduardo Soriano, Martí Pumarola and Joan J. Guinovart

ABSTRACT

Corpora amylacea (CA) are polyglucosan bodies (PGBs) that accumulate during aging in the brains of humans and other mammals. Here we compared the regional and cell-type localization and the protein composition of CA with those of Lafora bodies (LBs), the PGBs accumulated in Lafora disease (LD). For this purpose, we used normal aged mice and malin KO mice, the latter an LD model that we previously generated and described. Moreover, we studied the brain expression pattern of malin and glycogen synthase (MGS) during aging and evaluated the putative contribution of MGS to CA formation by analyzing MGS KO mice. Our results show strong similarities between CA and LBs, thereby suggesting a common mechanism for the formation of the two types of PGB. Here we demonstrate, for the first time, that MGS and therefore glycogen synthesis are required for brain CA formation during normal aging. These observations point to a new physiological role for glycogen machinery in neurodegenerative events.

INTRODUCTION

Glycogen is a polyglucosan –a polymer of glucose- known for its important energetic role, and it is the main carbohydrate storage of the human body (Brown, 2004). Liver and skeletal muscles are the most important glycogenic tissues of the body. In humans, there is around 100 g of glycogen in fed liver (6-8% of the tissue weight) and 400 g in resting skeletal muscle (1-2% of the tissue weight) (Brown, 2004; Shulman et al., 1995). Liver glycogen is released mainly as glucose into the blood stream when required to maintain normoglycemia. In contrast, muscle glycogen is consumed uniquely as a local energy source by skeletal muscle cells during exercise. Glycogen synthase (GS) is the only enzyme able to synthesize these large chains of glucose in mammals. There are two isoforms of GS. These receive the name of the main glycogen-accumulating tissues in which they are expressed. The *GYS1* gene codifies for Muscle Glycogen Synthase (MGS), which is expressed in muscle and other tissues, such as the brain and heart, but not in liver, this organ showing exclusive expression of the *GYS2* gene, codifying for Liver Glycogen Synthase (LGS). Glycogen Phosphorylase (GP) degrades the polysaccharide under glucose demand. There are three tissue-specific isoforms of GP in mammals, namely the muscle (MGP), liver (LGP) and brain (BGP) isoforms. Nevertheless, in addition to BGP, MGP is also expressed in brain tissue.

The human brain contains around 1 g of glycogen (0.1% of the tissue weight). This concentration is 10 times lower than that in skeletal muscle and 100 times lower than that in liver (Nelson et al., 1968). Thus, it is not surprising that the contribution of brain glycogen as an energy reserve for long-term activity has been overlooked and it is widely accepted that brain is energetically dependent of the delivery of glucose from the systemic circulation (Brown, 2004). However, brain glycogen content has been proposed to be a short-term energy source that supports local or specific neural activities, such as memory formation (Suzuki et al., 2011), sensory stimulation (Brown et al., 2003; Cruz and Dienel, 2002; Swanson et al., 1992), and sleep-wake cycles (Franken et al., 2003; Gip et al., 2002; Kong et al., 2002; Petit et al., 2002; Scharf et al., 2008). Furthermore, brain glycogen is protective under stress or pathological situations such as hypoglycemia (Brown et al., 2003; Herzog et al., 2008; Wender et al., 2000), exhaustive exercise (Matsui et al., 2011), ischemia (Brown et al., 2004), and seizures (Bernard-Helary et al., 2000; Cloix et al., 2010).

In this tissue, most glycogen is found in astroglial cells while most neurons do not accumulate this polysaccharide under normal conditions (Cataldo and Broadwell, 1986; Magistretti et al., 1993; Vilchez et al., 2007; Wender et al., 2000). These observations are in concordance with GP expression as MGP and BGP are found in astrocytes and only a few specific neurons have been reported to express the latter (Pfeiffer-Guglielmi et al., 2003). Nevertheless MGS is not expressed exclusively in astrocytes but is also present in neurons (Inoue et al., 1988; Pellegri et al., 1996; Valles-Ortega et al.,

2011). The finding that neurons express MGS and keep it inactive (Vilchez et al., 2007) suggests an alternative function for this enzyme in these cells.

Periodic Acid Schiff (PAS)-positive polyglucosan deposits, also named Polyglucosan Bodies (PGBs) are found in brain cells in several pathologies, such as Andersen Disease (GSD IV, OMIM232500), Adult Polyglucosan Body Disease (APBD, OMIM263570) and Lafora Disease (LD; EPM2, OMIM254780). The study of LD during the last decade has brought about a considerable amount of new data that have opened relevant questions regarding the function of glycogen metabolism, especially in the central nervous system. LD is a fatal epilepsy caused by mutations in two genes: *EPM2A*, which encodes laforin, a dual-specificity protein phosphatase with a functional carbohydrate-binding domain; and *EPM2B* (also known as *NHLRC1*), which encodes malin, an E3 ubiquitin ligase. Individuals with mutations in *EPM2A* or *EPM2B* are neurologically and histologically indistinguishable. Malin ubiquitinates and promotes the degradation of laforin (Gentry et al., 2005). These two proteins form a complex and have been described to regulate glycogen accumulation through ubiquitin-proteasome-dependent control of glycogen-related proteins, such as protein targeting to glycogen (PTG/R5), MGS, debranching enzyme (AGL) and neuronatin (Cheng et al., 2007; Sharma et al., 2011; Vilchez et al., 2007; Worby et al., 2008). Moreover, the phosphatase activity of laforin directly controls glycogen quality by preventing its hyperphosphorylation (Tagliabracci et al., 2011; Tagliabracci et al., 2007; Turnbull et al., 2010). In addition, it has been reported that laforin and malin are involved in cellular degradative systems such as the endosomal-lysosomal and autophagy pathways (Aguado et al., 2010; Criado et al., 2011; Knecht et al., 2010; Puri and Ganesh, 2010; Puri et al., 2011) and the clearance of misfolded proteins through the ubiquitin-proteasome system (Delgado-Escueta, 2007; Garyali et al., 2009; Rao et al., 2010a). Finally, it has been proposed that laforin-malin activities are protective against endoplasmic reticulum (Liu et al., 2009; Vernia et al., 2009) and thermal (Sengupta et al., 2011) stress. Given these recent lines of evidence, it is of interest to study whether glycogen machinery, in addition to its role in energy storage, is also linked to these cellular degradative pathways or to cell-stress responses.

In order to study this hypothetical link, a relevant feature of the CNS is the accumulation of Corpora amylacea (CA). CA are PGBs that are found in the brains of healthy aged humans and other mammals. In addition to polyglucosan, CA contain phosphate and proteins (Sakai et al., 1969), some of these related to cell stress, such as ubiquitin (Cisse et al., 1993) and heat-shock proteins (Cisse et al., 1993; Martin et al., 1991). These age-associated inclusions, which were first noted by J.E. Pukinje in 1837, have been widely characterized and well reviewed (Cavanagh, 1999). However, the originating cell type and especially the cause or the function of CA formation are still unclear. Interestingly, the accumulation of PGBs, normally referred to as CA, is enhanced by various stress insults such as anoxia (Abe and Yagishita, 1995) and ischemia (Botez and Rami, 2001) or neuropathological situations such as epilepsies (Das et al., 2011; Erdamar et al., 2000; Loiseau et al., 1992; Loiseau et al., 1993; Radhakrishnan et al., 2007), schizophrenia, Down's syndrome, Alzheimer's disease (Cavanagh, 1999; Cisse et al., 1993; Fleming et al., 1986; Nishi et al., 2003; Nishimura et al., 2000; Singhrao et al., 1993), and other neurodegenerative conditions (Kosaka et al., 1981; Nishi et al., 2003; Robitaille et al., 1980). These observations suggest that CA formation is related to cell stress or death rather than to glycogen metabolism disturbance.

Although CA are present in all mammals, their properties and regional localization within the brain differs between species. Moreover, although the appearance of these bodies is age-dependent, it is highly heterogeneous even within species (Cavanagh, 1999). Therefore, the study of CA and their comparison with other PGBs is challenging. Here we sought to compare several characteristics of the PGBs that accumulate during normal aging (CA) in mice with those present in LD (also called Lafora Bodies, LB) using a malin KO mouse model reported to overaccumulate MGS and polyglucosan (DePaoli-Roach et al., 2010; Valles-Ortega et al., 2011). Furthermore, in order to evaluate the contribution of MGS to the formation of CA, we generated MGS KO mice. Here we show that the polyglucosan matrix synthesized by MGS is required for CA formation during aging. We point out the remarkable similarities between CA and LB and finally we hypothesize that the formation of these two types of PGB corresponds to different stages, or to the impairment of different steps, of the same physiological event.

METHODS

Generation of transgenic mice

Epm2b-disrupted (malin KO) mice were generated as described previously (Valles-Ortega et al., 2011). *Gys1*-disrupted (MGS KO) ES C57BL/6N cells were obtained from the European Conditional Mouse Mutagenesis Program (EUCOMM), Wellcome Trust Sanger Institute, Hinxton (UK). In these cells, the *Gys1* gene is disrupted by the insertion of a cassette containing the *LacZ* and *NeoR* genes between exons 5 and 6 (Supplementary Figure 1). After confirmation of targeting by PCR analyses, we injected the cells into C57BL/6J blastocysts, and these were then implanted in the uterus of pseudo-pregnant C57BL/6J females for the generation of chimeric mice. One chimeric male positive for the disruption was mated with C57BL/6J females to test for germline transmission. Heterozygous F1 mice were intercrossed to generate the animals used in this study. Wt, heterozygous, and homozygous null mice were identified by PCR genotyping.

Animal manipulation

All procedures were approved by the Barcelona Science Park's Animal Experimentation Committee and were carried out in accordance with the European Community Council Directive and National guidelines for the care and use of laboratory animals. Mice were allowed free access to a standard chow diet and water and maintained on a 12-h/12-h light/dark cycle under specific pathogen-free conditions in the Animal Research Center at the Barcelona Science Park. After weaning the mice at 3 weeks of age, tail clippings were taken for genotyping by PCR.

Histology

Animals were anesthetized and perfused transcardiacally with phosphate buffered saline (PBS) containing 4% paraformaldehyde (PF). Brains were removed and postfixed for 12 h with PBS–4% PF, embedded in paraffin and sectioned coronally at 4 µm. To obtain cryosections, brains were cryoprotected with PBS-30% sucrose after postfixation, frozen, sectioned coronally at 30 µm, distributed in 10 series, and maintained at –20°C in PBS–30% glycerol–30% ethylene glycol for free-floating processing.

X-gal staining

For X-gal staining, animals were anesthetized and perfused transcardially with PBS containing 2% PF. Brains were removed, postfixed for 4h with PBS–2% PF, cryoprotected with PBS-30% sucrose, frozen and sectioned coronally at 30 µm. Sections were incubated at 37°C for 12 h in PBS containing 0.5% Triton X-100, 10 mM $MgCl_2$, 5 mM $K_3Fe(CN)_6$, 5 mM $K_4Fe(CN)_6$, and 4-chloro-5-bromo-3-indolyl P-D-galactopyranoside (X-Gal) at 0.6 mg/ml (Soriano et al., 1995). To discard the possibility of endogenous β-galactosidase activity contributing to the labeling pattern, brain sections were also obtained from control animals (wild-type littermates) and processed for X-gal. Labeled cells were not found in any control tissue.

Immunohistochemistry

Brain sections were stained with Haematoxylin and Eosin (HE), Periodic Acid-Schiff (PAS), Iodine (Lugol), Congo Red and Methenamine. The primary antibodies used in the immunohistochemical (IHC) studies were against MGS (1:200, Epitomics 1741), laforin (1:150, a generous gift from Dr. Rodríguez de Córdoba), advanced glycation end products (AGEP, 1:500, a generous gift from Dr. Rafael Salto), ubiquitin (1:300, Dakocytomation Z0458), HSP70 (1:50, MBL International Corporation SR810F), parvalbumin (PV, 1:3000, Sigma P3088), 200 KDa phosphorylated and non-phosphorylated neurofilament Clone 52 (NF200, 1:1000, Sigma N0142), α-synuclein (1:300, Chemicon AB5334P), and tau (1:500, Dako A0024). To minimize the background, the MOM kit (Vector laboratories Inc BMK-2202) was used in monoclonal mouse primary antibody IHC. For IHC based on rabbit primary antibodies, the anti-rabbit Envision-System-HRP (Dakocytomation K4011) kit was used. In all cases, the positive immunoreactivity was visualized with the 3, 3'-diaminobenzidine tetrahydrochloride (DAB) system included in the Envision-System-HRP (Dakocytomation K4011) kit.

Immunohistofluorescence

Fluorescent immunodetection of antigens was performed by free-floating on the 30-µm sections that were washed in PBS and PBS- 0.1% Triton X-100, blocked for 2 h at RT with PBS containing 10% of

normal goat serum (NGS), 0.2% gelatin, and F(ab')$_2$ fragment anti-mouse IgG when required. Primary antibodies were incubated with PBS–5% NGS overnight at 4°C. We used antibodies against parvalbumin (PV, 1:1000, Swant PV25), glial fibrillary acidic protein (GFAP, 1:500, Millipore MAB360), polyglucosan (1:50, Kamiya MC-253) and brain glycogen phosphorylase (BGP, 1:1000, (Vilchez et al., 2007)). Dye-labeled secondary antibodies and Hoechst 33342 were incubated for 2 h at RT in PBS–5% NGS, mounted in Mowiol, and stored at –20°C. Confocal images were taken with a Leica SP5 microscope. ImageJ software (Wayne Rasband, National Institute of Health, USA; http://imagej.nih.gov/ij) was used for image processing. Three-dimensional representations were obtained by Imaris® software (Bitplane AG).

RESULTS

Muscle glycogen synthase (MGS) and malin brain expression during age.

We previously described that neurons, such as astrocytes, express MGS (Valles-Ortega et al., 2011; Vilchez et al., 2007). In the present study, we analyzed changes in the expression pattern of this protein in several brain regions during aging. Immunostaining of MGS protein was performed with various specific antibodies in WT brains at 15 days, 21 days, 3 months, 6 months and 16 months of age (Figure 1, 2 and 3). In the 15-day postnatal brains, the MGS staining was stronger in astrocytes than in most neurons. However, Purkinje cells in the cerebellum (Figure 2) and GABAergic interneurons, especially those in the hippocampus (Figure 1), presented a signal comparable to astrocytes. The MGS expression in Purkinje neurons was maintained from 15 days to 16 months with no apparent changes (Figure 2). However, the expression of this enzyme in interneurons decayed with aging. While numerous intensely stained interneurons were detected in the hippocampus at 15 day, the signal was lower in 21-day-old mice and could scarcely be discerned from 3 months of age onwards (Figure 1). Although astrocytes expressed MGS during the entire study period, they showed a weaker and diffused signal from 21 days to 3 months while this signal was more intense and defined from 6 months on. Interestingly, 16-month-old brains showed MGS-positive deposits. These accumulations in aged mice were observed mainly in the hippocampus (Figure 1), the inner granular layer of the cerebellum (Figure 2) and the outer layers of the piriform cortex (Figure 3).

In order to analyse the brain expression pattern of malin during aging, we took advantage of the lacZ gene inserted under the *Epm2b*-promoter of the malin KO mice as a reporter of transcriptional activity (Valles-Ortega et al., 2011). This approach was especially useful because no valid antibody is available to detect endogenous levels of malin protein. X-gal staining of malin heterozygous brains from 15 days to 16 months revealed a wide malin reporter signal throughout the different brain areas, including the hippocampus (Figure 1), cerebellum (Figure 2) and piriform cortex (Figure 3). In the hippocampus and piriform cortex, this signal increased from 15 days to 21 days after birth, this increase being more obvious in the dentate gyrus (DG) (Figure 1). In the cerebellum, X-gal staining did not appear to increase from 15 days after birth onwards. Interestingly, the malin reporter signal decayed gradually in aged brains (Figure 1, 2 and 3), being especially visible in the inner granular layer of the cerebellum, one of the brain areas with a higher presence of MGS deposits (Figure 2). Since it has been reported that malin regulates MGS by inducing its proteasomal degradation (Vilchez et al., 2007) and that malin depletion causes MGS accumulation (Valles-Ortega et al., 2011), it is likely that the observed decrease in the transcription of the malin gene entailed a reduction in its protein levels and, consequently, diminished MGS proteasomal degradation. Remarkably, aged WT mice showed MGS accumulation in the same brain areas that were most affected in younger malin KO mice (Figure 4). We therefore focused our study on these areas.

Glycogen-related proteins accumulate on polyglucosan deposits in aged WT and LD mice.

As described before, CA in the brains of aged mammals contain polyglucosans and proteins (Brown, 2004; Cavanagh, 1999). Given that MGS catalyzes the synthesis of glycogen and this enzyme accumulated with age in the mice, we analyzed whether glycogen and glycogen metabolism-related proteins were present in the deposits of the aged WT mice. We compared these animals with malin KO mice, which have increased levels of MGS and accumulate it in the same brain areas as aged WT mice (Valles-Ortega et al., 2011). In addition, in order to evaluate the relevance of MGS in the formation of CA, we generated MGS KO mice (Supplementary Figure 1, see methods). This model showed a severe perinatal mortality with around 90% of the MGS-null pups dying from impaired

cardiac formation, in agreement with previously published observations for a similar model (Pederson et al., 2004). Nevertheless, the development of the surviving 10% MGS KO mice was morphologically normal. MGS KO mice did not have glycogen in muscle, heart or brain. No differences were observed in food intake, body weight or general behavior between the MGS KO mice we generated and their littermates (data not shown).

We compared WT, malin KO and MGS KO mouse brains of the same age (16 months). We first analyzed them for polyglucosan content. The deposits found in WT and malin KO brains, although larger and more numerous in the LD model, were equally positive for PAS staining (Figure 5A, 6A and 7A), gave a purplish colour with iodine staining (Figure 5B, 6B and 7B), indicative of the presence of poorly branched glycogen (Reed et al., 1968; Sakai et al., 1969), and immunoreacted with anti-polyglucosan antibody (Figure 8A), thereby confirming that both depostis contained aberrant glucose polymers and so they can be named PGBs. These PGBs were present mainly in the hippocampus (Figure 5), cerebellum (Figure 6) and piriform cortex (Figure 7) in WT and malin KO brains, coinciding with MGS accumulation (Figure 5A, 6A, 7A). In addition, laforin (Figure 5A, 6A, 7A) and BGP (Figure 8B) were also accumulated on PGBs from WT and malin KO brains. Neither polyglucosan, laforin, BGP (not shown) or, obviously, MGS accumulated in any brain region of MGS KO mice. Interestingly, laforin cellular localization appeared to be mainly nuclear in the absence of MGS (Figure 5, 6, 7).

CA markers accumulate only in the presence of polyglucosan deposits in aged mice and are overaccumulated in LD mice.

The presence of glial markers, such as GFAP, and of neuronal markers, such as 200 kDa neurofilaments (NF200), has been used in the bibliography to elucidate the cell type of origin of CA and has produced controversial results. The lack of consistent findings may be the result of the heterogeneity of the samples and the techniques used to determine the presence of these markers, as well as the heterogenic nature of CA themselves (Cavanagh, 1999). For instance, while many authors have found that CA react with antibodies against GFAP, many others have reported the opposite (reviewed in (Cavanagh, 1999)). By means of confocal imaging, we previously described the presence of LB highly associated with and inside the astrocytes of malin KO brains (Valles-Ortega et al., 2011) . Here we obtained confocal images from 16-month-old WT and malin KO mice in order to compare the distribution of the PGBs between brain cell types. Astrocytes showed a strong association with polyglucosan deposits in WT and malin KO mice, since anti-polyglucosan-reactive aggregates were found in the soma of GFAP-positive cells or surrounded by GFAP-positive processes (Figure 8A).

Next we evaluated the implication of neuronal cells in the PGBs formation by determining the presence of heavy chain neurofilament (NF200) and parvalbumin (PV) in these aggregates. We previously reported that PV-positive interneurons from the hippocampus express malin and MGS in WT mice, and that they accumulate PGBs and degenerate in malin KO mice (Valles-Ortega et al., 2011). PGBs containing PV (Figure 9A) and NF200 (Figure 9B) were found in WT and malin KO brains. Although PGBs from the hippocampus and cerebellum were slightly stained for NF200 and difficult to discern among the neuronal processes, those from the piriform cortex were clearly labelled with anti-NF200 antibodies. No PV- or NF200-containing aggregates were detected in MGS KO mice, while the normal staining of neurons with these markers was retained (Figure 9).

Since PGBs were associated with astrocytes and interneurons in WT and malin KO brains, we performed high resolution confocal imaging for polyglucosan, GFAP and PV in order to further analyze the interaction of the deposits with these cell types. PV-positive PGBs from interneuronal processes or attached to neuronal fragments were frequently found associated with GFAP-positive astroglial processes in both aged WT and malin KO mice (Figure 10 arrows). Strikingly, some PGBs detected in the soma of PV-positive interneurons from aged WT mice were detected at the interface between the intracellular and the extracellular compartment, where they were attached to astrocyte processes (Figure 10 arrowheads). Extraordinarily, even intracellular PGBs from malin KO interneurons showed association with astrocytes. GFAP-positive filaments entered the neuronal soma where they interacted with the polyglucosan deposits (Figure 10 arrowheads).

Previous studies have addressed the composition of the protein fraction of CA by immunostaining, and have related the presence of different markers with the formation of these deposits. Oxidative stress- and protein clearance-related markers, such as advanced glycation end-products (AGEP) (Iwaki et al., 1996; Kimura et al., 1998), ubiquitin (Cisse et al., 1993; Marquez et al., 2010) and heat-shock proteins (Cisse et al., 1993; Iwaki et al., 1996; Marquez et al., 2010) are present in CA. The PGBs found in WT and malin KO brain were positive for AGEP (Figure 11), ubiquitin (Figure 12A) and HSP70 (Figure 12B) while none of these markers accumulated in any region of same-aged MGS KO mice.

Protein aggregates related to other neurodegenerative disorders

Finally we analyzed other aggregate-prone proteins that, although known for their accumulation in other neurodegenerative diseases such as Alzheimer's and Parkinson's, have also been related to PGBs. This is the case of tau protein, which has been detected in CA and LBs from humans (Cavanagh, 1999; Loeffler et al., 1993), and in LBs from an LD mouse model (Puri et al., 2009), and alpha-synuclein, which accumulates in several cases of polyglucosan body diseases (Krim et al., 2005; Trivedi et al., 2003; Uchida et al., 2003). PGBs containing alpha-synuclein were found in WT and malin KO brains. However, alpha-synuclein-positive PGBs were difficult to identify in the cerebellum and were not found in the piriform cortex of WT brains. In contrast, they were easily detected in the hippocampus of WT brains and in these three regions of malin KO brains (Figure 13A). No accumulation of alpha-synuclein was detected in MGS KO mice (Figure 13A). Conversely, tau-positive PGBs were not observed in WT brains and they only slightly stained for tau in malin KO hippocampus (Figure 13B). No accumulation of alpha-synuclein or tau was found in MGS KO mice (Figure 13). In addition, PGBs were not stained for Congo Red or Methenamine (not shown), both of which are normally used to detect amyloid substances.

DISCUSSION

Here we compared the regional distribution, protein composition and cellular localization of PGBs in the brain of normal aged mice (corpora amylacea, CA) with those found in a model of LD (Lafora bodies, LBs), namely the malin KO mice. These KO animals show MGS protein and glycogen accumulated in LBs (Valles-Ortega et al., 2011). Furthermore, in order to analyze the role of MGS and its product glycogen in the formation of CA during aging, we generated and analyzed MGS KO mice. Our results indicated that polyglucosan synthesis was required for CA formation. Therefore, we propose that MGS and other proteins related to glycogen metabolism play a crucial role in brain-aging phenomena and that CA and LBs are distinct stages of the same physiopathological process.

We previously described that MGS is expressed not only in astrocytes but also in neurons (Valles-Ortega et al., 2011; Vilchez et al., 2007). Nevertheless, while MGS expression and glycogen content is widespread in astroglial cells (Brown, 2004; Prebil et al., 2011), in neurons the enzyme is kept in an inactive form (Vilchez et al., 2007), and glycogen has rarely been observed in this cell type under normal conditions (Brown, 2004; Cammermeyer and Fenton, 1981; Cavalcante et al., 1996). It has been hypothesized that these differences between astrocytes and neurons entail a moonlighting role for neuronal glycogen or MGS activity (Pfeiffer et al., 1995; Vilchez et al., 2007). Moreover, it has been proposed that glycogen metabolism has variable physiological functions for the two cell types during brain development (Pfeiffer et al., 1993). Here we analyzed the brain expression pattern of MGS from 15 days to 16 months of age in order to evaluate possible changes in the glycogen metabolism machinery between different cell types during normal aging. In concordance with the glycogen content, MGS was found in astrocytes during the whole study period. The distribution of MGS expression was homogeneous within the different brain regions of young animals. However, the presence of scattered MGS-strongly-stained astrocytes increased with aging. With regard to neuronal expression, MGS was detected only in some specific neuronal types where it was also differentially modulated with age. While MGS expression was maintained in the Purkinje cells of the cerebellum, the expression in hippocampal interneurons clearly decayed with age. Moreover, a striking result was the finding of MGS protein accumulations in the hippocampus, the granular layer of the cerebellum and the pirifom cortex of aged mice. The brain areas affected by these age-related deposits coincided with those we had previously described to contain MGS accumulation in malin KO mice (Valles-Ortega et al., 2011). In addition, the study of the malin expression pattern revealed a decrease in its levels in the same brain areas where MGS accumulated in aged mice. Given that the malin-laforin complex

induces MGS proteasomal degradation (Vilchez et al., 2007), our data suggest that aged-related deposits and LBs share a common origin that involves impaired or decreased MGS degradation.

In addition to its role controlling glycogen metabolism, it is noticeable that laforin and malin, the genes mutated in LD, are also associated with cellular degradative pathways (Aguado et al., 2010; Delgado-Escueta, 2007; Garyali et al., 2009; Knecht et al., 2010; Puri and Ganesh, 2010; Puri et al., 2011; Rao et al., 2010a). The cellular processes implicated in the CA formation have been widely debated. Many authors have described the immunocytochemical properties of these deposits in brains of humans and other mammals. Among others, proteins and other molecules related to misfolded-protein response and oxidative stress, and cell-type specific markers, are the most frequently reported (Cavanagh, 1999). In this study we validated the presence of several of these markers in the aged mouse CA and we further described similar characteristics of CA and malin KO LBs by identifying the presence of the same markers in both deposits. Advanced glycation end products (AGEP) result from the oxidative reaction between long-lived proteins and reducing sugars and they have been detected in several age-related diseases (Li et al., 1995; Uchiki et al., 2011; Yan et al., 1995) and in another model of LD, namely the laforin KO mouse (Ganesh et al., 2002). Heat-shock proteins have a key function as chaperone machinery. HSP70 has been recently proposed to play a crucial role in the triage of damaged and aberrant proteins for degradation via the ubiquitin-proteasome pathway (Pratt et al., 2010). Indeed, HSP70 interacts with malin and laforin to form a complex that suppresses the toxicity of misfolded proteins (Garyali et al., 2009; Rao et al., 2010b) and it has been found, together with ubiquitin, in LBs from human patients (Rao et al., 2010a). All together, the presence of AGEP, ubiquitin and HSP70 in both CA and LBs suggests that the two PGBs are related to cell stress processes that course with the accumulation of misfolded proteins. The link between PGB formation and protein misfolding is strengthened by the observation of α-synuclein accumulation in CA and LBs. This cytosolic protein accumulates in other neurodegenerative conditions such as Parkinson's disease (PD), where it is the main component of Lewy bodies (Bellucci et al., 2012). All together, these findings point to a putative role of glycogen metabolism machinery in the misfolded protein response, the impairment or overload of which would originate PGB accumulation during aging or disease.

CA and LBs are defined as polyglucosan bodies (PGBs) because of their content of poorly branched glucose polymers (Cavanagh, 1999). However, despite their physicochemical similarities, a common formation mechanism for these two PGBs has not been proposed to date. Moreover, although polyglucosan is the most abundant and the first material identified in CA, even recent publications fail to explain the origin of this polysaccharide and its implication in the formation of these deposits (Wilhelmus et al., 2011). Here we found that both age-related (CA) and malin KO (LBs) PGBs appeared in the same brain areas and contained MGS protein. In addition, other proteins involved in glycogen metabolism, such as laforin and BGP, were also detected in CA and LBs. These results reinforce the implication of glycogen in the formation of CA and LBs.

MGS is the only enzyme able to synthesize large chains of glucose in the brain and, consequently, the presence of polyglucosan in CA and LBs implies MGS activity. In fact, a recent publication showed that the depletion of PTG, an activator of MGS, prevents LB formation in mice (Turnbull et al., 2011). Nevertheless, given the observations described above, the accumulation of MGS protein in PGBs could be interpreted to be only a consequence of its misfolding in response to cellular stress. In order to elucidate the relevance of MGS in the formation of CA in aged WT brains, we analyzed age-matched MGS KO mice. Not surprisingly, these mice showed no CA, thus confirming that MGS is required for the formation of these deposits. More strikingly, however, none of the components we found in PGBs from WT and malin KO mice were detected in the brains of these animals. This observation suggests that polyglucosans serve as a matrix for the aggregation of several other waste molecules.

Differential functions have been proposed for MGS and glycogen in neuronal and glial cells. Given the central role of glycogen synthesis in the formation of CA, the identification of the cell-type origin of these deposits is an important issue, as this information would contribute to revealing the physiological significance of CA formation. A wide range of data, mainly based on the presence of cell-

type specific components, support the implication of neuronal (Cavanagh, 1999; Korzhevskii and Giliarov, 2007; Marquez et al., 2010; Selmaj et al., 2008) but also glial (Cavanagh, 1999; Marquez et al., 2010; Schipper, 2011) cells in the biogenesis of CA. In this regard, we found both CA and LBs containing PV and NF200 neuronal markers, although these deposits were frequently not associated with any neuronal structure. PV-positive cells are GABAergic interneurons that express MGS and malin. In malin KO mice, these cells accumulate LBs and degenerate (Valles-Ortega et al., 2011). It is worth noting that serum carnosinase, a dipeptidase that catalyzes the synthesis of GABA, has also been detected in CA (Jackson et al., 1994). The presence of PV in LBs and CA further relates GABAergic interneurons with the formation PGBs. GABAergic interneurons are inhibitory cells whose impairment is involved in epileptogenesis and seizure activity (Magloczky and Freund, 2005). In fact, the number of these cells decreases in some cases of epilepsy (Castro et al., 2011; Dinocourt et al., 2003). Interestingly, epilepsy is one of the pathological conditions where CA accumulation is increased (Cavanagh, 1999; Das et al., 2011; Kawamura et al., 2002; Radhakrishnan et al., 2007; Ribeiro Mde et al., 2003), and is the main clinical manifestation of LD. Taken together, these data demonstrate that some brain PGBs, if not all, originate inside neurons.

In malin KO mouse brains, LBs are highly associated with astrocytes and they can also be found inside these glial cells (Valles-Ortega et al., 2011). Here we show that not only LBs but also CA presented an astrocyte-related pattern. GIven that neuronal proteins were also identified as components of PGBs both in normal aged and malin KO mice, we further analyzed the cellular PGB distribution between GFAP-positive astrocytes and PV-positive interneurons. Extracellular PGBs containing PV protein were found surrounded by astrocyte processes in the vicinity of interneuronal cells. Strikingly, astrocyte processes were also observed to extend to and contact PGBs located in the soma of these interneurons. These observations suggest the transfer of the polyglucosan deposits from the body of interneurons to astroglial cells. In fact, the cell-to-cell transfer of non-polyglucosan bulk materials from neuronal perikarya by the active intervention of astrocyte processes has been previously proposed. Abnormal smooth membranes accumulated in Purkinje cells (Cavanagh and Gysbers, 1983) and lysosomal dense bodies deposited in hippocampal pyramidal cells (Cavanagh et al., 1990; Nolan and Brown, 1989; Norio and Koskiniemi, 1979) after chemical intoxication transfer to astroglial processes projecting into the neuronal body. Thus, the same waste-removing mechanism could be exerted on neuronal PGBs and would explain the presence of both neuronal and glial components in these deposits.

In summary, our results show that MGS-synthesized polyglucosan is required for CA formation. We attribute a putative functional role of neuronal glycogen metabolism to an efficient mechanism for avoiding potentially dangerous proteins following neuronal stress. Although other functions of neuronal glycogen cannot be ruled out, the physiological role described here would explain why neurons retain MGS expression, despite its potentially harmful activity (Magistretti and Allaman, 2007). We hypothesize that PGBs accumulate as the result of the overload or failure of this mechanism induced by the genetic deficiency of malin or laforin in LD or by the accumulation of cellular stresses during normal aging. Further studies on the implications of brain glycogen metabolism proposed here will help to unravel the pathological mechanisms that lead to brain deterioration in normal aging and neurological diseases.

FIGURES

Figure 1 Legend. MGS and malin expression in the hippocampus. Aged hippocampi showed MGS deposits. Hippocampal sections of WT (*left panel*) and malin heterozygous (*right panel*) mice of 15 days, 21 days, 3 months, 6 months and 16 months of age are shown. **Left panel:** Immunostaining with an antibody against MGS (brown). MGS-positive interneurons (arrowheads) and MGS deposits (arrows) are shown. **Right panel:** X-gal staining as a reporter of malin transcriptional activity. DG: Dentate gyrus, CA1: Cornum Amonnis 1, CA2: Cornum Amonnis 2. Scale bar = 200µm.

Figure 1

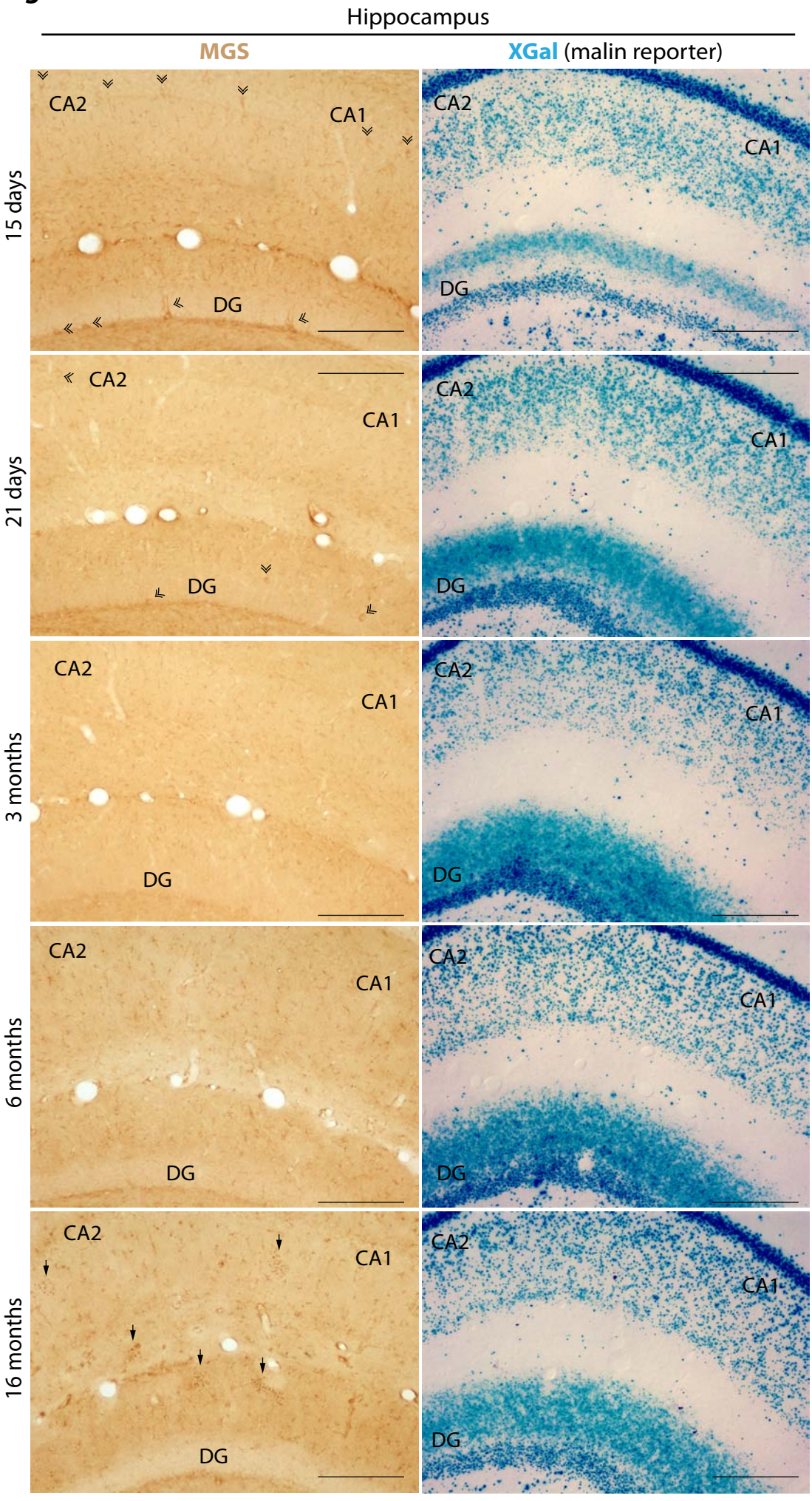
Hippocampus
MGS
XGal (malin reporter)
15 days
21 days
3 months
6 months
16 months
CA2
CA1
DG

Figure 2 Legend. MGS and malin expression in the cerebellum. Aged cerebella showed MGS deposits. Cerebellar sections of WT (*left panel*) and malin heterozygous (*right panel*) mice of 15 days, 21 days, 3 months, 6 months and 16 months of age are shown. **Left panel:** Immunostaining with an antibody against MGS (brown). MGS deposits (arrows) are shown. **Right panel:** X-gal staining as a reporter of malin transcriptional activity. igl: inner granullar layer, pcl: Purkinje cell layer, ml: molecular layer. Scale bar = 200μm.

Figure 2

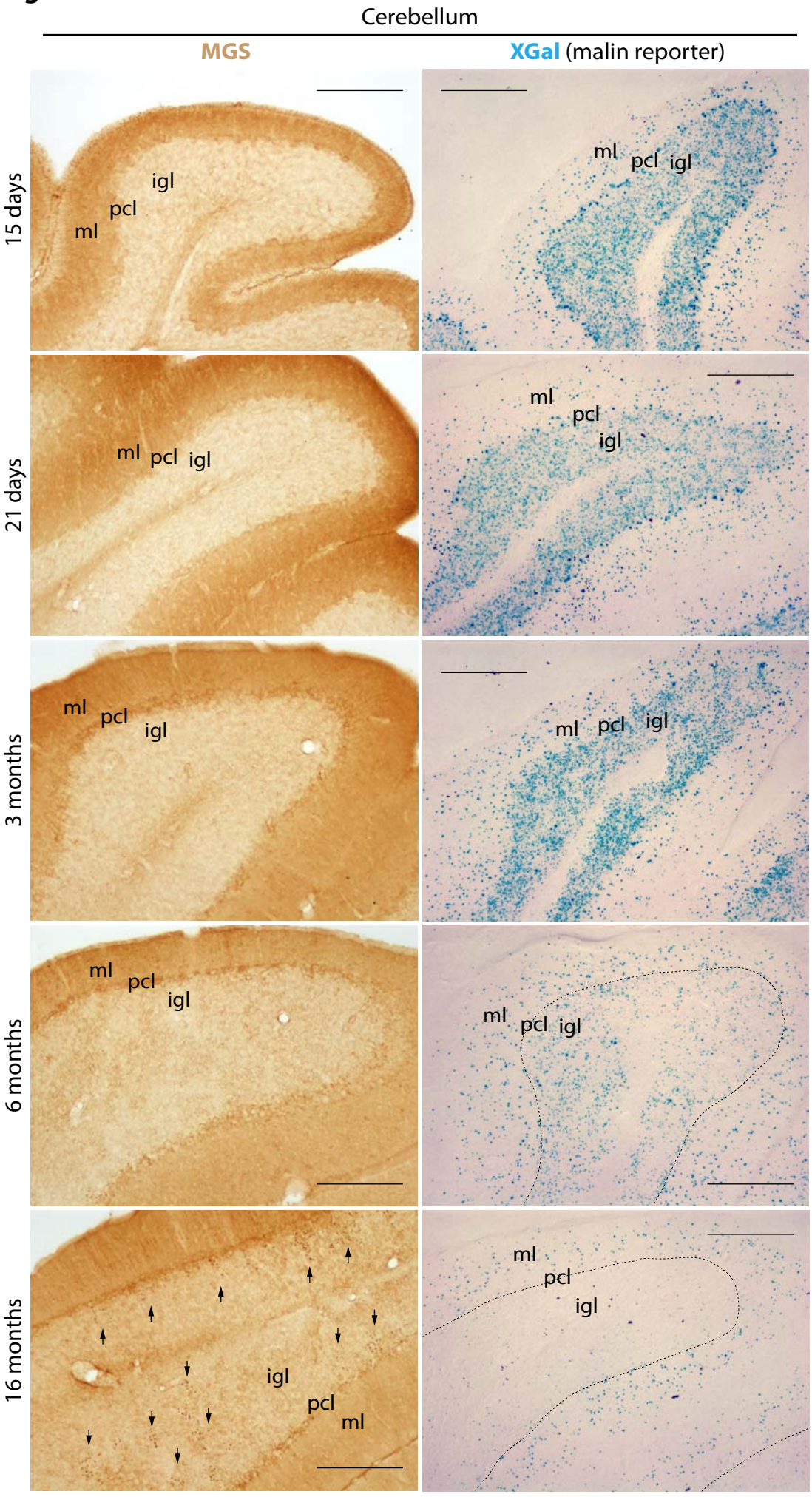
Cerebellum
MGS
XGal (malin reporter)
15 days
21 days
3 months
6 months
16 months
ml
pcl
igl

Figure 3 Legend. MGS and malin expression in the piriform cortex. Aged piriform cortex showed MGS deposits. Sections of the piriform cortex of WT (*left panel*) and malin heterozygous (*right panel*) mice of 15 days, 21 days, 3 months, 6 months and 16 months of age are shown. **Left panel:** Immunostaining with an antibody against MGS (brown). MGS deposits (arrows) are shown. **Right panel:** X-gal staining as a reporter of malin transcriptional activity. Scale bar = 200μm.

Figure 3

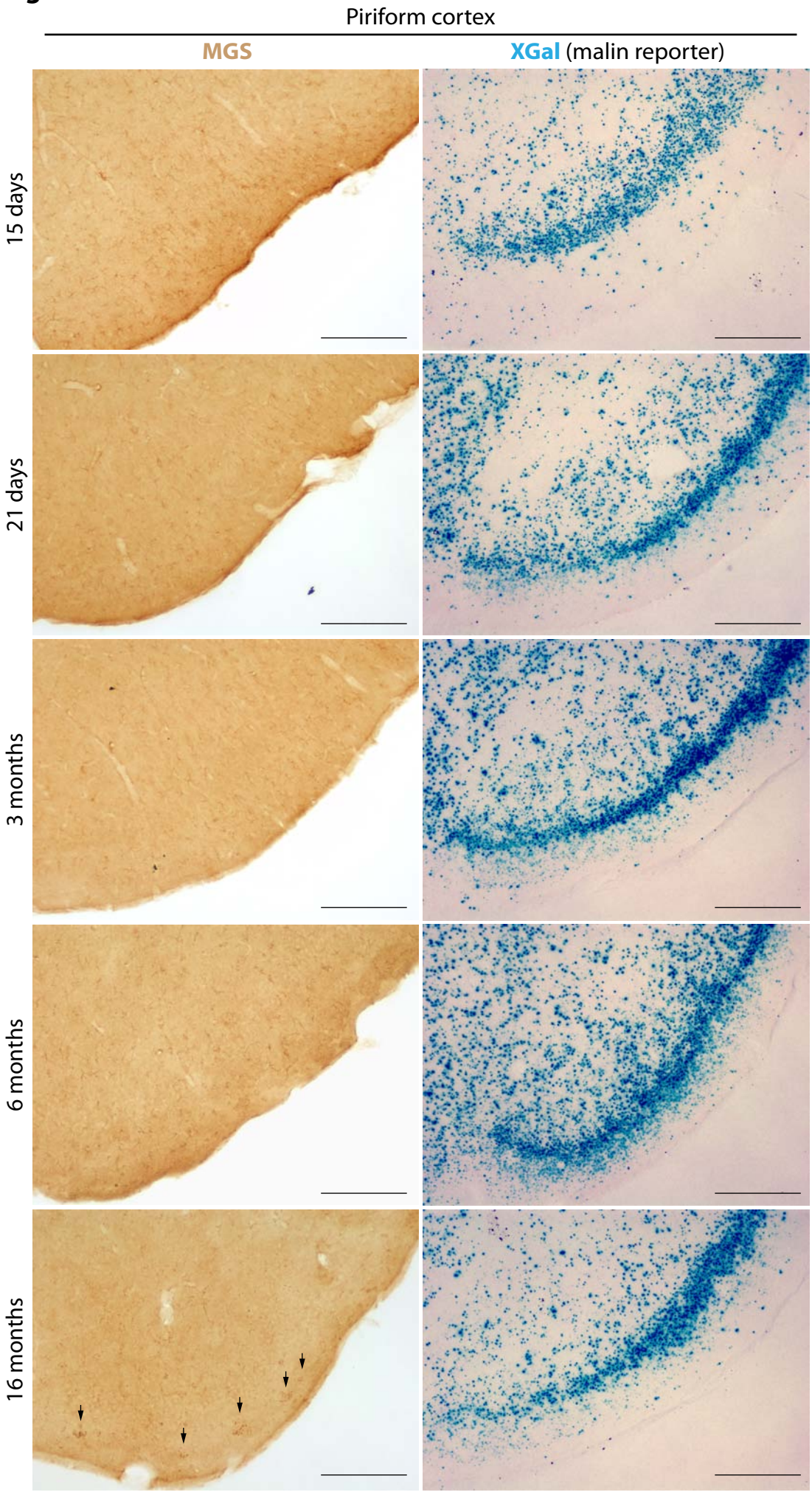
Piriform cortex
MGS
XGal (malin reporter)
15 days
21 days
3 months
6 months
16 months

Figure 4

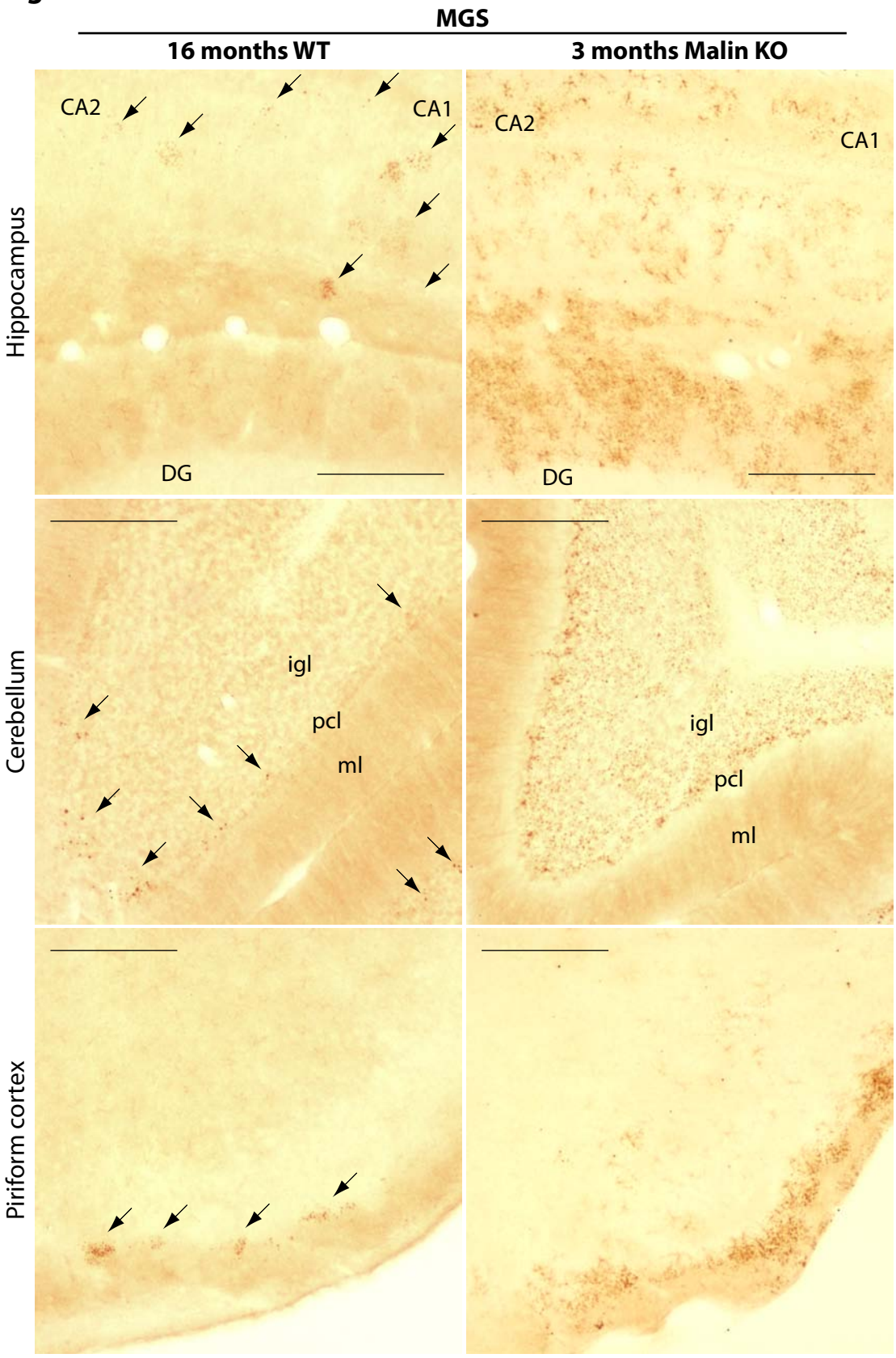

Figure 4 Legend. MGS deposits were found in the same brain regions of aged WT and young malin KO mice. Immunostaining with an antibody against MGS (brown). Hippocampus, cerebellum and piriform cortex sections from 16-month-old WT and 3-month-old malin KO brains are shown. MGS deposits in aged WT mice (arrows) were found in the same brain regions as in young malin KO mice. DG: Dentate gyrus, CA1: Cornum Amonnis 1, CA2: Cornum Amonnis 2, igl: inner granullar layer, pcl: Purkinje cell layer, ml: molecular layer. Scale bar = 200µm.

Figure 5

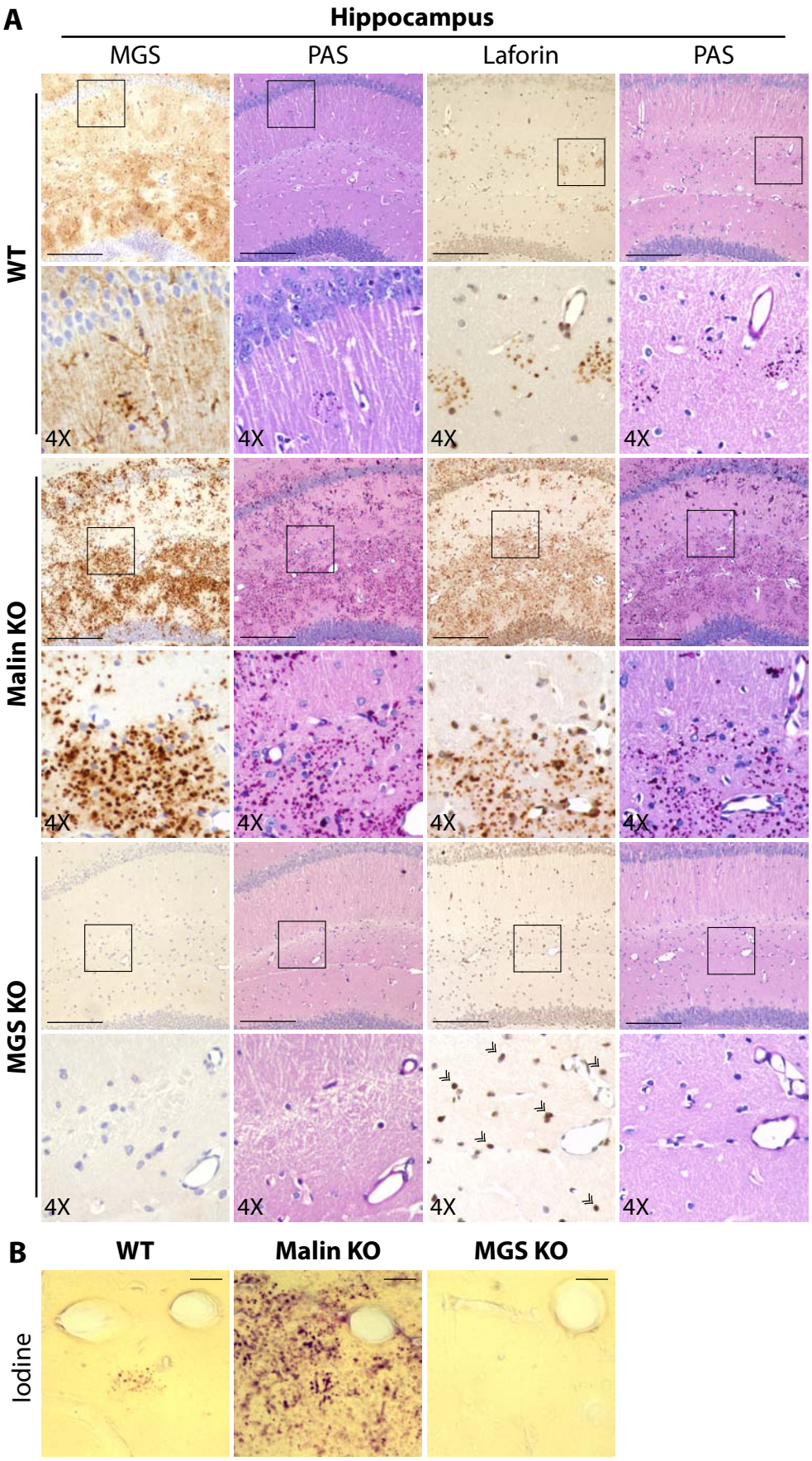

Figure 5 Legend. MGS and laforin proteins accumulated with polyglucosan bodies (PGBs) in the hippocampus of aged WT and malin KO mice. Aged MGS KO mice did not show these accumulations. 16 month-old WT, malin KO and MGS KO hippocampi are shown. **A)** Different 4 µm-thick consecutive sections stained with periodic acid-Schiff (PAS) and immunostained for MGS and laforin (brown). All the sections were counterstained with hematoxylin. Laforin staining presented nuclear localization in MGS KO mice (arrowheads). Scale bar = 200µm, 4X = 4-fold magnification. **B)** Iodine staining. Scale bar = 30µm.

Figure 6

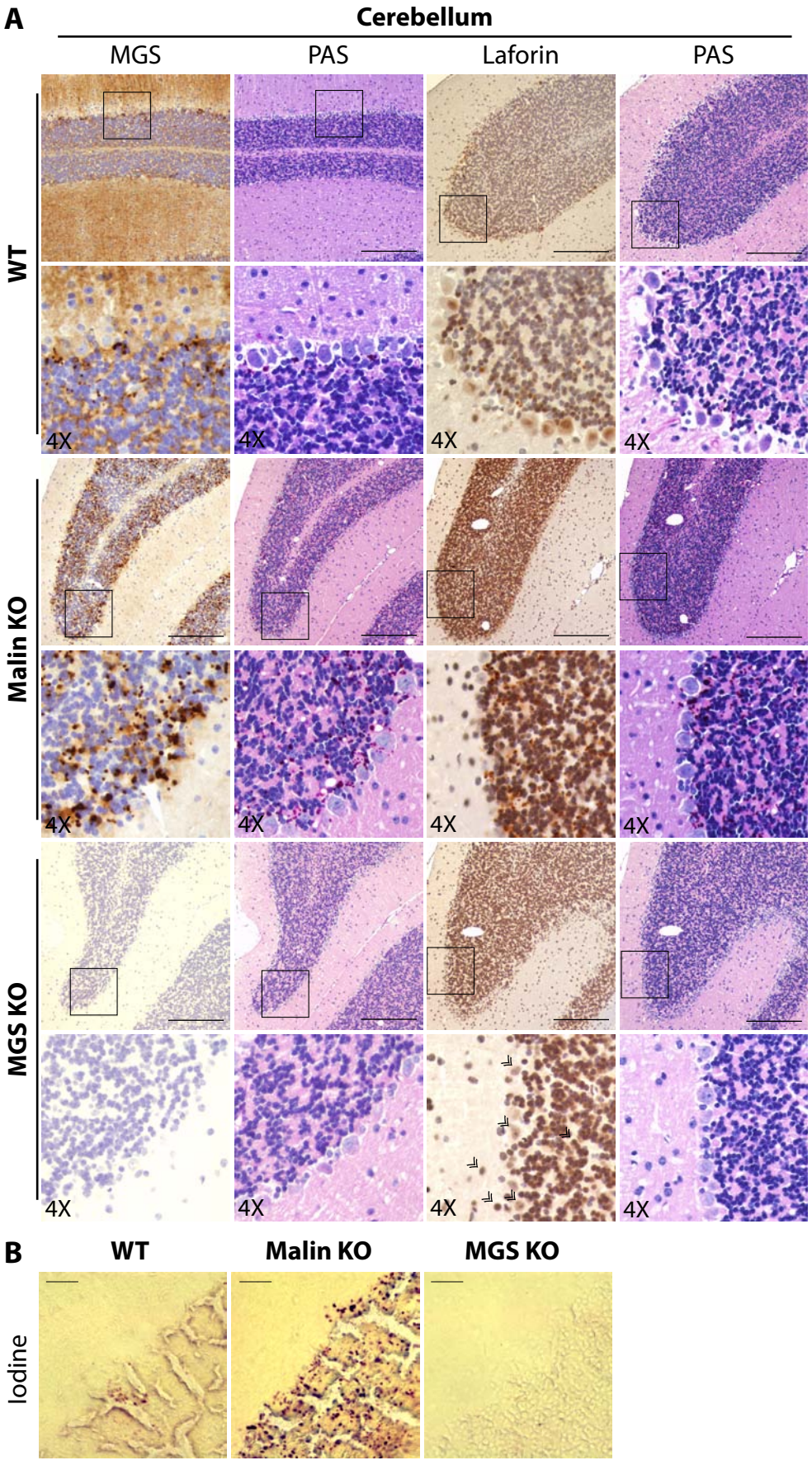

Figure 6 Legend. MGS and laforin proteins accumulated with polyglucosan bodies (PGBs) in the cerebellum of aged WT and malin KO mice. Aged MGS KO mice did not show these accumulations. 16- month-old WT, malin KO and MGS KO cerebella are shown. **A)** Different 4 µm-thick consecutive sections stained with periodic acid-Schiff (PAS) and immunostained for MGS and laforin (brown). All the sections were counterstained with hematoxylin. Laforin staining presented nuclear localization in MGS KO mice (arrowheads). Scale bar = 200µm, 4X = 4-fold magnification. **B)** Iodine staining. Scale bar = 30µm.

Figure 7

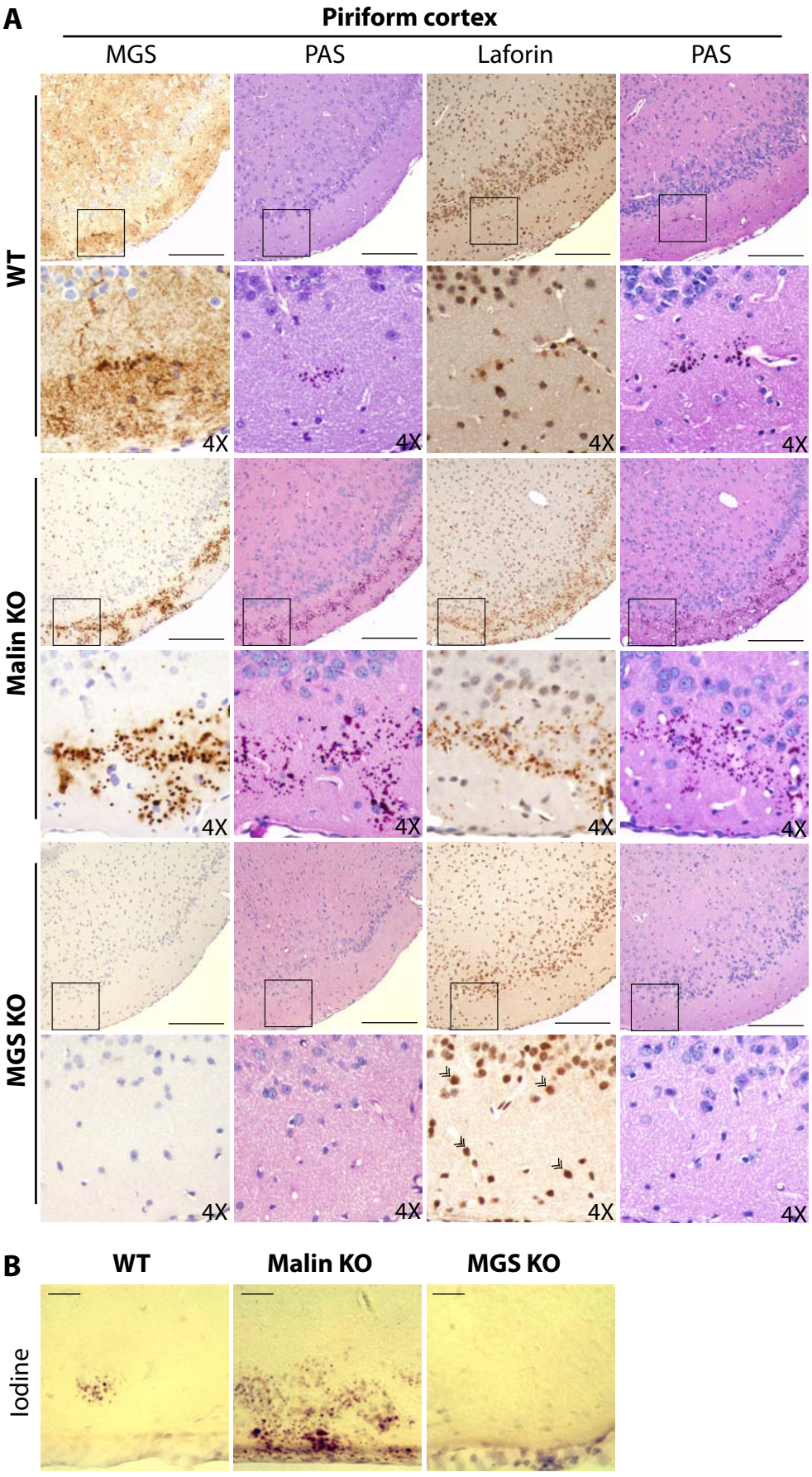

Figure 7 Legend. MGS and laforin proteins accumulated with polyglucosan bodies (PGBs) in the piriform cortex of aged WT and malin KO mice. Aged MGS KO mice did not show these accumulations. 16-month-old WT, malin KO and MGS KO piriform cortexes are shown. **A)** Different 4 µm-thick consecutive sections stained with periodic acid-Schiff (PAS) and immunostained for MGS and laforin (brown). All the sections were counterstained with hematoxylin. Laforin staining presented nuclear localization in MGS KO mice (arrowheads). Scale bar = 200µm, 4X = 4-fold magnification. **B)** Iodine staining. Scale bar = 30µm.

Figure 8

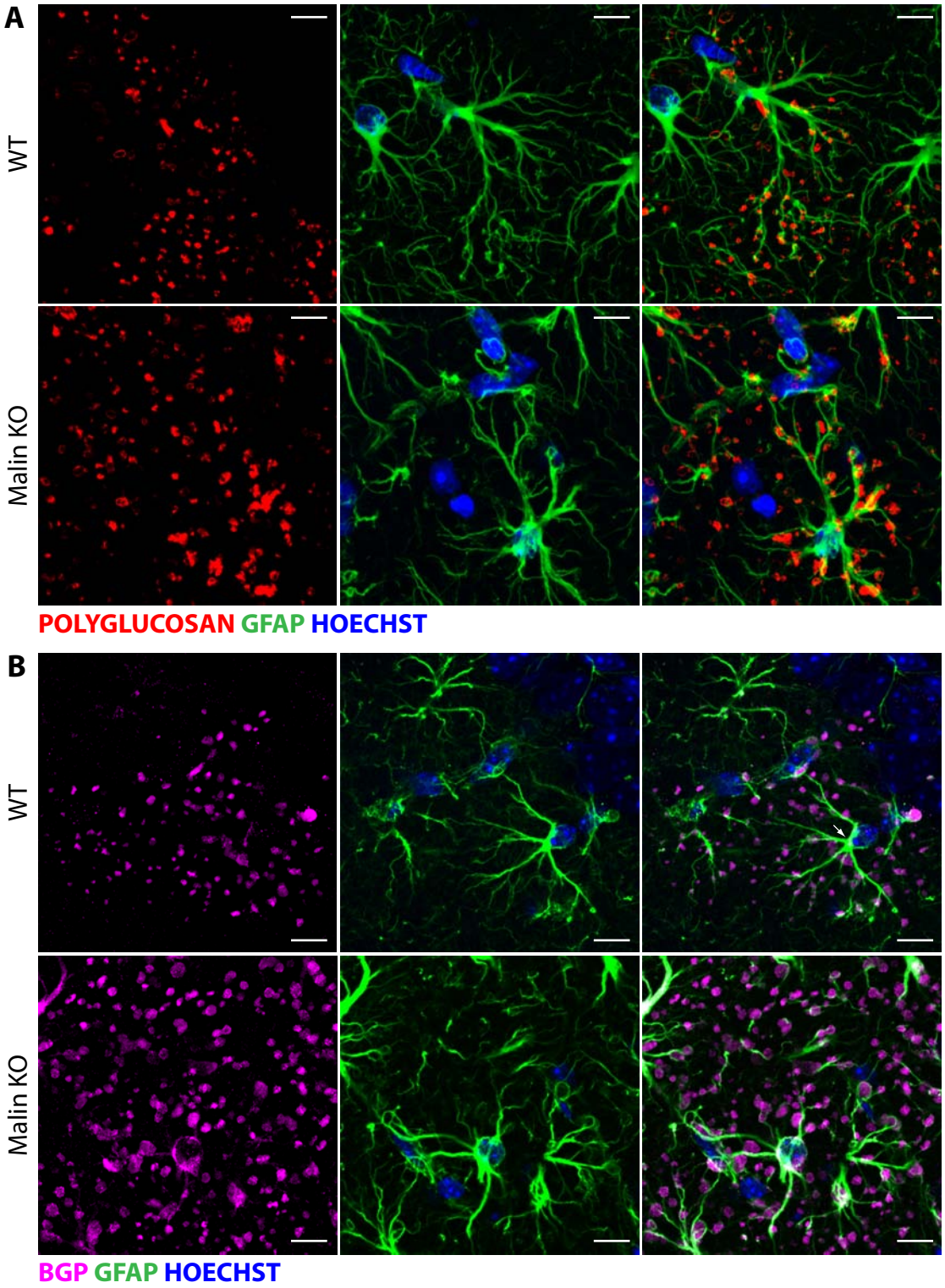

Figure 8 Legend. PGBs found in aged WT and malin KO mice accumulated glycogen phosphorylase and were associated with astrocytes. Confocal images are shown for 16-month-old WT and malin KO hippocampal regions. Antibodies were used against polyglucosan (red, *A*), brain glycogen phosphorylase (BGP) (magenta, *B*) and glial fibrillary acidic protein (GFAP) (green). Hoechst (blue) was used for nuclear staining. PGBs in both strains were found in the soma of astrocytes or surrounded by their processes. Scale bar = 10 µm.

Figure 9

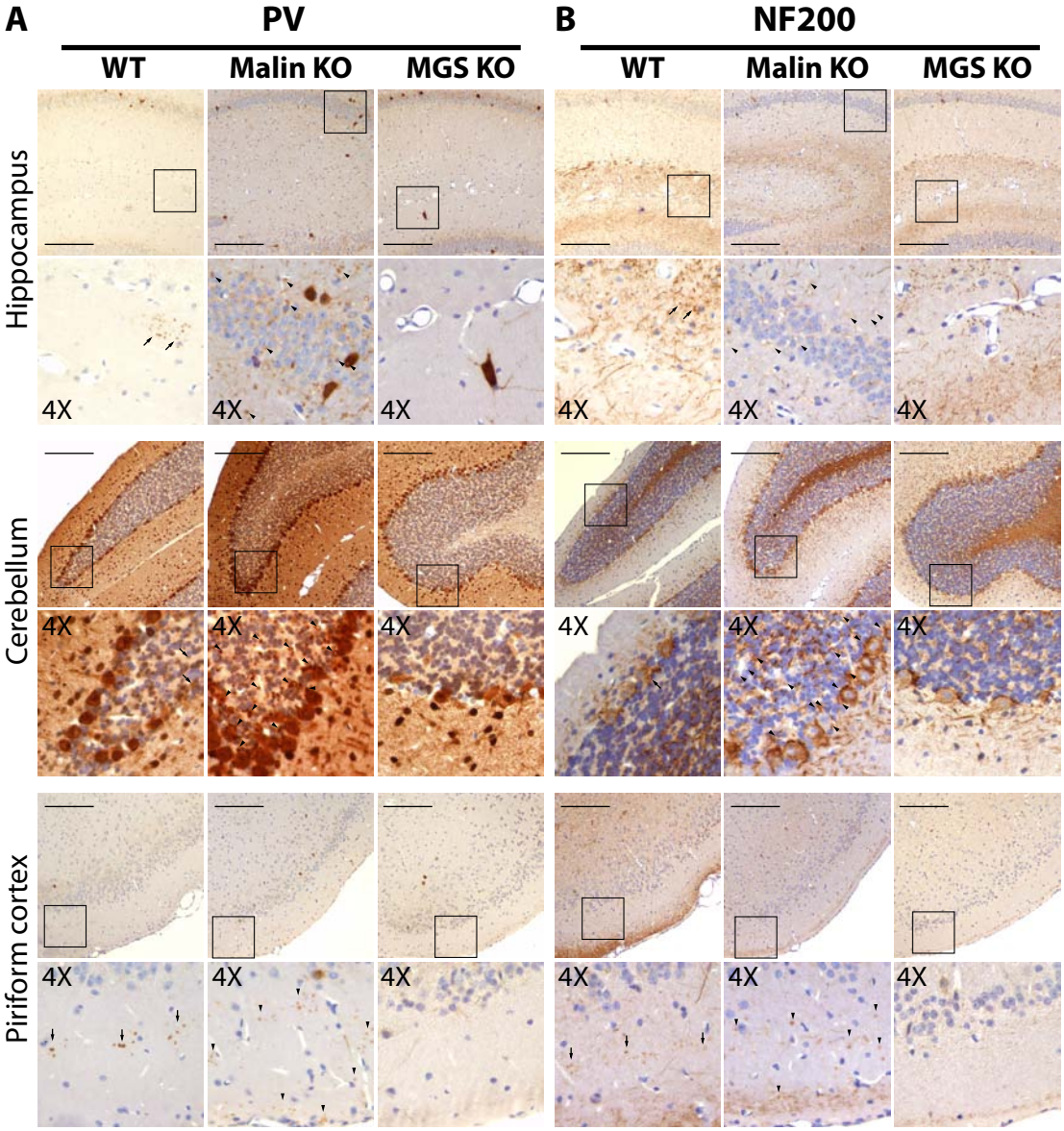

Figure 9 Legend. The neuronal markers parvalbumin (PV) and 200 kDa neurofilament (NF200) accumulated with polyglucosan bodies (PGBs) in aged WT and malin KO mice. Aged MGS KO mice did not show these accumulations. Hippocampus, cerebellum and piriform cortex regions from 16-month-old WT, malin KO and MGS KO mice are shown. 4 µm-thick sections consecutive to those stained with periodic acid-Schiff (PAS) were immunostained (brown) with antibodies against parvalbumin (PV, *A*) and 200 kDa neurofilament (NF200, *B*). All the sections were counterstained with hematoxylin. PV and NF200-positive PGBs were found in aged WT (arrows) and malin KO mice (arrowheads). Scale bar = 200µm, 4X = 4-fold magnification.

Figure 10

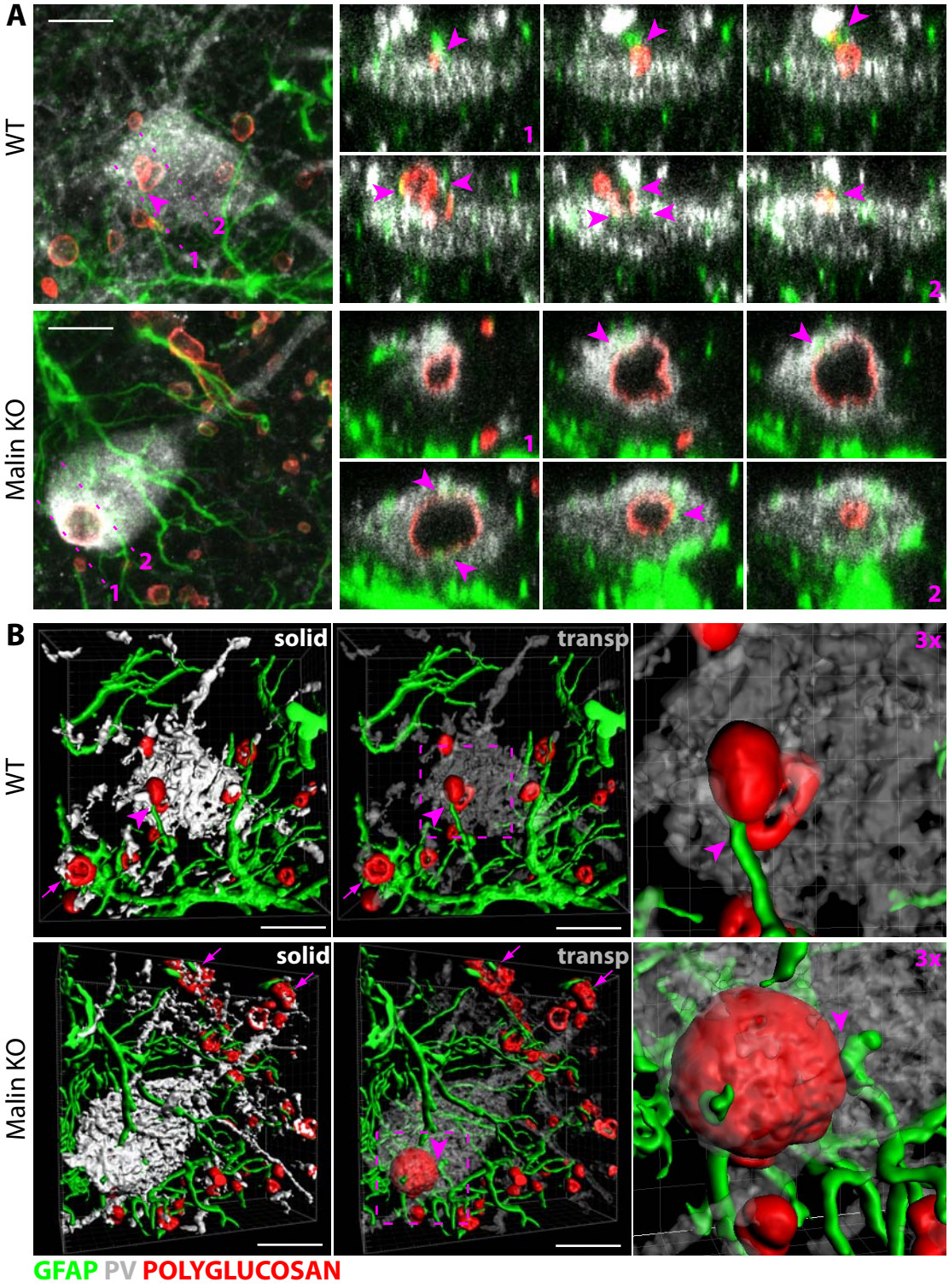

Figure 10 Legend. Localization of PGBs in astroglia and interneurons of aged WT and malin KO brains. **A)** Confocal images are shown for 16-month-old WT and malin KO hippocampal regions. Antibodies were used against glial fibrillary acidic protein (GFAP) (green), parvalbumin (PV) (grey) and polyglucosan (red). Consecutive orthogonal sections are shown between the planes represented by magenta broken lines (1 and 2). **B)** Three-dimensional representations of the images in (A). PV signal is represented as a solid (solid) and as a partially transparent (transp) surface. Extracellular PGBs containing PV (arrows) and PGBs in the soma of PV-positive interneurons (arrowheads) are shown associated with astrocytes both in aged WT and malin KO brains. Scale bar = 10 µm, 3X = 3-fold inset.

Figure 11

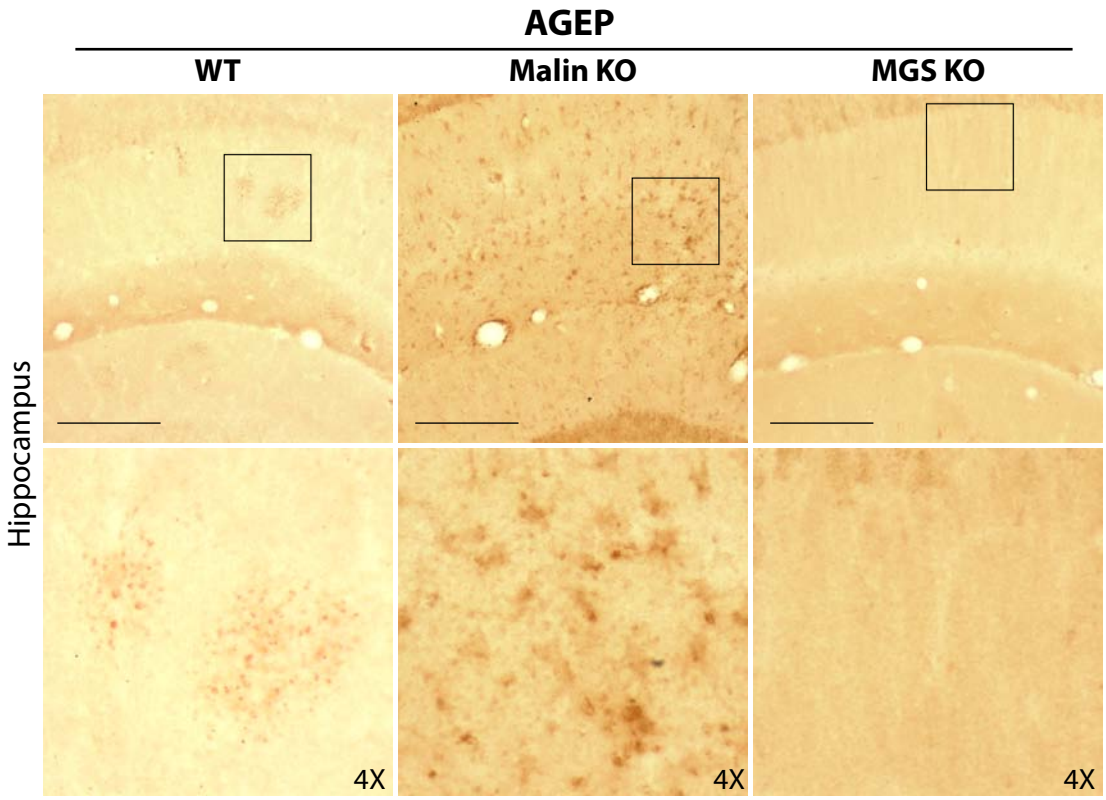

Figure 11 Legend. The polyglucosan bodies (PGBs) in aged WT and malin KO brains contained advanced glycation end products (AGEP). Aged MGS KO brains did not show AGEP-positive deposits. Hippocampi from 16-month-old WT, malin KO and MGS KO mice were immunostained with an antibody against AGEP (brown). Scale bar = 200µm, 4X = 4-fold magnification.

Figure 12

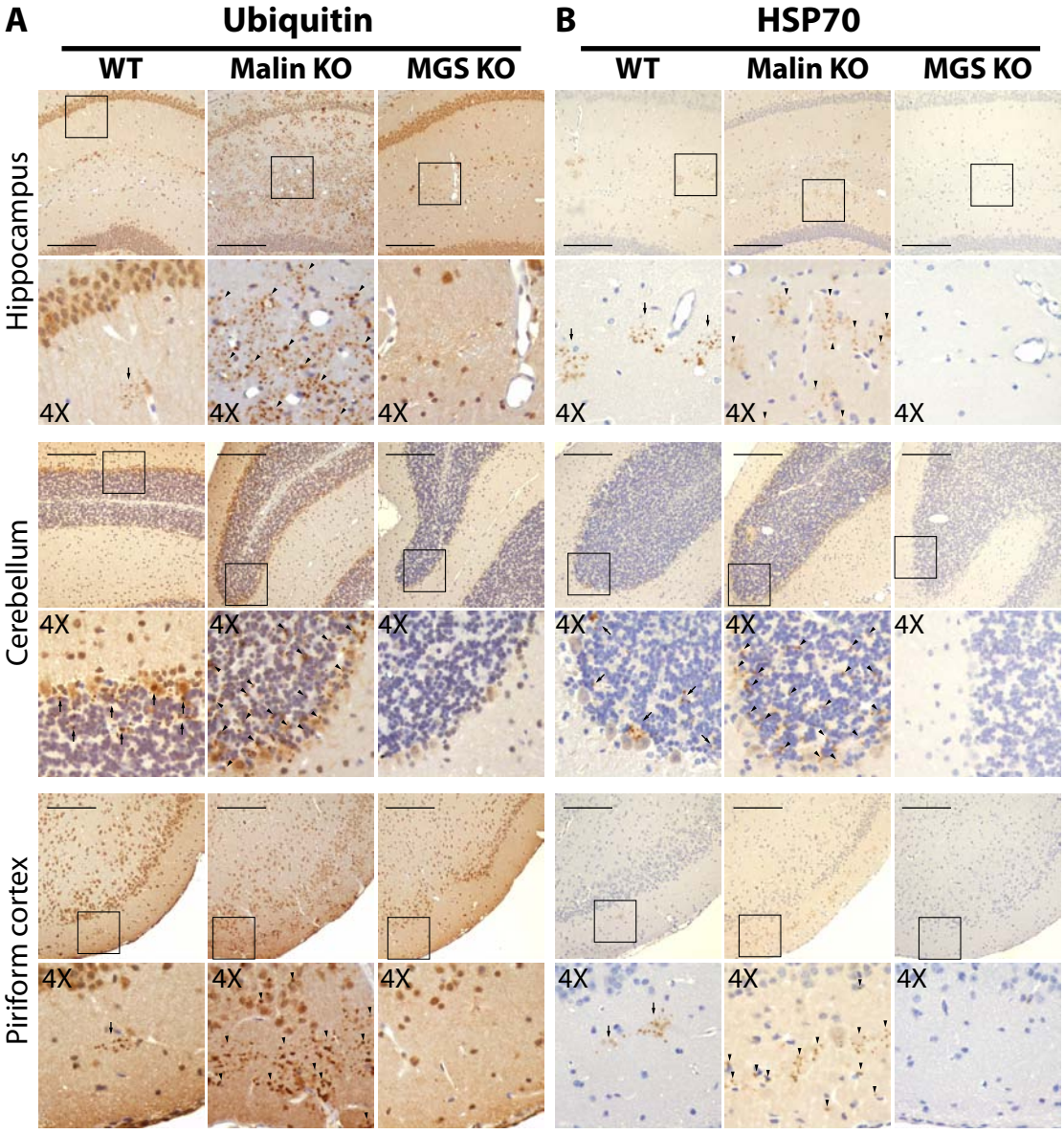

Figure 12 Legend. Ubiquitin and 70 kDa heat-shock protein (HSP70) accumulated with polyglucosan bodies (PGBs) in aged WT and malin KO mice. Aged MGS KO mice did not show these accumulations. Hippocampus, cerebellum and piriform cortex regions from 16-month-old WT, malin KO and MGS KO mice are shown. 4 µm-thick sections consecutive to those stained with periodic acid-Schiff (PAS) were immunostained (brown) with antibodies against ubiquitin (*A*) and 70 kDa heat-shock protein (HSP70, *B*). All the sections are counterstained with hematoxylin. Ubiquitin and HSP70-positive PGBs were found in aged WT (arrows) and malin KO mice (arrowheads) Scale bar = 200µm, 4X = 4-fold magnification.

Figure 13

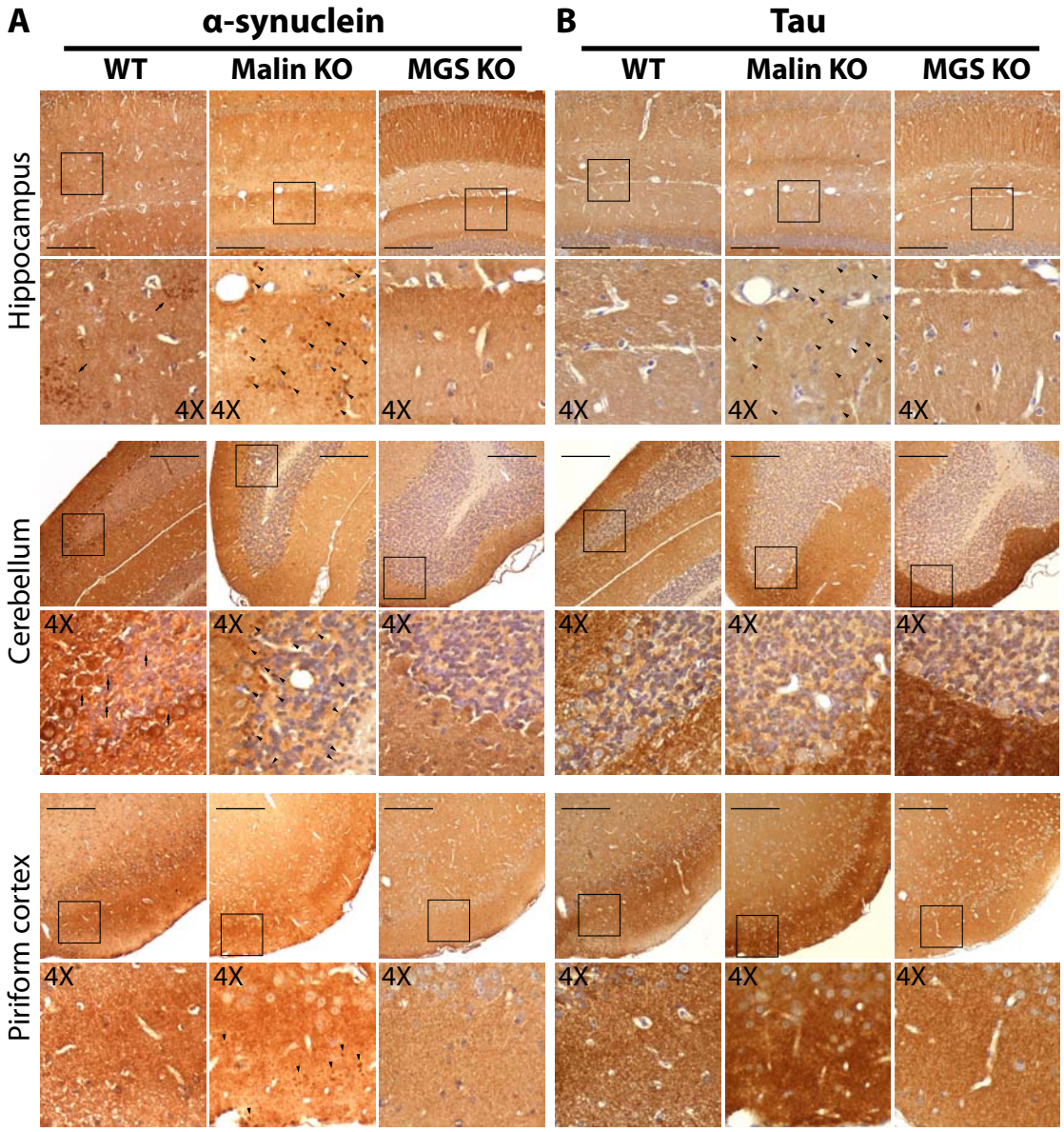

Figure 13 Legend. Analysis of the presence in PGBs of proteins aggregated in other neurodegenerative diseases. Hippocampus, cerebellum and piriform cortex regions from 16-month-old WT, malin KO and MGS KO mice are shown. 4 µm-thick sections consecutive to those stained with periodic acid-Schiff (PAS) are immunostained (brown) with antibodies against α-synuclein (*A*) and tau (*B*). All the sections were counterstained with hematoxylin. α-synuclein-positive PGBs were found in aged WT (arrows) and malin KO mice (arrowheads). Only malin KO PGBs were slightly positive for tau (arrowheads). Scale bar = 200µm, 4X = 4-fold magnification.

Supplementary figure 1

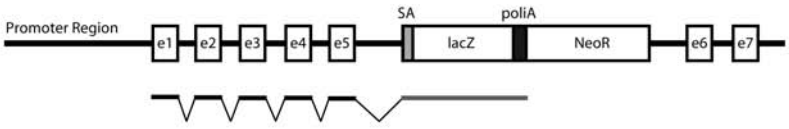

Supplementary Figure 1 Legend. Generation of the MGS KO mouse. Schematic representation of the targeted disruption.

REFERENCES

Abe, H., and Yagishita, S. (1995). Massive appearance of corpora amylacea in postnatal anoxic encephalopathy. Clin Neuropathol *14*, 207-210.

Aguado, C., Sarkar, S., Korolchuk, V. I., Criado, O., Vernia, S., Boya, P., Sanz, P., de Cordoba, S. R., Knecht, E., and Rubinsztein, D. C. (2010). Laforin, the most common protein mutated in Lafora disease, regulates autophagy. Hum Mol Genet *19*, 2867-2876.

Bellucci, A., Navarria, L., Zaltieri, M., Missale, C., and Spano, P. (2012). Alpha-synuclein synaptic pathology and its implications in the development of novel therapeutic approaches to cure Parkinson's disease. Brain Res *1432*, 95-113.

Bernard-Helary, K., Lapouble, E., Ardourel, M., Hevor, T., and Cloix, J. F. (2000). Correlation between brain glycogen and convulsive state in mice submitted to methionine sulfoximine. Life Sci *67*, 1773-1781.

Botez, G., and Rami, A. (2001). Immunoreactivity for Bcl-2 and C-Jun/AP1 in hippocampal corpora amylacea after ischaemia in humans. Neuropathol Appl Neurobiol *27*, 474-480.

Brown, A. M. (2004). Brain glycogen re-awakened. J Neurochem *89*, 537-552.

Brown, A. M., Baltan Tekkok, S., and Ransom, B. R. (2004). Energy transfer from astrocytes to axons: the role of CNS glycogen. Neurochem Int *45*, 529-536.

Brown, A. M., Tekkok, S. B., and Ransom, B. R. (2003). Glycogen regulation and functional role in mouse white matter. J Physiol *549*, 501-512.

Cammermeyer, J., and Fenton, I. M. (1981). Improved preservation of neuronal glycogen by fixation with iodoacetic acid-containing solutions. Exp Neurol *72*, 429-445.

Castro, O. W., Furtado, M. A., Tilelli, C. Q., Fernandes, A., Pajolla, G. P., and Garcia-Cairasco, N. (2011). Comparative neuroanatomical and temporal characterization of FluoroJade-positive neurodegeneration after status epilepticus induced by systemic and intrahippocampal pilocarpine in Wistar rats. Brain Res *1374*, 43-55.

Cataldo, A. M., and Broadwell, R. D. (1986). Cytochemical identification of cerebral glycogen and glucose-6-phosphatase activity under normal and experimental conditions. II. Choroid plexus and ependymal epithelia, endothelia and pericytes. J Neurocytol *15*, 511-524.

Cavalcante, L. A., Barradas, P. C., and Vieira, A. M. (1996). The regional distribution of neuronal glycogen in the opossum brain, with special reference to hypothalamic systems. J Neurocytol *25*, 455-463.

Cavanagh, J. B. (1999). Corpora-amylacea and the family of polyglucosan diseases. Brain Res Brain Res Rev *29*, 265-295.

Cavanagh, J. B., and Gysbers, M. F. (1983). Ultrastructural features of the Purkinje cell damage caused by acrylamide in the rat: a new phenomenon in cellular neuropathology. J Neurocytol *12*, 413-437.

Cavanagh, J. B., Nolan, C. C., and Brown, A. W. (1990). Glial cell intrusions actively remove detritus due to toxic chemicals from within nerve cells. Neurotoxicology *11*, 1-12.

Cisse, S., Perry, G., Lacoste-Royal, G., Cabana, T., and Gauvreau, D. (1993). Immunochemical identification of ubiquitin and heat-shock proteins in corpora amylacea from normal aged and Alzheimer's disease brains. Acta Neuropathol *85*, 233-240.

Cloix, J. F., Tahi, Z., Boissonnet, A., and Hevor, T. (2010). Brain glycogen and neurotransmitter levels in fast and slow methionine sulfoximine-selected mice. Exp Neurol *225*, 274-283.

Criado, O., Aguado, C., Gayarre, J., Duran, L., Garcia-Cabrero, A. M., Vernia, S., Millan, B. S., Heredia, M., Roma-Mateo, C., Mouron, S*., et al.* (2011). Lafora bodies and neurological defects in malin-deficient mice correlate with impaired autophagy. Hum Mol Genet.

Cruz, N. F., and Dienel, G. A. (2002). High glycogen levels in brains of rats with minimal environmental stimuli: implications for metabolic contributions of working astrocytes. J Cereb Blood Flow Metab *22*, 1476-1489.

Cheng, A., Zhang, M., Gentry, M. S., Worby, C. A., Dixon, J. E., and Saltiel, A. R. (2007). A role for AGL ubiquitination in the glycogen storage disorders of Lafora and Cori's disease. Genes Dev *21*, 2399-2409.

Das, A., Balan, S., Mathew, A., Radhakrishnan, V., Banerjee, M., and Radhakrishnan, K. (2011). Corpora amylacea deposition in the hippocampus of patients with mesial temporal lobe epilepsy: A new role for an old gene? Indian J Hum Genet *17 Suppl 1*, S41-47.

Delgado-Escueta, A. V. (2007). Advances in lafora progressive myoclonus epilepsy. Curr Neurol Neurosci Rep *7*, 428-433.

DePaoli-Roach, A. A., Tagliabracci, V. S., Segvich, D. M., Meyer, C. M., Irimia, J. M., and Roach, P. J. (2010). Genetic depletion of the malin E3 ubiquitin ligase in mice leads to lafora bodies and the accumulation of insoluble laforin. J Biol Chem *285*, 25372-25381.

Dinocourt, C., Petanjek, Z., Freund, T. F., Ben-Ari, Y., and Esclapez, M. (2003). Loss of interneurons innervating pyramidal cell dendrites and axon initial segments in the CA1 region of the hippocampus following pilocarpine-induced seizures. J Comp Neurol *459*, 407-425.

Erdamar, S., Zhu, Z. Q., Hamilton, W. J., Armstrong, D. L., and Grossman, R. G. (2000). Corpora amylacea and heat shock protein 27 in Ammon's horn sclerosis. J Neuropathol Exp Neurol *59*, 698-706.

Fleming, P. D., Cordoza, M. E., and Wood, S. G. (1986). Corpora amylacea increased in Alzheimer's disease. Neurology.

Franken, P., Gip, P., Hagiwara, G., Ruby, N. F., and Heller, H. C. (2003). Changes in brain glycogen after sleep deprivation vary with genotype. Am J Physiol Regul Integr Comp Physiol *285*, R413-419.

Ganesh, S., Delgado-Escueta, A. V., Sakamoto, T., Avila, M. R., Machado-Salas, J., Hoshii, Y., Akagi, T., Gomi, H., Suzuki, T., Amano, K*., et al.* (2002). Targeted disruption of the Epm2a gene causes formation of Lafora inclusion bodies, neurodegeneration, ataxia, myoclonus epilepsy and impaired behavioral response in mice. Hum Mol Genet *11*, 1251-1262.

Garyali, P., Siwach, P., Singh, P. K., Puri, R., Mittal, S., Sengupta, S., Parihar, R., and Ganesh, S. (2009). The malin-laforin complex suppresses the cellular toxicity of misfolded proteins by promoting their degradation through the ubiquitin-proteasome system. Hum Mol Genet *18*, 688-700.

Gentry, M. S., Worby, C. A., and Dixon, J. E. (2005). Insights into Lafora disease: malin is an E3 ubiquitin ligase that ubiquitinates and promotes the degradation of laforin. Proc Natl Acad Sci U S A *102*, 8501-8506.

Gip, P., Hagiwara, G., Ruby, N. F., and Heller, H. C. (2002). Sleep deprivation decreases glycogen in the cerebellum but not in the cortex of young rats. Am J Physiol Regul Integr Comp Physiol *283*, R54-59.

Herzog, R. I., Chan, O., Yu, S., Dziura, J., McNay, E. C., and Sherwin, R. S. (2008). Effect of acute and recurrent hypoglycemia on changes in brain glycogen concentration. Endocrinology *149*, 1499-1504.

Inoue, N., Matsukado, Y., Goto, S., and Miyamoto, E. (1988). Localization of glycogen synthase in brain. J Neurochem *50*, 400-405.

Iwaki, T., Hamada, Y., and Tateishi, J. (1996). Advanced glycosylation end-products and heat shock proteins accumulate in the basophilic degeneration of the myocardium and the corpora amylacea of the glia. Pathol Int *46*, 757-763.

Jackson, M. C., Scollard, D. M., Mack, R. J., and Lenney, J. F. (1994). Localization of a novel pathway for the liberation of GABA in the human CNS. Brain Res Bull *33*, 379-385.

Kawamura, T., Morioka, T., Nishio, S., Fukui, K., and Fukui, M. (2002). Temporal lobe epilepsy and corpora amylacea in the hippocampus: clinicopathologic correlation. Neurol Res *24*, 563-569.

Kimura, T., Takamatsu, J., Miyata, T., Miyakawa, T., and Horiuchi, S. (1998). Localization of identified advanced glycation end-product structures, N epsilon(carboxymethyl)lysine and pentosidine, in age-related inclusions in human brains. Pathol Int *48*, 575-579.

Knecht, E., Aguado, C., Sarkar, S., Korolchuk, V. I., Criado-Garcia, O., Vernia, S., Boya, P., Sanz, P., Rodriguez de Cordoba, S., and Rubinsztein, D. C. (2010). Impaired autophagy in Lafora disease. Autophagy *6*, 991-993.

Kong, J., Shepel, P. N., Holden, C. P., Mackiewicz, M., Pack, A. I., and Geiger, J. D. (2002). Brain glycogen decreases with increased periods of wakefulness: implications for homeostatic drive to sleep. J Neurosci *22*, 5581-5587.

Korzhevskii, D. E., and Giliarov, A. V. (2007). [Demonstration of nuclear protein neun in the human brain corpora amylacea]. Morfologiia *131*, 75-76.

Kosaka, K., Matsushita, M., Oyanagi, S., Uchiyama, S., and Iwase, S. (1981). Pallido-nigro-luysial atrophy with massive appearance of corpora amylacea in the CNS. Acta Neuropathol *53*, 169-172.

Krim, E., Vital, A., Macia, F., Yekhlef, F., and Tison, F. (2005). Atypical parkinsonism combining alpha-synuclein inclusions and polyglucosan body disease. Mov Disord *20*, 200-204.

Li, J. J., Surini, M., Catsicas, S., Kawashima, E., and Bouras, C. (1995). Age-dependent accumulation of advanced glycosylation end products in human neurons. Neurobiol Aging *16*, 69-76.

Liu, Y., Wang, Y., Wu, C., and Zheng, P. (2009). Deletions and missense mutations of EPM2A exacerbate unfolded protein response and apoptosis of neuronal cells induced by endoplasm reticulum stress. Hum Mol Genet *18*, 2622-2631.

Loeffler, K. U., Edward, D. P., and Tso, M. O. (1993). Tau-2 immunoreactivity of corpora amylacea in the human retina and optic nerve. Invest Ophthalmol Vis Sci *34*, 2600-2603.

Loiseau, H., Marchal, C., Vital, A., Vital, C., Rougier, A., and Loiseau, P. (1992). Occurrence of polyglucosan bodies in temporal lobe epilepsy. J Neurol Neurosurg Psychiatry *55*, 1092-1093.

Loiseau, H., Marchal, C., Vital, A., Vital, C., Rougier, A., and Loiseau, P. (1993). [Polysaccharide bodies: an unusual finding in a case of temporal epilepsy. Review of the literature]. Rev Neurol (Paris) *149*, 192-197.

Magistretti, P. J., and Allaman, I. (2007). Glycogen: a Trojan horse for neurons. Nat Neurosci *10*, 1341-1342.

Magistretti, P. J., Sorg, O., Yu, N., Martin, J. L., and Pellerin, L. (1993). Neurotransmitters regulate energy metabolism in astrocytes: implications for the metabolic trafficking between neural cells. Dev Neurosci *15*, 306-312.

Magloczky, Z., and Freund, T. F. (2005). Impaired and repaired inhibitory circuits in the epileptic human hippocampus. Trends Neurosci *28*, 334-340.

Marquez, M., Perez, L., Serafin, A., Teijeira, S., Navarro, C., and Pumarola, M. (2010). Characterisation of Lafora-like bodies and other polyglucosan bodies in two aged dogs with neurological disease. Vet J *183*, 222-225.

Martin, J. E., Mather, K., Swash, M., Garofalo, O., Leigh, P. N., and Anderton, B. H. (1991). Heat shock protein expression in corpora amylacea in the central nervous system: clues to their origin. Neuropathol Appl Neurobiol *17*, 113-119.

Matsui, T., Ishikawa, T., Ito, H., Okamoto, M., Inoue, K., Lee, M. C., Fujikawa, T., Ichitani, Y., Kawanaka, K., and Soya, H. (2011). Brain glycogen supercompensation following exhaustive exercise. J Physiol.

Nelson, S. R., Schulz, D. W., Passonneau, J. V., and Lowry, O. H. (1968). Control of glycogen levels in brain. J Neurochem *15*, 1271-1279.

Nishi, K., Tanegashima, A., Yamamoto, Y., Ushiyama, I., Ikemoto, K., Yamasaki, S., Nishimura, A., Rand, S., and Brinkmann, B. (2003). Utilization of lectin-histochemistry in forensic neuropathology: lectin staining provides useful information for postmortem diagnosis in forensic neuropathology. Leg Med (Tokyo) *5*, 117-131.

Nishimura, A., Ikemoto, K., Satoh, K., Yamamoto, Y., Rand, S., Brinkmann, B., and Nishi, K. (2000). The carbohydrate deposits detected by histochemical methods in the molecular layer of the dentate gyrus in the hippocampal formation of patients with schizophrenia, Down's syndrome and dementia, and aged person. Glycoconj J *17*, 815-822.

Nolan, C. C., and Brown, A. W. (1989). Reversible neuronal damage in hippocampal pyramidal cells with triethyllead: the role of astrocytes. Neuropathol Appl Neurobiol *15*, 441-457.

Norio, R., and Koskiniemi, M. (1979). Progressive myoclonus epilepsy: genetic and nosological aspects with special reference to 107 Finnish patients. Clin Genet *15*, 382-398.

Pederson, B. A., Chen, H., Schroeder, J. M., Shou, W., DePaoli-Roach, A. A., and Roach, P. J. (2004). Abnormal cardiac development in the absence of heart glycogen. Mol Cell Biol *24*, 7179-7187.

Pellegri, G., Rossier, C., Magistretti, P. J., and Martin, J. L. (1996). Cloning, localization and induction of mouse brain glycogen synthase. Brain Res Mol Brain Res *38*, 191-199.

Petit, J. M., Tobler, I., Allaman, I., Borbely, A. A., and Magistretti, P. J. (2002). Sleep deprivation modulates brain mRNAs encoding genes of glycogen metabolism. Eur J Neurosci *16*, 1163-1167.

Pfeiffer, B., Buse, E., Meyermann, R., and Hamprecht, B. (1995). Immunocytochemical localization of glycogen phosphorylase in primary sensory ganglia of the peripheral nervous system of the rat. Histochem Cell Biol *103*, 69-74.

Pfeiffer, B., Buse, E., Meyermann, R., Rocha, M. J., and Hamprecht, B. (1993). Glycogen phosphorylase activity and immunoreactivity during pre- and postnatal development of rat brain. Histochemistry *100*, 265-270.

Pfeiffer-Guglielmi, B., Fleckenstein, B., Jung, G., and Hamprecht, B. (2003). Immunocytochemical localization of glycogen phosphorylase isozymes in rat nervous tissues by using isozyme-specific antibodies. J Neurochem *85*, 73-81.

Pratt, W. B., Morishima, Y., Peng, H. M., and Osawa, Y. (2010). Proposal for a role of the Hsp90/Hsp70-based chaperone machinery in making triage decisions when proteins undergo oxidative and toxic damage. Exp Biol Med (Maywood) *235*, 278-289.

Prebil, M., Jensen, J., Zorec, R., and Kreft, M. (2011). Astrocytes and energy metabolism. Arch Physiol Biochem *117*, 64-69.

Puri, R., and Ganesh, S. (2010). Laforin in autophagy: a possible link between carbohydrate and protein in Lafora disease? Autophagy *6*, 1229-1231.

Puri, R., Suzuki, T., Yamakawa, K., and Ganesh, S. (2009). Hyperphosphorylation and aggregation of Tau in laforin-deficient mice, an animal model for Lafora disease. J Biol Chem *284*, 22657-22663.

Puri, R., Suzuki, T., Yamakawa, K., and Ganesh, S. (2011). Dysfunctions in endosomal-lysosomal and autophagy pathways underlie neuropathology in a mouse model for Lafora disease. Hum Mol Genet.

Radhakrishnan, A., Radhakrishnan, K., Radhakrishnan, V. V., Mary, P. R., Kesavadas, C., Alexander, A., and Sarma, P. S. (2007). Corpora amylacea in mesial temporal lobe epilepsy: clinico-pathological correlations. Epilepsy Res *74*, 81-90.

Rao, S. N., Maity, R., Sharma, J., Dey, P., Shankar, S. K., Satishchandra, P., and Jana, N. R. (2010a). Sequestration of chaperones and proteasome into Lafora bodies and proteasomal dysfunction induced by Lafora disease-associated mutations of malin. Hum Mol Genet *19*, 4726-4734.

Rao, S. N., Sharma, J., Maity, R., and Jana, N. R. (2010b). Co-chaperone CHIP stabilizes aggregate-prone malin, a ubiquitin ligase mutated in Lafora disease. J Biol Chem *285*, 1404-1413.

Reed, G. B., Jr., Dixon, J. F., Neustein, J. B., Donnell, G. N., and Landing, B. H. (1968). Type IV glycogenosis. Patient with absence of a branching enzyme alpha-1,4-glucan:alpha-1,4-glucan 6-glycosyl transferase. Lab Invest *19*, 546-557.

Ribeiro Mde, C., Barbosa-Coutinho, L., Mugnol, F., Hilbig, A., Palmini, A., da Costa, J. C., Paglioli Neto, E., and Paglioli, E. (2003). Corpora amylacea in temporal lobe epilepsy associated with hippocampal sclerosis. Arq Neuropsiquiatr *61*, 942-945.

Robitaille, Y., Carpenter, S., Karpati, G., and DiMauro, S. D. (1980). A distinct form of adult polyglucosan body disease with massive involvement of central and peripheral neuronal processes and astrocytes: a report of four cases and a review of the occurrence of polyglucosan bodies in other conditions such as Lafora's disease and normal ageing. Brain *103*, 315-336.

Sakai, M., Austin, J., Witmer, F., and Trueb, L. (1969). Studies of corpora amylacea. I. Isolation and preliminary characterization by chemical and histochemical techniques. Arch Neurol *21*, 526-544.

Scharf, M. T., Naidoo, N., Zimmerman, J. E., and Pack, A. I. (2008). The energy hypothesis of sleep revisited. Prog Neurobiol *86*, 264-280.

Schipper, H. M. (2011). Heme oxygenase-1 in Alzheimer disease: a tribute to Moussa Youdim. J Neural Transm *118*, 381-387.

Selmaj, K., Pawlowska, Z., Walczak, A., Koziolkiewicz, W., Raine, C. S., and Cierniewski, C. S. (2008). Corpora amylacea from multiple sclerosis brain tissue consists of aggregated neuronal cells. Acta Biochim Pol *55*, 43-49.

Sengupta, S., Badhwar, I., Upadhyay, M., Singh, S., and Ganesh, S. (2011). Malin and laforin are essential components of a protein complex that protects cells from thermal stress. J Cell Sci *124*, 2277-2286.

Sharma, J., Rao, S. N., Shankar, S. K., Satishchandra, P., and Jana, N. R. (2011). Lafora disease ubiquitin ligase malin promotes proteasomal degradation of neuronatin and regulates glycogen synthesis. Neurobiol Dis *44*, 133-141.

Shulman, R. G., Bloch, G., and Rothman, D. L. (1995). In vivo regulation of muscle glycogen synthase and the control of glycogen synthesis. Proc Natl Acad Sci U S A *92*, 8535-8542.

Singhrao, S. K., Neal, J. W., and Newman, G. R. (1993). Corpora amylacea could be an indicator of neurodegeneration. Neuropathol Appl Neurobiol *19*, 269-276.

Soriano, E., Dumesnil, N., Auladell, C., Cohen-Tannoudji, M., and Sotelo, C. (1995). Molecular heterogeneity of progenitors and radial migration in the developing cerebral cortex revealed by transgene expression. Proc Natl Acad Sci U S A *92*, 11676-11680.

Suzuki, A., Stern, S. A., Bozdagi, O., Huntley, G. W., Walker, R. H., Magistretti, P. J., and Alberini, C. M. (2011). Astrocyte-neuron lactate transport is required for long-term memory formation. Cell *144*, 810-823.

Swanson, R. A., Morton, M. M., Sagar, S. M., and Sharp, F. R. (1992). Sensory stimulation induces local cerebral glycogenolysis: demonstration by autoradiography. Neuroscience *51*, 451-461.

Tagliabracci, V. S., Heiss, C., Karthik, C., Contreras, C. J., Glushka, J., Ishihara, M., Azadi, P., Hurley, T. D., DePaoli-Roach, A. A., and Roach, P. J. (2011). Phosphate incorporation during glycogen synthesis and Lafora disease. Cell Metab *13*, 274-282.

Tagliabracci, V. S., Turnbull, J., Wang, W., Girard, J. M., Zhao, X., Skurat, A. V., Delgado-Escueta, A. V., Minassian, B. A., Depaoli-Roach, A. A., and Roach, P. J. (2007). Laforin is a glycogen phosphatase, deficiency of which leads to elevated phosphorylation of glycogen in vivo. Proc Natl Acad Sci U S A *104*, 19262-19266.

Trivedi, J. R., Wolfe, G. I., Nations, S. P., Burns, D. K., Bryan, W. W., and Dewey, R. B., Jr. (2003). Adult polyglucosan body disease associated with lewy bodies and tremor. Arch Neurol *60*, 764-766.

Turnbull, J., Depaoli-Roach, A. A., Zhao, X., Cortez, M. A., Pencea, N., Tiberia, E., Piliguian, M., Roach, P. J., Wang, P., Ackerley, C. A., and Minassian, B. A. (2011). PTG Depletion Removes Lafora Bodies and Rescues the Fatal Epilepsy of Lafora Disease. PLoS Genet *7*, e1002037.

Turnbull, J., Wang, P., Girard, J. M., Ruggieri, A., Wang, T. J., Draginov, A. G., Kameka, A. P., Pencea, N., Zhao, X., Ackerley, C. A., and Minassian, B. A. (2010). Glycogen hyperphosphorylation underlies lafora body formation. Ann Neurol *68*, 925-933.

Uchida, K., Kihara, N., Hashimoto, K., Nakayama, H., Yamaguchi, R., and Tateyama, S. (2003). Age-related histological changes in the canine substantia nigra. J Vet Med Sci *65*, 179-185.

Uchiki, T., Weikel, K. A., Jiao, W., Shang, F., Caceres, A., Pawlak, D., Handa, J. T., Brownlee, M., Nagaraj, R., and Taylor, A. (2011). Glycation-altered proteolysis as a pathobiologic mechanism that links dietary glycemic index, aging, and age-related disease (in nondiabetics). Aging Cell.

Valles-Ortega, J., Duran, J., Garcia-Rocha, M., Bosch, C., Saez, I., Pujadas, L., Serafin, A., Canas, X., Soriano, E., Delgado-Garcia, J. M.*, et al.* (2011). Neurodegeneration and functional impairments associated with glycogen synthase accumulation in a mouse model of Lafora disease. EMBO Mol Med.

Vernia, S., Rubio, T., Heredia, M., Rodriguez de Cordoba, S., and Sanz, P. (2009). Increased endoplasmic reticulum stress and decreased proteasomal function in lafora disease models lacking the phosphatase laforin. PLoS One *4*, e5907.

Vilchez, D., Ros, S., Cifuentes, D., Pujadas, L., Valles, J., Garcia-Fojeda, B., Criado-Garcia, O., Fernandez-Sanchez, E., Medrano-Fernandez, I., Dominguez, J.*, et al.* (2007). Mechanism suppressing glycogen synthesis in neurons and its demise in progressive myoclonus epilepsy. Nat Neurosci *10*, 1407-1413.

Wender, R., Brown, A. M., Fern, R., Swanson, R. A., Farrell, K., and Ransom, B. R. (2000). Astrocytic glycogen influences axon function and survival during glucose deprivation in central white matter. J Neurosci *20*, 6804-6810.

Wilhelmus, M. M., Verhaar, R., Bol, J. G., van Dam, A. M., Hoozemans, J. J., Rozemuller, A. J., and Drukarch, B. (2011). Novel role of transglutaminase 1 in corpora amylacea formation? Neurobiol Aging *32*, 845-856.

Worby, C. A., Gentry, M. S., and Dixon, J. E. (2008). Malin decreases glycogen accumulation by promoting the degradation of protein targeting to glycogen (PTG). J Biol Chem *283*, 4069-4076.

Yan, S. D., Yan, S. F., Chen, X., Fu, J., Chen, M., Kuppusamy, P., Smith, M. A., Perry, G., Godman, G. C., Nawroth, P., and et al. (1995). Non-enzymatically glycated tau in Alzheimer's disease induces neuronal oxidant stress resulting in cytokine gene expression and release of amyloid beta-peptide. Nat Med *1*, 693-699.

DISCUSSIÓ GENERAL

DISCUSSIÓ GENERAL

El glicogen és la major reserva energètica del SNC. La seva concentració és molt inferior a la d'altres teixits com el múscul i el fetge, i és clarament insuficient per a cobrir l'elevada i contínua demanda energètica del cervell, que depèn principalment de la glucosa que li arriba a través del reg sanguini. Malgrat això, el glicogen té un paper important com a suport energètic en determinades activitats neuronals o en situacions d'estrès tissular degut a patologies o privació energètica. Encara que la síntesi i degradació del glicogen cerebral sembla estar lligada a les necessitats energètiques derivades de l'activitat sinàptica, són els astròcits els que acumulen aquest polisacàrid i l'administren a les neurones en forma de lactat. D'aquesta manera, l'activitat cerebral depèn de la coordinació energètica entre les cèl·lules neuronals i glials. Així doncs, tot i que sembla que les neurones requereixen el glicogen cerebral per al seu funcionament òptim, en general, no s'ha observat que n'acumulin les seves pròpies reserves. Tot i això, en determinades situacions neurodegeneratives, les neurones acumulen polímers de glucosa poc ramificats coneguts com a cossos de poliglucosà (PGBs). Aquesta observació va ser la que va impulsar el nostre grup a investigar el metabolisme del glicogen neuronal.

En contra del que generalment es creu, no només els astròcits sinó també les neurones tenen la maquinària necessària per a sintetitzar glicogen. Malgrat aquest fet, mentre que l'expressió de MGS i el contingut de glicogen són generalitzats en les cèl·lules astroglials (Brown, 2004; Prebil et al., 2011), en neurones, l'enzim es manté inactivat per fosforilació (**Article 1**) i no s'observa glicogen en aquest tipus cel·lular en condicions normals (Brown, 2004; Cammermeyer and Fenton, 1981; Cavalcante et al., 1996). Aquestes diferències entre astròcits i neurones han portat a la hipòtesi que existeix un rol diferent per al glicogen o l'activitat MGS neuronals (Pfeiffer et al., 1995), **Article 1**). En els articles que conformen aquesta tesi doctoral, s'analitza el paper del metabolisme del glicogen neuronal mitjançant l'estudi i la comparació de dues situacions paradigmàtiques on es produeix acumulació de PGBs: 1)la malaltia de Lafora (LD), una epilèpsia mioclònica progressiva causada per mutacions en els gens que codifiquen per laforina o malina, en la que la presència de PGBs a les neurones (anomenats cossos de Lafora, LBs) n'és la característica diferencial i 2) l'envelliment, situació fisiològica en la que, per motius encara desconeguts, s'acumulen PGBs (anomenats Corpora Amylacea, CA) en el cervell de tots els mamífers.

L'expressió de MGS en neurones es va descriure inicialment en cultius primaris de ratolí, on es va demostrar l'existència d'un mecanisme, fins llavors desconegut, que regula l'acumulació de glicogen mitjançant la degradació proteasomal, mediada pel complex laforina-malina, de MGS i PTG. Donat que, en mamífers, la MGS és l'únic enzim capaç de sintetitzar polímers de glucosa en el cervell i la PTG propicia la seva acumulació, l'alteració d'aquest mecanisme com a conseqüència de la pèrdua de funció de laforina o malina pot explicar l'acumulació de cossos de

poliglucosà en neurones i en altres tipus cel·lulars que expressin normalment laforina i malina. El paper del complex laforina-malina en la degradació de PTG i altres proteïnes vinculades al metabolisme del glicogen com el DBE també ha estat descrit per altres autors (Cheng et al., 2007; Worby et al., 2008). L'alteració de la regulació sobre el DBE podria contribuir a la manca de ramificació del glicogen acumulat en els LBs.

A més, també es va observar que la sobreexpressió de PTG aconseguia activar la MGS neuronal i produïa acumulació de poliglucosà en aquestes neurones. Aquest fet estava associat a efectes perjudicials per a les cèl·lules neuronals, ja que activava el seu programa apoptòtic. Per tant, vam proposar que l'alteració del metabolisme del glicogen causada per deficiència de laforina o malina podia ser la causant de la formació dels LBs i del procés neurodegeneratiu en la LD (**Article 1**).

En aquesta direcció, la disrupció de laforina (laforina KO) en ratolins causava neurodegeneració, epilèpsia mioclònica i alteracions del comportament juntament amb la formació de LBs (Ganesh et al., 2002). A més, en concordança amb el mecanisme abans proposat, es va trobar un marcat increment en els nivells de MGS dels cervells d'aquest model animal (Tagliabracci et al., 2008). Per tal d'analitzar les conseqüències de la disrupció de l'altre gen conegut implicat en la LD, vam generar ratolins deficients en malina (malina KO). Dues publicacions anteriors a la nostra estudiaven ratolins malina KO de 3 mesos (DePaoli-Roach et al., 2010) i 6 mesos d'edat (Turnbull et al., 2010) però cap d'elles descrivia alteracions neurològiques. Nosaltres vam allargar l'estudi del nostre model fins als 11 mesos, edat en la qual els ratolins presentaven un fenotip neuropatològic evident (**Article 2**).

Els ratolins malina KO presentaven LBs en diverses regions del cervell però també en múscul esquelètic i cor (DePaoli-Roach et al., 2010); **Article2**), tal i com passa en pacients humans d'aquesta malaltia. Les zones del cervell on la presència de LBs eren més evidents són la capa granular del cerebel, l'hipocamp i el còrtex piriforme. El contingut de glicogen en els cervells d'aquests animals era més de dues vegades major que el dels WT i corresponia a una fracció insoluble i poc ramificada de polisacàrid. Aquesta observació dóna suport a la idea que l'augment en quantitat de glicogen correspon a les inclusions de poliglucosà. Els LBs no només contenien glicogen poc ramificat sinó també MGS, l'enzim responsable de la seva síntesi. L'acumulació de LBs tenia lloc inclús en presència d'un increment en els nivells de GP soluble. Aquest darrer resultat es pot entendre com una resposta a l'acumulació de poliglucosà i suggereix que el glicogen aberrant sintetitzat en els cervells malina KO és resistent a la degradació per GP. A més, també vam trobar augmentats els nivells de glicogenina en la fracció insoluble dels cervells KO, fet que suggereix que aquest enzim també és necessari per a la iniciació de la síntesi de poliglucosà.

En publicacions recents es demostra que el glicogen incorpora fosfats en els seus residus glucosídics com a conseqüència de l'error catalític de la GS i que aquest fosfat s'allibera

mitjançant l'activitat fosfatasa de la laforina. Segons postulen aquests treballs, la hiperfosforilació del glicogen portaria a una reducció de la seva solubilitat, essent aquesta característica el determinant que causaria la LD (Tagliabracci et al., 2008; Tagliabracci et al., 2011; Turnbull et al., 2010). Tot i que aquest argument podria explicar la formació de LBs en els casos de deficiència de laforina, resulta complicat entendre com contribuiria en la seva formació en els casos de pèrdua de funció de malina, en els quals la laforina es troba inalterada. A més, les nostres dades (**Article 2**) demostren que la laforina es manté inalterada a la fracció soluble, i fins i tot es troba augmentada en la fracció insoluble. Per tant, la causa de l'acumulació de LBs en el nostre model no pot ser atribuït a un decrement de l'activitat laforina fosfatasa disponible.

En concordança amb l'impressionant acumulació de MGS que s'observava per immunohistologia, l'anàlisi per western blot d'extractes de cervells malina KO va mostrar que la MGS total es trobava dràsticament incrementada i acumulada en la fracció insoluble. Vam trobar que l'enzim en els LBs estava menys fosforilat i, per tant, presumiblement més actiu. Sorprenentment, no vam detectar una major activitat GS ni tan sols fent el test en presència de G6P. L'acumulació de MGS que s'observa en els cervells malina KO (11 mesos) és comparable a la descrita per als cervells laforina KO (9-12 mesos) (Tagliabracci et al., 2008), on també es descriu aquesta descompensació entre la proteïna total i l'activitat de l'enzim (Tagliabracci et al., 2008). Aquests resultats poden indicar que la MGS és incapaç de desenvolupar la seva activitat sota les condicions de l'assaig perquè es troba atrapada en els LBs. Per altra banda, també podrien assenyalar que la MGS acumulada en els LBs es troba realment inactivada, ja sigui per canvis estructurals, agregació o modificacions postraduccionals desconegudes que impedeixin fins i tot l'activació al·lostèrica induïda per un excés de G6P. El que sí que podem concloure és que el mecanisme pel qual s'acumula MGS i s'altera la seva activitat és una característica comú de la LD causada per alteració tant de laforina com de malina.

Si els LBs es formen per una alteració del metabolisme del glicogen, l'estudi en profunditat de la seva acumulació requereix la identificació de les cèl·lules que expressen la maquinària necessària per a la síntesi de glicogen. L'anàlisi del patró d'expressió de MGS en el cervell de ratolins salvatges des del període de lactància (15 dies) fins a edats avançades (16 mesos) va mostrar que, d'acord amb el contingut de glicogen, la MGS es trobava en astròcits i la seva distribució era homogènia dins de les diferents regions del cervell en animals joves. Però, amb l'edat, augmentava la presència dispersa d'astròcits amb major senyal per a MGS. Per altra banda, només es va trobar MGS en alguns tipus específics de neurones en els quals s'observava una modulació diferencial de l'expressió de MGS depenent de l'edat. Mentre que l'expressió de MGS es mantenia constant en els cèl·lules de Purkinje del cerebel durant l'etapa analitzada, l'expressió en les interneurones hipocampals dequeia amb l'edat (**Article 3**).

Un resultat molt rellevant d'aquest estudi va ser la troballa d'acumulacions de MGS a l'hipocamp, la capa granular del cerebel i el còrtex piriforme dels ratolins vells. Les àrees del cervell afectades

per aquests dipòsits relacionats amb l'envelliment (Corpora Amylacea, CA) eren les mateixes que en els ratolins malina KO. A més, l'estudi del patró d'expressió de malina va revelar una disminució dels seus nivells en animals vells en aquelles àrees del cervell on s'acumula MGS amb l'edat. Tenint en compte que la malina indueix la degradació proteasomal de la MGS, aquestes dades suggereixen un origen comú per als dipòsits relacionats amb l'edat i els propis de la LD (LBs). Aquest origen comú implicaria la disminució o l'alteració de la degradació de MGS. A més, altres proteïnes involucrades en el metabolisme del glicogen com la laforina i la BGP també es van trobar en CA i LBs (**Article 3**). Aquests resultats reforcen la implicació del glicogen en la formació dels dos tipus de PGBs.

L'estudi de l'hipocamp dels ratolins malina KO va mostrar que tant els astròcits com les interneurones positives per parvalbúmina (PV+), que expressen MGS i malina en condicions normals, acumulaven LBs intracel·lulars com a conseqüència de la disrupció genètica de malina. La cronologia d'aparició dels LBs correlacionava amb el caràcter degeneratiu de la LD, ja que l'increment en els dipòsits de poliglucosà en els somes PV+ coincidia amb la pèrdua d'aquestes interneurones. Tot i això, és interessant destacar que la presència de LBs fora dels somes neuronals, més petits i associats als astròcits, s'observava ja en animals més joves, quan la pèrdua de neurones encara no era visible (**Article 2**). Malgrat la severa neurodegeneració que es va trobar en els ratolins malina KO, no vam detectar neurones apoptòtiques en les nostres preparacions. La mateixa observació va ser feta per als cervells dels ratolins laforina KO (Ganesh et al., 2002). L'estudi de malalties neurodegeneratives com les d'Alzheimer i Huntington i l'esclerosi amiotròfica lateral ha mostrat que és molt difícil detectar apoptosi *in vivo* (Mattson, 2000). Això passa perquè l'apoptosi és un procés curt (unes hores) i això dificulta la detecció de cèl·lules que presentin les característiques típiques d'aquest procés en un fenomen neurodegeneratiu que es produeix paulatinament durant mesos.

Es considera que el tipus i la localització cel·lular on es troben és una característica distintiva dels diferents tipus de PGBs. Així, els LBs s'han atribuït únicament al soma i les dentrites de les neurones. Encara que la seva presència en cèl·lules glials de pacients va ser qüestió de debat al començament del segle XX (del Río-Hortega, 1925; Lafora, 1913), les nostres observacions en els ratolins malina KO són les primeres en demostrar la presència de LBs també en astròcits (**Article 2**). Pel que fa als CA, la seva localització és més controvertida. S'ha descrit que es troben associats a processos astrocítics i en axons però no en el soma de neurones (Cavanagh, 1999). Així, la presència de LBs en el soma de les neurones, minoritaris en nombre però majors en mida, seria la característica diferencial dels PGBs associats a la LD i podria tenir una relació directa amb la neurodegeneració que pateixen els pacients d'aquesta malaltia.

Com ja s'ha comentat, s'han proposat funcions fisiològiques diferenciades per la MGS i el glicogen en cèl·lules neuronals i glials. Per tal d'entendre el significat de la formació dels PGBs, doncs, és important saber en quin tipus cel·lular s'origina. Existeix un ampli ventall d'informació,

principalment basada en la presència de components específics de tipus cel·lular, que donen suport a la implicació de cèl·lules neuronals (Cavanagh, 1999; Korzhevskii and Giliarov, 2007; Marquez et al., 2010; Selmaj et al., 2008) però també de les glials (Cavanagh, 1999; Marquez et al., 2010; Schipper, 2011) en la biogènesi de CA.

Els nostres resultats demostraven que tant els CA com els LBs contenien els marcadors neuronals PV i NF200 encara que aquests dipòsits, freqüentment, no estaven associats a cap estructura neuronal. Les interneurones PV+ són cèl·lules inhibidores GABAèrgiques, l'alteració de les quals està involucrada en epileptogènesi i generació de convulsions (Magloczky and Freund, 2005). En aquesta direcció, els ratolins malina KO patien una degeneració tardana de les interneurones PV+ de l'hipocamp. Per tant, l'excitabilitat sinàptica augmentada i la propensió a convulsions mioclòniques que es van observar en aquests animals podrien ser atribuïdes a la pèrdua d'aquestes neurones. De fet, s'ha descrit un decrement en el seu nombre en la malaltia d'Alzheimer (Brady and Mufson, 1997; Takahashi et al., 2010) i en alguns casos d'epilèpsia (Castro et al., 2011; Dinocourt et al., 2003), , situacions patològiques on, curiosament, l'acumulació de CA es troba augmentada (Cavanagh, 1999; Das et al., 2011; Kawamura et al., 2002; Radhakrishnan et al., 2007; Ribeiro Mde et al., 2003). A més, la carnosinasa sèrica, una dipeptidasa produïda en neurones que catalitza la síntesi de GABA, també ha estat trobada en els CA (Jackson et al., 1994). La presència de PV en els LBs i els CA estreta la relació entre les interneurones GABAèrgiques i la formació de PGBs.

Tenint en compte que tant els CA d'animals vells com els LBs dels ratolins malina KO presentaven una forta associació amb els astròcits i les interneurones PV+, vam analitzar en profunditat la distribució de les inclusions de poliglucosà en relació a aquests dos tipus cel·lulars. Tant en el cervell de l'animal vell com en el del model de LD, es van trobar PGBs extracel·lulars que contenien la proteïna PV i que eren envoltats per processos astrocítics en la proximitat de cèl·lules interneuronals. A més, sorprenentment, en els dos casos es van trobar prolongacions de processos astroglials que s'allargaven fins a PGBs localitzats al soma d'aquestes interneurones. Aquestes observacions suggereixen la transferència dels dipòsits de poliglucosà des dels processos o el soma de les interneurones cap a les cèl·lules astroglials. De fet, un mecanisme equivalent ja ha estat descrit per a la transferència d'altres materials cel·lulars, però mai per al poliglucosà. Acumulacions membranoses anormals en cèl·lules de Purkinje (Cavanagh and Gysbers, 1983) i cossos densos lisosomals dipositats en cèl·lules piramidals de l'hipocamp (Cavanagh et al., 1990; Nolan and Brown, 1989; Norio and Koskiniemi, 1979) després d'una intoxicació química, s'han observat sent transferides cap a processos dels astròcits que es projecten cap a l'interior del cos neuronal. En les nostres preparacions, mentre que el contacte astrocític tenia lloc amb els CA situats en la interfície entre l'espai intracel·lular i l'extracel·lular, en el cas dels LBs els processos astrocítics penetraven a l'interior del soma neuronal per contactar el LB intracel·lular. Tenint en compte que 1) durant l'envelliment s'observa una disminució de l'expressió de malina en les zones on s'acumulen CA, 2) només els LBs, i no els CA,

s'observen generalment en els somes neuronals (Cavanagh, 1999) 3) els LBs tenen una aparició tardana en els somes interneuronals dels ratolins malina KO i està associada a la pèrdua neuronal i 4) els LBs que s'observen en el soma d'interneurones malina KO són considerablement més grans que els CA de ratolins normals vells, aquests resultats poden ser interpretats com que els LBs i els CA són part del mateix procés de transferència de material de neurona a astròcit. L'acumulació de LBs podria ser la conseqüència de l'exacerbació, provocada per la deficiència genètica associada a la LD, d'un procés que té lloc de manera normal durant l'envelliment.

Moltes de les evidències descrites fins ara vinculen l'alteració de la maquinària enzimàtica del metabolisme del glicogen amb la formació dels LBs. Tot i això encara no s'ha pogut establir fins a quin punt aquest fenomen pot ser responsable de les manifestacions clíniques de la LD. Encara que els nostres resultats són consistents amb la hipòtesi que l'acumulació de glicogen aberrant causa les alteracions de la funció neuronal en aquesta malaltia, no podem excloure la possibilitat que altres dianes del complex laforina-malina estiguin involucrades en la patogènesi d'aquesta malaltia. En aquest sentit, no es pot obviar que s'ha descrit que laforina i malina estan implicades en sistemes cel·lulars degradatius com la ruta endosoma-lisosomal, l'autofagia (Aguado et al., 2010; Criado et al., 2011; Knecht et al., 2010; Puri and Ganesh, 2010; Puri et al., 2011b), o l'eliminació de proteïnes mal plegades a través del sistema ubiqüitina-proteasoma (Delgado-Escueta, 2007; Garyali et al., 2009; Rao et al., 2010a; Rao et al., 2010b), i s'ha proposat que aquestes activitats protegeixen contra l'estrès de reticle endoplàsmic (Liu et al., 2009; Vernia et al., 2009) i l'estrès tèrmic (Sengupta et al., 2011). De fet, l'estudi recent de les fases inicials de la malaltia en models de LD indica que els ratolins laforina KO i malina KO presenten alteracions neuronals abans que els LBs siguin detectats (Ganesh et al., 2002), fet que suggereix que una disminució de l'autofàgia pot ser la causa primària de la formació de LBs i dels efectes devastadors de la LD (Criado et al., 2011). Però, per altra banda, un altre treball recent (Turnbull et al., 2011) demostra que la depleció de PTG evita la formació de LBs i el fenotip epilèptic dels ratolins laforina KO. Tot plegat, fa que sigui interessant investigar si el metabolisme del glicogen, a més del seu paper com a reserva energètica, també està lligat a aquestes rutes cel·lulars degradatives i, en especial, a l'autofàgia.

Els processos cel·lulars implicats en la formació dels CA durant l'envelliment també han estat àmpliament debatuts. Molts autors han descrit les propietats immunoquímiques d'aquests dipòsits en cervells humans i de diferents mamífers. Entre d'altres, les proteïnes i altres molècules relacionades amb la resposta a proteïnes mal plegades, els marcadors d'estrès oxidatiu, i els marcadors específics de tipus cel·lular són probablement els que s'han estudiat amb més freqüència (Cavanagh, 1999). Els nostres resultats han validat la presència d'alguns d'aquests marcadors en els CA de ratolins vells i han aprofundit en la descripció de la similitud de les seves característiques dels CA amb les dels LBs dels ratolins malina KO mitjançant la identificació dels mateixos marcadors presents en els dos tipus de dipòsit. A continuació es discuteixen aquests resultats en detall.

Els productes finals de glicació avançada (*advanced glycation end products,* AGEP) són el resultat de la reacció oxidativa entre proteïnes de vida llarga i sucres reductors, i s'han detectat en diverses patologies relacionades amb l'envelliment (Li et al., 1995; Uchiki et al., 2011; Yan et al., 1995) i en els ratolins laforina KO (Ganesh et al., 2002). Les proteïnes de xoc tèrmic (*heat shock proteins,* HSP) tenen una funció important com chaperones. Recentment s'ha proposat que la HSP70 té un paper clau en el triatge de proteïnes aberrants o danyades cap a la degradació per la ruta ubiqüitina-proteasoma (Pratt et al., 2010). De fet, s'ha descrit que la HSP70 interactua amb malina i laforina per formar un complex que suprimeix la toxicitat de proteïnes mal plegades (Garyali et al., 2009; Rao et al., 2010b) i s'ha trobat, juntament amb ubiqüitina, en els LBs de pacients humans (Rao et al., 2010a). Aquestes evidències experimentals, sumades a la presència d'AGEP, ubiqütina i HSP70 tan en els CA com en els LBs observada en el nostre estudi, suggereixen que els dos PGBs poden estar relacionats amb un procés d'estrès cel·lular que cursa amb acumulació de proteïnes mal plegades.

Aquesta relació entre la formació de PGBs i proteïnes mal plegades va ser reforçada per la detecció de l'acumulació d'α-sinucleïna en CA i LBs. Aquesta proteïna és el principal component dels cossos de Lewy presents en la malaltia de Parkinson (PD). A més del sistema ubiqüitina-proteasoma (*ubiquitin-proteasome system*, UPS), cada cop hi ha més evidències que suggereixen l'existència d'un altre sistema selectiu depenent d'ubiqüitina per al control de qualitat de les proteïnes, la ruta agresoma-autofàgia. Quan la producció de proteïnes mal plegades supera la capacitat del sistema de replegament per chaperones i de la ruta de degradació UPS, les proteïnes mal plegades són segrestades en inclusions anomenades agresomes (Kaganovich et al., 2008; Olzmann and Chin, 2008). És probable, doncs, que s'indueixi aquest sistema durant l'envelliment i en malalties neurològiques, on l'activitat proteasomal no funciona correctament (Li and Li, 2011). Al contrari del que passa en l'autofàgia basal, la ruta agresoma-autofàgia propiciaria la neteja selectiva de proteïnes mal plegades i agregades en condicions d'estrès proteotòxic (Chin et al., 2010). De fet, recentment s'ha descrit que l'α-sinucleïna en cèl·lules neuronals és degradada mitjançant la ruta agresoma-autofàgia (Su et al., 2011).

L'α-sinucleïna –juntament amb la huntingtina (en la malaltia de Huntington, HD), la SOD-1 (en l'esclerosi amiotròfica lateral, ALS), tau i el pèptid Aβ (eb la malaltia d'Alzheimer, AD)- pertany a una classe de proteïnes l'agregació anormal de les quals juga un paper central en les malalties neurodegeneratives anomenades proteïnopaties. Resulta interessant que la deposició de PGBs no només s'ha descrit durant l'envelliment sinó també en totes aquestes proteïnopaties (Atsumi, 1981; Averback, 1981; Cavanagh, 1999; Garofalo et al., 1991; McDonald et al., 1993; Schiffer et al., 1994; Segers et al., 2011; Singhrao et al., 1995; Takahashi et al., 1977; Wilhelmus et al., 2011). A més a més, publicacions recents demostren que després de la inhibició del proteasoma, es formen agresomes que a més de material ubiqüitinilat també contenen les proteïnes laforina i

malina (Mittal et al., 2007) i poliglucosà (Puri et al., 2011a). Tots aquests fets indiquen que el glicogen i la seva maquinària enzimàtica poden tenir una funció en l'eliminació de proteïnes mal plegades a través de la ruta agresoma-autofàgia, l'alteració o sobrecàrrega de la qual podria originar l'acumulació de PGBs durant l'envelliment o els processos patològics. Un exemple que reforça aquesta idea és la malatia de Pompe (GSDII, OMIM232300), una patologia genètica causada per la deficiència d'α-glucosidasa àcida lisosomal (GAA) en la qual s'acumula glicogen als lisosomes (Shin, 2006). Curiosament, quan es sobrexpressa la GS en ratolins deficients en GAA, model de la malaltia de Pompe, aquests presenten cossos de poliglucosà (Raben et al., 2001).

La MGS és l'únic enzim que pot sintetitzar cadenes llargues de glucosa al cervell i, per tant, la presència de poliglucosà en CA i LBs implica activitat MGS. De fet, com s'ha comentat anteriorment, la depleció genètica de PTG, un activador de la MGS, evita la formació de LBs en ratolins laforina KO (Turnbull et al., 2011). Tot i això, tenint en compte les observacions exposades abans, l'acumulació de proteïna MGS en els PGBs podria ser interpretada com una conseqüència del seu plegament incorrecte degut a estrès cel·lular. Amb l'objectiu de determinar la importància de la MGS en la formació de CA, es van generar ratolins MGS KO i es va comparar el seu cervell amb el d'animals salvatges durant l'envelliment. El resultat va ser destacable, ja que no només els ratolins MGS KO no presentaven poliglucosans, sinó que cap dels altres components que s'havien detectat en els CA (i en els LBs) es van trobar acumulats en cap de les zones del cervell d'aquests animals. Aquest resultat indica que la MGS és necessària per a la formació de CA.

Cada cop hi ha més evidències que suggereixen que les proteïnes mal plegades agregades en les proteïnopaties, com la α-sinucleïna, comparteixen algunes propietats amb els prions (Lee et al., 2010; Steiner et al., 2011). Per exemple, s'ha proposat que aquestes proteïnes similars als prions podrien transferir-se des de la cèl·lula original cap a una altra, causant mal plegament i agregació de proteïnes en la nova cèl·lula infectada, encara que el mecanisme no està clar (Aguzzi, 2009; Brundin et al., 2010; Frost and Diamond, 2010; Olanow and Prusiner, 2009). En aquest punt, és important destacar que el poliglucosà és un component de les partícules priòniques que accelera la seva agregació i formació de fibriles (Dumpitak et al., 2005; Panza et al., 2008). Així doncs, si els PGBs poden ser partícules infectives similars als prions que podrien contribuir a l'escampament de proteïnes mal plegades o, pel contrari, afavorir al seu confinament és una pregunta interessant que mereix ser afrontada experimentalment. L'estudi exhaustiu dels animals MGS KO permetrà aportar respostes sobre aquesta i altres preguntes.

Tenint en compte els resultats exposats en aquesta tesi i les dades disponibles actualment, una de les funcions del metabolisme neuronal del glicogen es podria atribuir a un mecanisme eficient per evitar la presència de proteïnes perilloses en situació d'estrès cel·lular. Malgrat que no es pot descartar que el glicogen neuronal tingui altres funcions importants, aquest mecanisme fisiològic

justificaria la conservació de l'expressió de MGS, encara que aquesta sigui potencialment nociva per les neurones (Magistretti and Allaman, 2007). Aquest mecanisme, regulat pel complex laforina-malina, controlaria 1) la degradació proteasomal de proteïnes mal plegades 2) l'acumulació d'agresomes formats per poliglucosà i les proteïnes mal plegades que han sobrepassat el sistema proteasomal i la seva eliminació a través de la ruta agresoma-autofàgia 3) la transferència de neurona a astròcit dels agresomes que s'han dipositat després de sobrepassar el sistema d'autofàgia. A més, el funcionament d'aquest mecanisme implica que l'estrès cel·lular induiria l'acumulació de poliglucosà i que el complex laforina-malina bloquejaria aquesta acumulació mitjançant la degradació de MGS, PTG i DBE quan fos necessari. Hipotetitzem que els PGBs s'acumulen com a conseqüència d'una fallada d'aquest procés, ja sigui induït per la deficiència genètica de malina o laforina en la LD o per l'acumulació d'estressos i la disminució de l'activitat proteasomal o de l'autofàgia durant l'envelliment (**Esquema 1**).

Òbviament, el mecanisme proposat en aquesta tesi haurà de ser analitzat en treballs experimentals futurs. L'estudi de les implicacions del metabolisme neuronal del glicogen que aquí es descriuen ens ajudaran a entendre els mecanismes patològics relacionats amb l'envelliment i amb diferents malalties neurològiques.

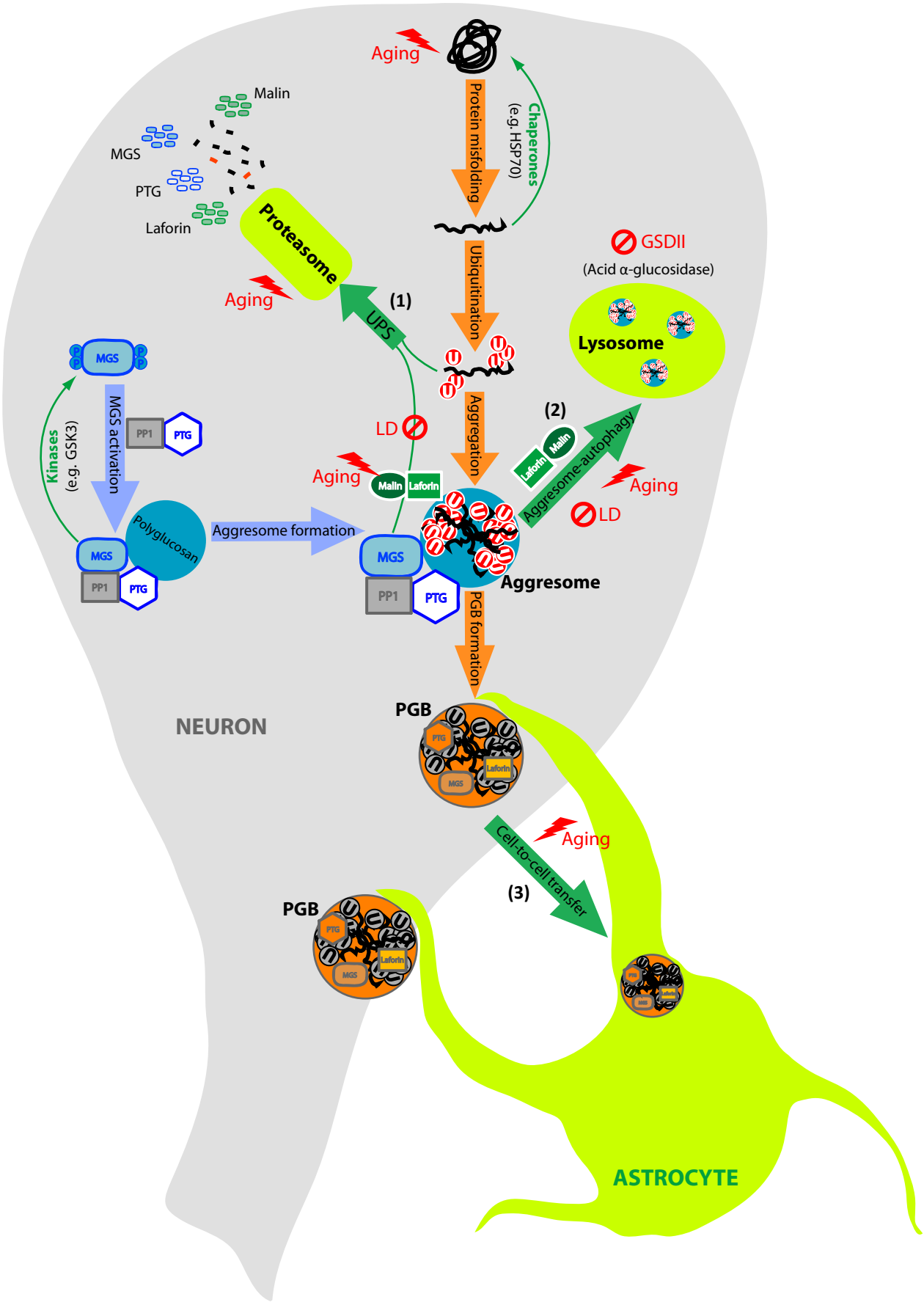

Esquema 1. Mecanisme d'acció proposat pel complex laforina-malina.
GSDII: malaltia de Pompe; LD: malaltia de Lafora; PGB: cos de poliglucosà; UPS: sistema ubiqüitina-proteasoma.

CONCLUSIONS

CONCLUSIONS

1- Els astròcits expressen la isoforma muscular de la glicogen sintasa (MGS) i acumulen glicogen. Les neurones també expressen la MGS, però la mantenen inactivada per fosforilació i no acumulen glicogen en condicions normals.

2- L'expressió neuronal de MGS varia amb l'edat i entre els diferents subtipus cel·lulars. Les cèl·lules de Purkinje del cerebel i les interneurones PV+ de l'hipocamp són les neurones on l'expressió de MGS és més elevada.

3- L'increment dels nivells de PTG porta a l'activació de la MGS, l'acumulació de glicogen poc ramificat i l'activació del programa apoptòtic de neurones en cultiu.

4- El complex format per laforina i malina, les dues proteïnes que es troben mutades en la malaltia de Lafora, bloqueja l'acumulació de glicogen induïda per PTG en neurones mitjançant un mecanisme que implica la degradació proteasomal de MGS i PTG.

5- La deficiència genètica de malina recapitula la malaltia de Lafora en ratolí ja que els ratolins malina KO presenten acumulació de cossos de Lafora (LBs), neurodegeneració i problemes neurològics relacionats amb la malaltia.

6- Els astròcits i les interneurones PV+ de l'hipocamp, a més de MGS, també expressen malina. En els ratolins malina KO els dos tipus cel·lulars presenten LBs. Aquests resultats vinculen la formació de LBs amb l'alteració del funcionament de la maquinària del metabolisme del glicogen i demostren per primer cop la presència de LBs en astròcits.

7- L'acumulació de LBs en el soma de les interneurones PV+ de l'hipocamp va acompanyada per una marcada pèrdua d'aquest tipus cel·lular i per gliosi en aquesta zona del cervell, indicant que l'acumulació anòmala de glicogen en neurones està vinculada amb el procés neurodegeneratiu que té lloc en la malaltia de Lafora. La degeneració d'aquestes interneurones GABAèrgiques pot estar relacionada amb l'epilèpsia que caracteritza aquesta patologia.

8- L'acumulació de Corpora Amylacea (CA) durant el procés normal d'envelliment correlaciona amb una baixada de l'expressió de malina i té lloc a les mateixes zones del cervell que presenten LBs en els ratolins malina KO. Aquest fet suggereix que la formació dels dos tipus de cos de poliglucosà (PGBs) té lloc per l'alteració d'un mecanisme cel·lular comú on intervé la malina.

9- A més d'acumular-se en les mateixes zones cerebrals i d'estar formats principalment per poliglucosà, els CA i els LBs també coincideixen en la presència dels mateixos components

proteics, fet que corrobora un mecanisme comú de formació. Tant en els CA com en els LBs s'hi acumula: .

- MGS, laforina i altres components de la maquinària del metabolisme glicogen
- components relacionats amb processos d'estrès cel·lular i/o d'acumulació de proteïnes mal plegades
- proteïnes neuronals, entre elles la PV, que relaciona les interneurones GABAèrgiques amb la formació d'aquests dos tipus de PGBs.

10- Els astròcits interaccionen tant amb els CA com amb els LBs que es formen en els somes de les interneurones PV+ en un mecanisme que suggereix la transferència dels dos tipus de PGBs d'un tipus cel·lular a l'altre.

11- Els ratolins MGS KO no presenten acumulació de poliglucosà ni de cap dels components descrits en els CA. La MGS i, per tant, la síntesi de glicogen, és necessària per a la formació de CA. El poliglucosà actua com a matriu sense la qual la resta de components dels CA no s'acumulen.

INFORME SOBRE l'ÍNDEX D'IMPACTE I LA CONTRIBUCIÓ DEL DOCTORAND EN CADA ARTICLE

Article 1

Mechanism suppressing glycogen synthesis in neurons and its demise in progressive myoclonus epilepsy. Vilchez D, Ros S, Cifuentes D, Pujadas L, Vallès J, García-Fojeda B, Criado-García O, Fernández-Sánchez E, Medraño-Fernández I, Domínguez J, García-Rocha M, Soriano E, Rodríguez de Córdoba S, Guinovart JJ. (2007). *Nature Neuroscience 10*, 1407-1413.

Índex d'impacte: 14,191
Contribució del doctorand en l'article: el Jordi Vallès va dur a terme l'anàlisi de ramificació del glicogen i va participar en altres experiments.

Article 2

Neurodegeneration and functional impairments associated with glycogen synthase accumulation in a mouse model of Lafora disease. Valles-Ortega J*, Duran J*, Garcia-Rocha M, Bosch C, Saez I, Pujadas L, Serafin A, Cañas X, Soriano E, Delgado-García JM, Gruart A, Guinovart JJ. (2011). *EMBO Molecular Medicine 3(11)*, 667-681.

Índex d'impacte: 8,830
Contribució del doctorand en l'article: el Jordi Vallès va participar en el disseny i la coordinació de l'estudi, va dur a terme les anàlisis histològiques dels cervells i de ramificació del glicogen, va quantificar les interneurones PV+, va estudiar els paràmetres apoptòtics i va redactar la primera versió del manuscrit.

Article 3

Central role of Glycogen Synthase in Corpora Amylacea formation: similarities between Lafora disease and physiological aging. Valles-Ortega J, Duran, J, Márquez, M, Vilchez, D, Pujadas, L, Soriano, E, Pumarola, M, Guinovart JJ.

Pendent de publicació
Contribució del doctorand en l'article: el Jordi Vallès va concebre, dissenyar i coordinar el treball. Va dur a terme l'estudi del patró de d'expressió de MGS i malina en el cervell, va realitzar l'anàlisi per immunohistofluorescència i microscopia Confocal, la determinació d'AGEP i la tinció amb iode, va participar en la resta d'assajos histològics i va redactar el manuscrit.

ARTICLE ANNEX

El doctorand també ha contribuït en l'article següent (veure Annex), que no formava part dels objectius d'aquesta tesi:

Hepatic overexpression of a constitutively active form of liver glycogen synthase improves glucose homeostasis. Ros S, Zafra D, Valles-Ortega J, García-Rocha M, Forrow S, Domínguez J, Calbó J, Guinovart JJ. (2010). *The Journal of Biological Chemistry 26; 285(48)*, 37170-7.

> **Índex d'impacte**: 5,328
> **Contribució del doctorand en l'article**: el Jordi Vallès va dur a terme l'anàlisi de ramificació del glicogen.

El director de la Tesi

Dr. Joan J. Guinovart Cirera

BIBLIOGRAFIA

BIBLIOGRAFIA

Abe, H., and Yagishita, S. (1995). Massive appearance of corpora amylacea in postnatal anoxic encephalopathy. Clin Neuropathol *14*, 207-210.

Aguado, C., Sarkar, S., Korolchuk, V. I., Criado, O., Vernia, S., Boya, P., Sanz, P., de Cordoba, S. R., Knecht, E., and Rubinsztein, D. C. (2010). Laforin, the most common protein mutated in Lafora disease, regulates autophagy. Hum Mol Genet *19*, 2867-2876.

Aguzzi, A. (2009). Cell biology: Beyond the prion principle. Nature *459*, 924-925.

Armstrong, C. G., Browne, G. J., Cohen, P., and Cohen, P. T. (1997). PPP1R6, a novel member of the family of glycogen-targetting subunits of protein phosphatase 1. FEBS Lett *418*, 210-214.

Atsumi, T. (1981). The ultrastructure of intramuscular nerves in amyotrophic lateral sclerosis. Acta Neuropathol *55*, 193-198.

Averback, P. (1981). Parasynaptic corpora amylacea in the striatum. Arch Pathol Lab Med *105*, 334-335.

Baskaran, S., Roach, P. J., DePaoli-Roach, A. A., and Hurley, T. D. (2010). Structural basis for glucose-6-phosphate activation of glycogen synthase. Proc Natl Acad Sci U S A *107*, 17563-17568.

Belanger, M., Allaman, I., and Magistretti, P. J. (2011). Brain energy metabolism: focus on astrocyte-neuron metabolic cooperation. Cell Metab *14*, 724-738.

Berman, H. K., O'Doherty, R. M., Anderson, P., and Newgard, C. B. (1998). Overexpression of protein targeting to glycogen (PTG) in rat hepatocytes causes profound activation of glycogen synthesis independent of normal hormone- and substrate-mediated regulatory mechanisms. J Biol Chem *273*, 26421-26425.

Bittar, P. G., Charnay, Y., Pellerin, L., Bouras, C., and Magistretti, P. J. (1996). Selective distribution of lactate dehydrogenase isoenzymes in neurons and astrocytes of human brain. J Cereb Blood Flow Metab *16*, 1079-1089.

Bloom, W., and Fawcett, D. (1968). A Textbook of Histology, (Philadelphia, London, Toronto: W.B. Saunders Co).

Bollen, M. (2001). Combinatorial control of protein phosphatase-1. Trends Biochem Sci *26*, 426-431.

Botez, G., and Rami, A. (2001). Immunoreactivity for Bcl-2 and C-Jun/AP1 in hippocampal corpora amylacea after ischaemia in humans. Neuropathol Appl Neurobiol *27*, 474-480.

Bouche, C., Serdy, S., Kahn, C. R., and Goldfine, A. B. (2004). The cellular fate of glucose and its relevance in type 2 diabetes. Endocr Rev *25*, 807-830.

Bouskila, M., Hunter, R. W., Ibrahim, A. F., Delattre, L., Peggie, M., van Diepen, J. A., Voshol, P. J., Jensen, J., and Sakamoto, K. (2010). Allosteric regulation of glycogen synthase controls glycogen synthesis in muscle. Cell Metab *12*, 456-466.

Brady, D. R., and Mufson, E. J. (1997). Parvalbumin-immunoreactive neurons in the hippocampal formation of Alzheimer's diseased brain. Neuroscience *80*, 1113-1125.

Brown, A. M. (2004). Brain glycogen re-awakened. J Neurochem *89*, 537-552.

Brown, A. M., Baltan Tekkok, S., and Ransom, B. R. (2004). Energy transfer from astrocytes to axons: the role of CNS glycogen. Neurochem Int *45*, 529-536.

Brown, A. M., Tekkok, S. B., and Ransom, B. R. (2003). Glycogen regulation and functional role in mouse white matter. J Physiol *549*, 501-512.

Browner, M. F., Fauman, E. B., and Fletterick, R. J. (1992). Tracking conformational states in allosteric transitions of phosphorylase. Biochemistry *31*, 11297-11304.

Brundin, P., Melki, R., and Kopito, R. (2010). Prion-like transmission of protein aggregates in neurodegenerative diseases. Nat Rev Mol Cell Biol *11*, 301-307.

Cardell, R. R., Jr., Michaels, J. E., Hung, J. T., and Cardell, E. L. (1985). SERGE, the subcellular site of initial hepatic glycogen deposition in the rat: a radioautographic and cytochemical study. J Cell Biol *101*, 201-206.

Carling, D., and Hardie, D. G. (1989). The substrate and sequence specificity of the AMP-activated protein kinase. Phosphorylation of glycogen synthase and phosphorylase kinase. Biochim Biophys Acta *1012*, 81-86.

Castro, O. W., Furtado, M. A., Tilelli, C. Q., Fernandes, A., Pajolla, G. P., and Garcia-Cairasco, N. (2011). Comparative neuroanatomical and temporal characterization of FluoroJade-positive neurodegeneration after status epilepticus induced by systemic and intrahippocampal pilocarpine in Wistar rats. Brain Res *1374*, 43-55.

Cavanagh, J. B. (1999). Corpora-amylacea and the family of polyglucosan diseases. Brain Res Brain Res Rev *29*, 265-295.
Cavanagh, J. B., and Gysbers, M. F. (1983). Ultrastructural features of the Purkinje cell damage caused by acrylamide in the rat: a new phenomenon in cellular neuropathology. J Neurocytol *12*, 413-437.
Cavanagh, J. B., Nolan, C. C., and Brown, A. W. (1990). Glial cell intrusions actively remove detritus due to toxic chemicals from within nerve cells. Neurotoxicology *11*, 1-12.
Cohen, P., and Hardie, D. G. (1991). The actions of cyclic AMP on biosynthetic processes are mediated indirectly by cyclic AMP-dependent protein kinase. Biochim Biophys Acta *1094*, 292-299.
Crerar, M. M., Karlsson, O., Fletterick, R. J., and Hwang, P. K. (1995). Chimeric muscle and brain glycogen phosphorylases define protein domains governing isozyme-specific responses to allosteric activation. J Biol Chem *270*, 13748-13756.
Criado, O., Aguado, C., Gayarre, J., Duran, L., Garcia-Cabrero, A. M., Vernia, S., Millan, B. S., Heredia, M., Roma-Mateo, C., Mouron, S.*, et al.* (2011). Lafora bodies and neurological defects in malin-deficient mice correlate with impaired autophagy. Hum Mol Genet.
Champe, P., and Harvey, R. A. (1994). Lippincott's Illustrated Reviews: Biochemistry, (Philadelphia: Lippincott, Williams & Wilkins).
Cheng, A., Zhang, M., Gentry, M. S., Worby, C. A., Dixon, J. E., and Saltiel, A. R. (2007). A role for AGL ubiquitination in the glycogen storage disorders of Lafora and Cori's disease. Genes Dev *21*, 2399-2409.
Chin, L. S., Olzmann, J. A., and Li, L. (2010). Parkin-mediated ubiquitin signalling in aggresome formation and autophagy. Biochem Soc Trans *38*, 144-149.
Das, A., Balan, S., Mathew, A., Radhakrishnan, V., Banerjee, M., and Radhakrishnan, K. (2011). Corpora amylacea deposition in the hippocampus of patients with mesial temporal lobe epilepsy: A new role for an old gene? Indian J Hum Genet *17 Suppl 1*, S41-47.
del Río-Hortega, P. (1925). Papel de la microglía en la formación de los cuerpos amiláceos del tejido nervioso. Boletín de la Sociedad española de Historia Natural.
Delgado-Escueta, A. V. (2007). Advances in lafora progressive myoclonus epilepsy. Curr Neurol Neurosci Rep *7*, 428-433.
DePaoli-Roach, A. A., Tagliabracci, V. S., Segvich, D. M., Meyer, C. M., Irimia, J. M., and Roach, P. J. (2010). Genetic depletion of the malin E3 ubiquitin ligase in mice leads to lafora bodies and the accumulation of insoluble laforin. J Biol Chem *285*, 25372-25381.
Diaz, A., Martinez-Pons, C., Fita, I., Ferrer, J. C., and Guinovart, J. J. (2011). Processivity and subcellular localization of glycogen synthase depend on a non-catalytic high affinity glycogen-binding site. J Biol Chem *286*, 18505-18514.
Dinocourt, C., Petanjek, Z., Freund, T. F., Ben-Ari, Y., and Esclapez, M. (2003). Loss of interneurons innervating pyramidal cell dendrites and axon initial segments in the CA1 region of the hippocampus following pilocarpine-induced seizures. J Comp Neurol *459*, 407-425.
Doherty, M. J., Moorhead, G., Morrice, N., Cohen, P., and Cohen, P. T. (1995). Amino acid sequence and expression of the hepatic glycogen-binding (GL)-subunit of protein phosphatase-1. FEBS Lett *375*, 294-298.
Dringen, R., and Hamprecht, B. (1992). Glucose, insulin, and insulin-like growth factor I regulate the glycogen content of astroglia-rich primary cultures. J Neurochem *58*, 511-517.
Dumpitak, C., Beekes, M., Weinmann, N., Metzger, S., Winklhofer, K. F., Tatzelt, J., and Riesner, D. (2005). The polysaccharide scaffold of PrP 27-30 is a common compound of natural prions and consists of alpha-linked polyglucose. Biol Chem *386*, 1149-1155.
Ferrer, J. C., Baque, S., and Guinovart, J. J. (1997). Muscle glycogen synthase translocates from the cell nucleus to the cystosol in response to glucose. FEBS Lett *415*, 249-252.
Flotow, H., and Roach, P. J. (1989). Synergistic phosphorylation of rabbit muscle glycogen synthase by cyclic AMP-dependent protein kinase and casein kinase I. Implications for hormonal regulation of glycogen synthase. J Biol Chem *264*, 9126-9128.
Freemont, P. S. (2000). RING for destruction? Curr Biol *10*, R84-87.
Frost, B., and Diamond, M. I. (2010). Prion-like mechanisms in neurodegenerative diseases. Nat Rev Neurosci *11*, 155-159.
Fukuda, T., Roberts, A., Ahearn, M., Zaal, K., Ralston, E., Plotz, P. H., and Raben, N. (2006). Autophagy and lysosomes in Pompe disease. Autophagy *2*, 318-320.
Ganesh, S., Delgado-Escueta, A. V., Sakamoto, T., Avila, M. R., Machado-Salas, J., Hoshii, Y., Akagi, T., Gomi, H., Suzuki, T., Amano, K.*, et al.* (2002). Targeted disruption of the Epm2a gene

causes formation of Lafora inclusion bodies, neurodegeneration, ataxia, myoclonus epilepsy and impaired behavioral response in mice. Hum Mol Genet *11*, 1251-1262.
Garofalo, O., Kennedy, P. G., Swash, M., Martin, J. E., Luthert, P., Anderton, B. H., and Leigh, P. N. (1991). Ubiquitin and heat shock protein expression in amyotrophic lateral sclerosis. Neuropathol Appl Neurobiol *17*, 39-45.
Garyali, P., Siwach, P., Singh, P. K., Puri, R., Mittal, S., Sengupta, S., Parihar, R., and Ganesh, S. (2009). The malin-laforin complex suppresses the cellular toxicity of misfolded proteins by promoting their degradation through the ubiquitin-proteasome system. Hum Mol Genet *18*, 688-700.
Geddes, R., and Stratton, G. C. (1977). The influence of lysosomes on glycogen metabolism. Biochem J *163*, 193-200.
Gentry, M. S., Worby, C. A., and Dixon, J. E. (2005). Insights into Lafora disease: malin is an E3 ubiquitin ligase that ubiquitinates and promotes the degradation of laforin. Proc Natl Acad Sci U S A *102*, 8501-8506.
Jackson, M. C., Scollard, D. M., Mack, R. J., and Lenney, J. F. (1994). Localization of a novel pathway for the liberation of GABA in the human CNS. Brain Res Bull *33*, 379-385.
Jiang, S., Heller, B., Tagliabracci, V. S., Zhai, L., Irimia, J. M., DePaoli-Roach, A. A., Wells, C. D., Skurat, A. V., and Roach, P. J. (2010). Starch binding domain-containing protein 1/genethonin 1 is a novel participant in glycogen metabolism. J Biol Chem *285*, 34960-34971.
Jiang, S., Wells, C. D., and Roach, P. J. (2011). Starch binding domain protein 1 (Stbd1) and glycogen metabolism: Identification of the Atg8 family interacting motif (AIM) in Stbd1 required for interaction with GABARAPL1. Biochem Biophys Res Commun.
Kaganovich, D., Kopito, R., and Frydman, J. (2008). Misfolded proteins partition between two distinct quality control compartments. Nature *454*, 1088-1095.
Kawamura, T., Morioka, T., Nishio, S., Fukui, K., and Fukui, M. (2002). Temporal lobe epilepsy and corpora amylacea in the hippocampus: clinicopathologic correlation. Neurol Res *24*, 563-569.
Knecht, E., Aguado, C., Sarkar, S., Korolchuk, V. I., Criado-Garcia, O., Vernia, S., Boya, P., Sanz, P., Rodriguez de Cordoba, S., and Rubinsztein, D. C. (2010). Impaired autophagy in Lafora disease. Autophagy *6*, 991-993.
Korzhevskii, D. E., and Giliarov, A. V. (2007). [Demonstration of nuclear protein neun in the human brain corpora amylacea]. Morfologiia *131*, 75-76.
Lafora, G. R. (1913). Nuevas investigaciones sobre los cuerpos amiláceos del interior de las células nerviosas. Trab Lab Investi Biológ Univ Madrid *11*, 29-42.
Lafora, G. R., and Glueck, B. (1911). Beitrag zur Histopathologie der myoklonischen Epilepsie. Zeitschrift für die gesamte Neurologie und Psychiatrie *6*, 1-14.
Lee, S. J., Desplats, P., Sigurdson, C., Tsigelny, I., and Masliah, E. (2010). Cell-to-cell transmission of non-prion protein aggregates. Nat Rev Neurol *6*, 702-706.
Li, J. J., Surini, M., Catsicas, S., Kawashima, E., and Bouras, C. (1995). Age-dependent accumulation of advanced glycosylation end products in human neurons. Neurobiol Aging *16*, 69-76.
Li, X. J., and Li, S. (2011). Proteasomal dysfunction in aging and Huntington disease. Neurobiol Dis *43*, 4-8.
Liu, Y., Wang, Y., Wu, C., and Zheng, P. (2009). Deletions and missense mutations of EPM2A exacerbate unfolded protein response and apoptosis of neuronal cells induced by endoplasm reticulum stress. Hum Mol Genet *18*, 2622-2631.
Magistretti, P. J., and Allaman, I. (2007). Glycogen: a Trojan horse for neurons. Nat Neurosci *10*, 1341-1342.
Magistretti, P. J., Pellerin, L., Rothman, D. L., and Shulman, R. G. (1999). Energy on demand. Science *283*, 496-497.
Magistretti, P. J., Sorg, O., Yu, N., Martin, J. L., and Pellerin, L. (1993). Neurotransmitters regulate energy metabolism in astrocytes: implications for the metabolic trafficking between neural cells. Dev Neurosci *15*, 306-312.
Magloczky, Z., and Freund, T. F. (2005). Impaired and repaired inhibitory circuits in the epileptic human hippocampus. Trends Neurosci *28*, 334-340.
Marquez, M., Perez, L., Serafin, A., Teijeira, S., Navarro, C., and Pumarola, M. (2010). Characterisation of Lafora-like bodies and other polyglucosan bodies in two aged dogs with neurological disease. Vet J *183*, 222-225.
Mathews, C. K., and Van Holde, K. E. (1990). Biochemistry, (Redwood City, Calif.: Benjamin/Cummings Pub. Co.).

Matsui, T., Ishikawa, T., Ito, H., Okamoto, M., Inoue, K., Lee, M. C., Fujikawa, T., Ichitani, Y., Kawanaka, K., and Soya, H. (2011). Brain glycogen supercompensation following exhaustive exercise. J Physiol.

Mattson, M. P. (2000). Apoptosis in neurodegenerative disorders. Nat Rev Mol Cell Biol *1*, 120-129.

McDonald, T. D., Faust, P. L., Bruno, C., DiMauro, S., and Goldman, J. E. (1993). Polyglucosan body disease simulating amyotrophic lateral sclerosis. Neurology *43*, 785-790.

Minassian, B. A. (2002). Progressive myoclonus epilepsy with polyglucosan bodies: Lafora disease. Adv Neurol *89*, 199-210.

Mittal, S., Dubey, D., Yamakawa, K., and Ganesh, S. (2007). Lafora disease proteins malin and laforin are recruited to aggresomes in response to proteasomal impairment. Hum Mol Genet *16*, 753-762.

Montori-Grau, M., Guitart, M., Garcia-Martinez, C., Orozco, A., and Gomez-Foix, A. M. (2011). Differential pattern of glycogen accumulation after protein phosphatase 1 glycogen-targeting subunit PPP1R6 overexpression, compared to PPP1R3C and PPP1R3A, in skeletal muscle cells. BMC Biochem *12*, 57.

Munro, S., Ceulemans, H., Bollen, M., Diplexcito, J., and Cohen, P. T. (2005). A novel glycogen-targeting subunit of protein phosphatase 1 that is regulated by insulin and shows differential tissue distribution in humans and rodents. Febs J *272*, 1478-1489.

Nelson, S. R., Schulz, D. W., Passonneau, J. V., and Lowry, O. H. (1968). Control of glycogen levels in brain. J Neurochem *15*, 1271-1279.

Nielsen, J. N., Derave, W., Kristiansen, S., Ralston, E., Ploug, T., and Richter, E. A. (2001). Glycogen synthase localization and activity in rat skeletal muscle is strongly dependent on glycogen content. J Physiol *531*, 757-769.

Nolan, C. C., and Brown, A. W. (1989). Reversible neuronal damage in hippocampal pyramidal cells with triethyllead: the role of astrocytes. Neuropathol Appl Neurobiol *15*, 441-457.

Norio, R., and Koskiniemi, M. (1979). Progressive myoclonus epilepsy: genetic and nosological aspects with special reference to 107 Finnish patients. Clin Genet *15*, 382-398.

Olanow, C. W., and Prusiner, S. B. (2009). Is Parkinson's disease a prion disorder? Proc Natl Acad Sci U S A *106*, 12571-12572.

Olzmann, J. A., and Chin, L. S. (2008). Parkin-mediated K63-linked polyubiquitination: a signal for targeting misfolded proteins to the aggresome-autophagy pathway. Autophagy *4*, 85-87.

Ozen, H. (2007). Glycogen storage diseases: new perspectives. World J Gastroenterol *13*, 2541-2553.

Panza, G., Stohr, J., Birkmann, E., Riesner, D., Willbold, D., Baba, O., Terashima, T., and Dumpitak, C. (2008). Aggregation and amyloid fibril formation of the prion protein is accelerated in the presence of glycogen. Rejuvenation Res *11*, 365-369.

Parodi, A. J., Mordoh, J., Krisman, C. R., and Leloir, L. F. (1970). Action patterns of phosphorylase and glycogen synthetase on glycogen. Eur J Biochem *16*, 499-507.

Pfeiffer, B., Buse, E., Meyermann, R., and Hamprecht, B. (1995). Immunocytochemical localization of glycogen phosphorylase in primary sensory ganglia of the peripheral nervous system of the rat. Histochem Cell Biol *103*, 69-74.

Pfeiffer-Guglielmi, B., Fleckenstein, B., Jung, G., and Hamprecht, B. (2003). Immunocytochemical localization of glycogen phosphorylase isozymes in rat nervous tissues by using isozyme-specific antibodies. J Neurochem *85*, 73-81.

Pratt, W. B., Morishima, Y., Peng, H. M., and Osawa, Y. (2010). Proposal for a role of the Hsp90/Hsp70-based chaperone machinery in making triage decisions when proteins undergo oxidative and toxic damage. Exp Biol Med (Maywood) *235*, 278-289.

Printen, J. A., Brady, M. J., and Saltiel, A. R. (1997). PTG, a protein phosphatase 1-binding protein with a role in glycogen metabolism. Science *275*, 1475-1478.

Puri, R., and Ganesh, S. (2010). Laforin in autophagy: a possible link between carbohydrate and protein in Lafora disease? Autophagy *6*, 1229-1231.

Puri, R., Jain, N., and Ganesh, S. (2011a). Increased glucose concentration results in reduced proteasomal activity and the formation of glycogen positive aggresomal structures. FEBS J *278*, 3688-3698.

Puri, R., Suzuki, T., Yamakawa, K., and Ganesh, S. (2011b). Dysfunctions in endosomal-lysosomal and autophagy pathways underlie neuropathology in a mouse model for Lafora disease. Hum Mol Genet.

Raben, N., Danon, M., Lu, N., Lee, E., Shliselfeld, L., Skurat, A. V., Roach, P. J., Lawrence, J. C., Jr., Musumeci, O., Shanske, S., *et al.* (2001). Surprises of genetic engineering: a possible model of polyglucosan body disease. Neurology *56*, 1739-1745.

Radhakrishnan, A., Radhakrishnan, K., Radhakrishnan, V. V., Mary, P. R., Kesavadas, C., Alexander, A., and Sarma, P. S. (2007). Corpora amylacea in mesial temporal lobe epilepsy: clinico-pathological correlations. Epilepsy Res *74*, 81-90.

Rao, S. N., Maity, R., Sharma, J., Dey, P., Shankar, S. K., Satishchandra, P., and Jana, N. R. (2010a). Sequestration of chaperones and proteasome into Lafora bodies and proteasomal dysfunction induced by Lafora disease-associated mutations of malin. Hum Mol Genet *19*, 4726-4734.

Rao, S. N., Sharma, J., Maity, R., and Jana, N. R. (2010b). Co-chaperone CHIP stabilizes aggregate-prone malin, a ubiquitin ligase mutated in Lafora disease. J Biol Chem *285*, 1404-1413.

Ribeiro Mde, C., Barbosa-Coutinho, L., Mugnol, F., Hilbig, A., Palmini, A., da Costa, J. C., Paglioli Neto, E., and Paglioli, E. (2003). Corpora amylacea in temporal lobe epilepsy associated with hippocampal sclerosis. Arq Neuropsiquiatr *61*, 942-945.

Roach, P. J. (1990). Control of glycogen synthase by hierarchal protein phosphorylation. FASEB J *4*, 2961-2968.

Roach, P. J. (2002). Glycogen and its metabolism. Curr Mol Med *2*, 101-120.

Roach, P. J., Cao, Y., Corbett, C. A., DePaoli-Roach, A. A., Farkas, I., Fiol, C. J., Flotow, H., Graves, P. R., Hardy, T. A., Hrubey, T. W., and et al. (1991). Glycogen metabolism and signal transduction in mammals and yeast. Adv Enzyme Regul *31*, 101-120.

Roach, P. J., DePaoli-Roach, A. A., and Larner, J. (1978). Ca2+-stimulated phosphorylation of muscle glycogen synthase by phosphorylase b kinase. J Cyclic Nucleotide Res *4*, 245-257.

Roach, P. J., Takeda, Y., and Larner, J. (1976). Rabbit skeletal muscle glycogen synthase. I. Relationship between phosphorylation state and kinetic properties. J Biol Chem *251*, 1913-1919.

Robitaille, Y., Carpenter, S., Karpati, G., and DiMauro, S. D. (1980). A distinct form of adult polyglucosan body disease with massive involvement of central and peripheral neuronal processes and astrocytes: a report of four cases and a review of the occurrence of polyglucosan bodies in other conditions such as Lafora's disease and normal ageing. Brain *103*, 315-336.

Sakai, M., Austin, J., Witmer, F., and Trueb, L. (1969). Studies of corpora amylacea. I. Isolation and preliminary characterization by chemical and histochemical techniques. Arch Neurol *21*, 526-544.

Schiffer, D., Attanasio, A., Chio, A., Migheli, A., and Pezzulo, T. (1994). Ubiquitinated dystrophic neurites suggest corticospinal derangement in patients with amyotrophic lateral sclerosis. Neurosci Lett *180*, 21-24.

Schipper, H. M. (2011). Heme oxygenase-1 in Alzheimer disease: a tribute to Moussa Youdim. J Neural Transm *118*, 381-387.

Segers, K., Kadhim, H., Colson, C., Duttmann, R., and Glibert, G. (2011). Adult Polyglucosan Body Disease Masquerading as "ALS With Dementia of the Alzheimer Type": An Exceptional Phenotype in a Rare Pathology. Alzheimer Dis Assoc Disord.

Selmaj, K., Pawlowska, Z., Walczak, A., Koziolkiewicz, W., Raine, C. S., and Cierniewski, C. S. (2008). Corpora amylacea from multiple sclerosis brain tissue consists of aggregated neuronal cells. Acta Biochim Pol *55*, 43-49.

Sengupta, S., Badhwar, I., Upadhyay, M., Singh, S., and Ganesh, S. (2011). Malin and laforin are essential components of a protein complex that protects cells from thermal stress. J Cell Sci *124*, 2277-2286.

Shearer, J., and Graham, T. E. (2004). Novel aspects of skeletal muscle glycogen and its regulation during rest and exercise. Exerc Sport Sci Rev *32*, 120-126.

Shin, Y. S. (2006). Glycogen storage disease: clinical, biochemical, and molecular heterogeneity. Semin Pediatr Neurol *13*, 115-120.

Shulman, R. G., Bloch, G., and Rothman, D. L. (1995). In vivo regulation of muscle glycogen synthase and the control of glycogen synthesis. Proc Natl Acad Sci U S A *92*, 8535-8542.

Singh, S., and Ganesh, S. (2009). Lafora progressive myoclonus epilepsy: a meta-analysis of reported mutations in the first decade following the discovery of the EPM2A and NHLRC1 genes. Hum Mutat *30*, 715-723.

Singhrao, S. K., Morgan, B. P., Neal, J. W., and Newman, G. R. (1995). A functional role for corpora amylacea based on evidence from complement studies. Neurodegeneration *4*, 335-345.

Skurat, A. V., Wang, Y., and Roach, P. J. (1994). Rabbit skeletal muscle glycogen synthase expressed in COS cells. Identification of regulatory phosphorylation sites. J Biol Chem *269*, 25534-25542.

Stapleton, D., Nelson, C., Parsawar, K., McClain, D., Gilbert-Wilson, R., Barker, E., Rudd, B., Brown, K., Hendrix, W., O'Donnell, P., and Parker, G. (2010). Analysis of hepatic glycogen-associated proteins. Proteomics *10*, 2320-2329.

Steiner, J. A., Angot, E., and Brundin, P. (2011). A deadly spread: cellular mechanisms of alpha-synuclein transfer. Cell Death Differ *18*, 1425-1433.

Su, M., Shi, J. J., Yang, Y. P., Li, J., Zhang, Y. L., Chen, J., Hu, L. F., and Liu, C. F. (2011). HDAC6 regulates aggresome-autophagy degradation pathway of alpha-synuclein in response to MPP+-induced stress. J Neurochem *117*, 112-120.

Suzuki, A., Stern, S. A., Bozdagi, O., Huntley, G. W., Walker, R. H., Magistretti, P. J., and Alberini, C. M. (2011). Astrocyte-neuron lactate transport is required for long-term memory formation. Cell *144*, 810-823.

Tagliabracci, V. S., Girard, J. M., Segvich, D., Meyer, C., Turnbull, J., Zhao, X., Minassian, B. A., Depaoli-Roach, A. A., and Roach, P. J. (2008). Abnormal metabolism of glycogen phosphate as a cause for Lafora disease. J Biol Chem *283*, 33816-33825.

Tagliabracci, V. S., Heiss, C., Karthik, C., Contreras, C. J., Glushka, J., Ishihara, M., Azadi, P., Hurley, T. D., Depaoli-Roach, A. A., and Roach, P. J. (2011). Phosphate Incorporation during Glycogen Synthesis and Lafora Disease. Cell Metab *13*, 274-282.

Takahashi, H., Brasnjevic, I., Rutten, B. P., Van Der Kolk, N., Perl, D. P., Bouras, C., Steinbusch, H. W., Schmitz, C., Hof, P. R., and Dickstein, D. L. (2010). Hippocampal interneuron loss in an APP/PS1 double mutant mouse and in Alzheimer's disease. Brain Struct Funct *214*, 145-160.

Takahashi, K., Iwata, K., and Nakamura, H. (1977). Intra-axonal corpora amylacea in the CNS. Acta Neuropathol *37*, 165-167.

Tang, P. M., Bondor, J. A., Swiderek, K. M., and DePaoli-Roach, A. A. (1991). Molecular cloning and expression of the regulatory (RG1) subunit of the glycogen-associated protein phosphatase. J Biol Chem *266*, 15782-15789.

Thorens, B., Cheng, Z. Q., Brown, D., and Lodish, H. F. (1990). Liver glucose transporter: a basolateral protein in hepatocytes and intestine and kidney cells. Am J Physiol *259*, C279-285.

Turnbull, J., Depaoli-Roach, A. A., Zhao, X., Cortez, M. A., Pencea, N., Tiberia, E., Piliguian, M., Roach, P. J., Wang, P., Ackerley, C. A., and Minassian, B. A. (2011). PTG Depletion Removes Lafora Bodies and Rescues the Fatal Epilepsy of Lafora Disease. PLoS Genet *7*, e1002037.

Turnbull, J., Wang, P., Girard, J. M., Ruggieri, A., Wang, T. J., Draginov, A. G., Kameka, A. P., Pencea, N., Zhao, X., Ackerley, C. A., and Minassian, B. A. (2010). Glycogen hyperphosphorylation underlies lafora body formation. Ann Neurol *68*, 925-933.

Uchiki, T., Weikel, K. A., Jiao, W., Shang, F., Caceres, A., Pawlak, D., Handa, J. T., Brownlee, M., Nagaraj, R., and Taylor, A. (2011). Glycation-altered proteolysis as a pathobiologic mechanism that links dietary glycemic index, aging, and age-related disease (in nondiabetics). Aging Cell.

Vannucci, S. J., Maher, F., and Simpson, I. A. (1997). Glucose transporter proteins in brain: delivery of glucose to neurons and glia. Glia *21*, 2-21.

Vernia, S., Rubio, T., Heredia, M., Rodriguez de Cordoba, S., and Sanz, P. (2009). Increased endoplasmic reticulum stress and decreased proteasomal function in lafora disease models lacking the phosphatase laforin. PLoS One *4*, e5907.

Villar-Palasi, C., and Guinovart, J. J. (1997). The role of glucose 6-phosphate in the control of glycogen synthase. FASEB J *11*, 544-558.

Wang, J., Stuckey, J. A., Wishart, M. J., and Dixon, J. E. (2002). A unique carbohydrate binding domain targets the lafora disease phosphatase to glycogen. J Biol Chem *277*, 2377-2380.

Wilhelmus, M. M., Verhaar, R., Bol, J. G., van Dam, A. M., Hoozemans, J. J., Rozemuller, A. J., and Drukarch, B. (2011). Novel role of transglutaminase 1 in corpora amylacea formation? Neurobiol Aging *32*, 845-856.

Wilson, W. A., Skurat, A. V., Probst, B., de Paoli-Roach, A., Roach, P. J., and Rutter, J. (2005). Control of mammalian glycogen synthase by PAS kinase. Proc Natl Acad Sci U S A *102*, 16596-16601.

Worby, C. A., Gentry, M. S., and Dixon, J. E. (2008). Malin decreases glycogen accumulation by promoting the degradation of protein targeting to glycogen (PTG). J Biol Chem *283*, 4069-4076.

Yan, S. D., Yan, S. F., Chen, X., Fu, J., Chen, M., Kuppusamy, P., Smith, M. A., Perry, G., Godman, G. C., Nawroth, P., and et al. (1995). Non-enzymatically glycated tau in Alzheimer's disease induces neuronal oxidant stress resulting in cytokine gene expression and release of amyloid beta-peptide. Nat Med *1*, 693-699.

ANNEX

THE JOURNAL OF BIOLOGICAL CHEMISTRY VOL. 285, NO. 48, pp. 37170–37177, November 26, 2010

Hepatic Overexpression of a Constitutively Active Form of Liver Glycogen Synthase Improves Glucose Homeostasis*

Received for publication, June 23, 2010, and in revised form, August 12, 2010 Published, JBC Papers in Press, September 14, 2010, DOI 10.1074/jbc.M110.157396

Susana Ros[‡§¶1], Delia Zafra[‡§], Jordi Valles-Ortega[‡§1], Mar García-Rocha[‡§], Stephen Forrow[‡], Jorge Domínguez[‡§], Joaquim Calbó[‡§], and Joan J. Guinovart[‡§¶2]

From the [‡]Institute for Research in Biomedicine, the [§]CIBER de Diabetes y Enfermedades Metabólicas, and the [¶]Department of Biochemistry and Molecular Biology, University of Barcelona, Baldiri Reixac 10, E-08028 Barcelona, Spain

In this study, we tested the efficacy of increasing liver glycogen synthase to improve blood glucose homeostasis. The overexpression of wild-type liver glycogen synthase in rats had no effect on blood glucose homeostasis in either the fed or the fasted state. In contrast, the expression of a constitutively active mutant form of the enzyme caused a significant lowering of blood glucose in the former but not the latter state. Moreover, it markedly enhanced the clearance of blood glucose when fasted rats were challenged with a glucose load. Hepatic glycogen stores in rats overexpressing the activated mutant form of liver glycogen synthase were enhanced in the fed state and in response to an oral glucose load but showed a net decline during fasting. In order to test whether these effects were maintained during long term activation of liver glycogen synthase, we generated liver-specific transgenic mice expressing the constitutively active LGS form. These mice also showed an enhanced capacity to store glycogen in the fed state and an improved glucose tolerance when challenged with a glucose load. Thus, we conclude that the activation of liver glycogen synthase improves glucose tolerance in the fed state without compromising glycogenolysis in the postabsorptive state. On the basis of these findings, we propose that the activation of liver glycogen synthase may provide a potential strategy for improvement of glucose tolerance in the postprandial state.

The liver responds to an increase in blood glucose concentration in the postprandial state by net uptake of glucose and conversion to glycogen, which is subsequently mobilized in the postabsorptive state to maintain blood glucose homeostasis. Various attempts have been made to improve blood glucose homeostasis through the modulation of the expression or activity of proteins involved in the control of liver glycogen metabolism. Glucokinase (GK)[3] catalyzes the first step in hepatic glucose metabolism and exerts high control on liver glycogen synthesis (1). Previous studies using either transgenic models (2, 3) or adenoviral vectors targeting the liver (4) demonstrated improved glucose tolerance and/or a lowering of blood glucose in basal conditions. However, GK overexpression also increases flux through glycolysis, and in some circumstances this leads to hypertriglyceridemia (4).

An alternative approach to modulating liver glycogen metabolism without stimulating glycolysis and triglyceride formation is through modifying the enzymes that are involved exclusively in glycogen synthesis and degradation or regulatory proteins that may affect the activity of the former, such as protein targeting to glycogen (PTG) (5). Overexpression of PTG in the liver by means of an adenoviral vector increases glucose tolerance without perturbing lipid homeostasis (6). However, a limitation of this experimental model is that it leads to the progressive accumulation of glycogen because PTG promotes the inactivation of glycogen phosphorylase (GP) also during fasting, and consequently there is negligible depletion of glycogen in the postabsorptive state and during a prolonged fast. Similarly, G_L targeting subunit overexpression in the livers of streptozotocin-induced diabetic rats causes a large increase in liver glycogen stores but only a transient decrease in blood glucose levels. The glycemia-reducing effect can be prolonged in time by using a truncated version of the scaffolding proteins G_M and G_L, termed $G_M\Delta C$, which does not compromise the response to glycogenolytic signals (7–9).

Another approach is the use of inhibitors of GP, which promote the dephosphorylation of the enzyme (conversion of GPa to GPb) and the subsequent activation of glycogen synthase (GS) (10, 11). GP inhibitors reduce blood glucose in animal models of diabetes and improve glucose tolerance in the postprandial state. An alternative strategy has been to selectively modify the interaction between GPa and the glycogen-targeting protein G_L by mutating the terminal GPa binding domain or by using small molecules that prevent the interaction of GPa with G_L (12). In this way, the negative control exerted by GPa on LGS activation is released without altering the activation state of GPa.

A common end point of all of the above strategies is that they aim to induce the activation of liver GS (LGS) through indirect mechanisms. However, to date, the strategy of directly activating LGS, independently of the rate of glucose phosphorylation or the activation state of GP, to regulate blood glucose homeostasis has not been addressed.

* This work was supported by Ministry of Education and Science, Spain, Grants BFU2005-02253 and SAF2007-64722, Autonomous Government of Catalonia Grant 2005-SGR-00570, and a grant from the Fundación Marcelino Botín. The CIBER de Diabetes y Enfermedades Metabólicas Asociadas is an ISCIII project.

[1] Recipient of a predoctoral fellowship from the Spanish government.

[2] To whom correspondence should be addressed: Inst. for Research in Biomedicine, Barcelona Science Park, Baldiri Reixac 10-12, E-08028 Barcelona, Spain. Tel.: 34-934037163; E-mail: guinovart@irbbarcelona.org.

[3] The abbreviations used are: GK, glucokinase; GP, glycogen phosphorylase; GS, glycogen synthase; LGS, liver glycogen synthase; NEFA, non-esterified fatty acid; BHBA, 3-hydroxybutyrate; PEPCK, phosphoenolpyruvate carboxykinase; PTG, protein targeting to glycogen; IPGTT, intraperitoneal glucose tolerance test.

To this end, we examined the impact of the adenovirus-mediated overexpression of wild-type LGS and a constitutively active LGS variant (13) on livers of healthy rats. In addition, we generated liver-specific transgenic mice expressing the activated mutant LGS. Using these approaches, we have demonstrated the relevance of the phosphorylation state of LGS in the control of blood glucose homeostasis and in the regulation of hepatic glycogen storage.

EXPERIMENTAL PROCEDURES

Preparation of Recombinant Adenoviruses—Recombinant adenoviruses encoding for the bacterial enzyme β-galactosidase (β-gal), wild-type *Rattus norvegicus* LGS (WT LGS) (14), or a constitutively active *Rattus norvegicus* LGS variant mutated at phosphorylation sites 2 and 3b (activated mutant LGS) (13) were amplified and purified for injection into animals, following procedures described previously (15).

Animal Studies—All procedures were approved by the Barcelona Science Park's Animal Experimentation Committee and were carried out in accordance with the European Community Council Directive and National Institutes of Health guidelines for the care and use of laboratory animals.

Rat Studies—Male Wistar rats (Charles River Laboratories) weighing 200–250 g were housed for 1 week before any procedure and were allowed free access to water and standard laboratory chow (Harlan Tekland Laboratory diet 7001). After procedures, the rats were caged individually under a standard 12-h light/12-h dark cycle to allow monitoring of food and water intake. Two experimental protocols were performed. In the first, rats were anesthetized with 2% isofluorane (Isoba vet, Schering Plough) and infused with 1×10^{12} particles of activated mutant LGS-, WT LGS-, or β-gal-encoding purified adenoviruses. 96 h after adenovirus administration, animals were either fasted for 18 h or allowed to continue to feed *ad libitum*. In the second protocol, animals were infused with the same titer of adenovirus, and after 96 h, they were fasted for 18 h. This was followed by an intraperitoneal glucose injection (intraperitoneal glucose tolerance test (IPGTT); 2 g/kg body weight). Blood samples from the tail vein were collected immediately before administration of the bolus and at the time intervals indicated in order to measure circulating glucose concentrations. In all procedures, tissue samples were obtained from anesthetized animals (sodium thiopental (Tiobarbital Braun), 0.1 g/kg body weight intraperitoneally), rapidly snap-frozen in liquid nitrogen, and stored at −80 °C for further analysis.

Transgenic Mouse Generation and Studies—The *Mus musculus Gys2* cDNA sequence (clone ID 5051685, pCMV-SPORT6 vector, Invitrogen) previously mutated at sites 2 and 3b (Ser → Ala mutations, by site-directed mutagenesis using the following primers: for site 2, GCCGCTCCTTGCCGGTGACATCCCTTG (sense) and CAAGGGATGTCACCGGCAAGGAGCGGC (antisense); site 3b, GCTTTAAGTATCCCAGGCCCTCCGCAGTACCACC (sense) and GGTGGTACTGCGGAGGGCCTGGGATACTTAAAGC (antisense), respectively) was subcloned between the intron II of the rabbit β-globin gene and the rabbit β-globin and SV40 polyadenylation signals of the pSG5 plasmid (a generous gift from Dr. P. Chambon, Université Louis Pasteur). This fragment was then subcloned into the EcoRV site of the p2335-1 plasmid (a generous gift from Dr. K. Khono, Nara Institute of Science and Technology), which contains the mouse albumin enhancer/promoter, generating the palbpSG5MmLGS-2 + 3b vector. A 5-kb NotI/SalI digestion fragment was excised, microdialyzed, and microinjected into the pronuclei of fertilized mouse eggs (C57BL/6J × C57BL/6J) at the Mouse Mutant Core Facility, Institute for Research in Biomedicine (Barcelona, Spain). Embryos were implanted into pseudopregnant foster females (ICR), and transgenic pups were identified. DNA samples from tail clips of subsequent litters were screened by PCR with primers (forward, ATCCCCCGGGCTGCAGGAAT; reverse, GCACGTTGCCCAGGAGCTGT) that amplified a 638-bp fragment of the transgene. The transgene was maintained on the C57BL/6J background throughout the study. Transgenic and wild-type mice were allowed free access to a standard chow diet and water and maintained on a 12-h/12-h light/dark cycle under specific pathogen-free conditions in the Animal Research Center at the Barcelona Science Park. After weaning at 3 weeks of age, tail clippings were taken for genotyping by PCR. Glucose tolerance tests were carried out using 20-week male mice after fasting by injecting 2 g/kg glucose intraperitoneally. Glucose levels were measured from tail bleeds at 0, 5, 15, 30, 60, 90, and 120 min. For the determination of liver glycogen content and LGS activity and expression, fed and 18 h-fasted male mice were given a lethal dose of anesthesia (sodium thiopental (Tiobarbital Braun), 0.2 g/kg body weight intraperitoneally), and tissues were rapidly snap-frozen in liquid nitrogen and stored at −80 °C for further analyses.

Enzyme Activity and Metabolite Determination—To measure GS activity, tissue samples (100 mg) were added to 1 ml of ice-cold homogenization buffer containing 10 mM Tris-HCl (pH 7), 150 mM KF, 15 mM EDTA, 15 mM 2-mercaptoethanol, 0.6 M sucrose, 1 mM benzamidine, 1 mM phenylmethanesulfonyl fluoride, 25 nM okadaic acid, 10 μg/ml leupeptin, 10 μg/ml aprotinin, and 10 μg/ml pepstatin and were then homogenized (Polytron) at 4 °C. GS activity was measured in whole homogenates in the absence or presence of 6.6 mM glucose 6-phosphate, representing active or total activity, respectively (16). The −/+ glucose 6-phosphate activity ratio is an estimation of the activation state of the enzyme.

Electrophoresis and Immunoblotting—Immunoreactivity was determined by resolving homogenates (20 μg of protein) by 10% SDS-PAGE. The protein was transferred onto a nitrocellulose membrane and probed with the following antibodies: a rabbit antibody against rat LGS (17), a mouse antibody against glyceraldehyde-3-phosphate dehydrogenase (GAPDH; Sigma), and a mouse antibody against actin (Sigma). Secondary antibodies conjugated to horseradish peroxidase against rabbit (GE Healthcare) or mouse (DakoCytomation) immunoglobulins were used. Immunoreactive bands were visualized using an ECL Plus kit (GE Healthcare), following the manufacturer's instructions.

Blood Parameters—Blood glucose was measured using a HemoCue glucose analyzer (HemoCue AB, Angelholm, Sweden). Plasma aspartate-aminotransferase activity was measured spectrophotometrically by standard techniques (HORIBA ABX) adapted to a COBAS Mira analyzer (Roche Applied Science). Only

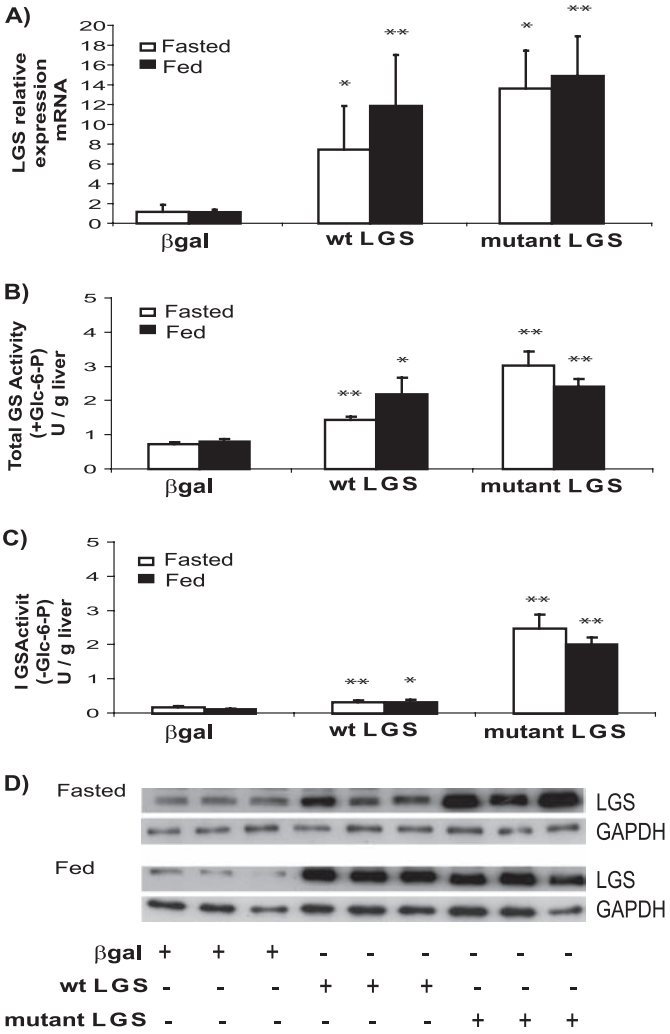

FIGURE 1. **Effects of the overexpression of WT LGS or activated mutant LGS on hepatic GS activity in rat liver.** *A*, RT-PCR analysis of LGS mRNA levels in livers of rats overexpressing β-gal, WT LGS, or a constitutively active mutant LGS form (mutant LGS). *B*, total GS activity (units (*U*)/g of liver) of liver homogenates from fasted (*white bars*) or fed (*black bars*) rats overexpressing β-gal, WT LGS, or mutant LGS. *C*, GS activity (units/g of liver) calculated in the absence of glucose 6-phosphate. In all cases (*A–C*), data represent the mean ± S.E. (*error bars*) of the following: seven fasted and seven fed β-gal-overexpressing rats; five fasted and six fed WT LGS-overexpressing rats; and five fasted and five fed mutant LGS-overexpressing rats. * or **, statistical difference for comparisons with β-gal group at the same metabolic state with $p < 0.05$ or $p < 0.005$, respectively. *D*, representative Western blot analysis of three liver extracts of fasted or fed rats with antibodies against LGS or GAPDH as a load control. In all cases, 20 μg of protein were analyzed per lane.

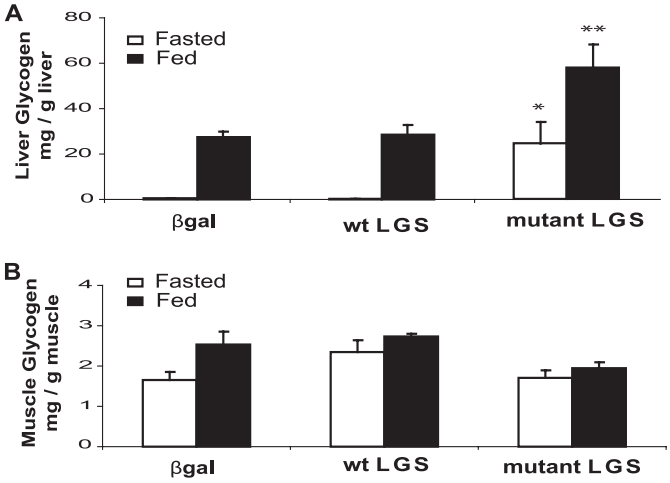

FIGURE 2. **Effects of the overexpression of WT LGS and activated mutant LGS on glycogen content in rat liver and muscle.** *A*, liver glycogen content (mg/g of liver) measured in rats overexpressing β-gal, WT LGS, or mutant LGS. *B*, muscle glycogen content (mg/g of muscle) determined in the same animals. In all cases, data represent the mean ± S.E. (*error bars*) of the following: seven fasted and seven fed β-gal-overexpressing rats; five fasted and six fed WT LGS-overexpressing rats; and five fasted and five fed mutant LGS-overexpressing rats. * or **, statistical difference for comparisons with β-gal group at the same metabolic state with $p < 0.05$ or $p < 0.005$, respectively.

animals with blood plasma aspartate aminotransferase concentrations lower than 200 units/liter (indicative of the absence of virus-induced liver damage) were used for further study (18). Plasma lactate (HORIBA ABX), triglycerides (Sigma), and 3-hydroxybutyrate (BHBA; Sigma) concentrations were measured spectrophotometrically by standard techniques adapted to a COBAS Mira analyzer. Plasma non-esterified fatty acids (NEFAs; Wako) were measured by colorimetric determination adapted to a Freedom Evo Tekan analyzer. Plasma insulin levels were measured by immunoassay (Spi Bio).

RNA Purification and Retrotranscription—Total RNA was isolated from rat liver tissue by homogenizing (Polytron) 100 mg of the sample in 1 ml of TRIzol (Invitrogen). After centrifugation at 12,000 × *g* for 5 min, 0.2 ml of chloroform was added to the supernatant, and it was then centrifuged again at 12,000 × *g* for 15 min at 4 °C to separate it into two phases. Adding 0.5 ml of isopropyl alcohol to the aqueous phase then precipitated total RNA. After an incubation of 10 min at room temperature, samples were centrifuged at 12,000 × *g* for 10 min at 4 °C. Pellets were washed with 1 ml of 70% ethanol and centrifuged at 7500 × *g* for 5 min at 4 °C. The desiccated pellets were resuspended in 100 μl of RNase-free water. 5 μg of total RNA from each sample was reverse-transcribed for 50 min at 42 °C in a 15-ml reaction volume using 200 units of SuperScript III reverse transcriptase (SuperScript First-strand Synthesis System for RT-PCR, Invitrogen) in the presence of 50 ng of random hexamers.

Quantitative Real-time PCR—PCR tests were performed following the standard real-time PCR protocol of the ABI Prism 7900 Detection System, together with the appropriate ready-made TaqMan primer/probe sets (Applied Biosystems) at the Genomic Unit of Core Scientific Services at the University of Barcelona. Each sample was analyzed from triplicate wells. The temperature profile consisted of 40 cycles of 15 s at 95 °C and 1 min at 60 °C. Data were analyzed with the $2^{\Delta\Delta Ct}$ method using 18 S rRNA as endogenous control.

Glycogen Analysis—Liver glycogen content was determined by an amyloglucosidase-based assay (19). To assess glycogen branching, the method described by Krisman (20) was used.

Electron Microscopy Analysis—Rat liver biopsies were fixed in 2.5% glutaraldehyde solution for 24 h, rinsed in Sorensen's phosphate buffer, and postfixed in 1% osmium tetroxide in Sorensen's phosphate buffer. The fixed tissue was dehydrated in an ascending series of graded ethanol solutions. It was then rinsed with propylene oxide, embedded in Eponate 12, and polymerized at 60 °C for more than 48 h. Thin sections were prepared with a diamond knife on an Leica Ultracut UCT ultratome at the Electron Microscopy Unit of the Core Scientific

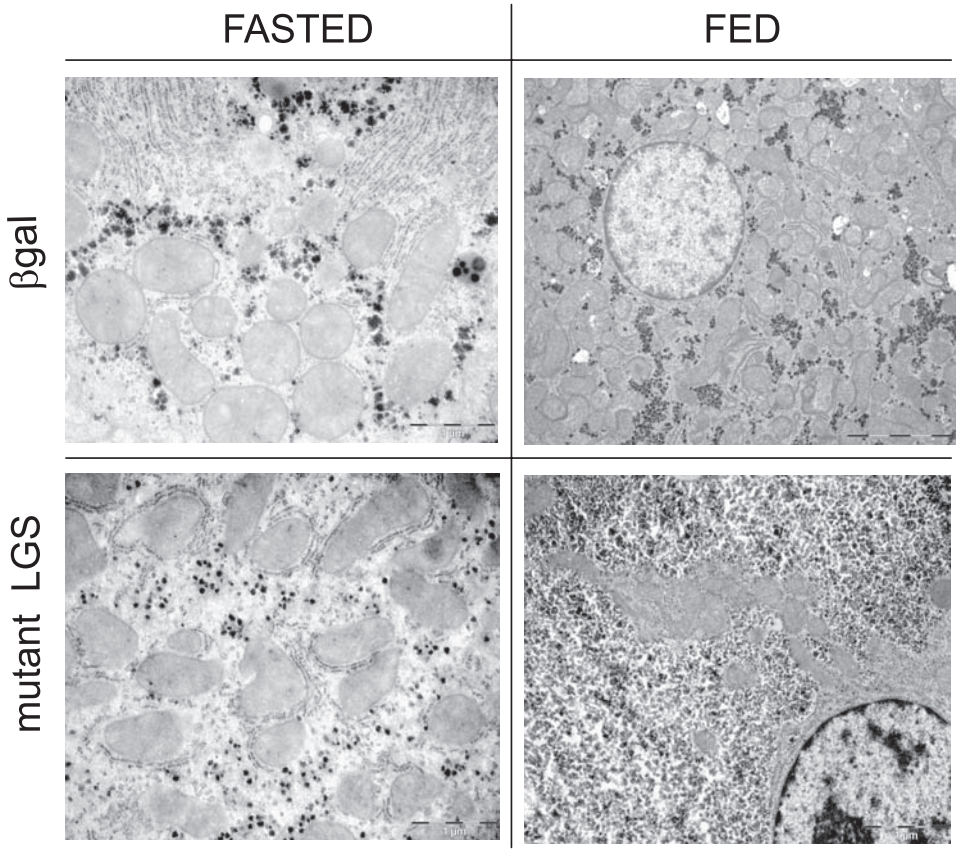

FIGURE 3. **Effects of activated mutant LGS overexpression on ultracellular structure as shown by electron microscopy analysis of rat liver sections.** Cellular ultrastructure analysis by electron microscopy of liver biopsies from the rats overexpressing β-gal or the constitutively active mutant form of LGS, fasted for 18 h or fed *ad libitum*. *Scale bar*, 5 μm (fed rats) or 1 μm (fasted rats).

TABLE 1

Degree of branching of liver glycogen isolated from fed rats

Glycogen samples isolated from the livers of fed rats were complexed with iodine, and spectra were recorded to measure the degree of branching of the accumulated glycogen. Results are expressed as the mean ± S.E. of four β-gal- overexpressing rats, four WT LGS-overexpressing rats, four activated mutant-LGS-overexpressing rats. Commercial rabbit liver glycogen and commercial corn amylopectin were used as controls for high and low degree of branching, respectively.

Polysaccharide	λ_{max} (20)
β-gal liver glycogen	490 ± 2
WT LGS liver glycogen	493 ± 2
Mutant LGS liver glycogen	502 ± 7
Rabbit liver glycogen	491 ± 2
Starch amylopectin	563 ± 4[a]

[a] Statistical difference for comparisons with mutant LGS group with $p < 10^{-6}$.

Services at the University of Barcelona, and sections were then collected on copper grids. Sections were then stained with 2% uranyl acetate in water and lead citrate solution. Cell structure was assessed by transmission electron microscopy JEM-1010 (Jeol).

Immunocytofluorescence—Liver biopsies were fixed in a 4% paraformaldehyde solution for 24 h. Cryoprotection was done by increasing saccharose gradients up to 30% in PBS solution. Liver was then frozen in the presence of water-soluble glycols and resins (Tissue-Tek O.C.T. compound, Sakura). Cryostat sections (10 μm, Leica CM1900) were washed with PBS and permeabilized for 20 min with 0.2% (v/v) Triton X-100 (in PBS). After 10 min of blocking with 3% BSA (w/v in PBS), incubation with the primary antibody against rat total LGS (in PBS) was done for 12 h at 4 °C. After washing with PBS, sections were incubated with the secondary antibody (Texas Red-conjugated donkey and rabbit IgG, Jackson) for 2 h at room temperature. They were then washed with PBS and mounted onto glass slides using Mowiol (Sigma).

Statistical Analysis—Data are expressed as mean ± S.E. Statistical significance was determined by unpaired Student's *t* test using Microsoft Excel (version XP; Microsoft Corp., Redmond, WA). Statistical significance was assumed at $p \leq 0.05$.

RESULTS

Overexpression of WT LGS and Activated Mutant LGS in Rat Liver—Rats were injected with adenovirus encoding for either WT LGS or a constitutively active LGS mutant form (mutations Ser → Ala at 2 and 3b phosphorylation sites, activated mutant LGS), and the control group was injected with adenovirus coding for β-gal. After 96 h postinjection, animals were subdivided into two groups, one of which was submitted to an 18-h fast while the other was allowed to feed *ad libitum*. The efficiency of adenovirus transfection in liver was confirmed by the significant increase in mRNA expression (Fig. 1*A*) and LGS immunoreactivity and total GS activity (Fig. 1, *B* and *D*) in both the WT LGS and activated mutant LGS groups compared with the control. Active GS (measured in the absence of glucose 6-phosphate) was only moderately increased in the group overexpressing WT LGS but was markedly increased in the activated mutant LGS-overexpressing group (Fig. 1*C*). There was no detectable immunoreactivity to LGS in adipose tissue, pancreas, kidney, testes, lung, or skeletal muscle (data not shown), thereby confirming preferential transgene delivery to liver, in agreement with previous studies (21, 22).

Effects on Liver Glycogen in Fasted and Fed Rats—Liver glycogen content in the fed rats was enhanced ~2-fold in the activated mutant LGS group but was unchanged in the WT LGS one (Fig. 2*A*), despite similar levels of total GS activity and protein in the two groups (Fig. 1, *B* and *D*). In the fasted state, the glycogen content of the activated mutant LGS-overexpressing group was decreased compared with the fed state, thereby indicating net mobilization of liver glycogen. Transmission electron microscopy confirmed a higher cytoplasmic glycogen content in the livers of rats overexpressing the activated mutant LGS compared with controls but did not show any other structural changes (Fig. 3). Furthermore, glycogen isolated from liver of the former group was normally branched (Table 1). Addi-

TABLE 2

Blood parameters in rats overexpressing β-gal, WT LGS, or activated mutant LGS

After sacrificing the animals, blood samples were taken to measure the metabolites and hormones indicated. Glucose was measured in whole blood, whereas the rest of the parameters were determined in plasma. In all cases, data represent the mean ± S.E. of the following: seven fasted and seven fed β-gal-overexpressing rats; five fasted and six fed WT LGS-overexpressing rats; and five fasted and five fed mutant LGS-overexpressing rats. ND, not determined; TG, triglycerides.

	Fasted			Fed		
	β-gal	WT LGS	Mutant LGS	β-gal	WT LGS	Mutant LGS
Glucose (mg/dl)	68 ± 3	73 ± 4	84 ± 8	124 ± 5	115 ± 6	96 ± 3[a]
Insulin (ng/ml)	0.4 ± 0.2	ND	0.5 ± 0.2	1.4 ± 0.3	ND	1.1 ± 0.4
TG (mg/dl)	99 ± 12	71 ± 8	104 ± 15	146 ± 23	120 ± 21	183 ± 46
Lactate (mg/dl)	35 ± 4	26 ± 5	28 ± 1	45 ± 7	67 ± 19	55 ± 9
NEFAs (mmol/liter)	0.12 ± 0.02	ND	0.10 ± 0.01	0.02 ± 0.01	ND	0.06 ± 0.03
BHBA (mg/dl)	19 ± 4	23 ± 1	8 ± 3[a]	2.2 ± 0.6	4.3 ± 0.9	3.3 ± 0.3

[a] Significant differences relative to β-gal-overexpressing rats, with $p < 0.05$.

tionally, there was no difference in muscle glycogen content between the experimental and control groups (Fig. 2*B*).

Effects on Blood Parameters in Fasted and Fed Rats—We examined the impact of LGS expression on the concentration of glucose and other metabolites in the blood. In the fed state, blood glucose concentrations were slightly decreased in the activated mutant LGS group but not in the WT LGS group, whereas plasma triglycerides and other blood metabolites were unchanged (Table 2); nor was plasma insulin altered with respect to controls. In the fasted state, there were no differences in glycemia; however, the concentration of plasma BHBA was significantly decreased in the activated mutant LGS group.

Expression of GP, GK, PEPCK, and GLUT2 in Fasted and Fed Rats—We tested whether the overexpression of LGS and/or the increased accumulation of glycogen caused secondary changes in the expression of key players of hepatic glucose metabolism. The mRNA levels of GK, GLUT2, PEPCK, and GP were determined by quantitative real-time PCR. Although fasting caused the expected decrease in GK expression and increase in PEPCK expression (23) (Fig. 4*A*), there were no further significant differences in the mRNA levels of these genes caused by activated mutant LGS overexpression when compared with the other experimental groups in the same nutritional state (Fig. 4, *B* and *C*).

Intraperitoneal Glucose Tolerance Test—To further study the effects of WT or activated mutant LGS overexpression on blood glucose homeostasis, we performed an IPGTT to a new group of rats. 96 h after postadenoviral injection, rats were subjected to an 18-h fast and were then given an intraperitoneal glucose load (2 g/kg body weight). Blood glucose concentration determined between 15 min and 3 h after the glucose load was markedly diminished in the activated mutant LGS group compared with the β-gal and WT LGS groups, with a decrease in area under the curve of 30% (Fig. 5*A*). Liver glycogen content of β-gal or WT LGS-overexpressing rats showed a marked increase at the final point of the IPGTT (180 min) compared with that for β-gal-overexpressing fasted rats (Fig. 5*B*, *inset*). Overexpression of activated mutant LGS resulted in a much larger increase in the storage of this polymer compared with the other groups (Fig. 5*B*). Similarly, only activated mutant LGS-overexpressing animals showed significantly improved glucose tolerance. Several blood parameters were measured upon ending the test. There was no difference in the concentrations of insulin, lactate, or triglycerides between the experimental groups and the controls (Table 3). However, plasma BHBA concentrations were significantly decreased in the activated mutant LGS group, similar to the changes observed in the fasted activated mutant LGS-overexpressing rats (Table 2).

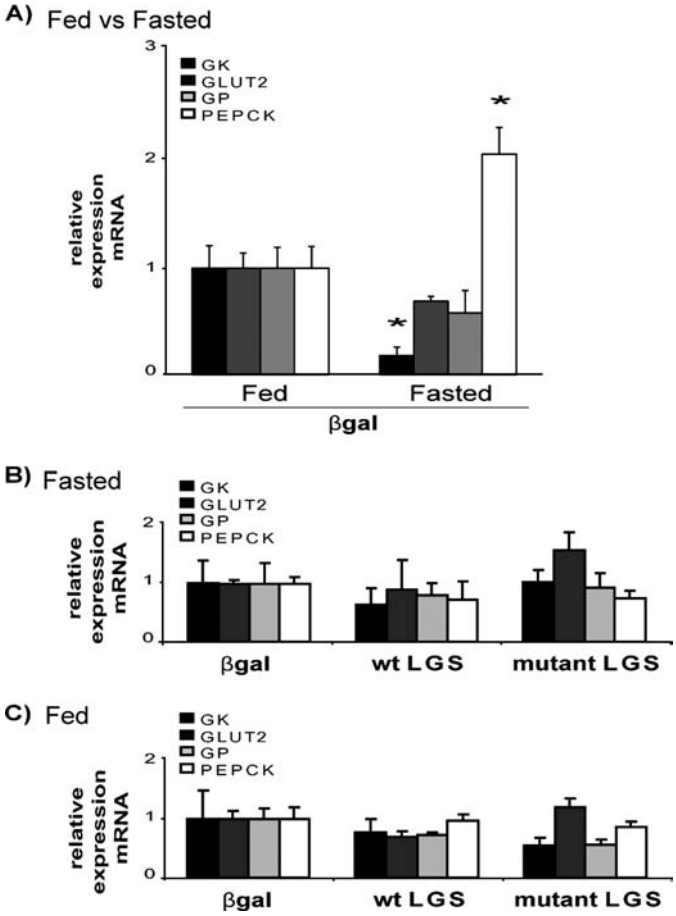

FIGURE 4. **Effects of the overexpression of WT LGS and activated mutant LGS on glucokinase, GLUT2, glycogen phosphorylase, and phosphoenolpyruvate carboxykinase expression levels in rat liver.** *A*, RT-PCR analysis of liver GK, GLUT2, GP, and PEPCK mRNA levels in livers of fed and fasted rats overexpressing β-gal; data are relative to the fed β-gal group. *B*, RT-PCR analysis in fasted overexpressing β-gal, WT LGS, or mutant LGS rats; data are relative to the fasted β-gal group of rats. *C*, RT-PCR analysis in fed overexpressing β-gal, WT LGS, or mutant LGS rats; data are relative to the fed β-gal group of rats. In all cases, relative expression levels were calculated with the $2^{-\Delta\Delta Ct}$ method using 18 S rRNA as endogenous control, and data represent the mean ± S.E. (*error bars*) of the following: seven fasted and seven fed β-gal-overexpressing rats; five fasted and six fed WT LGS-overexpressing rats; and five fasted and five fed mutant LGS-overexpressing rats. In *A* the *asterisk* indicates significant difference, with $p < 0.05$.

Intracellular Distribution of LGS after the IPGTT—Previous *in vitro* studies reported that the incubation of isolated hepatocytes

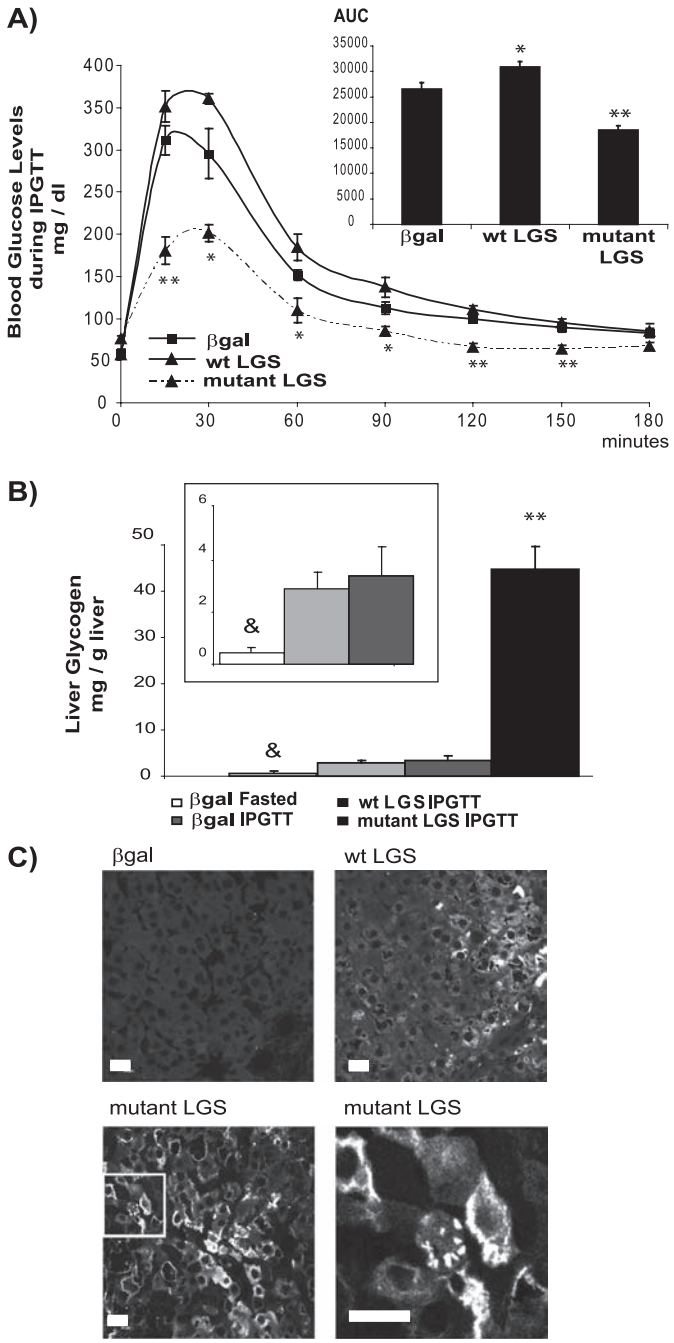

FIGURE 5. **Intraperitoneal glucose tolerance test.** *A*, rats overexpressing β-gal, WT LGS, or activated mutant LGS were fasted for 18 h before receiving an intraperitoneal glucose bolus of 2 g/kg body weight. Tail vein blood samples were taken, and glucose concentrations were measured at the times indicated after the glucose bolus. The area under the curve was measured for each experimental group (*AUC*, *inset*). *B*, liver glycogen content (mg/g of liver) determined at the starting point (β-gal-fasted) and at the end point of the IPGTT (180 min). The *inset* shows a *lower scale graph*. In all cases, data are mean ± S.E. (*error bars*) for seven fasted β-gal-overexpressing rats and nine β-gal-, six WT LGS-, and five mutant LGS-overexpressing animals from the IPGTT. *C*, liver samples taken after the IPGTT were processed for immunofluorescence analysis with an antibody against LGS. Representative confocal microscopy images of liver sections from rats overexpressing β-gal, WT LGS, or activated mutant LGS. Laser intensity was adjusted so that the endogenous LGS signal (β-gal-overexpressing animals) was hardly observable. *Lower right panel*, magnification of the mutant LGS image (*area inside* the *box*) to show the aggregated, peripheral distribution of LGS. *Scale bar*, 20 μm. In *A*, the *single* or *double asterisks* indicate those time points at which blood glucose concentrations were significantly lower in rats overexpressing mutant LGS than in rats overexpressing β-gal, with $p < 0.05$ or $p < 0.005$ respectively; in *B* the *double asterisk* denotes statistical difference for comparisons with the β-gal IPGTT group with $p < 0.005$, and the *ampersand* denotes statistical difference between the fasted β-gal group and the β-gal IPGTT group, with $p < 0.005$.

TABLE 3

Blood parameters after the IPGTT in rats overexpressing β-gal, WT LGS, or activated mutant LGS

At the end of the IPGTT (180 min), blood samples were taken in order to measure the metabolites and hormones indicated. Glucose was measured in whole blood, whereas the rest of the parameters were determined in plasma. Data are expressed as the mean ± S.E. for nine β-gal-, six WT LGS-, and five mutant LGS-overexpressing rats.

	β-gal	WT LGS	Mutant LGS
Glucose (mg/dl)	83 ± 6	91 ± 6	67 ± 4
Insulin (ng/ml)	2.3 ± 1	2.7 ± 1	2.8 ± 1
Triglycerides (mg/dl)	52 ± 10	47 ± 14	63 ± 8
Lactate (mg/dl)	27 ± 7	35 ± 3	40 ± 11
BHBA (mg/dl)	11 ± 2	13 ± 1	4 ± 1[a]

[a] Significant differences relative to β-gal-overexpressing rats, with $p < 0.05$.

with glucose activates LGS but also causes its translocation from a homogeneous cytoplasmic distribution to the cell periphery (17, 24). In the present study, we studied the subcellular distribution of LGS in all of the experimental groups after the IPGTT by means of immunofluorescence (Fig. 5*C*). There was a clear localization of LGS in the cell periphery in the activated mutant LGS group compared with the β-gal-overexpressing rats.

Liver-specific Transgenic Mice Expressing the Activated Mutant LGS—We wanted to investigate if longer (chronic) expression of the activated mutant LGS resulted in the loss of the ability to efficiently reduce blood glucose levels as a consequence of limited glycogen storage capacity. Because experiments using adenovirally transduced rats are time-limited, we undertook a completely new approach to address the issue of permanent activation of LGS as a potential strategy to chronically improve glucose tolerance. Thus, we generated transgenic mice expressing the activated mutant LGS under the control of albumin enhancer/promoter (liver-specific). Although transgenic animals expressed moderate levels of the recombinant protein as revealed by Western blot analysis (Fig. 6*A*; note the increased mobility due to reduced phosphorylation level), it was sufficient to drastically increase the LGS activity ratio (Fig. 6*B*). In addition, fed transgenic mice showed increased liver glycogen content when compared with WT animals in the same metabolic state, although this difference disappeared upon 18 h of fasting (Fig. 6*C*), indicating that these mice were capable of fully mobilizing their glycogen stores. Furthermore, activated mutant LGS liver-specific transgenic mice showed improved glucose tolerance when challenged with a glucose bolus (IPGTT; 2 g/kg body weight) (Fig. 6*D*).

DISCUSSION

The liver plays a major role in the clearance of blood glucose in the postprandial state (25), and several proteins involved in the control of hepatic glucose metabolism, including GK, GP, and glycogen-targeting proteins, have been proposed as potential targets for antihyperglycemic therapy for type 2 diabetes. GK overexpression and inhibition of GP activity are both effective in improving glucose tolerance. However, there are certain critical issues associated with these strategies. GK overexpression increases flux through glycolysis, and in some circum-

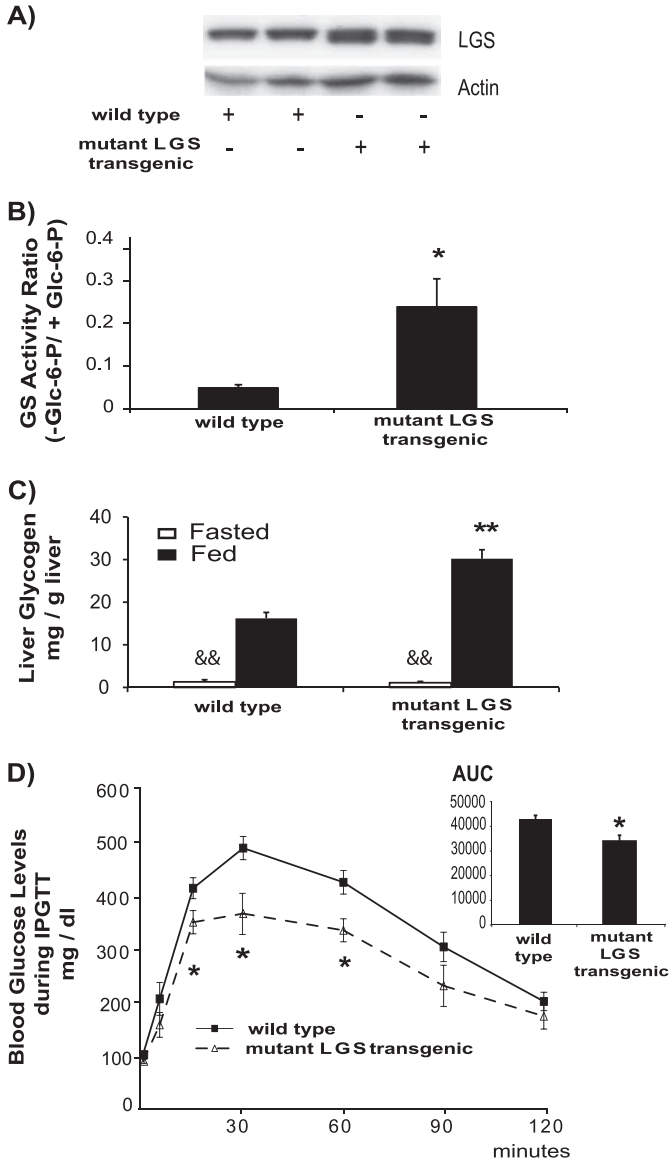

FIGURE 6. **Characterization of transgenic mice expressing activated mutant LGS in liver.** *A*, representative Western blot analysis of liver extracts of wild type and activated mutant LGS transgenic mice (two samples of each) with antibodies against LGS or actin as a load control. In all cases, 20 μg of protein were analyzed per lane. *B*, GS activity ratio (−glucose 6-phosphate/+glucose 6-phosphate (*−Glc-6-P/+Glc-6-P*)) of liver homogenates from wild type ($n = 8$) and mutant LGS transgenic ($n = 4$) mice. Data represent the mean ± S.E. (*error bars*). *C*, liver glycogen content (mg/g of liver) measured in fasted (*white bars*) or fed (*black bars*) wild type and mutant LGS transgenic mice. Data represent the mean ± S.E. of six fasted and four fed wild type mice and five fasted and four fed mutant LGS transgenic mice. *D*, wild type ($n = 9$) and mutant LGS transgenic ($n = 6$) mice were fasted for 18 h before receiving an intraperitoneal glucose bolus of 2 g/kg body weight. Tail vein blood samples were taken, and glucose concentrations were measured at the times indicated after the glucose bolus. The area under the curve was measured for each experimental group (*AUC, inset*). Data represent the mean ± S.E. The *single* or *double asterisks* denote statistical difference for comparisons with WT group at the same metabolic state with $p < 0.05$ or $p < 0.005$, respectively. The *double ampersand* denotes statistical difference ($p < 0.005$) between the fasted and fed states for each group of mice.

stances, this can lead to an increase in plasma triglycerides (4). GP inhibition may have potentially negative effects on skeletal muscle function during exercise (26). Studies using glycogen-targeting proteins have shown that sustained efficacy in improving glucose tolerance can be achieved only by enhancing glycogen synthesis in the postprandial state without compromising glycogenolysis in the postabsorptive state (6, 9). Accordingly, although overexpression of PTG markedly enhances glycogen storage in isolated hepatocytes *in vitro* (27), it is only mildly effective at improving glucose clearance in fasted glucose-challenged rats, because glycogenolysis is markedly curtailed in the fasted state and hepatic glycogen stores are therefore nearly saturated prior to glucose loading (6). A common feature of all of the above mentioned strategies is that they lead to secondary activation of LGS. Nevertheless, the direct effects of activation of this enzyme as the primary target to modulate blood glucose homeostasis have not been addressed. We have recently shown that the activity of LGS in primary cultured hepatocytes can be modulated by expression of constitutively active forms of the enzyme (13). Thus, our objective was to determine the effects of the expression of a constitutively active form of LGS on blood glucose homeostasis *in vivo*.

Two key findings have emerged from this study. First, the overexpression of a constitutively active variant of LGS (Ser → Ala mutations at 2 and 3b phosphorylation sites) lowered blood glucose in the fed but not in the fasted state, and these changes were paralleled by corresponding alterations in hepatic glycogen content. Worthy of note is that the glycogen synthesized showed a normal degree of ramification. Furthermore, it also markedly enhanced glucose clearance when fasted animals were challenged with a glucose load. Importantly, overexpression of the wild-type protein had a negligible effect on hepatic glycogen storage and on blood glucose homeostasis. Consequently, this finding indicates that the amount of LGS in the normal physiological state is not limiting for hepatic glycogen synthesis and that strategies simply aiming to increase LGS protein are not likely to improve glucose homeostasis. Second, the overexpression of a constitutively active form of LGS had no effect on plasma insulin, lactate, NEFAs, or triglycerides, thereby being free of some of the negative side effects detected in other approaches. Furthermore, this strategy also prevents the increase in ketogenesis because rats expressing an activated mutant LGS had a lower concentration of BHBA in the fasted state and after a glucose challenge, when compared with controls. Changes in the plasma concentration of ketone bodies generally parallel the plasma concentration of NEFAs. However, because the NEFA levels of the rats expressing a constitutively active LGS form were similar to those of controls, we propose that intrahepatic regulation of ketogenesis by the elevated glycogen content is a plausible explanation for the lower levels of BHBA. Further experiments would be necessary to address this hypothesis. Moreover, expression of LGS (either wild-type or active form) had no effect on the expression of the main glucose metabolism-related enzymes and glucose transporters, such as GK, GP, PEPCK, and GLUT2. Interestingly, although the rats overexpressing a constitutively active form of LGS showed markedly elevated GS activity in the fed and fasted states, blood glucose concentrations were decreased only in the former state, thereby indicating that other mechanisms have an overriding role on glycogen metabolism in the fasted state.

A central result in this study is the marked improvement of glucose tolerance shown by 18 h-fasted rats when challenged with a glucose load, with a decrease in area under the curve of 30%. This can be explained almost entirely by the prominent increase in the storage of hepatic glycogen in this experimental group. In fact, the overexpressed activated mutant LGS was located at the cellular periphery, where glycogen synthesis is initiated (17, 24). Although the hepatic glycogen accumulation in rats overexpressing the activated mutant form of LGS was already higher than the other groups after an 18-h fast, this surplus of glycogen did not limit the capacity of posterior accumulation of the polysaccharide in liver. Thus, rats overexpressing this constitutively active LGS mutant had the capacity to remove the excess of glucose in blood and then deliver it to glycogen synthesis more efficiently than the other groups. However, a permanent activation of LGS could potentially cause the saturation of the liver capacity to store glycogen, thus limiting its glycemia-lowering effects (8). The results obtained with liver-specific transgenic mice chronically expressing the activated mutant LGS largely reproduce the observations from the experiments with rats: increased LGS activity and glycogen accumulation in the fed state, capacity to mobilize glycogen stores upon fasting, and improved glucose tolerance when these mice were challenged with a glucose load.

On the basis of our findings, we propose that the direct activation of LGS is an effective method to improve glucose tolerance in the postprandial state as a result of its capacity to enhance glucose storage without affecting other metabolic pathways. Therefore, our observations may provide the basis for a novel therapeutic approach to reduce hyperglycemia in diabetes.

Acknowledgments—We thank Professor P. Chambon (Université Louis Pasteur, Strasbourg, France) and Dr. K. Kohno (Nara Institute of Science and Technology, Japan) for the generous gift of the pSG5 and p2335-1 plasmids, respectively. We also thank Dr. R. Gasa, (Diabetes and Obesity Laboratory of Institut d'Investigaciones Biomediques Pi i Sunyer-Hospital Clínic, Barcelona University) for valuable assistance with the purification of the adenoviruses. We thank the Mutant Mouse Platform (Institute for Research in Biomedicine, Barcelona), the Animal Research Center (Barcelona Science Park), and the Electron Microscopy Unit of the Core Scientific Services at Barcelona University for help with the assessment and the equipment necessary to carry out this study. We are also grateful to A. Adrover, L. Babin, E. Veza, and N. Plana for technical support. We thank T. Yates for correcting the English version of the manuscript and Professor L. Agius (University of Newcastle) for helpful suggestions.

REFERENCES

1. Agius, L., Peak, M., Newgard, C. B., Gomez-Foix, A. M., and Guinovart, J. J. (1996) *J. Biol. Chem.* **271,** 30479–30486
2. Hariharan, N., Farrelly, D., Hagan, D., Hillyer, D., Arbeeny, C., Sabrah, T., Treloar, A., Brown, K., Kalinowski, S., and Mookhtiar, K. (1997) *Diabetes* **46,** 11–16
3. Niswender, K. D., Shiota, M., Postic, C., Cherrington, A. D., and Magnuson, M. A. (1997) *J. Biol. Chem.* **272,** 22570–22575
4. O'Doherty, R. M., Lehman, D. L., Télémaque-Potts, S., and Newgard, C. B. (1999) *Diabetes* **48,** 2022–2027
5. Printen, J. A., Brady, M. J., and Saltiel, A. R. (1997) *Science* **275,** 1475–1478
6. O'Doherty, R. M., Jensen, P. B., Anderson, P., Jones, J. G., Berman, H. K., Kearney, D., and Newgard, C. B. (2000) *J. Clin. Invest.* **105,** 479–488
7. Yang, R., Cao, L., Gasa, R., Brady, M. J., Sherry, A. D., and Newgard, C. B. (2002) *J. Biol. Chem.* **277,** 1514–1523
8. Yang, R., and Newgard, C. B. (2003) *J. Biol. Chem.* **278,** 23418–23425
9. Gasa, R., Clark, C., Yang, R., DePaoli-Roach, A. A., and Newgard, C. B. (2002) *J. Biol. Chem.* **277,** 1524–1530
10. Agius, L. (2007) *Best Pract. Res. Clin. Endocrinol. Metab.* **21,** 587–605
11. Treadway, J. L., Mendys, P., and Hoover, D. J. (2001) *Expert. Opin. Investig. Drugs* **10,** 439–454
12. Kelsall, I. R., Munro, S., Hallyburton, I., Treadway, J. L., and Cohen, P. T. (2007) *FEBS Lett.* **581,** 4749–4753
13. Ros, S., García-Rocha, M., Domínguez, J., Ferrer, J. C., and Guinovart, J. J. (2009) *J. Biol. Chem.* **284,** 6370–6378
14. Gomis, R. R., Ferrer, J. C., and Guinovart, J. J. (2000) *Biochem. J.* **351,** 811–816
15. Becker, T. C., Noel, R. J., Coats, W. S., Gómez-Foix, A. M., Alam, T., Gerard, R. D., and Newgard, C. B. (1994) *Methods Cell Biol.* **43,** 161–189
16. Thomas, J. A., Schlender, K. K., and Larner, J. (1968) *Anal. Biochem.* **25,** 486–499
17. García-Rocha, M., Roca, A., De La Iglesia, N., Baba, O., Fernández-Novell, J. M., Ferrer, J. C., and Guinovart, J. J. (2001) *Biochem. J.* **357,** 17–24
18. An, J., Muoio, D. M., Shiota, M., Fujimoto, Y., Cline, G. W., Shulman, G. I., Koves, T. R., Stevens, R., Millington, D., and Newgard, C. B. (2004) *Nat. Med.* **10,** 268–274
19. Chan, T. M., and Exton, J. H. (1976) *Anal. Biochem.* **71,** 96–105
20. Krisman, C. R. (1962) *Anal. Biochem.* **4,** 17–23
21. Trinh, K. Y., O'Doherty, R. M., Anderson, P., Lange, A. J., and Newgard, C. B. (1998) *J. Biol. Chem.* **273,** 31615–31620
22. Herz, J., and Gerard, R. D. (1993) *Proc. Natl. Acad. Sci. U.S.A.* **90,** 2812–2816
23. Salavert, A., and Iynedjian, P. B. (1982) *J. Biol. Chem.* **257,** 13404–13412
24. Fernández-Novell, J. M., Bellido, D., Vilaró, S., and Guinovart, J. J. (1997) *Biochem. J.* **321,** 227–231
25. Cherrington, A. D. (1999) *Diabetes* **48,** 1198–1214
26. Baker, D. J., Greenhaff, P. L., MacInnes, A., and Timmons, J. A. (2006) *Diabetes* **55,** 1855–1861
27. Berman, H. K., O'Doherty, R. M., Anderson, P., and Newgard, C. B. (1998) *J. Biol. Chem.* **273,** 26421–26425